

**Conversion of Indian Agro-waste to Bio-ethanol  
via Syngas Platform- Detailed Process  
Modelling with Thermodynamic,  
Techno-Economic and Life Cycle Analysis**

Thesis Submitted by

**Soumitra Pati**

**Doctor of Philosophy (Engineering)**

Department of Mechanical Engineering

Faculty Council of Engineering & Technology

Jadavpur University

Kolkata, India

2023

**1. Title of the Thesis:** Conversion of Indian Agro-waste to Bio-ethanol via Syngas Platform- Detailed Process Modelling with Thermodynamic, Techno-Economic and Life Cycle Analysis.

**2. Name, Designation & Institution of the**

**Supervisors: Dr. Sudipta De**

Professor  
Department of Mechanical  
Engineering, Jadavpur  
University,  
Kolkata – 700 032, India

**Dr. Ranjana Chowdhury**

Professor  
Department of Chemical  
Engineering, Jadavpur  
University,  
Kolkata- 700 032, India

**3. List of Publications:**

**Book Chapters**

1. **Pati, S.**, Manna, D., De, S., & Chowdhury, R.\* (2023). Thermodynamic and phase equilibrium models of syngas generation through gasification. In *Advances in Synthesis Gas: Methods, Technologies and Applications* (pp. 3-42). Elsevier.  
DOI: <https://doi.org/10.1016/B978-0-323-91879-4.00007-2>

**International journal**

1. **Pati, S.**, De, S., & Chowdhury, R.\* (2023). Integrated techno-economic, investment risk and life cycle analysis of Indian lignocellulosic biomass valorisation via co-gasification and syngas fermentation. **Journal of Cleaner Production, (Elsevier)**  
DOI: <https://doi.org/10.1016/j.jclepro.2023.138744>
2. **Pati, S.**, De, S., & Chowdhury, R.\* (2023). Exploring the hybrid route of bio-ethanol production via biomass co-gasification and syngas fermentation from wheat straw and sugarcane bagasse: model development and multi-objective optimization. **Journal of Cleaner Production (Elsevier)**.  
DOI: <https://doi.org/10.1016/j.jclepro.2023.136441>

3. **Pati, S.**, De, S., & Chowdhury, R.\* (2021). Process modelling and thermodynamic performance optimization of mixed Indian lignocellulosic waste co-gasification. **International Journal of Energy Research, (Wiley)**. DOI: <https://doi.org/10.1002/er.6052>
4. **Pati, S.**, & De, S.\* (2021). Model development and thermodynamic analysis of biomass co-gasification using Aspen plus®. **Indian Chemical Engineer, (Taylor and Francis)**. DOI: <https://doi.org/10.1080/00194506.2021.1887770>

**List of Patents**      Nil

**List of Presentations in National / International / Conferences/Workshops/Symposiums**

1. **Pati, S.**, De, S., Chowdhury, R. (2020) Exergetic analysis of a combined gasificationfermentation hybrid model. **International Conference on Energy and Sustainable Development, 2020**. Organised by Jadavpur University, 2020.
2. **Pati, S.**, De, S., Chowdhury, R. (2019) Process Modelling of Gasification and Co-gasification of Individual and Mixed Indian Lignocellulosic Waste - Optimization of Energy Efficiency. **11th International Exergy, Energy and Environment Symposium**, Organised by SRM University, 2019.

## “Statement of Originality”

I Shri Soumitra Pati registered on 27<sup>th</sup> April, 2018 do hereby declare that this thesis entitled “**Conversion of Indian Agro-waste to Bio-ethanol via Syngas Platform- Detailed Process Modelling with Thermodynamic, Techno-Economic and Life Cycle Analysis**” contains literature survey and original research work done by the undersigned candidate as part of Doctoral studies. All information in this thesis have been obtained and presented in accordance with existing academic rules and ethical conduct. I declare that, as required by these rules and conduct, I have fully cited and referred all materials and results that are not original to this work. I also declare that I have checked this thesis as per the “Policy on Anti Plagiarism, Jadavpur University, 2019”, and the level of similarity as checked by iThenticate software is 1 %.

Signature of Candidate: *Soumitra Pati*

Date: 20.05.2024

Certified by Supervisors:  
(Signature with date, seal)

1.

*S-v*  
20/5/24

Professor  
Dept. of Mechanical Engineering  
Jadavpur University, Kolkata-32

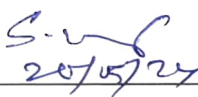
2.

*Ranjana Chowdhury*  
20/5/2024

**Dr. Ranjana Chowdhury**  
Professor  
Chemical Engineering Department  
JADAVPUR UNIVERSITY  
Kolkata-700 032

## Certificate from the Supervisors

This is to certify that the thesis entitled “**Conversion of Indian Agro-waste to Bio-ethanol via Syngas Platform- Detailed Process Modelling with Thermodynamic, Techno-Economic and Life Cycle Analysis**” submitted by Shri. Soumitra Pati, who got his name registered on 27<sup>th</sup> April, 2018 for the award of Ph.D (Engg.) degree of Jadavpur University is absolutely based upon his own work under the joint supervision of Dr. Sudipta De and Dr. Ranjana Chowdhury and that neither his thesis nor any part of the thesis has been submitted for any degree or any other academic award anywhere before.

1.  20/5/24

(Dr. Sudipta De)  
Professor  
Department of Mechanical Engineering  
Jadavpur University  
Kolkata 700032, India  
**Signature of Supervisor  
and date with office Seal**

*Professor  
Dept. of Mechanical Engineering  
Jadavpur University, Kolkata-32*

2.  20/5/2024

(Dr. Ranjana Chowdhury)  
Professor  
Department of Chemical Engineering  
Jadavpur University  
Kolkata 700032, India  
**Signature of Co-supervisor  
and date with office Seal**

**Dr. Ranjana Chowdhury**  
Professor  
Chemical Engineering Department  
JADAVPUR UNIVERSITY  
Kolkata-700 032

*Dedicated to*

*My Teachers*

## Acknowledgements

Research has been defined as the systematized effort to gain new knowledge. This journey to new insights becomes easier when one receives proper direction and encouragement. During my journey of Ph.D. work, there were many ups and downs. I would like to express my sincere gratitude to those people who helped me to overcome all the hurdles throughout my PhD period.

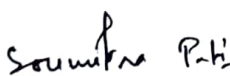
First and foremost, I would like to gratefully acknowledge my PhD supervisors, Prof. Sudipta De and Prof. Ranjana Chowdhury. It is not an exaggeration to say that my curiosity and eagerness in research was evoked by Prof. Sudipta De and Prof. Ranjana Chowdhury. I would like to thank them for inspiring me to pursue excellence. The discussions with both of them stimulated new ideas. The importance of supervision is well-known to anyone who conducts research. In this context, I would thank my supervisors for their unconditional support.

I would also like to express gratitude to my grandmother (Smt. Snehalata Pati) and my parents (Sri. Sanjit Kumar Pati and Smt. Rita Panda) for standing by me always and keeping faith in me. It can't be expressed in words what my family did for me and are still doing for me. I must thank them for helping me in every step of my life and pampering me so much.

Next, I would also like to thank Mrs. Titir Chakraborty for being there for me in my vulnerable moments and being a source of constant motivation.

Next, I would like to thank my friends, seniors and juniors from Jadavpur University for making this decade long university life what it is. I also like to thank my lab mates specially Dr. Avishek Roy, Dr. Sayan Das, Dr. Shiladitya Ghosh, Dr. Sumona Das, Mr. Sujit Saha, Mr. Amit Bhowmick, Dr. Prasun Dutta, Mr. Satyajit Das Karmakar, Mr. Dinabandhu Manna, Dr. Biswajit Debnath, Mr. Rishav Dutta for their continuous support. I would like to thank Mr. Binoy Shukla and all other staff of Heat Power Laboratory of Mechanical Engineering Department, Jadavpur University for their help and continuous support.

Signature:

 20.05.2024

---

(Soumitra Pati)

## Abstract

Biofuels are considered to be one of the most sustainable solutions towards the problem of fuel crisis and environmental pollution growing rapidly around the globe. This study aims to focus on the hybrid route of biofuel production in the theoretical and analytical context. Focused biofuel in this study is bio-ethanol and the hybrid route is a combination of the thermochemical route of gasification especially co-gasification and the biochemical route of synthesis gas fermentation. It can be stated after significant literature review that this route is less explored but has a lot of commercialization potential. Three Indian lignocellulosic biomass, namely rice straw, wheat straw and sugarcane bagasse, have been chosen according to their local availability. Using these biomass in a combination of two a non-stoichiometric equilibrium model of biomass co-gasification has been developed in process simulation software Aspen plus. It has been observed that the model can successfully predict the syngas composition with an average error of less than 10%. Significant sensitivity on the thermodynamic performance of the co-gasification process has been noticed with the variation of process parameters like temperature and equivalence ratio. Optimization of independent variables has been performed to maximize the energy and exergy efficiency of the process. Afterwards, kinetic modelling has been developed for the co-gasification process to predict the combined effect of biomass mixing ratio, temperature and equivalence ratio on the thermodynamic performance. Response surface methodology has been implemented on the model for that purpose. After developing these two models of co-gasification synthesis gas fermentation has been incorporated in simulation. The bio-ethanol production module has been developed to study the theoretical ethanol productivity. Also in this study, response surface methodology has been used to optimize various process parameters. Ethanol production potential of about 283 kg per ton of biomass has been predicted through this process. Some modifications in the model including heat integration and resource recovery have been observed to improve the overall sustainability and resource efficiency of the process. The economic viability, investment risk and environmental feasibility of the process have been tested theoretically. It has been observed that the minimum selling price of ethanol produced in this process is less than the current market price. Uncertainty of the economic parameters has lesser impact on the profitability of the route. It has been established by conducting life cycle analysis that the syngas fermentation route combining co-gasification of pairs of Indian lignocellulosic feedstocks under study and syngas fermentation is environmentally more sustainable compared to the bio-ethanol production via sugar platform.



## **Title of the thesis**

**Conversion of Indian Agro-waste to  
Bio-ethanol via Syngas Platform- Detailed  
Process Modelling with Thermodynamic,  
Techno-Economic and Life Cycle Analysis**

# CONTENTS

<b>Abstract.....</b>	<b>i</b>
<b>Title of the thesis .....</b>	<b>ii</b>
<b>CONTENTS.....</b>	<b>iii</b>
<b>LIST OF FIGURES .....</b>	<b>vi</b>
<b>LIST OF TABLES.....</b>	<b>ix</b>
<b>SYMBOLS AND ABBREVIATIONS .....</b>	<b>xi</b>
<b>Chapter 1. Introduction.....</b>	<b>1</b>
1.1 Indian lignocellulosic biomass.....	3
1.2 Gasification .....	4
1.3 Co-gasification of biomass .....	7
1.4 Syngas fermentation.....	8
1.5 Process modelling .....	11
1.6 Mathematical modelling of gasification .....	12
1.6.1 Thermochemical equilibrium modelling.....	12
1.6.2 Kinetic Modelling of gasification .....	26
1.7 Mathematical modelling syngas fermentation: .....	26
1.8 Techno-economic analysis .....	28
1.9 Investment risk analysis.....	29
1.10 Life cycle analysis.....	29
1.11 Thesis Overview.....	30
<b>Chapter 2. Literature review .....</b>	<b>33</b>
2.1 Introduction.....	33
2.2 Equilibrium modelling of gasification and co-gasification in Aspen plus.....	33
2.2.1 Research gaps in equilibrium modelling of biomass .....	41
2.3 Kinetic modelling of gasification and co-gasification .....	42
2.3.1 Research gaps in kinetic modelling of biomass .....	49
2.4 Literatures on modelling of ethanol production following syngas platform .....	49
2.4.1 Research gaps in modelling of ethanol production following syngas platform.....	55
2.5 Economic, life cycle and risk assessment of bio-ethanol production technologies.....	56
2.5.1 Research gaps in economic, life cycle and risk assessment of bio-ethanol production technologies: .....	65
2.6 Research objectives.....	66
2.7 Scope of the research work .....	67

<b>Chapter 3. Materials and Methods.....</b>	<b>69</b>
3.1 Introduction.....	69
3.2 Materials .....	69
3.3 Methodology of modelling in Aspen plus.....	70
3.3.1 Aspen plus simulation of equilibrium models .....	70
3.4 Aspen plus modelling of syngas fermentation .....	76
3.5 Chapter summary .....	76
<b>Chapter 4. Equilibrium modelling and thermodynamic analysis of Indian lignocellulosic biomass co-gasification using Aspen plus .....</b>	<b>77</b>
4.1 Objective of the chapter .....	77
4.2 Modelling aspect.....	77
4.3 Thermodynamic Performance Assessment .....	79
4.4 Results and Discussions.....	81
4.4.1 Model Validation.....	81
4.4.2 Thermodynamic performance results .....	82
4.4.3 Statistical analysis using Response Surface Methodology .....	87
4.4.4 Optimization of process parameters.....	95
4.5 Chapter summary .....	96
<b>Chapter 5. Kinetic modelling and thermodynamic performance optimization of Indian lignocellulosic biomass co-gasification .....</b>	<b>97</b>
5.1 Objective of the chapter .....	97
5.2 Methodology .....	97
5.3 Model development .....	99
5.4 Thermodynamic performance analysis .....	100
5.5 Experimental design.....	101
5.6 Results and discussions.....	101
5.6.1 Model Validation.....	101
5.6.2 Optimization of the performance of mixed biomass gasification process.....	103
5.7 Chapter summary .....	117
<b>Chapter 6. Bio-ethanol production via syngas platform: model development and multi-objective optimization.....</b>	<b>119</b>
6.1 Objective of the chapter .....	119
6.2 Feedstock selection and mathematical background.....	119
6.2.1 Feedstock selection .....	119
6.2.2 Mathematical methodology .....	119
6.3 Model development .....	120
6.4 Response Surface Methodology .....	123
6.5 Performance parameters.....	123

6.6 Results and Discussions.....	124
6.6.1 Model validation .....	124
6.6.2 Sensitivity analysis.....	126
6.6.3 Statistical analysis results .....	130
6.6.4 Multi-objective optimization .....	144
6.7 Chapter summary .....	144
<b>Chapter 7. Integration of power generation and heat and resource recovery in the co-gasification- syngas fermentation model.....</b>	<b>145</b>
7.1 Objective of the chapter .....	145
7.2 Model development .....	145
7.3 Results and discussions.....	147
7.3.1 Mass and energy balance .....	147
7.4 Chapter summary .....	148
<b>Chapter 8. Techno-economic analysis, investment risk analysis and life cycle analysis of the co-gasification fermentation model.....</b>	<b>149</b>
8.1 Objective of the chapter .....	149
8.2 Methodology .....	149
8.2.1 Methodology of Techno-economic analysis .....	149
8.2.2 Methodology of investment risk analysis .....	151
8.2.3 Life cycle impact assessment methodology.....	151
8.3 Results and discussions.....	156
8.3.1 Capital investment and MFSP estimation:.....	156
8.3.2 Comparison of economic indicators .....	158
8.3.3 Uncertainty analysis on NPV .....	159
8.3.4 Life cycle assessment results .....	162
8.4 Chapter summary .....	168
<b>Chapter 9. Conclusions and future scope .....</b>	<b>169</b>
9.1 Conclusions.....	169
9.2 Scope for future work .....	171
<b>References.....</b>	<b>173</b>
<b>Appendix .....</b>	<b>196</b>

# LIST OF FIGURES

Figure 1.1: Different types of gasifiers (A: Updraft; B) Downdraft; C) Fluidized bed; D) Entrained Bed.....	6
Figure 1.2: Simplified pathway for syngas fermentation.....	10
Figure 1.3: Four stages of life cycle analysis (ISO 14040/44) .....	30
Figure 3.1: Methodical representation of Aspen plus equilibrium modelling .....	70
Figure 3.2: Process flow diagram of Aspen plus equilibrium modelling .....	73
Figure 3.3: Process flow diagram of Aspen plus kinetic modelling .....	75
Figure 4.1: Co-gasification model developed in Aspen plus .....	78
Figure 4.2: Comparison of volume percentage between model and experimental results of Sharma et al. 2015.....	82
Figure 4.3: Variation of LHV of syngas with gasification temperature.....	83
Figure 4.4: Variation of LHV of syngas with equivalence ratio .....	84
Figure 4.5: Variation of LHV of syngas with steam to biomass ratio.....	84
Figure 4.6: Variation of (a) energy efficiency and (b) exergy efficiency with Temperature (°C) at an equivalence ratio 0.35 and steam/biomass ratio 0.5.....	85
Figure 4.7: Variation of (a) energy efficiency and (b) exergy efficiency with equivalence ratio at a gasifier temperature 750°C and steam/biomass ratio 0.5 .....	86
Figure 4.8: Variation of (a) energy efficiency and (b) exergy efficiency with steam/biomass ratio at gasifier temperature 750°C and equivalence ratio 0.35.....	87
Figure 4.9: Deviation of the actual responses from predicted response values of energy efficiency regression model (RS-SCB).....	90
Figure 4.10: Deviation of the actual responses from predicted response values of exergy efficiency regression model (RS-SCB).....	91
Figure 4.11: Deviation of the actual responses from predicted response values of energy efficiency regression model (WS-SCB).....	94
Figure 4.12: Deviation of the actual responses from predicted response values of exergy efficiency regression model (WS-SCB).....	95
Figure 5.1: Aspen plus flow sheet for kinetic model of co-gasification .....	100
Figure 5.2: Bar chart showing the comparison of experimental to simulated values .....	103
Figure 5.3: Deviation of the actual responses from predicted response values of regression model (RS-SCB).....	107

Figure 5.4: Deviation of the actual responses from predicted response values of regression model (WS-SCB).....	109
Figure 5.5: Effect of biomass ratio and gasification temperature on energy efficiency ( $\eta$ ).....	111
Figure 5.6: Effect of biomass ratio and equivalence ratio on energy efficiency ( $\eta$ ).....	112
Figure 5.7: Effect of biomass ratio and gasification temperature on exergy efficiency ( $\psi$ ).....	113
Figure 5.8: Effect of biomass ratio and equivalence ratio on exergy efficiency ( $\psi$ ) .....	115
Figure 5.9: Effect of gasification temperature and equivalence ratio on exergy efficiency ( $\psi$ ) .....	116
Figure 6.1: Co-gasification and fermentation simulation flow-sheet in Aspen plus.....	121
Figure 6.2: Variation of model yields with experimental results .....	126
Figure 6.3: Variation of syngas and ethanol yield with temperature .....	127
Figure 6.4: Variation of (a) LHV of syngas and H <sub>2</sub> /CO ratio and (b) CGE and overall energy efficiency with temperature .....	128
Figure 6.5: Variation of syngas and ethanol yield with equivalence ratio .....	129
Figure 6.6: Variation of (a) LHV of syngas and H <sub>2</sub> /CO ratio and (b) CGE and overall energy efficiency with equivalence ratio .....	130
Figure 6.7: Deviation of the actual responses from predicted response values of regression model.....	133
Figure 6.8: Interaction effects of input variables on Ethanol production rate .....	135
Figure 6.9: Interaction effect of input variables on syngas LHV (MJ/Nm <sup>3</sup> ) .....	137
Figure 6.10: Interaction effect of input variables on cold gas efficiency (CGE).....	139
Figure 6.11: Interaction effect of input variables on energy efficiency .....	141
Figure 6.12: Interaction effect of input variables on CO <sub>2</sub> emission.....	143
Figure 7.1: Aspen plus flowsheet of the modified co-gasification and fermentation process including power generation and heat and resource recovery. ....	146
Figure 7.2: Mass and energy balance block diagram.....	148
Figure 8.1: System boundary of the system for life cycle assessment.....	154
Figure 8.2: Equipment purchase cost distribution of various units in the simulated co-gasification fermentation plant .....	156
Figure 8.3: Probability distribution histogram for total NPV variation.....	161
Figure 8.4: Sensitivity of NPV on the operating variables .....	162
Figure 8.5: Percentage of environmental impact in ReCiPe 2016 Midpoint (H) 1.13 method for different unit processes .....	164
Figure 8.6: Midpoint comparison of impacts of three different ethanol production	

methodologies .....	167
Figure 8.7: Endpoint comparison of ethanol production methodologies.....	167
Figure 1-A: Diagnostic plots for energy efficiency optimization for RS-SCB mixture in equilibrium modelling.....	189
Figure 2-A: Diagnostic plots for exergy efficiency optimization for RS-SCB mixture ..	190

# LIST OF TABLES

Table 1.1: Top ten agro-wastes of India according to their surplus potential (Hiloidhari et al., 2014). .....	4
Table 1.2: Array of reactions in gasifiers (La Villetta et al., 2017; Marcantonio et al., 2020; Safarian et al., 2019; Silva et al., 2019).....	7
Table 1.3: All reactions involved in syngas fermentation (Gunes, 2021; Phillips et al., 2017; Shen et al., 2018; Wang et al., 2018; Wang et al., 2017; Zhang et al., 2013) .....	10
Table 1.4: Chemical characteristic of gases in the ideal-gas state at reference state $T = 298.15$ K, $P = 0.1$ MPa (Perry & Green, 2007).....	14
Table 2.1: Literatures on equilibrium modelling of gasification and co-gasification in Aspen plus.....	33
Table 2.2: Literatures on kinetic modelling of gasification and co-gasification.....	42
Table 2.3: Literatures on modelling of ethanol production following syngas platform ....	49
Table 2.4: Literatures on economic, life cycle and risk assessment of bio-ethanol production technologies .....	56
Table 3.1: Elemental analysis of the feedstock (Livingston, 1991; Miles et al., 1995).....	69
Table 4.1: Description of the blocks used in co-gasification model .....	78
Table 4.2: Elemental analysis of the feedstock used in the experiments of Sharma et al., 2015 .....	81
Table 4.3: List of independent variables .....	87
Table 4.4: ANOVA table of energy efficiency (RS-SCB).....	88
Table 4.5: ANOVA table of exergy efficiency (RS-SCB).....	89
Table 4.6: ANOVA table of energy efficiency (WS-SCB).....	92
Table 4.7: ANOVA table of exergy efficiency (WS-SCB).....	93
Table 5.1: Rate constants for different gasification reactions (Eikeland et al., 2015; Gremyachkin, 2006; Umeki et al., 2012).....	98
Table 5.2: List of independent variables .....	101
Table 5.3: Elemental analysis of the feedstock used in the experiments of (Monir et al., 2020) .....	102
Table 5.4: yield variation between experimental and simulation results .....	102
Table 5.5: Results of the experimental conditions. ....	104
Table 5.6: ANOVA table of the response variables (RS-SCB) .....	105



Table 5.7: Modified ANOVA table of the response models (RS-SCB) .....	106
Table 5.8: Modified ANOVA table of the response models (WS-SCB) .....	108
Table 6.1: Elemental analysis of the feedstock to be used for validation purpose .....	125
Table 6.2: ANOVA results for response variables of the hybrid model .....	131
Table 8.1: LCA inventory for 1 ton of mixed biomass use .....	155
Table 8.2: Assessment of total capital investment .....	157
Table 8.3: Results of economic analysis and economic indicators .....	158
Table 8.4: Comparison of the economic indicators of the CGF, EHF and SF route .....	159
Table 8.5: Probability distribution and specifications of the input variables .....	160
Table 8.6: Environmental impacts according to ReCiPe 2016 Midpoint (H) methodology for various ethanol production pathway .....	166

# SYMBOLS AND ABBREVIATIONS

## Abbreviations

LB	Lignocellulosic biomass
LHV	Lower heating value
ER	Equivalence ratio
SBR	Steam to biomass ratio
rmse	Root mean square error
RSM	Response surface methodology
ANOVA	Analysis of variance
CGE	Cold gas efficiency
SCB	Sugarcane Bagasse
RS	Rice straw
WS	Wheat straw
MESP	Minimum ethanol selling price
CEPCI	Chemical engineering plant cost index
TCI	Total capital investment
TEPC	Total equipment purchase cost
TDC	Total direct cost
TIC	Total indirect cost
NPV	Net present value
ACC	Annualised capital cost
IRR	Internal rate of return
PBP	Payback period
LCA	Life cycle analysis
CGF	Co-gasification fermentation
EHF	Enzymatic hydrolysis and fermentation
SF	Sugar fermentation
GWP	Global warming potential

## Symbols

$G_i$	Gibbs free energy of $i^{\text{th}}$ component
$N_i$	Total number of moles in $i^{\text{th}}$ component
$c$	Total number of components
$T$	Temperature
$P$	Total pressure
$V$	Volume
$R$	Universal Gas constant
$U$	Internal energy
$M$	Mass
$C$	Concentration
$y_i$	Mole fraction of $i^{\text{th}}$ component
$f_i$	Fugacity of $i^{\text{th}}$ component
$\bar{f}$	Fugacity coefficients of pure component

$\bar{f}_i$	Fugacity coefficients of pure component i in reaction mixture
$\bar{G}_i$	Partial molar Gibbs energy of i <sup>th</sup> component
$\bar{\bar{G}}_i$	Pure molar Gibbs energy of i <sup>th</sup> component
$\bar{G}_i^o$	Gibbs energy of species at standard temperature and pressure
$a_i$	Activity of i <sup>th</sup> component
$T_R$	Reference temperature
$\Delta_{rxn}G^o$	Total Gibbs energy of reaction
$\Delta G_{fi}^o$	Standard heat of formation i <sup>th</sup> component
$S_i$	Entropy of i <sup>th</sup> component
$\bar{S}_i$	Partial molar entropy of i <sup>th</sup> component
$H_i$	Enthalpy of i <sup>th</sup> component
$\Delta_{rxn}H^o$	Total heat of reaction
$c_{pi}$	Constant pressure heat capacity of i <sup>th</sup> component
$K_a$	Equilibrium constant
$N_i^k$	Total number of moles of i <sup>th</sup> component in k <sup>th</sup> phase
$\bar{G}_i^k$	Partial molar Gibbs energy of i <sup>th</sup> component in k <sup>th</sup> phase
$F$	Degrees of freedom
$r$	Number of independent reactions
$MW$	Molecular weight
$w$	Weight fraction
$\Delta \dot{H}$	Rate of change of enthalpy
$\Delta \dot{E}_k$	Rate of change of kinetic energy
$\Delta \dot{E}_p$	Rate of change of potential energy
$\dot{Q}$	Rate of heat transfer between the system and the surroundings
$\dot{W}_s$	Shaft work
$\hat{h}_f^o$	Molar heat of formation
$\Delta \hat{h}$	Specific enthalpy change associated with sensible heat
$\dot{S}_{gen}$	Specific entropy of generation
$\mu_i$	chemical potential of i <sup>th</sup> species
$a_{ik}$	Number of atoms of the k <sup>th</sup> element in each molecule of i
$A_k$	Total number of atomic masses of the k <sup>th</sup> element
$W$	Number of atoms present in the system
$L$	Lagrangian function
$E_a$	Activation energy
$A$	Frequency factor
$k$	Rate constant
$EX$	Exergy
$I$	Irreversibility
$Y$	yield coefficient
$V_g$	Gas phase volume
$V_l$	Liquid phase volume
$N_{Gout}$	Molar flow rate of outlet gas
$V_i$	Inlet volume
$V_o$	Outlet volume
$C^*$	Equilibrium concentration
$Q_{Gout}$	Volumetric flow rate of outlet gas
$r_i$	Reaction rate of i <sup>th</sup> component

$H_i$	Henry's constant of $i^{\text{th}}$ component
$X$	Concentration of biomass

### Greek Symbols

$\vartheta_i$	Stoichiometric coefficient of $i^{\text{th}}$ component
$\xi$	Extent of reaction
$\pi$	Number of phases
$\mu_i$	Chemical potential of $i^{\text{th}}$ species
$\lambda$	Lagrangian multiplier
$\eta$	Energy efficiency
$\psi$	Exergy efficiency
$\beta$	factor for calculating exergy
$\mu_{max}$	Maximum specific growth rate
$\mu$	Specific growth rate

---

## Chapter 1. Introduction

---

Fuel is keeping alive and carrying further the modern day civilization. But over time the human civilization has drained the fossil fuel reserve stored inside the earth up to a great extent. Also, the continuous increase in the living standards, rapid urbanization and non-sustainable power production have tremendously increased environmental pollution.

Scientists have unanimously agreed that if this situation continues then the rise in the global average temperature will rise up to  $2.7^{\circ}\text{C}$  by the end of this century causing serious threat to the livelihood of one third of the total world population (Lenton et al., 2023). To deal with this grave concern the United Nations have outlined a plan of action that has been taken up by all 196 countries in the general assembly known as the famous Paris Agreement taken up in December 2015. In the Paris agreement all the countries have agreed to a common goal of mitigating climate change by limiting global warming at  $1.5^{\circ}\text{C}$  by the end of 2030 (Horowitz, 2016). To achieve this ambitious target 17 sustainable development goals have also been adopted by the UN which are expected to lead the path towards a 'Net Zero' society. Obtaining 'Net Zero' emission understandably requires major shift in the power production approach that is currently predominant in our society and various renewable and waste resources are supposed to play a significant role in this 'Energy transition'.

The fuels derived from biomass, i.e., bio-fuels are apparently environment friendly. During the conversion processes, chemical energy in the biomass is usually converted to that of a low-carbon fuel/fuel substitute, e.g., bioethanol, long chain fatty acid esters, higher alcohols (butanol, hexanol etc.), hydrogen, biogas etc.. Bioelectricity can also be produced by the conversion of chemical energy of biomass using microbial fuel cells. Bio-fuels, when produced from plant-based waste biomass, serve dual purposes. While on one hand biofuels solve the problem of solid waste utilization, on the other hand, they provide alternative low/zero -carbon energy resources ensuring reduction in  $\text{CO}_2$  emission. If the processes used for biofuel generation are sustainable, all biofuels are expected to be either  $\text{CO}_2$  neutral or  $\text{CO}_2$  negative if the  $\text{CO}_2$  utilization during the production of biomass through photosynthesis is accounted. Bio-ethanol is a particular type of biofuel that can be used as a gasoline substitute in internal combustion engines. The conventional way of producing first generation bioethanol is by fermenting sugar, food crop and other starchy food grains in the presence of yeast,

*Saccharomyces cerevisiae* (Gunatilake et al., 2014). To ensure food security, the food-fuel competition should be avoided and hence the researchers should keep away from using first generation biofuel generation processes based on food. From this perspective, lignocellulosic biomass (LB) is a potential feedstock for the production of biofuels. The energy resources generated from lignocellulosic biomass are called second generation (2G) biofuels. As India has an abundantly available LB resource in the form Agro-wastes, it can contribute largely in the 2G-biofuel generation. According to the '**National Policy on Biofuels (2018)**' of the Government of India (GoI), a guideline for 'Ethanol blending' with a target of 20% blending-with-gasoline by 2025 has already been announced. Although GoI has permitted the use of maize, broken rice etc. for ethanol generation for ethanol production for the time being, an efficient generation of 2G-bioethanol can only make the blending target reachable (*Roadmap for Ethanol Blending in India 2020-25*)

2G-bioethanol cannot be directly produced by the fermentation of LBs because none of the structural carbohydrate polymers, namely cellulose, hemicelluloses and lignin can be assimilated by any of the microorganisms used for ethanol production. As LBs are not directly fermentable, they are converted to ethanol either through (I) reducing **sugar** via the generation of hexose (glucose) and pentose (xylose) sugars or (II) **syngas** platform via syngas production. In sugar platform, the reducing sugars are produced from LBs are produced through medium temperature pretreatment (120-200°C) processes. After the pretreatment of LBs a liquid phase product, called hydrolysate and pretreated solid containing mostly the recalcitrant lignin and the major portion of LB cellulose are produced. During pretreatment the hemicellulose and amorphous cellulose parts of LBs are depolymerised to release xylose and glucose respectively and they appear in the liquid hydrolysate. The cellulosic part of the pretreated solid is enzymatically hydrolysed to glucose, while the lignin part remains almost unchanged. The glucose, thus produced, is conventionally converted to bio-ethanol through microbial route using *Saccharomyces cerevisiae*. Because of recalcitrance of lignin, the sugar platform is not very suitable for dry and high-lignin biomass. Many of the agricultural wastes are lignin rich and hence syngas platform can be used for them to produce bio-ethanol. Syngas platform follows a combination of thermochemical and biochemical processes and thus represents a hybrid route of ethanol production. This process firstly follows the thermochemical route of producing synthesis gas (mixture of  $H_2$  and  $CO$ ) via gasification from LBs, and then follows the biochemical route of fermentation of the product gas to a mixture of acetic acid and ethanol using anaerobic and mesophilic bacterial strains (Sun et al., 2018). As GoI targets 20% ethanol-

gasoline blending by 2025, the all possibilities of conversion of Indian Agro wastes to 2G-bioethanol should be explored. It is expected that syngas platform will be effective for the generation of bioethanol from Agro-wastes of India. As there is a wide variation of characteristics of Indian agro-wastes, their gasification performance is also expected to vary their properties. The performance of the gasification of mixed agro-waste, i.e. the co-gasification, is expected to be a function of the ratio of weight fraction of each type of biomass, besides other gasification parameters like temperature, quantity of gasifying agent, i.e., air or oxygen etc. The performance of the fermentation process will be directly dependent on the composition of syngas. Thus the alcohol production will be indirectly dependent on all factors affecting the co-gasification performance. As the agro-wastes have to be handled in large quantities, the assessment and optimization of large scale 2G-bioethanol production via syngas platform is necessary. For the development of a guideline to take the strategic decision on the setting up of 2G-Bio-ethanol plants using mixed Indian Agro-wastes in near future, simulation and process modeling can serve as an important tool to save the expenditure of real time large scale experiments. It will be also useful to get the immediate understanding of the effects of different variables on 2G-Bio-ethanol production from Agricultural wastes of India via syngas platform. Based on the understanding the input variables can further be optimized to maximize the bio-ethanol production. For the ultimate implementation of Agro-based 2G-Bio-ethanol production process in large scale the sustainability and techno-economic viability must be checked.

### **1.1 Indian lignocellulosic biomass**

The array of Indian lignocellulosic biomass includes agricultural waste, forestry waste, municipal organic waste etc. However, being an agriculture dominated economy, India has an abundance of agricultural waste biomass. India has a 179.8 million hectares of land area which produces around 500 Mt/year of agricultural waste (Bhuvaneshwari et al., 2019). These agro-wastes have some usage as animal feed or organic fertilizer but a large amount of it is either burnt away or remains unutilized. Indian agricultural sector is responsible for the 18% of the annual greenhouse gas (GHG) emission in India (Kapoor et al., 2020). A significant portion of it is because of the stubble burning that take place in between cultivations. Mitigating this stubble burning has a potential of reducing up to 520 kg  $CO_2$  eq./he/year which is a huge number considering the current environmental situation the whole world is in (Sapkota et al., 2019). Top ten agro-wastes of India according to their surplus potentials have been listed in Table 1.1

**Table 1.1:** Top ten agro-wastes of India according to their surplus potential (Hiloidhari et al., 2014).

Crop	Waste type	Surplus potential (Mt/year)	Lower heating value (LHV) (MJ/kg)
<b>Sugarcane</b>	Bagasse	55.7	17.71
	Top and leaves		
<b>Cotton</b>	Stalk	46.9	17
	Husk		
	Boll shell		
<b>Rice</b>	Straw	43.5	13.95
	Husk		
<b>Wheat</b>	Straw	28.5	16.45
	Pod		
<b>Banana</b>	Peel	12.3	17.4
<b>Coconut</b>	Frond	9.7	15
	Husk		
<b>Maize</b>	Cob	9	17.39
	stalk		
<b>Bajra</b>	Cob	5.1	17.40
	Husk		
	Stalk		
<b>Mustard and rapeseed</b>	Stalk	4.9	17
<b>Soybean</b>	Stalk	4.6	17

The table suggests that India has huge potential of utilizing this naturally unused source of energy stored in LBs in the form of energy or fuel. However, the possible options of biomass conversion to fuel are versatile but our work here is limited to the assessment of the co-gasification and syngas fermentation route of bio-ethanol production.

## 1.2 Gasification

Gasification is a complex chemical phenomena where carbonaceous compounds react with suitable gasifying agent to produce combustible gas known as synthesis gas (syngas). Syngas is mainly constituted of  $CO$ ,  $CO_2$ ,  $H_2$ ,  $H_2O$ ,  $CH_4$ , and some condensable volatiles (tar). Gasification of solids containing  $C$ ,  $H$ ,  $N$ ,  $O$ , and  $S$  is one of the major routes of production of syngas. The solids are partially oxidized using gasifying agents like oxygen or air and steam. The solid feedstock, usually used for the production of syngas include low-grade coal,



agricultural biomass, algal biomass, woody biomass, and municipal solid wastes to name a few (Chowdhury et al., 2018). A solid stream containing unconverted char and ash is also produced during the process of syngas generation. From the perspective of moving patterns of solid feedstock and the gasifying medium the gasifiers can be categorized into three types, namely, a) moving bed, b) fluidized bed and c) entrained bed (Puig-Arnavat et al., 2010). Different configurations of syngas reactors are schematically represented in Figure 1.1. The moving bed gasifiers can again be classified as updraft and downdraft ones. In both types of moving bed reactors, the solid feedstock is fed from the top of the reactor and the gasifying medium is fed either from the bottom (updraft) or from the top (downdraft) of the gasifiers (Patra & Sheth, 2015). In the updraft and downdraft reactors, the solid-fluid movement is in counter-current and co-current patterns, respectively. The downdraft gasifier is more popularly used because the concentration of condensable volatiles (tar) in the product syngas stream is much less compared to updraft ones (Sharma et al., 2020). Large-sized particles can be handled in the moving bed gasifiers. In the fluidized bed gasifiers, the superficial velocity of the gasifying medium is sufficient enough to fluidize the solid particles and hence the gasifier behaves like a continuous stirred tank reactor (Nikoo & Mahinpey, 2008). The heat and mass transfer between the fluid and the solid particles is better in comparison to the moving bed versions. The residence time is in the order of minutes to seconds. In the entrained bed gasifiers micron-sized particles are handled in a co-current pattern with the gasifying medium. Usually, high temperature and very short residence time (in order of seconds) are maintained in the reactor and the solids are usually in the slagging state (Ku et al., 2019).

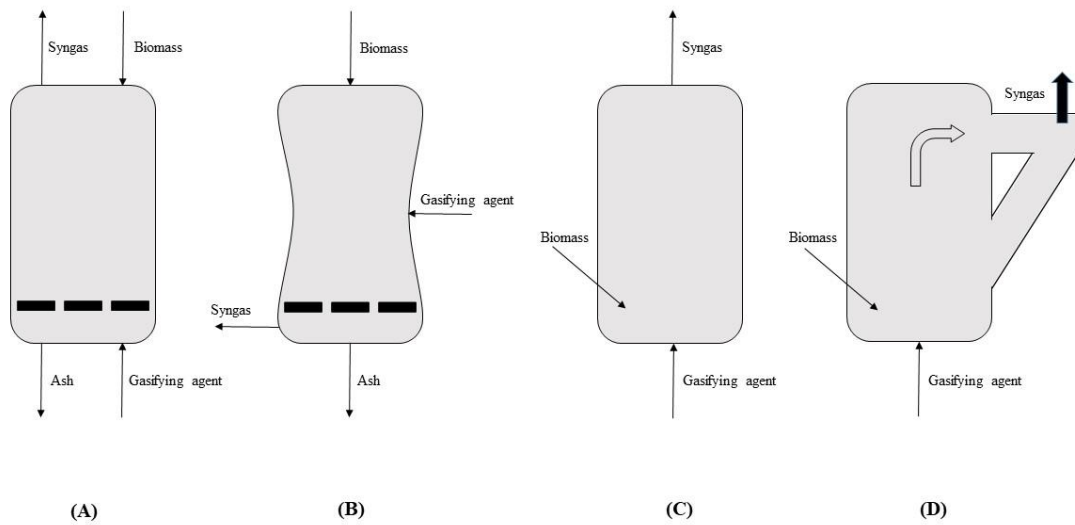


**Figure 1.1:** Different types of gasifiers (A: Updraft; B) Downdraft; C) Fluidized bed; D) Entrained Bed

Gasification is a complex process involving physical and chemical changes. Mainly four stages, namely, drying, pyrolysis, combustion, reduction, and gasification are involved in the process. Drying of feedstock occurs at  $<150^{\circ}\text{C}$  and causes the removal of moisture (Puig-Arnavat et al., 2010). During pyrolysis ( $150\text{--}700^{\circ}\text{C}$ ) thermal degradation of feedstock leads to the formation of char and volatiles. While the non-condensable volatile product, i.e., the gaseous part is constituted of  $\text{H}_2$ ,  $\text{CO}$ ,  $\text{CO}_2$ ,  $\text{CH}_4$ , and some other light hydrocarbon gases, the condensable non-aqueous volatile part is mainly high molecular weight hydrocarbons, namely tar (Chowdhury & Sarkar, 2012). In the combustion zone ( $700\text{--}1500^{\circ}\text{C}$ ), some of the solid feedstock are combusted to form  $\text{CO}_2$  and  $\text{H}_2\text{O}$ . During reduction ( $800\text{--}1100^{\circ}\text{C}$ ),  $\text{CO}_2$  reacts with char to form  $\text{CO}$  (Boudouard reaction). Besides, a further reaction between  $\text{H}_2\text{O}$  with  $\text{CO}$  (Water- shift reaction),  $\text{CH}_4$  (methane reforming), and methanation (reaction of char with hydrogen) can also occur (Patra & Sheth, 2015). While combustion reaction is exothermic in nature, reduction and gasification reactions are endothermic. Some tar cracking reactions and the formation of ammonia and  $\text{H}_2\text{S}$  can also occur during gasification. The heat required for endothermic reactions is supplied by exothermic combustion reaction, and hence the process can be run in a self-sustained way. Different reactions which may occur during gasification are provided in Table 1.2.

**Table 1.2:** Array of reactions in gasifiers (La Villetta et al., 2017; Marcantonio et al., 2020; Safarian et al., 2019; Silva et al., 2019)

Reaction	Reaction Name	Heat of reaction ( $\Delta H$ ) (kJ/mol)	Reaction Number
$Biomass_{wet} \rightarrow Biomass_{dry} + H_2O_{(g)}$	-	-	(R1)
$Biomass_{dry} \rightarrow Gas + Tar + Char$	-	-	(R2)
$C + O_2 \rightarrow CO_2$	Complete combustion	-394	(R3)
$C + 0.5 O_2 \rightarrow CO$	Char partial combustion	-111	(R4)
$C + CO_2 \leftrightarrow 2CO$	Boudouard reaction	+172	(R5)
$C + H_2O \leftrightarrow CO + H_2$	Water-gas	+131	(R6)
$C + 2H_2 \leftrightarrow CH_4$	Methane formation	-74.8	(R7)
$CO + 0.5 O_2 \rightarrow CO_2$	CO partial combustion	-284	(R8)
$H_2 + 0.5 O_2 \rightarrow H_2O$	Hydrogen combustion	-242	(R9)
$CO + H_2O \leftrightarrow CO_2 + H_2$	Water-gas shift (WGS)	-41.2	(R10)
$CH_4 + H_2O \leftrightarrow CO + 3H_2$	Methane reforming	+206	(R11)
$CH_4 + 1.5 O_2 \rightarrow CO + 2H_2O$	Methane partial combustion	-520	(R12)
$H_2 + S \rightarrow H_2S$	H <sub>2</sub> S formation	-	(R13)
$3H_2 + N_2 \rightarrow 2NH_3$	NH <sub>3</sub> formation	-	(R14)
$pC_nH_x \rightarrow qC_mH_y + rH_2$	Tar cracking	-	(R15)
$C_nH_x + nH_2O \rightarrow \left(n + \frac{x}{2}\right)H_2 + nCO$	Steam reforming of tar	-	(R16)
$C_nH_x + nCO_2 \rightarrow \left(\frac{x}{2}\right)H_2 + 2nCO$	Dry reforming of tar	-	(R17)
$C_nH_x \rightarrow nC + \left(\frac{x}{2}\right)H_2$	Carbon formation	-	(R18)

### 1.3 Co-gasification of biomass

Co-gasification process is defined as the gasification process where two feedstocks are simultaneously fed in the gasifier to generate syngas. There can be multiple variation of feedstock possible in co-gasification. Coal, biomass, plastic, municipal solid waste, sludge etc.

can be treated to produce syngas by co-gasification. Co-gasification technology is gaining interest among researchers in recent years because of its flexibility and versatility in feedstock selection and operation. There are four stages of co-gasification namely drying, pyrolysis, combustion and gasification. The reactions involved in co-gasification are same as listed in Table 1.2. The most common type of co-gasification is where biomass is blended with coal to improve its emission characteristics as well as syngas quality. Various researchers have observed synergistic effect of biomass in coal gasification. However, using coal in co-gasification comes with the adverse effect of enhanced environmental pollution and fossil fuel depletion. Therefore, it is essential to delve into the avenues of biomass co-gasification.

#### 1.4 Syngas fermentation

The syngas fermentation is the process of converting the mixture of  $CO$ ,  $CO_2$ , and  $H_2$  to alcohols and organic acids in the presence of acetogenic bacteria. This is a process where gas is converted to liquid at normal temperature without any mechanical interventions. The acetogenic bacteria plays a vital role here in terms of the gas-liquid mass transfer. In 1932,  $H_2$  and  $CO_2$  converting organisms were discovered but they could only convert  $H_2$  and  $CO_2$  to acetic acid (Ragsdale & Pierce, 2008). *Moorella thermoacetica* (formerly called *C. thermoacetica*) has been the oldest acetogen to be studied in lab scale for syngas fermentation in 1942 (Ragsdale, 2008). Other important acetogens used in this regard are *C. Ljungdahlii*, *C. aceticum*, *C. carboxidivorans*, *Acetobacterium woodii*, *C. ragsdalei*, and *C. autoethanogenum*. Till now, there are more than 100 species of acetogens that have been developed by different researchers for the purpose of syngas fermentation. These microorganisms have been collected from different sources like land, sludge, sediments, intestinal tracts of animals etc. These microorganisms are mesophilic in nature and experiments suggest that 30°C- 40°C is the favourable temperature range for these microorganisms to facilitate gas-liquid mass transfer.

Harland Goff Wood and Lars Gerhard Ljungdahl first used *Moorella thermoacetica* to determine the acetyl-Coenzyme A (Acetyl- CoA) pathway enzymology in their laboratories. The bioconversion of the syngas following the acetyl-CoA pathway is therefore also known as the Wood- Ljungdahl pathway. This pathway is found to be a linear pathway that occurs in both oxidative and reductive direction. The reductive direction is the conversion of  $CO_2$  to acetate and the oxidative direction is the conversion of acetate to  $CO_2$ . Two branches namely methyl and carbonyl branches are involved in the production of acetyl- CoA from  $CO$  and  $CO_2$  respectively, which is further converted to alcohol and acetate having acetaldehyde and acetyl

phosphate as their respective precursors. There are various literatures that describe the bio-chemistry involved in this process in detail (Bengelsdorf et al., 2013; Henstra et al., 2007). Acetyl-CoA is considered to be a metabolic intermediate in acetogens and is utilized to produce ethanol, butanol, hexanol, acetate, butyrate, hexanoate, and cell mass. The conversion process from Acetyl- CoA to ethanol is known as solventogenesis and the conversion of Acetyl- CoA to acetate is known as acetogenesis. The chemical equations for the production of bio-ethanol are as follows.



However, these reactions do not take place naturally as phase change and gas- liquid mass transfer is involved in this process. In the acetyl- CoA pathway, the acetogens are responsible for metabolising the  $H_2$ ,  $CO$  and  $CO_2$  and produce ethanol and acetate. The required electrons for the reduction process is generated by oxidising the  $H_2$  by hydrogenase and also by the oxidation of  $CO$  by carbon monoxide dehydrogenase (CODH). This donated reducing power is in the form of electrons, is carried by electron carrier pairs NADH/NAD<sup>+</sup>, NADPH/NADP<sup>+</sup> or ferredoxin. Adenosine triphosphate (ATP) is responsible for the transport of chemical energy required for metabolism in the cells. The ATP is converted to adenosine diphosphate (ADP) by the energy released in hydrolysis of phosphate bonds. Generation of ATP for cell growth necessitates production of acetate from Acetyl- CoA. The reduced products like acetaldehyde, ethanol etc. are produced by the reduction of acetate. The pathway of fermentative production of ethanol from syngas is represented in Figure 1.2 (Gunes, 2021; Shen et al., 2018; Zhang, et al., 2013).

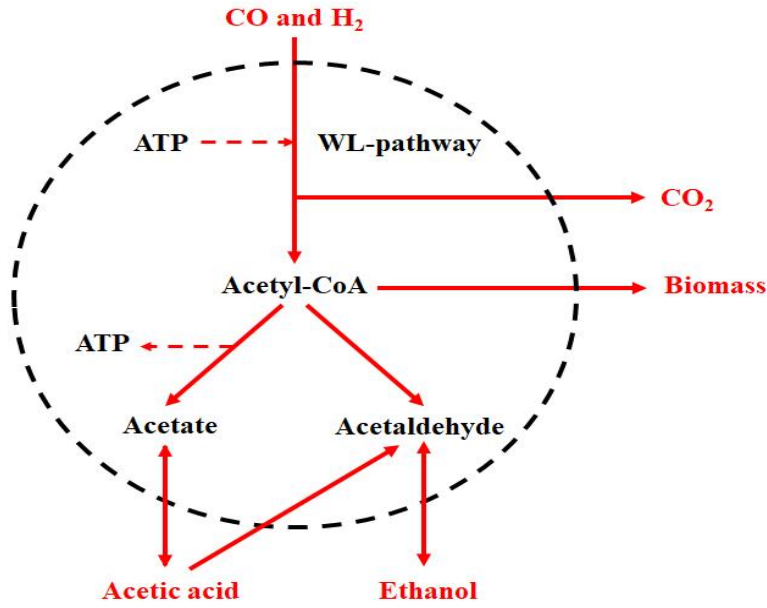


**Figure 1.2:** Simplified pathway for syngas fermentation

During formation of acetyl-CoA, some amount of  $CO_2$  is produced. Acetyl-CoA is then either integrated in cellular biomass or converted to metabolic products (acetate and acetaldehyde). Ethanol and acetic acid are produced from acetate and acetaldehyde respectively. All possible reactions for syngas fermentation have been reported in the Table 1.3.

**Table 1.3:** All reactions involved in syngas fermentation (Gunes, 2021; Phillips et al., 2017; Shen et al., 2018; Wang et al., 2018; Wang et al., 2017; Zhang et al., 2013)

Product	Biochemical reactions	Reaction number	$\Delta G^\circ$ (kJ/mol)
<b>Ethanol</b>	$6H_2 + 2CO_2 \rightarrow C_2H_5OH + 3H_2O$	(R21)	-96.0
	$6CO + 3H_2O \rightarrow C_2H_5OH + 4CO_2$	(R19)	-220.6
	$5CO + H_2 + 2H_2O \rightarrow C_2H_5OH + 3CO_2$	(R23)	-197.3
	$4CO + 2H_2 + H_2O \rightarrow C_2H_5OH + 2CO_2$	(R24)	-177.3
	$3CO + 3H_2 \rightarrow C_2H_5OH + CO_2$	(R25)	-157.2
	$2CO + 4H_2 \rightarrow C_2H_5OH + H_2O$	(R26)	-137.1
<b>Acetate</b>	$4H_2 + 2CO_2 \rightarrow C_2H_3O_2^- + H^+ + 2H_2O$	(R27)	-74.4
	$4H_2 + 2HCO_3^- + H^+ \rightarrow C_2H_3O_2^- + 4H_2O$	(R28)	-87.8
	$4CO + 2H_2O \rightarrow C_2H_3O_2^- + H^+ + 3CO_2$	(R29)	-172.2
<b>Acetic acid</b>	$C_2H_3O_2^- + C_2H_5OH \rightarrow C_4H_7O_2^- + H_2O$	(R30)	-38.5
	$C_2H_3O_2^- + 6H_2 + 2CO_2 \rightarrow C_4H_7O_2^- + H_2O$	(R31)	-143.0

## 1.5 Process modelling

The complexity of any chemical or biological process is determined by the number of correlating factors the said process is dependent on. In gasification the quality and quantity of the syngas are extremely dependent on various operating parameters like the mass flow rate of feedstock, type of gasifying agents, gasification temperature, pressure inside the gasifier and equivalence ratio for instance. The thermo-chemical property and elemental composition of the primary feedstock also affect the production of syngas up to a certain extent (Baruah & Baruah, 2014). In case of syngas fermentation the output of ethanol is dependent on the type of reactor, size of reactor, gas flow rate inside the reactor, the temperature, pressure and pH of the nutrient media, specific gas uptake rate of the micro-organism present in the reactor to name a few. Therefore, it is economically infeasible as well as sufficiently time-consuming to experimentally determine the optimum condition of the gasification process for any particular feedstock. It is worth mentioning that the operating parameter variation leaves a combined effect on the gasification system. Mathematical modelling of gasification and fermentation reactors is necessary for (i) *a priori* prediction of performance with the variation of input parameters such as feedstock properties, temperature, solid to gasifying agent ratio, and pressure for example; (ii) scaling up from lab-scale to pilot and industrial scales; (iii) optimization of reactor design and performance (de Souza-Santos, 2010). Mathematical modelling has enabled the researchers to virtually model the gasification and syngas fermentation process and optimize the process parameters providing a lot of convenience in experimental studies. The main aim of a mathematical model is to virtually replicate the physical and chemical processes taking place inside a reactor up to as much extent as possible. As the amount of complicity of the model is increased, it will provide more realistic results. These complexities are typically based on the chemical reactions of gasification and syngas fermentation and the dynamic behaviour of gas and solid particles as well as the gas and liquid particles inside the reactors (Silva et al., 2019). The extent of the implication of such complexity in any mathematical model determines its exactness in turn. However, it is a common practice among researchers to simplify the model up to a certain extent within a certain range of permissible tolerance. These simplifications are based on some assumptions regarding the physical and chemical changes of matter inside the reactors and regarding the elemental composition of the products (Basu, 2010).

Based on the principles of development, the gasification and co-gasification models can be

broadly categorized as A) thermodynamic equilibrium models and B) kinetic models (Baruah & Baruah, 2014). The syngas fermentation models can also be of two types namely A) Equilibrium models and B) Kinetic models. The process modelling can be done by directly implementing the mathematical equations of mass- energy balance and reaction rates in any programming languages like FORTRAN, MATLAB, C, C++, PYTHON etc. or it can be done using different available software of chemical process simulation like Aspen plus, Aspen HYSYS, CHEMCAD, SuperPro Designer etc..

## 1.6 Mathematical modelling of gasification

It has been already discussed that based on the mass and energy balance and chemical behaviour inside the gasifier two types of modelling is possible.

- A) Thermochemical equilibrium modelling
- B) Kinetic modelling

### 1.6.1 Thermochemical equilibrium modelling

As the name suggests, thermochemical equilibrium (TCE) models are based on the principle of attainment of equilibrium. The predictions of the models are independent of the reactor design and fluid dynamics. However, TCE models can predict the maximum possible yield of a gasifier achievable using a particular set of operating parameters. The TCE models can be categorized as I) **Stoichiometric** (based on equilibrium constants of a set of pre-selected array of reaction) and II) **Non-stoichiometric** ones (based on minimization of Gibbs free energy). All TCE models are based on the following assumptions (La Villetta et al., 2017).

1. Gasifier is operated isothermally under atmospheric pressure.
2. Residence time of the reactants in the gasifier is infinite and hence steady state is attained.
3. The exact mechanism of pyrolysis reaction and the accounting of intermediates are not considered.
4. The reactor is well mixed and transient behaviour and spatial gradient of temperature and pressure are negligible.
5. No unreacted oxygen escapes the gasifier.
6. Nitrogen behaves almost as an inert gas during the gasification.
7. There is no change in kinetic and potential energy within the reactor.



8. Oxidizing agent is sufficient to convert all carbon entering through biomass or coal fed to the gasifier.
9. Gas phase behaves ideally.
10. Energy content of ash, i.e., the mixture of unconverted carbon and mineral matter, escaping through the effluent solid stream, is negligible.
11. The condensable volatiles, i.e., tar formed during pyrolysis are in vapour state and behave as an ideal gas as the temperature inside the gasifier is very high.
12. Heat loss to the environment is negligible.

In the case of non-stoichiometric equilibrium model, the volatile pyro-products are only to be specified according to the quantity of different elements present. Under stoichiometric equilibrium model distribution of moles of different components is necessary. Typically, the components like  $CO$ ,  $CO_2$ ,  $CH_4$ ,  $H_2$ ,  $H_2O$ , and  $N_2$  are considered. The equivalent quantities of  $C$ ,  $H_2$ ,  $N_2$ ,  $O_2$ ,  $Cl_2$ , and  $S$  fed to the gasifier appear in the product syngas. In both stoichiometric and non- stoichiometric equilibrium models, char is considered as inert carbon during pyrolysis. Although the approaches are different, it has already been established that both types of equilibrium modelling yield the same results. The principles of the two types of modelling are described in the following sections.

#### **1.6.1.1 Stoichiometric equilibrium model**

The product syngas stream is composed of  $CO$ ,  $CO_2$ ,  $CH_4$ ,  $H_2$ ,  $H_2O$ , and  $N_2$ . This method of modelling is based on the equilibrium constants of a selected array of reactions taking place in the gasification process. Table 1.4 lists out the standard properties of all the gaseous elements participating in the gasification process.

**Table 1.4:** Chemical characteristic of gases in the ideal-gas state at reference state T = 298.15 K, P = 0.1 MPa (Perry & Green, 2007)

Chemical species	Standard enthalpy of formation (kJ/mol)	Standard Gibbs free energy of formation (kJ/mol)	Standard absolute entropy (J/kmol K)	constant coefficients for constant pressure heat capacity (Temperature range 273K-1800K)			
				a	b	c	d
<b>Carbon monoxide (CO)</b>	-110.257	-137.163	197.653	28.16	0.167 $\times 10^{-2}$	0.537 $\times 10^{-5}$	-2.222 $\times 10^{-9}$
<b>Hydrogen (H<sub>2</sub>)</b>	0	0	130.680	29.11	- 0.1916 $\times 10^{-2}$	0.4003 $\times 10^{-5}$	- 0.8704 $\times 10^{-9}$
<b>Carbon dioxide (CO<sub>2</sub>)</b>	-393.522	-394.389	213.795	22.26	5.981 $\times 10^{-2}$	-3.501 $\times 10^{-5}$	-7.469 $\times 10^{-9}$
<b>Methane (CH<sub>4</sub>)</b>	-74.873	-50.768	186.251	19.89	5.204 $\times 10^{-2}$	1.269 $\times 10^{-5}$	-11.01 $\times 10^{-9}$
<b>Water (H<sub>2</sub>O<sub>(g)</sub>)</b>	-241.826	-228.582	188.834	32.24	0.1923 $\times 10^{-2}$	1.055 $\times 10^{-5}$	-3.595 $\times 10^{-9}$
<b>Nitrogen (N<sub>2</sub>)</b>	0	0	191.609	28.90	- 0.1571 $\times 10^{-2}$	0.8081 $\times 10^{-5}$	-2.873 $\times 10^{-9}$

Chemical equilibrium in a single-phase system is considered. One of the main criteria of chemical equilibrium is that the entropy, S and Gibbs energy, G are maximum and minimum respectively (Stanley Sandler, 2006a). This leads to

$$\sum_{i=1}^c \nu_i \bar{G}_i = 0 \quad (1.1)$$

where,  $\bar{G}_i$ ,  $\nu_i$  and c are partial molar Gibbs energy and stoichiometric coefficient of i<sup>th</sup> component and total number of components respectively.

The above equation along with the atom balance equations and the constraint equations of state variables can be used to identify the equilibrium state. The total Gibbs energy for a gaseous system can be represented as follows:

$$G = \sum_{i=1}^c N_i \bar{G}_i(T, P, y) = \sum_{i=1}^c N_i \bar{G}_i(T, P) + \sum_{i=1}^c N_i (\bar{G}_i(T, P, y) - \bar{G}_i(T, P)) \quad (1.2)$$

$\bar{G}_i(T, P)$  and  $\bar{G}_i(T, P, y)$  are the pure and partial molar Gibbs energy of  $i^{\text{th}}$  component at the condition of reaction. Equation (1.2) can also be written as

$$G = \sum_{i=1}^c N_i \bar{G}_i(T, P) + \sum_{i=1}^c N_i RT \ln \frac{\bar{f}_i(T, P, y)}{\bar{f}_i(T, P)} \quad (1.3)$$

$$= \sum_{i=1}^c N_i \bar{G}_i(T, P) + \sum_{i=1}^c N_i RT \ln \frac{(y_i P) \frac{\bar{f}_i(T, P, y)}{(y_i P)}}{(P) \frac{\bar{f}_i(T, P)}{(P)}} \quad (1.4)$$

$\frac{\bar{f}_i(T, P)}{(P)}$  and  $\frac{\bar{f}_i(T, P, y)}{(y_i P)}$  are the fugacity coefficients of pure component  $i$  and when in the reaction mixture, respectively. Considering the ideal gas behavior, all fugacity coefficients can be set at unity. Therefore,

$$G = \sum_{i=1}^c N_i \bar{G}_i(T, P) + RT \sum_{i=1}^c N_i \ln(y_i) \quad (1.5)$$

The first term on the RHS represents the summation of Gibbs energy of all pure components and the second term represents the Gibbs free energy change. As the reactions proceed, the number of moles and hence the mole fraction of any component change. They are guided by the extent of reactions,  $\xi$  and the stoichiometric coefficients,  $\nu$  of the components in different reactions.

For any component,  $i$ , participating in a single reaction,

$$N_i = N_{i0} + \nu_i \xi$$

or  $\xi = \frac{N_i - N_{i0}}{\nu_i} \quad (1.6)$

For multiple reactions, for  $i^{\text{th}}$  component participating in several reactions,

$$N_i = N_{i0} + \sum_j \nu_{ij} \xi_j \quad (1.7)$$

where  $j$  represents any reaction

The value of  $\nu_i$  is positive for reaction products and negative for reactants. Mathematically, the equilibrium state can be identified by the criterion that  $G$  will be minimum, i.e.,

$$G = \text{minimum, } dG = 0 \quad (1.8)$$

$$\text{or, } \left( \frac{\partial G}{\partial \xi} \right)_{T, P} = 0 \quad (1.9)$$

This equation is solved to determine the value of  $\xi$  at equilibrium, i.e.,  $\xi^*$ . From that the equilibrium mole fraction of each species is determined.

In general, the following equation is valid under equilibrium:

$$-\frac{\sum_{i=1}^c \vartheta_i \bar{G}_i}{RT} = \sum_{i=1}^c \ln y_i^{\vartheta_i} = \ln \prod_{i=1}^c y_i^{\vartheta_i} \quad (1.10)$$

Again, under equilibrium,

$$\sum_{i=1}^c \bar{G}_i(T, P, \vartheta_i) = 0 \quad (1.11)$$

$$G = \sum_{i=1}^c N_i \bar{G}_i(T, P) + \sum_{i=1}^c N_i RT \ln \frac{\bar{f}_i(T, P, y)}{\bar{f}_i(T, P)} \quad (1.12)$$

$$\text{Or, } G = \sum_{i=1}^c N_i \bar{G}_i(T, P) + \sum_{i=1}^c N_i RT \ln \frac{(y_i P)^{\frac{\bar{f}_i(T, P, y)}{(y_i P)}}}{(P)^{\frac{\bar{f}_i(T, P)}{(P)}}} \quad (1.13)$$

$$\text{For general single phase reaction, } \bar{G}_i(T, P, \xi_i) = \bar{G}_i^o + [\bar{G}_i(T, P, \xi_i) - \bar{G}_i^o] \quad (1.14)$$

$\bar{G}_i^o$  is the standard Gibbs energy of species, i. (T=298K; P=1bar and initial  $\xi_i$ ,  $\xi_i^o$ ).

$$\text{Again, } \bar{G}_i(T, P, \xi_i) = \bar{G}_i^o(T = 298K, P = 1bar, \xi_i^o) + RT \ln \frac{\bar{f}_i(T, P, \xi_i)}{\bar{f}_i^o(T, P, \xi_i^o)} \quad (1.15)$$

$$\frac{\bar{f}_i(T, P, \xi_i)}{\bar{f}_i^o(T, P, \xi_i^o)} = a_i = \text{activity of } i^{\text{th}} \text{ species} \quad (1.16)$$

Therefore,

$$a_i = \exp \left( \frac{\bar{G}_i(T, P, \xi_i) - \bar{G}_i^o(T=298K, P=1bar, \xi_i^o)}{RT} \right) \quad (1.17)$$

$$\text{under equilibrium, } -\frac{\Delta_{rxn} G^o}{RT} = \ln \prod_{i=1}^c a_i^{\vartheta_i} \quad (1.18)$$

Equilibrium constant is defined as follows:

$$K_a(T) = \prod_{i=1}^c a_i^{\vartheta_i} = \exp \left( -\frac{\Delta_{rxn} G^o}{RT} \right) \quad (1.19)$$

This equation can be used to predict the values of variables under equilibrium state.

$$\Delta_{rxn} G^o = \sum_{i=1}^c \vartheta_i \Delta G_{fi}^o \quad (1.20)$$

$\Delta G_{fi}^o$  = standard heat of formation of  $i^{\text{th}}$  component

$$\frac{\partial}{\partial T} \left( \frac{\bar{G}_i}{T} \right)_P = \frac{1}{T} \left( \frac{\partial \bar{G}_i}{\partial T} \right)_P - \frac{\bar{G}_i}{T^2} = -\frac{\bar{S}_i}{T} - \frac{\bar{H}_i}{T^2} + \frac{\bar{S}_i}{T} = -\frac{\bar{H}_i}{T^2} \quad (1.21)$$

$$\ln K_a = -\frac{\sum_{i=1}^c \vartheta_i \Delta G_{fi}^o}{RT} \quad (1.22)$$

Therefore,

$$\left( \frac{d \ln K_a}{dT} \right)_P = -\frac{1}{R} \frac{d}{dT} \left( \frac{\sum_{i=1}^c \vartheta_i \Delta G_{fi}^o}{T} \right) = \frac{1}{RT^2} \sum_{i=1}^c \vartheta_i \Delta_f H_i^o = \frac{\Delta_{rxn} H^o}{RT^2} \quad (\text{van'tHoff equation}) \quad (1.23)$$

$$(1.24) \quad \Delta_{rxn} H^o = \sum_{i=1}^c \vartheta_i \Delta_f H_i^o$$

Functionality of constant-pressure heat capacity on temperature is as follows:

$$c_{pi} = a_i + b_i T + c_i T^2 + d_i T^3 \quad (1.25)$$

The value of the constants are listed in Table 1.4.

Now, the relationship between the heat of reaction at any temperature T and that at the reference

temperature,  $T_R$  is as follows:

$$\Delta_{rxn}H^o(T) = \Delta_{rxn}H^o(T_R) + \Delta a(T - T_R) + \frac{\Delta b}{2}(T^2 - T_R^2) + \frac{\Delta c}{2}(T^3 - T_R^3) + \frac{\Delta d}{2}(T^4 - T_R^4) - \Delta e\left(\frac{1}{T} - \frac{1}{T_R}\right) \quad (1.26)$$

$$\ln \frac{K_a(T)}{K_a(T_R)} = -\frac{\Delta_{rxn}H^o(T_R)}{R}\left(\frac{1}{T} - \frac{1}{T_R}\right) + \frac{\Delta_{rxn}c_p}{R} \ln \frac{T}{T_R} + \frac{\Delta_{rxn}c_p}{R}\left(\frac{T_R}{T} - 1\right) \quad (1.27)$$

$$K_a(T) = \prod_{i=1}^C a_i^{\vartheta_i} \quad (1.28)$$

$$a_i = \frac{y_i P}{1 \text{ bar}} \quad (1.29)$$

$$\text{Therefore, } K_a(T) = \prod_{i=1}^C \left(\frac{y_i P_{rxn}}{1 \text{ bar}}\right)^{\vartheta_i} \quad (1.30)$$

For any reaction,  $\alpha A + \beta B \rightarrow \gamma C + \delta D$

$$K_a(T) = \frac{y_C^\gamma y_D^\delta}{y_A^\alpha y_B^\beta} (P^{\gamma+\delta-\alpha-\beta}) \quad (1.31)$$

### Combined phase and chemical equilibrium

Total number of moles of species I in all P phases is given by,

$$\sum_{k=1}^P N_i^k = N_{i0} + \sum_{j=1}^M \vartheta_{ij} \xi_j \quad (1.32)$$

Total Gibbs free energy is given by,

$$G = \sum_{k=1}^P \sum_{i=1}^C N_i^k \bar{G}_i^k \quad (1.33)$$

The condition of phase equilibrium should be satisfied for all species in each phase and chemical reactions are in equilibrium. Therefore, the following equation is valid:

$$\frac{\partial G}{\partial \xi_j} = 0 = \sum_{k=1}^P \sum_{i=1}^C N_i^k \left(\frac{\partial \bar{G}_i^k}{\partial \xi_j}\right) - \sum_{i=1}^C a_i \vartheta_{ij} = 0 \quad (1.34)$$

$$\text{Again, } \sum_{i=1}^C \vartheta_{ij} \bar{G}_i^k = 0 \quad (1.35)$$

This signifies that all reactions are at equilibrium in each phase.

Phase rule is applied in PVT system to obtain the number of independent variables to be specified, i.e., the number of degrees of freedom,  $F$  of a system under equilibrium (Perry & Green, 2007). The phase rule is stated as follows:

$$F = 2 - \pi + N - r \quad (1.36)$$

where,

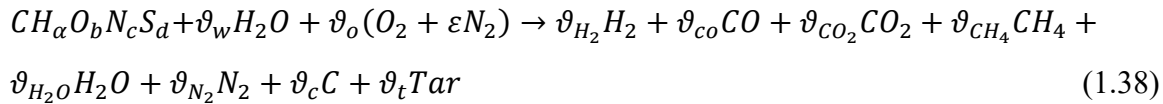
$F$  = degrees of freedom;  $\pi$  = number of phases;  $r$  = number of independent reactions

This rule is applied to determine the unknown composition.

For the application of the above principles in case of synthesis gas production, the following steps are followed:

## Step-I

Generalized stoichiometric equation representing the syngas production is usually written as the first step of the stoichiometric modelling:



where, the molecular formula of the biomass is based on  $C$ -mole and hence

$$\alpha = \frac{w_H(MW)_C}{w_C(MW)_H}; b = \frac{w_O(MW)_C}{w_C(MW)_O}; c = \frac{w_N(MW)_C}{w_C(MW)_N}; d = \frac{w_S(MW)_C}{w_C(MW)_S} \quad (1.39)$$

$w_C, w_H, w_O, w_N$  and  $w_S$  are the weight fraction of  $C, H, O, N$  and  $S$  respectively determined through the elemental analysis of the biomass.

Similarly,  $(MW)_C, (MW)_H, (MW)_O, (MW)_N$  and  $(MW)_S$  are the molar mass of  $C, H, O, N$  and  $S$ . The molar ratio of nitrogen to oxygen in air is  $\varepsilon \left( = \frac{y_{N_2}}{y_{O_2}} = \frac{0.79}{0.21} = 3.76 \right)$ .

The phase rule (Eq. 1.36) is applied to determine the unknown composition. Under this situation,

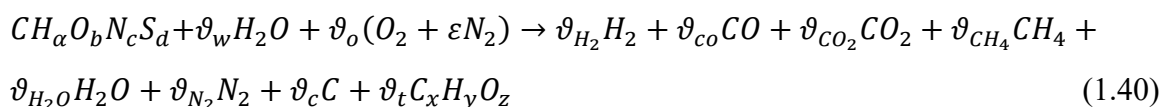
$$F = 2 - \pi + N - r = 2 - 3 + 11 - 1 = 9$$

Therefore, specification of temperature and pressure three atom balance equations [Step II], three equilibrium constants [Step III], and one energy balance equation [Step IV] leads to the evaluation of equilibrium composition of syngas.

## Step-II

Based on the stoichiometric equation, I, the atom balance equations are written to determine the number of moles of product components, i.e.,  $H_2, CO, CO_2, CH_4, H_2O, N_2, C$ , and Tar. Tar is a complex combination of different hydrocarbons and is generally represented by  $C_xH_yO_z$ . For simplification, in some literature, tar is considered to be  $C_6H_6$  (Gagliano et al., 2017a) and thus,  $x=6, y=6$  and  $z=0$ . In another reported article  $CH_{1.003}O_{0.33}$  has been used to represent tar (i.e.,  $x=1, y=1.003, z=0.33$ ) (Tinaut et al., 2008). Tar formation is a function of temperature and other input parameters.

In terms of the generalized representation of chemical formula,  $C_xH_yO_z$  of tar equation I can be represented as follows:



Atom balance equations for  $C, H$  and  $O$  are as follows:

$$\mathbf{C}: \mathbf{1} = \vartheta_{co} + \vartheta_{CO_2} + \vartheta_{CH_4} + \vartheta_c + x\vartheta_t$$

$$\text{Or, } \vartheta_{co} + \vartheta_{CO_2} + \vartheta_{CH_4} + \vartheta_c + x\vartheta_t - 1 = 0 \quad (1.41)$$

$$\mathbf{H}: \mathbf{a} + 2\vartheta_w = 2\vartheta_{H_2} + 4\vartheta_{CH_4} + 2\vartheta_{H_2O} + y\vartheta_t$$

$$\text{Or, } 2\vartheta_{H_2} + 4\vartheta_{CH_4} + 2\vartheta_{H_2O} + y\vartheta_t - a - 2\vartheta_w = 0 \quad (1.42)$$

$$\mathbf{O}: \mathbf{b} + \vartheta_w + 2\vartheta_o = \vartheta_{co} + 2\vartheta_{CO_2} + \vartheta_{H_2O} + z\vartheta_t$$

$$\vartheta_{co} + 2\vartheta_{CO_2} + \vartheta_{H_2O} + z\vartheta_t - b - \vartheta_w - 2\vartheta_o = 0 \quad (1.43)$$

### Step-III

Since the reactions involving oxygen are expected to be completed under gasification condition, most of the reported articles consider that the attainment of equilibrium of two or three reactions among R5, R6, R7, R10 and R11 influence the exit product composition (Silva et al., 2019):

$$\text{According to equation 1.19, } K(T) = \prod_{i=1}^c a_i^{\vartheta_i} = \exp\left(-\frac{\Delta_{rxn}G^o}{RT}\right)$$

$$\text{Since according to equation 4.29, } a_i = \frac{y_i P}{1 \text{ bar}},$$

$$K_a(T) = \prod_{i=1}^c \left(\frac{y_i P_{rxn}}{1 \text{ bar}}\right)^{\vartheta_i} = \exp\left(-\frac{\Delta_{rxn}G^o}{RT}\right) \quad (1.44)$$

Applying Equation 1.36,

$$K_{aI}(T) = \frac{(y_{CO})^2}{y_{CO_2}^1} \left(\frac{P_{rxn}}{P=1 \text{ bar}}\right)^{2-1} = \frac{(y_{CO})^2}{y_{CO_2}} \frac{P_{rxn}}{P=1 \text{ bar}} \quad (1.45)$$

Therefore,

$$\frac{(y_{CO})^2}{y_{CO_2}} \frac{P_{rxn}}{P=1 \text{ bar}} = \exp\left(-\frac{\Delta_{rxn,I}G^o}{RT}\right) \quad (1.46)$$

$$K_{aII}(T) = \frac{y_{CO}^1 y_{H_2}^1}{y_{H_2O}^1} \left(\frac{P_{rxn}}{P=1 \text{ bar}}\right)^{1+1-1} = \frac{y_{CO} y_{H_2}}{y_{H_2O}} \left(\frac{P_{rxn}}{P=1 \text{ bar}}\right) \quad (1.47)$$

Therefore,

$$\frac{y_{CO} y_{H_2}}{y_{H_2O}} \left(\frac{P_{rxn}}{P=1 \text{ bar}}\right) = \exp\left(-\frac{\Delta_{rxn,II}G^o}{RT}\right) \quad (1.48)$$

$$K_{aIII}(T) = \frac{y_{CH_4}^1}{y_{H_2}^2} \left(\frac{P_{rxn}}{P=1 \text{ bar}}\right)^{1-2} = \frac{y_{CH_4}^1}{y_{H_2}^2} \left(\frac{P_{rxn}}{P=1 \text{ bar}}\right)^{-1} \quad (1.49)$$

Therefore,

$$\frac{y_{CH_4}}{y_{H_2}^2} \left(\frac{P_{rxn}}{P=1 \text{ bar}}\right)^{-1} = \exp\left(-\frac{\Delta_{rxn,III}G^o}{RT}\right) \quad (1.50)$$

$$K_{aIV}(T) = \frac{y_{CO_2}^1 y_{H_2}^1}{y_{CO}^1 y_{H_2O}^1} \left(\frac{P_{rxn}}{P=1 \text{ bar}}\right)^{1+1-1-1} = \frac{y_{CO_2} y_{H_2}}{y_{CO} y_{H_2O}} \quad (1.51)$$

Therefore,

$$\frac{y_{CO_2} y_{H_2}}{y_{CO} y_{H_2O}} = \exp \left( -\frac{\Delta_{rxn,IV} G^0}{RT} \right) \quad (1.52)$$

$$K_{aV}(T) = \frac{y_{CO_2}^1 y_{H_2}^3}{y_{CH_4}^1 y_{H_2O}^1} \left( \frac{P_{rxn}}{P=1bar} \right)^{1+3-1-1} = \frac{y_{CO_2} y_{H_2}}{y_{CH_4} y_{H_2O}} \left( \frac{P_{rxn}}{P=1bar} \right)^2 \quad (1.53)$$

$$\frac{y_{CO_2} y_{H_2}}{y_{CH_4} y_{H_2O}} \left( \frac{P_{rxn}}{P=1bar} \right)^2 = \exp \left( -\frac{\Delta_{rxn,V} G^0}{RT} \right) \quad (1.54)$$

According to Eq. 1.20,  $\Delta_{rxn} G^0 = \sum_{i=1}^c \nu_i \Delta G_{fi}^0$

Where,  $\Delta G_{fi}^0$  = standard heat of formation of  $i^{th}$  component

Chemical equilibria of three reactions, namely, methane formation, water gas shift reaction, and char reforming reaction are the most common ones which are considered by the researchers in the stoichiometric equilibrium modelling of syngas production (Jarungthammachote & Dutta, 2007; Zainal et al., 2001). Some of the researchers have also considered as water gas shift reaction and methane reforming (Barman et al., 2012). Methane formation and methane reforming have also been considered by some other researchers (Mendiburu et al., 2014).

#### Step-IV

Generalized energy balance equation for a flow system is as follows:

$$\Delta \dot{H} + \Delta \dot{E}_k + \Delta \dot{E}_p = \dot{Q} - \dot{W}_s \quad (1.55)$$

where,

$\Delta \dot{H}$  = rate of change of enthalpy;  $\Delta \dot{E}_k$  = Rate of change of kinetic energy;

$\Delta \dot{E}_p$  = Rate of change of potential energy;

$\dot{Q}$  = Rate of heat transfer between the system and the surroundings;

$\dot{W}_s$  = shaft work

$$\text{For the reactor, } \Delta \dot{E}_k = \Delta \dot{E}_p = \dot{W}_s = 0. \quad (1.56)$$

Therefore,

$$\Delta \dot{H} = \dot{Q} \quad (1.57)$$

When nonstoichiometric amounts of reactants and products enter and leave respectively at different temperatures the following steps have to be followed:

- Declare a reference state (usually 25°C and 1 atm)
- Calculate enthalpies of each stream. For each stream, three components of enthalpy may be involved:
  - a) heat of formation; b) sensible heat relative to the reference state; c) latent heat if phase change is involved



Therefore, if no phase change is considered,

$$\sum_{i=reactant} \dot{n}_i \left( \hat{h}_{f,i}^o + \Delta \hat{h}_i(T_{i,in}) \right) + \dot{Q}_{in} = \sum_{p=product} \dot{n}_p \left( \hat{h}_{f,p}^o + \Delta \hat{h}_p(T_{j,rxn}) \right) + \dot{Q}_{out} \quad (1.58)$$

$\hat{h}_{f,i}^o$  and  $\hat{h}_{f,p}^o$  are the heats of formation per mole of reactant, i and product, p, respectively.  $\Delta \hat{h}_i$  and  $\Delta \hat{h}_p$  are the specific enthalpy change associated with sensible heat relative to reference state for reactant, i and product, p.

Under adiabatic condition, there is no heat exchange with surroundings and hence,

$$\dot{Q}_{in} = \dot{Q}_{out} = 0$$

Therefore,

$$\sum_{i=reactant} \dot{n}_i \left( \hat{h}_{f,i}^o + \Delta \hat{h}_i(T_{i,in}) \right) = \sum_{p=product} \dot{n}_p \left( \hat{h}_{f,p}^o + \Delta \hat{h}_p(T_{j,rxn}) \right) \quad (1.59)$$

If inert components are also fed to the reactor involved,

$$\sum_{in} \dot{n}_{in} \left( \hat{h}_{f,in}^o + \Delta \hat{h}_{in}(T_{i,in}) \right) = \sum_{out} \dot{n}_{out} \left( \hat{h}_{f,out}^o + \Delta \hat{h}_{out}(T_{j,rxn}) \right) \quad (1.60)$$

$\hat{h}_{f,in}^o$  and  $\hat{h}_{f,out}^o$  are the specific heats of formation of inlet and outlet components, respectively.  $\Delta \hat{h}_{in}$  and  $\Delta \hat{h}_{out}$  are the specific enthalpy change associated with sensible heat relative to reference temperature,  $T_R$  for inlet and outlet components, respectively. Standard heats of formation of most of the conventional compounds are available in the literature (Perry & Green, 2007).

For multiple reactions, the energy balance equation for an adiabatic reactor reduces to

$$\sum_{reactions} \sum \xi_j \Delta H_{rxn,j}^o + \sum_{out} \dot{n}_{out} \left( \Delta \hat{h}_{out}(T_{j,rxn}) \right) - \sum_{in} \dot{n}_{in} \left( \Delta \hat{h}_{in}(T_{i,in}) \right) = 0 \quad (1.61)$$

Sensible enthalpy  $\left( \sum_{out} \dot{n}_{out} \left( \Delta \hat{h}_{out}(T_{rxn}) \right) \right)$  and  $\sum_{in} \dot{n}_{in} \left( \Delta \hat{h}_{in}(T_{in}) \right)$  relative to reference temperature,  $T_R$  are as follows:

$$\sum_{out} \dot{n}_{out} \left( \Delta \hat{h}_{out}(T_{j,rxn}) \right) = \sum_{out} \dot{n}_{out} c_{p,out} \int_{T_R}^{T_{rxn}} c_{p,out} dT \quad (1.62)$$

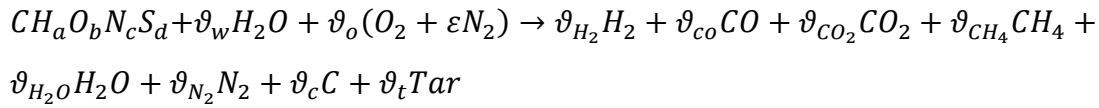
$$\sum_{in} \dot{n}_{in} \left( \Delta \hat{h}_{in}(T_{i,in}) \right) = \sum_{in} \dot{n}_{in} c_{p,in} \int_{T_R}^{T_{in}} c_{p,in} dT \quad (1.63)$$

The correlation of molar specific heat capacity at constant pressure with temperature (in K) is as follows:

$$c_{pi} = a_i + b_i T + c_i T^2 + d_i T^3 \quad (1.64)$$

Standard heats of formation for most of the conventional compounds are available in the literature (Perry & Green, 2007).

Following **Step I**, the generalized stoichiometric equation of overall gasification reaction is represented by equation 4.40 as follows:



Therefore, according to equation 1.55, the energy balance equation reduces to the following one:

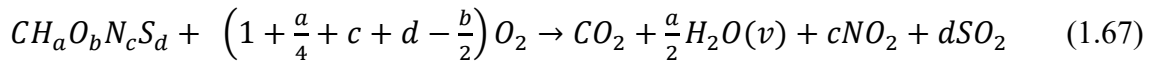
$$\begin{aligned} \hat{h}_{f,Biomass}^o + \Delta \hat{h}_{Biomass}(T_{i,in}) + \vartheta_w (\hat{h}_{f,w}^o + \Delta \hat{h}_w(T_{i,in})) + \vartheta_o (\hat{h}_{f,O_2}^o + \Delta \hat{h}_{O_2}(T_{i,in})) + \\ \vartheta_o \varepsilon (\hat{h}_{f,N_2}^o + \Delta \hat{h}_{N_2}(T_{i,in})) = \vartheta_{H_2} (\hat{h}_{f,H_2}^o + \Delta \hat{h}_{H_2}(T_{i,in})) + \vartheta_{co} (\hat{h}_{f,co}^o + \Delta \hat{h}_{co}(T_{i,in})) + \\ \vartheta_{CO_2} (\hat{h}_{f,CO_2}^o + \Delta \hat{h}_{CO_2}(T_{i,in})) + \vartheta_{CH_4} (\hat{h}_{f,CH_4}^o + \Delta \hat{h}_{CH_4}(T_{i,in})) + \vartheta_{H_2O} (\hat{h}_{f,H_2O}^o + \\ \Delta \hat{h}_{H_2O}(T_{i,in})) + \vartheta_{N_2} (\hat{h}_{f,N_2}^o + \Delta \hat{h}_{N_2}(T_{i,in})) + \vartheta_c (\hat{h}_{f,c}^o + \Delta \hat{h}_c(T_{i,in})) + \vartheta_t (\hat{h}_{f,t}^o + \Delta \hat{h}_t(T_{i,in})) \end{aligned} \quad (1.65)$$

Since the standard heat of formation of  $O_2$ ,  $N_2$ , and  $H_2$  are zero.

$$\begin{aligned} \hat{h}_{f,Biomass}^o + \Delta \hat{h}_{Biomass}(T_{i,in}) + \vartheta_w (\hat{h}_{f,w}^o + \Delta \hat{h}_w(T_{i,in})) + = + \vartheta_{co} (\hat{h}_{f,co}^o + \Delta \hat{h}_{co}(T_{i,in})) + \\ \vartheta_{CO_2} (\hat{h}_{f,CO_2}^o + \Delta \hat{h}_{CO_2}(T_{i,in})) + \vartheta_{CH_4} (\hat{h}_{f,CH_4}^o + \Delta \hat{h}_{CH_4}(T_{i,in})) + \vartheta_{H_2O} (\hat{h}_{f,H_2O}^o + \\ \Delta \hat{h}_{H_2O}(T_{i,in})) + \vartheta_c (\hat{h}_{f,c}^o + \Delta \hat{h}_c(T_{i,in})) + \vartheta_t (\hat{h}_{f,t}^o + \Delta \hat{h}_t(T_{i,in})) \end{aligned} \quad (1.66)$$

Heat of formation of biomass is calculated from the lower heating value (LHV) of biomass.

The combustion reaction of biomass can be represented as follows:



$$LHV = -\Delta H_{c,Biomass}^o = \hat{h}_{f,Biomass}^o - \hat{h}_{f,CO_2}^o - \frac{a}{2} \hat{h}_{f,H_2O}^o(v) - c \hat{h}_{f,NO_2}^o - d \hat{h}_{f,SO_2}^o \quad (1.68)$$

$$\text{Or, } \hat{h}_{f,Biomass}^o = LHV + \hat{h}_{f,CO_2}^o + \frac{a}{2} \hat{h}_{f,H_2O}^o(v) + c \hat{h}_{f,NO_2}^o + d \hat{h}_{f,SO_2}^o \quad (1.69)$$

The value of  $\hat{h}_{f,Biomass}^o$  obtained using Equation 1.63 is substituted in Equation 1.56.

### Solution of stoichiometric equilibrium model

In the simplest models without considering the yield of char and tar, three mass balance equations (Equation 1.33-1.35) two equilibrium reaction equations selected from Equations 1.39, 1.42, 1.44, 1.46 and 1.48 and one energy balance equation (Equation 1.60) are solved. When tar and char yields are considered, more equilibrium reactions are chosen from reactions III to VII. All equations are solved using Newton-Raphson method. Two strategies are followed. In Strategy-I, the equivalence ratio (ER) is the input. All equations are solved simultaneously using Newton Raphson method and the temperature is determined. In Strategy-II, temperature is the input and all the mass balance equations and the equilibrium equations

are solved. In the next step, the energy balance equation is solved to determine the temperature. The input value of temperature and the determined value are compared until their convergence.

### 1.6.1.2 Non-stoichiometric equilibrium model

Gibbs free energy minimization approach is a suitable option for modelling when the product of gasification is known but their chemical reactions are unknown.

For closed system, the energy balance equation is as follows (Stanley Sandler, 2006b):

$$\frac{dU}{dt} = \dot{Q} + \dot{W}_s - P \frac{dV}{dt} \quad (1.70)$$

$$\text{and } \frac{dS}{dt} = \frac{\dot{Q}}{T} + \dot{S}_{gen}$$

For multi-component non-reactive system,

$$U = \sum_{i=1}^c N_i \bar{U}_i(T, P, y) \quad (1.71)$$

$$S = \sum_{i=1}^c N_i \bar{s}_i(T, P, y) \quad (1.72)$$

Equilibrium criteria are again the maximum and minimum values of entropy and Gibbs energy respectively.

Gibbs energy for reactive system can be written as follows:

$$G = \sum_{i=1}^c N_i \bar{G}_i = \sum_{i=1}^c (N_{i0} + \vartheta_i \xi) \bar{G}_i \quad (1.73)$$

At constant temperature and pressure, the extent of reaction,  $\xi$  is the only variable.

$$\text{Hence, the equilibrium criterion is } \left( \frac{\partial G}{\partial \xi} \right)_{T,P} = 0 \quad (1.74)$$

$$\text{This leads to } \sum_{i=1}^c \vartheta_i \bar{G}_i = 0 \quad (1.75)$$

This correlation is also valid when the temperature and pressure are not constant.

For a system undergoing M number of multiple reactions, number of moles of  $i^{\text{th}}$  component can be written as  $N_i = \sum_{j=1}^M (N_{i0} + \vartheta_{ij} \xi_j)$  (1.76)

Total Gibbs energy can be written as follows:

$$G = \sum_{i=1}^c N_i \bar{G}_i = \sum_{i=1}^c (N_{i0} + \sum_{j=1}^M \vartheta_{ij} \xi_j) \bar{G}_i = \sum_{i=1}^c N_{i0} \bar{G}_i + \sum_{i=1}^c \sum_{j=1}^M (\vartheta_{ij} \xi_j \bar{G}_i) \quad (1.77)$$

If chemical equilibrium is attained,

$$G = \text{minimum}, dG = 0 \text{ or, } \left( \frac{\partial G}{\partial \xi_j} \right)_{T,P,y_{i \neq j}} = 0, \quad j = 1, 2, \dots, M$$

$$\text{Or, } \sum_{i=1}^c \vartheta_{ij} \bar{G}_i + \sum_{i=1}^c N_i \left( \frac{\partial \bar{G}_i}{\partial \xi_j} \right)_{T,P,y_{i \neq j}} = 0 \quad (1.78)$$

According to Gibbs- Duhem equation,

$$\sum_{i=1}^c N_i \left( \frac{\partial \bar{G}_i}{\partial \xi_j} \right)_{T,P,y_{i \neq j}} = 0 \quad (1.79)$$

$$\text{Therefore, } \sum_{i=1}^c \nu_{ij} \bar{G}_i = 0, \quad j=1,2,\dots,M \quad (1.80)$$

Equation 1.80 implies that if chemical equilibrium is achieved, all simultaneous reactions are in equilibrium.

According to Gibbs- Duhem equation,

$$\sum_{i=1}^c N_i \left( \frac{\partial G}{\partial \xi_j} \right)_{T,P,\nu_{i \neq j}} = 0 \quad (1.81)$$

$$\text{Therefore, } \sum_{i=1}^c \nu_{ij} \bar{G}_i = 0, \quad j=1,2,\dots,M \quad (1.82)$$

$$G = H - TS \quad (1.83)$$

$$d(nG) = -nSdT + nVdP + \sum_i \mu_i dn_i \quad (1.84)$$

The quantity  $\mu_i$  is called chemical potential of species i and it plays an important role in phase and chemical equilibria. This is actually partial molar Gibbs energy. Therefore,

$$\mu_i = \left( \frac{\partial nG}{\partial n_i} \right)_{T,P,n_j} \quad (1.85)$$

$$\left( \frac{\partial \mu_i}{\partial P} \right)_{T,n} = \bar{v}_i \quad (1.86)$$

$$\left( \frac{\partial \mu_i}{\partial T} \right)_{P,n} = -\bar{S}_i \quad (1.87)$$

where,  $\mu_i$  is the chemical potential of ith species.

$$\mu = f(T, P) \quad (1.88)$$

$$d\mu_i = \bar{v}_i dP - \bar{S}_i dT = d\bar{G}_i \quad (1.89)$$

$$G = \sum_i \mu_i n_i \quad (4.90)$$

$n_i$  is number of moles.

$$\sum_i n_i a_{ik} = A_k \quad (k = 1, 2, \dots, W); \quad (4.91)$$

$a_{ik}$  = number of atoms of the kth element in each molecule of i

$A_k$  is the total number of atomic masses of the kth element

$W$  = No. of atoms present in the system

Chemical potential is calculated using the following equation

$$\mu_i = RT \left[ \ln \left( \frac{f_i P}{P_0} \right) + \ln y_i + G_i^o(T, P_0) \right] \quad (1.92)$$

The values of standard free energy of formation are utilized for the prediction of chemical change through minimization of Gibbs free energy.

$$\Delta G^o = \Delta H^o - T\Delta S^o \quad (1.93)$$

### **Solution of non-stoichiometric model**

The solution of this model involves minimization of the Gibbs free energy function. The

minimization is carried out by various optimization methods such as Lagrange Multipliers method, Morley method, Gordon and McBride method and RAND method to name a few (Liu et al., 2020).

### **Lagrange Multipliers method**

Most of the non-stoichiometric equilibrium model equations are solved using Lagrange Multipliers method. The equation obtained by applying Lagrangean multipliers method and using Equations 1.81-1.84 is as follows:

$$\sum_k \lambda_k (\sum_k n_i a_{ik} - A_k)_i = 0 \quad (1.94)$$

$$\mu_i + \sum_k n_i a_{ik} = 0 \quad (1.95)$$

The minimization technique involves the minimization of the function G with respect to  $n_i$ . For this purpose, the Lagrangian function L is formed with the help of mass balance constraints as (Stanley Sandler, 2006a)

$$L = G - \sum_k \lambda_k (\sum_k n_i a_{ik} - A_k)_i \quad (1.96)$$

The minimum point of this function is calculated by setting the partial derivative of L with respect to  $n_i$  equal to zero.

$$\frac{\delta L}{\delta n_i} = 0 \quad (1.97)$$

This equation 1.97 creates a nonlinear equation for each species in the reactor. For multiple species a set of equations is created and solved by an iterative technique using Newton-Raphson method.

### **Morley method**

This optimization technique is basically a modification of Newton Raphson method proposed by Morley, 2005 (Morley, 2005). In this technique the next value of the function  $\frac{\delta L}{\delta n_i}$  is approximated by a first order Taylor development of  $\frac{\delta L}{\delta n_i}$  function. This method is limited to gas species only, solid materials cannot be handled by this method.

### **Gordon and McBride method**

Gordon and McBride (Gordon & McBride, 1971) proposed this method which is much more improved than the Morley method. In this method they used a first order Taylor expansion of  $C_i = \ln(n_i)$  and  $D = \ln(\sum_i^{N_G} n_i)$  to fit the data much better with the evolution of G.

## **RAND algorithm**

RAND algorithm which has been widely used in various non-stoichiometric equilibrium modelling has been proposed by Gautam et al. (Gautam & Seider, 1979). According to this algorithm a quadratic Taylor development is approximated to use it as a vector of mole numbers for next iterations. This technique is also used in Aspen plus software for calculating Gibbs free energy minimization at RGibbs block (Gagliano et al., 2017b; Ramzan et al., 2011).

Along with these algorithms Linear programming, Genetic algorithm, Monte Carlo method can also be utilised for the minimization of Gibbs free energy (Liu et al., 2020).

### **1.6.2 Kinetic Modelling of gasification**

The gasification process can be modelled more realistically if kinetics of the gasification reactions is taken into consideration. Unlike equilibrium modelling, kinetic modelling deals with complex physical and chemical phenomena like gas solid mass transport, fluid dynamics and different reaction kinetic models of gas-solid interaction. In kinetic Modelling reactor hydrodynamics is coupled with the reaction kinetics inside the gasifier. There are various reaction taking inside the gasifier that have been listed in Table 1.2. Some reactions are heterogeneous and some are homogeneous. The heterogeneous reactions (R3-R8) are modelled using three different char gasification models namely

- (i) Shrinking core model
- (ii) Shrinking particle model and
- (iii) Volumetric reaction model

### **1.7 Mathematical modelling syngas fermentation:**

There can be various types of bioreactors involved in the process of syngas fermentation like continuous stirred tank reactor (CSTR), bubble column reactor, trickle bed reactor and membrane bioreactor to name a few. However, most common type of bioreactor used for the syngas fermentation is the continuous stirred tank reactor. The fermentation process here, is carried out by continuously agitating the reactor with the help of a motor and agitator. The agitation process helps to develop a constant temperature and concentration inside the reactor volume. The CSTR has a continuous gas supply into the liquid phase, while agitator controls the gas-liquid mass transfer. Higher agitation speeds lead to a higher mass transfer rate between the substrate gases and the microbes. However, in industrial-scale fermenters, higher agitation speeds increase the agitator's power consumption, thus increasing the operational cost. Transfer

of sparingly soluble gases to suspended growth cultures in STRs require substantial amount of energy (1–10 kW/m<sup>3</sup>). High agitation speed breaks up the large bubbles into smaller bubbles which have less rise velocity, smaller surface/volume ratios and longer liquid contact time. Other limitations of CSTRs include possible damage to shear sensitive microorganisms, low lucrative cell concentrations due to biomass wash out at short hydraulic retention times, and poor mixing in stirred tanks with large diameters.

*Peptostreptococcus productus* was one of the first bacteria ever studied for the fermentation of syngas compounds to liquid fuels.

The modelling of syngas fermentation in CSTR reactor is based on the following assumptions:

- i.  $CO$  is the rate limiting substrate.
- ii. Other nutrients were supplied in the culture media.

Following these basic assumptions mass balance equations have been developed.

In gas phase

$CO$  balance,

$$V_g \frac{dC_{CO,g}}{dt} = V_i \frac{P}{TR} - V_o C_{CO,g} - V_l (k_l a_g)_{CO} \left[ \left( \frac{p_{CO,g}}{H_{CO}} \right) - C_{CO,l} \right] \quad (1.98)$$

$CO_2$  balance,

$$V_g \frac{dC_{CO_2,g}}{dt} = -V_o C_{CO_2,g} - V_l (k_l a_g)_{CO_2} \left[ \left( \frac{p_{CO_2,g}}{H_{CO_2}} \right) - C_{CO_2,l} \right] \quad (1.99)$$

In liquid phase,

$CO$  balance,

$$\frac{dC_{CO,l}}{dt} = (k_l a)_{CO} \left[ \left( \frac{C_{CO,g}}{H_{CO}} \right) - C_{CO,l} \right] - \left[ \frac{\mu X}{Y_{X/CO}} \right] \quad (1.100)$$

$CO_2$  balance,

$$\frac{dC_{CO_2,l}}{dt} = (k_l a)_{CO_2} \left[ \left( \frac{C_{CO_2,g}}{H_{CO_2}} \right) - C_{CO_2,l} \right] - \left[ \frac{\mu X}{Y_{X/CO_2}} \right] \quad (1.101)$$

where,

$$Y_{X/CO} = \frac{\text{biomass produced (g/L)}}{\text{CO consumed (moles/L)}} \text{ and } Y_{X/CO_2} = \frac{\text{biomass produced (g/L)}}{\text{CO}_2 \text{ consumed (moles/L)}}$$

Represent the yield of biomass per unit consumption of the substrates.

The product balance has been provided as,

$$Y_P \mu = \frac{1}{X} \frac{dp}{dt} \quad (1.102)$$

where  $Y_P = \frac{\text{product formed (moles/L)}}{\text{biomass generated (g/L)}}$  represents the corresponding yield of the product.

For acetic acid,

$$\frac{dAA}{dt} = X \left( \mu Y_{\frac{AA}{X}} \right) \quad (1.103)$$

For ethanol,

$$\frac{dE}{dt} = X \left( \mu Y_{\frac{E}{X}} \right) \quad (1.104)$$

Molar flow rate of the outlet gas

$$N_{Gout} = \frac{V_i P}{RT} - V_l (k_l a_g)_{CO} \left[ \left( \frac{p_{CO,g}}{H_{CO}} \right) - C_{CO,l} \right] - V_l (k_l a_g)_{CO_2} \left[ \left( \frac{p_{CO_2,g}}{H_{CO_2}} \right) - C_{CO_2,l} \right] \quad (1.105)$$

Now,

$$Q_{out} = \frac{N_{Gout} RT}{P} \quad (1.106)$$

The overall conversion rate of  $CO$  and production rate of  $CO_2$  is now is given as

$$r_{CO} = \left( \frac{\mu}{Y_{\frac{X}{CO}}} + Y_{CO/E} \right) X \quad (1.107)$$

$$r_{CO_2} = \left( \mu Y_{CO_2/X} + Y_{CO_2/E} r_{ET}^{AA} \right) X \quad (1.108)$$

Now solving the differential equations 1.98-1.104 the concentration of ethanol and other components can be calculated at any given instance of time.

## 1.8 Techno-economic analysis

Techno-economic analysis (TEA) of any process determines the technical efficiency and economic feasibility of it. A detailed techno-economic analysis provides significant commentary on the economically feasibility of any technology. It also aims to provide a combination of process simulation and cash flow analysis to determine the mass and energy flow as well as an array of economic parameter matrices that might be useful in measuring the viability of any process before it is commercialized. The TEA conducted by the academia and industries are significantly different. The TEAs conducted in academia primarily focuses on the total capital expenditure (CAPEX) and total operating and maintenance expenditure (OPEX) to determine the minimum selling price of any product. This is because in academia the primary goal of conducting TEA is to prepare necessary ground for any technology to be acceptable in the world for large scale production. Whereas the industrial purpose of it is to maximize the profitability of the process. Generally n<sup>th</sup> plant economics is used in conducting the TEA of any simulation model or lab scale process. Along with the minimum selling price the cash flow analysis also provides net present value (NPV), internal rate of return (IRR) and



payback period (PBP) of any given process. The detailed discussion regarding these economic parameters will be conducted in the next chapter.

## **1.9 Investment risk analysis**

Investment risk in any commercial process in terms of the net present value (NPV) is an important aspect of its financial viability. Taking into account the uncertainty involved in various economic parameters involved in the TEA, risk analysis determines the probability of a non-negative NPV. This is particularly suitable in determining the profitability of the process under consideration in adverse conditions.

## **1.10 Life cycle analysis**

Every product naturally or artificially developed in this world has a self-life. Different stages of this product life is known as life cycle. Life cycle analysis (LCA) is such a tool which is used in decision making for a product to check whether it can be suitable towards sustainable development. As per ISO 14040/14044 definition, LCA is “compilation and evaluation of the inputs and outputs and the potential environmental impacts of a product system throughout its life cycle”. There are five stages in any product life cycle namely, raw material extraction, manufacturing and transportation, use and end of life. According to the ISO definition the LCA determines the environmental impact at each of these stages of any product. In this study the bio-ethanol produced is regarded as the primary product and life cycle analysis has been conducted around that. The life cycle analysis consist of four steps.

- i. Goal and scope definition
- ii. Life cycle inventory
- iii. Impact analysis
- iv. Interpretation of the results

The goal and scope definition is regarded as the most important step in any life cycle analysis. Here the functional unit, scope and boundary of the study is defined. Inventory analysis is conducted by developing an input output material flow. Impact analysis is the process of determining the impact of inventory processes on the environment by choosing a suitable impact assessment method. Finally, the interpretation provides an overview whether the product or process is sustainable towards the environment or not.

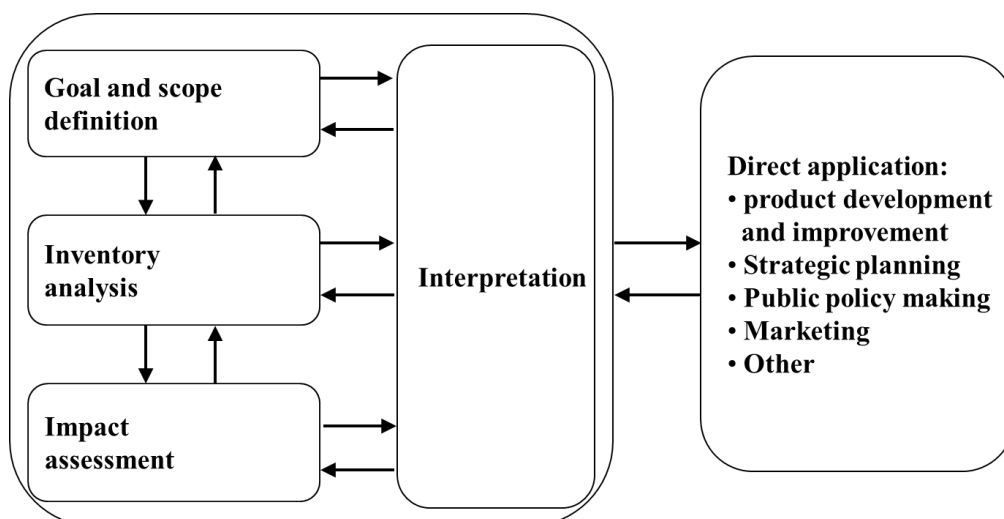


**Figure 1.3:** Four stages of life cycle analysis (ISO 14040/44)

### 1.11 Thesis Overview

Keeping all these perspectives under consideration, the present research studies will be focused in the following directions: (I) Determination of best possible combination of Indian agricultural waste for syngas production; (II) Optimization of performance of continuous production of 2<sup>nd</sup> Generation (2G)-Bioethanol from mixed Indian agro-wastes via syngas platform; (III) Sustainability analysis of the 2G-Bioethanol process under optimum condition; (IV) Techno-economic analysis of the 2G-Bioethanol process under optimum condition. In absence of real time data in large scale all studies will be conducted based on the predictions of process simulation modelling.

The chapterization of the thesis has been done in the following manner

#### **Chapter 1: Introduction**

In this chapter the motivation and the basic mathematical background of the study has been navigated in details.

#### **Chapter 2: Literature review**

The salient literatures have been studied and analyzed to determine the current state-of-the-art of the research topic and to find out the existing research gaps of the hybrid technology of co-gasification fermentation. The objectives of the research have also been discussed in this chapter.

### **Chapter 3: Materials and methods**

This chapter deals with the feedstock used and simulation methodology followed to develop the co-gasification as well as the co-gasification fermentation models.

### **Chapter 4: Equilibrium modelling and thermodynamic analysis of Indian lignocellulosic biomass co-gasification using Aspen plus**

In this chapter, thermodynamic performance of co-gasification of various Indian agricultural wastes have been studied for syngas production. Optimization of the process parameters have also been conducted to maximize the energy and exergy efficiency of the co-gasification process.

### **Chapter 5: Kinetic modelling and thermodynamic performance optimization of Indian lignocellulosic biomass co-gasification**

In this chapter, kinetic modelling aspect of biomass co-gasification has been explored using two of the most efficient biomass combinations selected in the previous chapter. Based on the thermodynamic performance of the biomass mixtures best combination is selected for further modelling of the hybrid route.

### **Chapter 6: Bio-ethanol production via syngas platform: model development and multi-objective optimization**

This chapter deals with the development of an equilibrium model of biomass co-gasification and syngas fermentation for the production of bio-ethanol. Optimization of ethanol production and overall energy efficiency of the system has also been conducted in this chapter.

### **Chapter 7: Integration of power generation and heat and resource recovery in the co-gasification- syngas fermentation model**

Integration of power generation from the excess syngas as well as heat and resource recovery from the process has been included in the previously developed model to improve utilization efficiency of the model.

## **Chapter 8: Techno-economic analysis, investment risk analysis and life cycle analysis of the co-gasification fermentation model**

Techno-economic, life cycle and investment risk analysis have been conducted in the modified co-gasification fermentation model to determine the overall sustainability of the process.

## **Chapter 9: Conclusions and future scope**

This chapter discusses the conclusion and the scope of future work of the study.

---

## Chapter 2. Literature review

---

### 2.1 Introduction

A chronological and comprehensive literature survey has been performed on the modelling of co-gasification as well as syngas fermentation for the period of ten years to update the existing knowledge in the area. The state-of-the-art in the current topic has been identified and possible research gap is also outlined to enlist the possible objectives of the research work.

### 2.2 Equilibrium modelling of gasification and co-gasification in Aspen plus

Modelling of gasification has been successfully carried out in different literatures following thermodynamic equilibrium. Aspen plus has been utilized to develop the gasification and co-gasification process following Gibbs free energy minimization technique. Various literatures involving Aspen plus modelling of biomass gasification and co-gasification have been conducted in Table 2.1.

**Table 2.1:** Literatures on equilibrium modelling of gasification and co-gasification in Aspen plus

Literature	Details	Observations
Zhang et al., 2023	<ul style="list-style-type: none"><li>• <b>Feedstock:</b> Chlorella Vulgaris and petroleum industry sludge</li></ul>	<ul style="list-style-type: none"><li>• Generation of syngas promoted by the mixing of petroleum industry sludge with chlorella vulgaris.</li><li>• Highest amount of <math>H_2</math> is achieved at 700°C.</li><li>• Equivalence ratio adversely effects the syngas production</li></ul>
	<ul style="list-style-type: none"><li>• <b>Property method:</b> Not mentioned</li></ul>	
	<ul style="list-style-type: none"><li>• <b>Modelling procedure:</b> Gibbs free energy minimization</li></ul>	
	<ul style="list-style-type: none"><li>• <b>Validation:</b> NA</li></ul>	
	<ul style="list-style-type: none"><li>• <b>Thermodynamic performance analysis:</b> NA</li></ul>	

	<ul style="list-style-type: none"> <li>• <b>Whether co-gasification:</b> yes</li> </ul>	
Rosha & Ibrahim, 2022	<ul style="list-style-type: none"> <li>• <b>Feedstock:</b> Paper mill sludge and Pine wood</li> <li>• <b>Property method:</b> PR- BM</li> <li>• <b>Modelling procedure:</b> Gibbs free energy minimization</li> <li>• <b>Validation:</b> Literature data</li> <li>• <b>Thermodynamic performance analysis:</b> NA</li> </ul>	<ul style="list-style-type: none"> <li>• Moisture in paper mill sludge increases <math>H_2</math> production but reduces <math>CO</math> production</li> <li>• Increase in temperature increased the LHV of syngas</li> </ul>
	Whether co-gasification: yes	
Zaman & Ghosh, 2021	<ul style="list-style-type: none"> <li>• <b>Feedstock:</b> Various biomass waste</li> <li>• <b>Property method:</b> Peng-Robinson (Peng-Rob)</li> <li>• <b>Modelling procedure:</b> Gibbs free energy minimization with full conversion of Sulphur.</li> <li>• <b>Validation:</b> Literature data</li> <li>• <b>Thermodynamic performance analysis:</b> NA</li> <li>• <b>Whether co-gasification:</b> No</li> </ul>	<ul style="list-style-type: none"> <li>• Optimum gasification condition was achieved at temperatures between 780°C and 790°C and steam to biomass ratio of 0.7.</li> <li>• Optimum cold gas efficiency (CGE) and LHV were found to be 70% and 15 MJ/kg respectively.</li> </ul>
Safarian et al., 2020	<ul style="list-style-type: none"> <li>• <b>Feedstock:</b> Various biomass</li> </ul>	<ul style="list-style-type: none"> <li>• The Aspen plus model has been used to devise an artificial neural network</li> </ul>

	<ul style="list-style-type: none"> <li>• <b>Property method:</b> Peng- Rob with Boston Mathias alpha function (PR-BM)</li> <li>• <b>Modelling procedure:</b> Gibbs free energy minimization with two stage gasification modelling</li> <li>• <b>Validation:</b> NA</li> <li>• <b>Energy and exergy analysis:</b> NA</li> <li>• <b>Whether co-gasification:</b> No</li> </ul>	<p>model for predicting the syngas yield of gasification more accurately.</p>
Monir et al., 2020	<ul style="list-style-type: none"> <li>• <b>Feedstock:</b> Forest residue and wood charcoal</li> <li>• <b>Property method:</b> PR-BM</li> <li>• <b>Modelling procedure:</b> Gibbs free energy minimization</li> <li>• <b>Validation:</b> Literature data</li> <li>• <b>Thermodynamic performance analysis:</b> exergy analysis</li> <li>• <b>Whether co-gasification:</b> yes</li> </ul>	<ul style="list-style-type: none"> <li>• Mixing wood charcoal with forest residue increased the exergy efficiency.</li> <li>• Specific H<sub>2</sub> yield also increased with the blending of wood charcoal.</li> </ul>
Safarian et al., 2019	<ul style="list-style-type: none"> <li>• <b>Feedstock:</b> sawdust, wood chips and mixed paper waste</li> <li>• <b>Property method:</b> PR- BM</li> </ul>	<ul style="list-style-type: none"> <li>• High temperature positively and high equivalence ratio (ER) adversely affects the</li> </ul>

	<ul style="list-style-type: none"> <li>• <b>Modelling procedure:</b> Gibbs free energy minimization</li> <li>• <b>Validation:</b> Literature data</li> <li>• <b>Energy and exergy analysis:</b> NA</li> <li>• <b>Whether co-gasification:</b> No</li> </ul>	syngas production and its heating value.
	<ul style="list-style-type: none"> <li>• <b>Property method:</b> IDEAL</li> </ul>	
	<ul style="list-style-type: none"> <li>• <b>Modelling procedure:</b> Gibbs free energy minimization and restricted chemical equilibrium with tar consideration</li> <li>• <b>Validation:</b> Literature data</li> <li>• <b>Thermodynamic performance analysis:</b> Both energy and exergy analysis</li> <li>• <b>Whether co-gasification:</b> No</li> </ul>	<ul style="list-style-type: none"> <li>• A range of <math>H_2</math> production between 50-170g <math>H_2</math>/g of Biomass has been achieved.</li> <li>• Increased temperature adversely affected the <math>H_2</math> production while favored the <math>CO</math> production.</li> <li>• Steam supply has increased the <math>CO</math> production but has not affected the steam <math>H_2</math> production.</li> </ul>
Mehrpooya et al., 2018		
Lan et al., 2018	<ul style="list-style-type: none"> <li>• <b>Feedstock:</b> Sanya wood flour</li> </ul>	<ul style="list-style-type: none"> <li>• Elevated ER increased the <math>CO</math> and <math>H_2</math> production.</li> </ul>
	<ul style="list-style-type: none"> <li>• <b>Property method:</b> PR-BM and Redlich- Kwong Soave with Boston Mathias alpha function</li> </ul>	<ul style="list-style-type: none"> <li>• Increase in temperature significantly increases the <math>CO</math> yield.</li> </ul>



	<ul style="list-style-type: none"> <li>• <b>Modelling procedure:</b> Gibbs free energy minimization</li> <li>• <b>Validation:</b> Literature data</li> <li>• <b>Thermodynamic performance analysis:</b> NA</li> <li>• <b>Whether co-gasification:</b> No</li> </ul>	
Han et al., 2017	<ul style="list-style-type: none"> <li>• <b>Feedstock:</b> Hardwood chips of red oak</li> <li>• <b>Property method:</b> IDEAL</li> <li>• <b>Modelling procedure:</b> Gibbs free energy minimization with restricted chemical equilibrium</li> <li>• <b>Validation:</b> Literature data</li> <li>• <b>Thermodynamic performance analysis:</b> NA</li> <li>• <b>Whether co-gasification:</b> No</li> </ul>	<ul style="list-style-type: none"> <li>• <math>H_2/CO</math> ratio and LHV increased from 500°C to 650°C and then decreased.</li> <li>• Equivalence ratio adversely effected the <math>H_2</math> and <math>CO</math> production.</li> <li>• Increase in moisture content slightly increased the <math>H_2</math> production.</li> </ul>
Gagliano et al., 2017	<ul style="list-style-type: none"> <li>• <b>Feedstock:</b> Pallets and rubber wood</li> <li>• <b>Property method:</b> Peng-Rob</li> <li>• <b>Modelling procedure:</b> Gibbs free energy minimization with calibration using empirical</li> </ul>	<ul style="list-style-type: none"> <li>• Calibrated model shows good agreement with experimental literatures.</li> <li>• Biomass moisture content (MC) adversely effects <math>H_2</math> and <math>CO</math> production and LHV of syngas.</li> </ul>

	<p>relation between moisture content and ER</p> <ul style="list-style-type: none"> <li>• <b>Validation:</b> Literature data</li> <li>• <b>Thermodynamic performance analysis:</b> NA</li> <li>• <b>Whether co-gasification:</b> No</li> </ul>	<ul style="list-style-type: none"> <li>• High ER helps in removing tar from the syngas but it reduces its heating value.</li> </ul>
Ali et al., 2017	<ul style="list-style-type: none"> <li>• <b>Feedstock:</b> Coal, petroleum coke, rice straw and wood</li> <li>• <b>Property method:</b> PR-BM</li> <li>• <b>Modelling procedure:</b> Gibbs free energy minimization based entrained flow gasification</li> <li>• <b>Validation:</b> Literature data</li> <li>• <b>Thermodynamic performance analysis:</b> NA</li> <li>• <b>Whether co-gasification:</b> yes</li> </ul>	<ul style="list-style-type: none"> <li>• No significant change can be noticed in terms of <math>CO</math> and <math>H_2</math> yield against gasification temperature.</li> <li>• <math>H_2/CO</math> ratio significantly increased with the increase of steam/<math>O_2</math> ratio.</li> </ul>
Rupesh et al., 2016a	<ul style="list-style-type: none"> <li>• <b>Feedstock:</b> Saw dust</li> <li>• <b>Property method:</b> NA</li> <li>• <b>Modelling procedure:</b> Gibbs free energy minimization</li> <li>• <b>Validation:</b> Literature data</li> <li>• <b>Thermodynamic performance analysis:</b></li> </ul>	<ul style="list-style-type: none"> <li>• A maximum of mole fraction 31.17% of <math>H_2</math> is reached at 900K temperature.</li> <li>• Sorbent enabled <math>CO_2</math> capture improved the gasification efficiency and <math>H_2</math> production.</li> </ul>

	Hydrogen production efficiency	
	<ul style="list-style-type: none"> <li>• <b>Whether co-gasification:</b> No</li> </ul>	
Tapasvi et al., 2015	<ul style="list-style-type: none"> <li>• <b>Feedstock:</b> Torrefied Leucaena</li> <li>• <b>Property method:</b> NA</li> <li>• <b>Modelling procedure:</b> Gibbs free energy minimization with tar consideration</li> <li>• <b>Validation:</b> NA</li> <li>• <b>Thermodynamic performance analysis:</b> Both energy and exergy analysis</li> <li>• <b>Whether co-gasification:</b> No</li> </ul>	<ul style="list-style-type: none"> <li>• Production of <math>H_2</math> and <math>CO_2</math> and production of <math>CO</math> decreases with the increase of steam to biomass ratio (SBR).</li> <li>• Production of <math>H_2</math> slightly decreases and <math>CO</math> slightly increases with the increase in gasification temperature.</li> <li>• Increase in ER adversely affect the syngas production.</li> <li>• Increase in SBR, ER and temperature reduces both energy and exergy efficiency.</li> </ul>
Begum et al., 2014	<ul style="list-style-type: none"> <li>• <b>Feedstock:</b> Municipal solid waste</li> <li>• <b>Property method:</b> RKS-BM</li> <li>• <b>Modelling procedure:</b> Gibbs free energy minimization</li> <li>• <b>Validation:</b> Literature data</li> <li>• <b>Thermodynamic performance analysis:</b> NA</li> </ul>	<ul style="list-style-type: none"> <li>• Increase in ER increases the carbon conversion whereas increase in temperature reduces carbon conversion and promotes the production of <math>CO</math> and <math>H_2</math>.</li> </ul>

	<ul style="list-style-type: none"> <li>• <b>Whether co-gasification:</b> No</li> </ul>	
Barrera et al., 2014	<ul style="list-style-type: none"> <li>• <b>Feedstock:</b> coal water slurry and dry coal</li> <li>• <b>Property method:</b> Not mentioned</li> <li>• <b>Modelling procedure:</b> Gibbs free energy minimization with reactor hierarchy</li> <li>• <b>Validation:</b> Literature data</li> <li>• <b>Thermodynamic performance analysis:</b> 3 type of energy analysis</li> <li>• <b>Whether co-gasification:</b> No</li> </ul>	<ul style="list-style-type: none"> <li>• Feeding technology significantly effects the energy parameters.</li> <li>• Process and global efficiency were higher for the slurry feeding method whereas the cold gas efficiency was higher for the dry feeding technology.</li> </ul>
Doherty et al., 2013	<ul style="list-style-type: none"> <li>• <b>Feedstock:</b> Wood chips</li> <li>• <b>Property method:</b> PR-BM</li> <li>• <b>Modelling procedure:</b> Gibbs free energy minimization with restricted equilibrium approach</li> <li>• <b>Validation:</b> Various literatures</li> <li>• <b>Thermodynamic performance analysis:</b> NA</li> <li>• <b>Whether co-gasification:</b> No</li> </ul>	<ul style="list-style-type: none"> <li>• With increase in gasification temperature, the production of <math>H_2</math> and <math>CO</math> increases whereas the production of <math>CO_2</math> and <math>CH_4</math> decreases.</li> <li>• Biomass moisture content has very little impact on the syngas composition.</li> <li>• With the increase in SBR ratio the production of <math>H_2</math> and <math>CO_2</math> increases while the production of <math>CO</math> and <math>CH_4</math> decreases.</li> </ul>

---

	<ul style="list-style-type: none"> <li>• Over SBR of 1.35, the SBR has very less impact on the syngas composition.</li> <li>• ER adversely effects the <math>H_2</math> and <math>CO</math> production.</li> </ul>
Chen et al., 2013	<ul style="list-style-type: none"> <li>• <b>Feedstock:</b> Municipal solid waste</li> <li>• <b>Property method:</b> Peng-Rob</li> <li>• <b>Modelling procedure:</b> Gibbs free energy minimization</li> <li>• <b>Validation:</b> Literature</li> <li>• <b>Thermodynamic performance analysis:</b> Cold gas efficiency</li> <li>• <b>Whether co-gasification:</b> yes</li> <li>• The production of <math>CO_2</math> increases with the increase of both temperature and ER.</li> <li>• Combustion flue gas if introduced in the gasification section improves the heat conversion efficiency and LHV of syngas.</li> </ul>

---

### 2.2.1 Research gaps in equilibrium modelling of biomass

The literature review suggest that equilibrium modelling of biomass gasification in Aspen plus is an important research direction among researchers. However, there is limited studies of biomass co-gasification in Aspen plus environment. Thermodynamic analysis of the system in terms of energy and exergy is also an important aspect in biomass co-gasification. There is also significant gap in research articles regarding the performance analysis of co-gasification system in terms of energy and exergy efficiency.

### 2.3 Kinetic modelling of gasification and co-gasification

Along with the equilibrium modelling, kinetic modelling of the biomass gasification and co-gasification process is also important to include the reaction kinetics of gasification in the simulation process. This makes the simulation more realistic in nature. There are various modelling tools to implement the kinetic model mathematically. Among them Aspen plus is becoming increasingly important. The literatures catering to this particular topic have been enlisted in Table 2.2.

**Table 2.2:** Literatures on kinetic modelling of gasification and co-gasification

Literature	Details	Observations
Rabea et al., 2022	<ul style="list-style-type: none"> <li>• <b>Feedstock:</b> wood chips</li> <li>• <b>Modelling aspect:</b> Kinetic modelling in Aspen plus with combined MATLAB code for the prediction of temperature profile.</li> <li>• <b>Validation:</b> Literature data</li> <li>• <b>Thermodynamic performance analysis:</b> Cold gas efficiency</li> <li>• <b>Whether co-gasification:</b> No</li> </ul>	<ul style="list-style-type: none"> <li>• Highest CGE for the gasification process is achieved to be 71% at any increased air flow rate.</li> <li>• With the increase in moisture content of the biomass, a significant increase in the gasifier performance can be observed.</li> </ul>
Catalanotti et al., 2022	<ul style="list-style-type: none"> <li>• <b>Feedstock:</b> Not mentioned</li> <li>• <b>Modelling aspect:</b> Kinetic modelling of downdraft gasification using plug flow reactors.</li> <li>• <b>Validation:</b> Literature data</li> </ul>	<ul style="list-style-type: none"> <li>• With the increase in char reactivity factor the yield of <math>H_2</math> initially increases significantly.</li> <li>• Reduced char reactivity factor to 7-8 converts less char to gas.</li> </ul>

	<ul style="list-style-type: none"> <li>• <b>Thermodynamic performance analysis:</b> NA</li> <li>• <b>Tar consideration:</b> Mixture of benzene and naphthalene</li> <li>• <b>Whether co-gasification:</b> No</li> </ul>	
Cao et al., 2022	<ul style="list-style-type: none"> <li>• <b>Feedstock:</b> Rice husk, sawdust and bamboo dust</li> <li>• <b>Modelling aspect:</b> Circulating fluidized bed gasification with kinetic modelling in aspen plus</li> <li>• <b>Validation:</b> Literature data</li> <li>• <b>Thermodynamic performance analysis:</b> Cold gas efficiency</li> <li>• <b>Tar consideration:</b> Not considered</li> <li>• <b>Whether co-gasification:</b> yes</li> </ul>	<ul style="list-style-type: none"> <li>• Increasing temperature increases the <math>H_2</math> and <math>CO</math> content and reduce <math>CO_2</math> content of the produced gas.</li> <li>• Highest CGE has been obtained at 900°C.</li> <li>• Increase in ER increases the <math>H_2</math> and <math>CO_2</math> content.</li> <li>• For both biomass blends (Rice husk+ sawdust and Rice husk +bamboo dust) increasing SBR decreased the CGE of the process.</li> </ul>
Cao et al., 2021	<ul style="list-style-type: none"> <li>• <b>Feedstock:</b> Pine sawdust</li> <li>• <b>Modelling aspect:</b> kinetic modelling of the gasification part in Aspen plus and</li> </ul>	<ul style="list-style-type: none"> <li>• Syngas yield increased with increasing SBR.</li> <li>• HHV of syngas initially increased with increasing ER</li> </ul>

	equilibrium modelling of the rest of the sections.	then reduced with further increase.
	<ul style="list-style-type: none"> <li>• <b>Validation:</b> Literature data</li> <li>• <b>Thermodynamic performance analysis:</b> Cold gas efficiency</li> <li>• <b>Tar consideration:</b> considered</li> <li>• <b>Whether co-gasification:</b> No</li> </ul>	<ul style="list-style-type: none"> <li>• <i>CO</i> content initially increased with increasing temperature but the n reduced after 750°C.</li> <li>• <i>CH<sub>4</sub></i> yield initially dropped to 1.5% v/v then increased to 3.56% with the increase in ER.</li> </ul>
Barontini et al., 2021	<ul style="list-style-type: none"> <li>• <b>Feedstock:</b> Woodchips with organic fraction of MSW, sewage sludge and hazelnut shells respectively</li> <li>• <b>Modelling aspect:</b> separate kinetic modelling of throat and under throat portion of the gasifier in Aspen plus</li> <li>• <b>Validation:</b> self-experiment</li> <li>• <b>Thermodynamic performance analysis:</b> Cold gas efficiency</li> <li>• <b>Tar consideration:</b> Not considered</li> <li>• <b>Whether co-gasification:</b> yes</li> </ul>	<ul style="list-style-type: none"> <li>• For all the three mixtures LHV of syngas was higher than 5.18 MJ/Nm<sup>3</sup>.</li> <li>• The CGE value was maximum for wood chips and organic fraction of MSW mixture at a value of 76.2%.</li> <li>• CGE is found to be increasing with increasing ER.</li> <li>• High air temperature at the inlet of gasifier improves the gasification efficiency.</li> </ul>



Smith et al., 2019	<ul style="list-style-type: none"> <li>• <b>Feedstock:</b> Not mentioned</li> <li>• <b>Modelling aspect:</b> Kinetic model of downdraft gasification in Aspen plus</li> <li>• <b>Tar consideration:</b> Acetone, benzene, naphthalene, propionic acid, toluene and phenol</li> <li>• <b>Validation:</b> Literature</li> <li>• <b>Thermodynamic performance analysis:</b> Not performed</li> <li>• <b>Whether co-gasification:</b> No</li> </ul>	<ul style="list-style-type: none"> <li>• Kinetic model predicts the syngas volume fraction more accurately than equilibrium model.</li> <li>• High gasification temperature, low moisture content improves the gasifier performance.</li> <li>• Between ER values of 0.2 and 0.3 the <math>CO</math> yield is found to be maximum.</li> <li>• Tar content of 1-3% of the total gas volume was recorded in the modelling.</li> </ul>
Yu & Smith, 2018	<ul style="list-style-type: none"> <li>• <b>Feedstock:</b> wood pallets and sewage sludge</li> <li>• <b>Modelling aspect:</b> Aspen plus kinetic model of updraft gasifier with two step gasification</li> <li>• <b>Validation:</b> Literature</li> <li>• <b>Tar consideration:</b> yes</li> <li>• <b>Thermodynamic performance analysis:</b> Not performed</li> <li>• <b>Whether co-gasification:</b> Both single biomass</li> </ul>	<ul style="list-style-type: none"> <li>• Volume fraction of <math>CO</math> first increases than decreases with increasing ER for the kinetic model.</li> <li>• Volume fraction of <math>H_2</math> slightly decreases with the increase in ER.</li> <li>• <math>CH_4</math> volume fraction decreases with increasing ER.</li> <li>• Mixing of sewage sludge reduces the <math>CO</math> and <math>H_2</math> production which in turn reduces the LHV of syngas.</li> </ul>

	gasification and co-gasification	<ul style="list-style-type: none"> <li>Higher moisture content of the biomass may result in ignition difficulty in gasifiers.</li> </ul>
Kaushal & Tyagi, 2017	<ul style="list-style-type: none"> <li><b>Feedstock:</b> woody biomass</li> <li><b>Modelling aspect:</b> Aspen plus kinetic model with tar modelling consideration</li> </ul>	<ul style="list-style-type: none"> <li>High temperature favored the gasification process.</li> </ul>
	<ul style="list-style-type: none"> <li><b>Validation:</b> Literature</li> <li><b>Tar consideration:</b> yes</li> <li><b>Thermodynamic performance analysis:</b> Not performed</li> <li><b>Whether co-gasification:</b> No</li> </ul>	<ul style="list-style-type: none"> <li>Steam is not so much effective in improving the syngas production. However, it is effective for the conversion of tar.</li> </ul>
Pauls et al., 2016	<ul style="list-style-type: none"> <li><b>Feedstock:</b> Pine sawdust</li> <li><b>Modelling aspect:</b> temperature dependent empirical equations for pyrolysis and user defined kinetics for gasification in Aspen plus.</li> </ul>	<ul style="list-style-type: none"> <li>Over 800°C the conversion of <math>CO</math> to <math>CO_2</math> becomes more dominant.</li> </ul>
	<ul style="list-style-type: none"> <li><b>Validation:</b> Literature data</li> <li><b>Tar consideration:</b> Not considered</li> </ul>	<ul style="list-style-type: none"> <li>Temperature has the maximum influence over the <math>H_2</math> production.</li> <li>ER and SBR does not have much influence over <math>H_2</math> production.</li> </ul>

	<ul style="list-style-type: none"> <li>• Thermodynamic performance analysis: Not performed</li> <li>• Whether co-gasification: No</li> </ul>	
Adeyemi & Janajreh, 2015	<ul style="list-style-type: none"> <li>• <b>Feedstock:</b> Kentucky Coal and wood waste</li> <li>• <b>Modelling aspect:</b> Aspen plus kinetic modelling with RKS property method</li> <li>• <b>Validation:</b> Self experiment</li> <li>• <b>Tar component:</b></li> <li>• <b>Thermodynamic performance analysis:</b> NA</li> <li>• <b>Whether co-gasification:</b> No</li> </ul>	<ul style="list-style-type: none"> <li>• Rise in gasifier diameter increases the syngas production.</li> <li>• Increase in gasifier height increases the <math>CO</math> and <math>H_2</math> production.</li> <li>• Syngas mole fraction is less in wood waste than Kentucky coal.</li> </ul>
Beheshti et al., 2015	<ul style="list-style-type: none"> <li>• <b>Feedstock:</b> Wood chips</li> <li>• <b>Modelling aspect:</b> Aspen plus modelling with bed hydrodynamics</li> <li>• <b>Validation:</b> literature</li> <li>• <b>Tar component:</b> Not categorized as tar</li> <li>• <b>Thermodynamic performance analysis:</b> <math>H_2</math> production efficiency and cold gas efficiency</li> </ul>	<ul style="list-style-type: none"> <li>• Increasing temperature from <math>600^{\circ}C</math> to <math>800^{\circ}C</math> increases the <math>H_2</math> and <math>CO</math> yield but decreases the yield of <math>CH_4</math> and <math>CO_2</math>.</li> <li>• ER adversely affects the syngas production increasing the <math>CO_2</math> Yield.</li> <li>• Increase in SBR improves the <math>H_2</math> and <math>CO_2</math> production but reduces the <math>CO</math> production by shifting the water gas shift reaction.</li> </ul>

	<ul style="list-style-type: none"> <li>• <b>Whether co-gasification:</b> No</li> </ul>	<ul style="list-style-type: none"> <li>• CGE initially increases with increasing ER.</li> </ul>
Eikeland et al., 2015	<ul style="list-style-type: none"> <li>• <b>Feedstock:</b> Not mentioned</li> <li>• <b>Modelling aspect:</b> separate equilibrium and kinetic modelling in aspen plus</li> <li>• <b>Validation:</b> Literature</li> <li>• <b>Thermodynamic performance analysis:</b> Not performed</li> <li>• <b>Whether co-gasification:</b> No</li> </ul>	<ul style="list-style-type: none"> <li>• For kinetic modelling, the <math>CO</math> concentration decreases with the increase in temperature whereas the <math>H_2</math> concentration increases.</li> <li>• Increased residence time produces more <math>H_2</math> and <math>CO_2</math>.</li> <li>• 8 Sec of residence time gives best match of experimental data predicted by the model.</li> </ul>
Zheng & Morey, 2014	<ul style="list-style-type: none"> <li>• <b>Feedstock:</b> Corn stover</li> <li>• <b>Modelling aspect:</b> Fluidized bed gasification including bed hydrodynamics and two phase reaction kinetics in MATLAB</li> <li>• <b>Validation:</b> Literature</li> <li>• <b>Thermodynamic performance analysis:</b> NA</li> <li>• <b>Whether co-gasification:</b> No</li> </ul>	<ul style="list-style-type: none"> <li>• Increase in superficial gas velocity increases the production of syngas.</li> <li>• Increased SBR increases the production of <math>H_2</math> and <math>CO_2</math> while decreasing the production of <math>CO</math> and <math>CH_4</math>.</li> <li>• Water-gas shift reaction and residence time are significant factors while deciding the syngas production.</li> </ul>

### 2.3.1 Research gaps in kinetic modelling of biomass

After reviewing all the above mentioned literatures, it can be summarized that the most of the researchers have put the emphasis on accurately predicting the syngas composition in different type of models of gasification. Various type of modelling arrangements have been considered to improve the quality of prediction. Overall methane yield have improved significantly with the kinetic considerations. However, studies involving kinetic modelling of co-gasification is limited in terms of both simulation and analysis. Optimization of the gasification parameters in terms of thermodynamic performance is also another less trotted path. Use of response surface methodology in optimization of the gasification parameters is another important aspect that has been less utilized.

### 2.4 Literatures on modelling of ethanol production following syngas platform

After conducting the literature review on co-gasification models, it is important to look into the aspect of syngas fermentation for ethanol production. Ethanol production following the syngas platform involves gas-liquid mass transfer which has been in literature for a long time but the hybrid route of co-gasification and syngas fermentation has not been researched to that much extent. The literature review on the topic of ethanol production following the syngas platform involving both standalone and hybrid route has been assessed in Table 2.3.

**Table 2.3:** Literatures on modelling of ethanol production following syngas platform

Literature	Details	Observations
Ruggiero et al., 2022	<ul style="list-style-type: none"> <li>• <b>Process type:</b> Syngas fermentation</li> <li>• <b>Modelling aspect:</b> Kinetic modelling of syngas fermentation in MATLAB, kinetic parameters were calculated using regression analysis</li> <li>• <b>Validation:</b> NA</li> </ul>	<ul style="list-style-type: none"> <li>• Maximum cell growth achieved in this study was <math>0.37 \text{ h}^{-1}</math></li> <li>• <math>CO</math> mass transfer increases with the increase in agitation speed and syngas volumetric flow rate.</li> <li>• Decreasing the agitation speed from 250 rpm to</li> </ul>

	<ul style="list-style-type: none"> <li>• <b>Analysis conducted:</b> sensitivity analysis of product concentration with time along with sensitivity of volumetric gas input, agitation speed and filling ratio</li> <li>• <b>Optimization:</b> Yes</li> </ul>	<p>182 rpm increased the cell growth up to 3.5%.</p>
<p><b>Ma et al., 2022</b></p>	<ul style="list-style-type: none"> <li>• <b>Process type:</b> Biomass gasification and syngas fermentation</li> <li>• <b>Feedstock:</b> Different biomass including softwood, wood chips, rice husk and rice straw</li> <li>• <b>Modelling aspect:</b> Aspen plus modelling with PR-BM equation of state for gasification</li> <li>• <b>Validation:</b> NA</li> <li>• <b>Analysis conducted:</b> Sensitivity analysis of gasification parameters on syngas yield, effect of substrate conversion on ethanol yield and energy efficiency, optimization of fermentation process.</li> <li>• <b>Optimization:</b> yes</li> </ul>	<ul style="list-style-type: none"> <li>• Conversion of woodchips into ethanol can produce 69,595 ton of ethanol with 200,000 ton of woodchips.</li> <li>• This optimized production can be obtained at 900°C temperature and 0.1 SBR.</li> <li>• Increase in both <math>CO</math> and <math>H_2</math> conversion increase the ethanol production and energy efficiency.</li> </ul>

Okolie et al., 2021	<ul style="list-style-type: none"> <li>• <b>Process type:</b> Biomass gasification and syngas fermentation</li> <li>• <b>Feedstock:</b> Crude glycerol</li> <li>• <b>Modelling aspect:</b> Aspen plus modelling of hydrothermal gasification and syngas fermentation using NRTL equation of state</li> <li>• <b>Validation:</b> NA</li> <li>• <b>Analysis conducted:</b> Energy efficiency</li> <li>• <b>Optimization:</b> NA</li> </ul>	<ul style="list-style-type: none"> <li>• With 500000 ton/ year of water and 50000 ton/year of glycerol supply, the achieved bioethanol production was 17,002 ton/ year.</li> <li>• Inclusion of bio-methane production and electrolysis unit increased the energy efficiency of the process from 30% to 35.1%.</li> </ul>
Safarian et al., 2020	<ul style="list-style-type: none"> <li>• <b>Process type:</b> Biomass gasification and syngas fermentation</li> <li>• <b>Feedstock:</b> Garden waste</li> <li>• <b>Modelling aspect:</b> Aspen plus modelling with three stages namely gasification, fermentation and ethanol recovery</li> <li>• <b>Validation:</b> NA</li> <li>• <b>Analysis conducted:</b> Sensitivity analysis of bio-ethanol and syngas against temperature, ER. Thermodynamic performance</li> </ul>	<ul style="list-style-type: none"> <li>• At 800°C temperature, highest CGE was recorded to be 44.5% while keeping ER constant.</li> <li>• 54.2% of CGE was recorded at 0.2 ER keeping constant temperature.</li> <li>• Increase in gasification temperature increased the ethanol yield whereas ER affected the ethanol production negatively.</li> </ul>

	analysis in terms of CGE of syngas	
	<ul style="list-style-type: none"> <li>• <b>Optimization:</b> NA</li> </ul>	
Michailos et al., 2019	<ul style="list-style-type: none"> <li>• <b>Process type:</b> Biomass gasification and syngas fermentation</li> <li>• <b>Feedstock:</b> sugarcane bagasse</li> <li>• <b>Modelling aspect:</b> Aspen plus modelling with RKS-BM equation of state, processes include bagasse pretreatment and drying along with gasification-fermentation and ethanol recovery. 70% of <math>CO</math> and 50% of <math>H_2</math> is assumed to be converted to ethanol.</li> <li>• <b>Validation:</b> Literature data for syngas production</li> <li>• <b>Thermodynamic performance analysis:</b> Energy and exergy efficiency</li> <li>• <b>Optimization:</b> NA</li> </ul>	<ul style="list-style-type: none"> <li>• An ethanol production of 22.7 t/h per 100 ton of bagasse is achieved.</li> <li>• Highest energy and exergy efficiency is achieved to be 43% and 39%.</li> <li>• 25.5 MW of electricity is generated from the unfermented syngas.</li> </ul>
Pardo-Planas et al., 2017	<ul style="list-style-type: none"> <li>• <b>Process type:</b> Biomass gasification and syngas fermentation</li> <li>• <b>Feedstock:</b> Switch grass</li> <li>• <b>Modelling aspect:</b> Equilibrium modelling of gasification and syngas</li> </ul>	<ul style="list-style-type: none"> <li>• Maximum syngas production was achieved at 0.405 ER, 730°C temperature and zero steam flow.</li> </ul>



	<p>fermentation in Aspen plus. <math>CO</math> and <math>H_2</math> conversion to ethanol considered to be 90%.</p> <ul style="list-style-type: none"> <li>• <b>Property method:</b> RKS-BM for gasification and NRTL for syngas fermentation.</li> <li>• <b>Validation:</b> Literature data</li> <li>• <b>Thermodynamic performance analysis:</b> NA</li> <li>• <b>Optimization:</b> NA</li> </ul>	<ul style="list-style-type: none"> <li>• Production of ethanol per dry ton of biomass is recorded to be 370 liter.</li> <li>• Reactor volume decreases if the gas uptake rate is increased.</li> </ul>
de Medeiros et al., 2017	<ul style="list-style-type: none"> <li>• <b>Process type:</b> Biomass gasification and syngas fermentation</li> <li>• <b>Feedstock:</b> corn stover</li> <li>• <b>Modelling aspect:</b> Aspen plus simulation of equilibrium model of gasification, heat recovery, syngas fermentation and distillation</li> <li>• <b>Validation:</b> Not conducted</li> <li>• <b>Thermodynamic performance analysis:</b> NA</li> <li>• <b>Optimization:</b> NA</li> </ul>	<ul style="list-style-type: none"> <li>• An ethanol production of 0.33 m<sup>3</sup> per dry ton of biomass is achieved.</li> <li>• Around 30% of carbon converted to ethanol.</li> <li>• It has also been suggested that some amount of syngas might be used for power generation purpose.</li> </ul>
Diederichs et al., 2016	<ul style="list-style-type: none"> <li>• <b>Process type:</b> comparison of different jet-fuel production technologies including gasification and syngas fermentation</li> </ul>	<ul style="list-style-type: none"> <li>• An ethanol production of 217 kg/ ton of dry biomass is obtained.</li> <li>• Jet fuel to mass of fuel ration in cases of the</li> </ul>

	<ul style="list-style-type: none"> <li>• <b>Modelling aspect:</b> Aspen plus modelling of biomass gasification and syngas fermentation with gasification conducted in a dual fluidized bed gasifier.</li> <li>• <b>Validation:</b> NA</li> <li>• <b>Thermodynamic performance analysis:</b> NA</li> <li>• <b>Optimization:</b> NA</li> </ul>	<p>gasification and syngas fermentation process reached up to 88%.</p>
Chen et al., 2015	<ul style="list-style-type: none"> <li>• <b>Process type:</b> Syngas fermentation</li> <li>• <b>Modelling aspect:</b> Kinetic modelling of syngas fermentation in a bubble column reactor in MATLAB environment</li> <li>• <b>Validation:</b> Literature data</li> <li>• <b>Thermodynamic performance analysis:</b> NA</li> <li>• <b>Optimization:</b> NA</li> </ul>	<ul style="list-style-type: none"> <li>• At higher <math>CO</math> concentrations the ethanol production reduces which in turn improves the acetate production.</li> <li>• Ethanol production is enhanced by high gas velocity.</li> <li>• Improved gas- liquid mass transfer enhanced the <math>CO</math> and <math>H_2</math> conversion.</li> </ul>
Ardila et al., 2014	<ul style="list-style-type: none"> <li>• <b>Process type:</b> Both gasification and syngas fermentation</li> <li>• <b>Modelling aspect:</b> gasification and syngas fermentation modelling in Aspen plus with gasification kinetics.</li> </ul>	<ul style="list-style-type: none"> <li>• Good agreement can be found between literature and model data.</li> <li>• <math>CO</math> production decreases with increasing SBR.</li> </ul>

	<ul style="list-style-type: none"> <li>• <b>Validation:</b> Model predicted syngas production validated with literature data</li> <li>• <b>Thermodynamic performance analysis:</b> NA</li> <li>• <b>Optimization:</b> NA</li> </ul>	<ul style="list-style-type: none"> <li>• Production of Acetic acid and ethanol increases with increasing ER.</li> </ul>
	<ul style="list-style-type: none"> <li>• <b>Process type:</b> Only syngas fermentation</li> <li>• <b>Modelling aspect:</b> Kinetic modelling of syngas fermentation using Luong and Monod kinetics for <math>CO</math> and <math>H_2</math> uptake respectively. Development of the suitable kinetic model for combined prediction of the model parameters.</li> <li>• <b>Validation:</b> NA</li> <li>• <b>Thermodynamic performance analysis:</b> NA</li> <li>• <b>Optimization:</b> NA</li> </ul>	<ul style="list-style-type: none"> <li>• Modified Gompertz model successfully predicted the fermentation kinetics.</li> <li>• Model confirmed Inhibitory effect of <math>CO</math> on gas uptake at higher <math>CO</math> concentrations.</li> </ul>

Mohammadi  
et al., 2014

### 2.4.1 Research gaps in modelling of ethanol production following syngas platform

The modelling studies, so far reported, are majorly developed based on the literature data on stand-alone syngas fermentation processes. The modelling of the whole hybrid process that include both gasification and syngas fermentation has just started in the last decade. So, there is a huge scope of research to develop mathematical models for the entire hybrid process. The previous literatures on modelling the gasification-fermentation process majorly focused on the ethanol yield. Literature having thermodynamic performance assessment of this process is very

rare. Very few previous research employed response surface methodology to estimate the combined effect of various parameters on response variables. Optimization of various process parameters is also lacking in this regard.

## 2.5 Economic, life cycle and risk assessment of bio-ethanol production technologies

To determine the overall sustainability of the ethanol production process it is necessary to determine the economic, environmental and investment risk of the process. The literature review on this topic is listed in Table 2.4.

**Table 2.4:** Literatures on economic, life cycle and risk assessment of bio-ethanol production technologies

Literature	Details	Observations
Regis et al., 2023	<ul style="list-style-type: none"> <li>• <b>Product/Products:</b> Ethanol</li> </ul>	
	<ul style="list-style-type: none"> <li>• <b>Ethanol production technology:</b> Switchgrass gasification and syngas fermentation</li> </ul>	<ul style="list-style-type: none"> <li>• With a switchgrass feeding rate of 1000 t/y, the minimum ethanol selling price is 7.04 \$/L. However, this MESP reduced to 1.07 \$/L with a switchgrass feeding rate of 750000 t/y.</li> </ul>
	<ul style="list-style-type: none"> <li>• <b>Economic assessment:</b> Yes, calculation of MESP</li> </ul>	
	<ul style="list-style-type: none"> <li>• <b>Life cycle analysis:</b> NA</li> <li>• <b>Risk analysis:</b> NA</li> </ul>	
Ma et al., 2022	<ul style="list-style-type: none"> <li>• <b>Product/Products:</b> Ethanol</li> </ul>	<ul style="list-style-type: none"> <li>• Economic evaluation of the process concluded an ethanol production cost of 430 €/t of ethanol.</li> </ul>
	<ul style="list-style-type: none"> <li>• <b>Ethanol production technology:</b> Gasification and syngas fermentation</li> </ul>	
	<ul style="list-style-type: none"> <li>• <b>Economic assessment:</b> Yes, Ethanol production cost calculation and optimization of total annual and product sales</li> </ul>	<ul style="list-style-type: none"> <li>• Optimized total annual cost was 19.9 M€ and total production cost of ethanol was 64.5 M€.</li> </ul>

	<ul style="list-style-type: none"> <li>• <b>Life cycle analysis:</b> NA</li> <li>• <b>Risk analysis:</b> NA</li> </ul>	
Baccar et al., 2022	<ul style="list-style-type: none"> <li>• <b>Product/Products:</b> Ethanol</li> <li>• <b>Ethanol production technology:</b> Tunisian waste date pretreatment, enzymatic hydrolysis and fermentation</li> <li>• <b>Economic assessment:</b> NA</li> <li>• <b>Life cycle analysis:</b> <p><b>Scope-</b> Cradle to gate</p> <p><b>System boundary-</b> date collection and ethanol production</p> <p><b>Functional unit-</b> 1 MJ of ethanol</p> <p><b>Comparison-</b> Standalone ethanol production unit</p> <p><b>Platform-</b> SimaPro 8</p> </li> <li>• <b>Risk analysis:</b> NA</li> </ul>	<ul style="list-style-type: none"> <li>• For the base case scenario, bio-ethanol production system produced 0.07 kg <math>CO_2</math> eq. per MJ of ethanol.</li> <li>• Acidification potential of the process was 0.34 g <math>SO_2</math> eq. per MJ of ethanol.</li> <li>• Use of renewable energy as the source of electricity successfully reduced the <math>CO_2</math> emission of the system.</li> </ul>
Okolie et al., 2021	<ul style="list-style-type: none"> <li>• <b>Product/Products:</b> Ethanol, bio-methane and <math>O_2</math></li> <li>• <b>Ethanol production technology:</b> Biomass gasification and syngas fermentation</li> </ul>	<ul style="list-style-type: none"> <li>• The MESP for ethanol production with carbon capture, electrolysis and bio-methane generation is 0.31\$/L.</li> <li>• Ethanol selling price is most sensitive towards the</li> </ul>

	<ul style="list-style-type: none"> <li>• <b>Economic assessment:</b> Yes, comparison of standalone ethanol production unit with multi-generation unit</li> <li>• <b>Life cycle analysis:</b> NA</li> <li>• <b>Risk analysis:</b> NA</li> </ul>	<ul style="list-style-type: none"> <li>• crude glycerol and electricity price.</li> </ul>
Michailos et al., 2019	<ul style="list-style-type: none"> <li>• <b>Product/Products:</b> Ethanol and Power</li> <li>• <b>Ethanol production technology:</b> Gasification of sugarcane bagasse and syngas fermentation</li> <li>• <b>Economic assessment:</b> Yes, calculation of ethanol selling price and other economic parameters like NPV, IRR and payback period</li> <li>• <b>Life cycle analysis:</b> Only GHG emission</li> <li>• <b>Risk analysis:</b> Yes, probability of non-negative NPV</li> </ul>	<ul style="list-style-type: none"> <li>• A mean profit of 40 M\$ was calculated for a minimum ethanol selling price of 0.71 \$/L.</li> <li>• Calculated payback period was 8 years.</li> <li>• Increase in CO conversion led to minimized production cost.</li> <li>• Increase in ER reduced the production cost of ethanol.</li> <li>• 11.5 g CO<sub>2</sub> eq. per MJ of ethanol was calculated with a wastewater generation of 1550 kg.</li> </ul>
Li et al., 2019	<ul style="list-style-type: none"> <li>• <b>Product/Products:</b> Jet fuel</li> <li>• <b>Ethanol production technology:</b> Biomass gasification of corn stalk followed by Fischer- Tropsh synthesis</li> </ul>	<ul style="list-style-type: none"> <li>• The jet fuel production without heat recovery is highly sensitive towards the electricity consumed by the process.</li> </ul>

	<ul style="list-style-type: none"> <li>• <b>Economic assessment:</b> Yes, Calculation of production cost followed by sensitivity analysis</li> <li>• <b>Life cycle analysis:</b>  <b>Scope-</b> Cradle to grave  <b>System boundary-</b> Corn cultivation, stalk procurement, gasification and FT synthesis of jet fuel, utilization  <b>Functional unit-</b> 1 ton of jet fuel  <b>Comparison-</b> Between jet fuel production modules with or without heat recovery  <b>Platform-</b> SimaPro 7.2</li> <li>• <b>Risk analysis:</b> NA</li> </ul>	<ul style="list-style-type: none"> <li>• Both of the scenarios are sensitive to the price of crude oil.</li> <li>• GHG emission of the jet fuel production scenario with heat recovery is 899.57 Kg <math>CO_2</math> eq. per ton of jet fuel whereas without heat recovery this emission was 1200 kg <math>CO_2</math> eq.</li> </ul>
<p><b>Hasanly et al., 2018</b></p>	<ul style="list-style-type: none"> <li>• <b>Product/Products:</b> Ethanol</li> <li>• <b>Ethanol production technology:</b> Simultaneous saccharification and co-fermentation</li> <li>• <b>Economic assessment:</b> Yes, calculation of minimum selling price of ethanol for different scenarios with sensitivity analysis</li> <li>• <b>Life cycle analysis:</b> NA</li> </ul>	<ul style="list-style-type: none"> <li>• For a production capacity of 316 t/day, the minimum selling price of ethanol was calculated 1.407 \$ l<sup>-1</sup>.</li> <li>• Minimum ethanol selling price is directly proportional to the production capacity of the bio-ethanol plant.</li> <li>• Inclusion of transportation cost breaks the monotonic nature of the MESP vs</li> </ul>

	<ul style="list-style-type: none"> <li>• <b>Risk analysis:</b> Yes</li> </ul>	<p>Production capacity curve.</p> <ul style="list-style-type: none"> <li>• For an MESP of 1.4 \$ l<sup>-1</sup> the probability of a non-negative NPV is 52%.</li> </ul>
Silva et al., 2017	<ul style="list-style-type: none"> <li>• <b>Product/Products:</b> Furfural and ethanol</li> <li>• <b>Ethanol production technology:</b> 1<sup>st</sup> generation ethanol production</li> <li>• <b>Economic assessment:</b> Yes, comparison of economic performance of simple 1G bio-ethanol production with small scale and large scale furfural production.</li> <li>• <b>Life cycle analysis:</b> NA</li> <li>• <b>Risk analysis:</b> Yes, probability of non-negative NPV</li> </ul>	<ul style="list-style-type: none"> <li>• The 1G bioethanol facility estimated an ethanol production cost of 1.15 \$/kg of ethanol.</li> <li>• Integration of small and medium scale furfural production plant reduced the ethanol production cost to 1.01\$/kg and 0.91\$/kg respectively.</li> <li>• The probability of a non-negative NPV for the 1G bio-ethanol production is 75.7% whereas the other two scenarios showed 100% probability of non-negative NPV.</li> </ul>
de Medeiros et al., 2017	<ul style="list-style-type: none"> <li>• <b>Product/Products:</b> Ethanol and electricity</li> <li>• <b>Ethanol production technology:</b> Biomass gasification and syngas fermentation</li> <li>• <b>Economic assessment:</b> Yes, calculation of minimum selling</li> </ul>	<ul style="list-style-type: none"> <li>• Minimum selling price of ethanol was found to be 706 US\$/m<sup>3</sup>.</li> <li>• Uncertainties are considered in fixed capital investment and in raw material price.</li> </ul>



	<p>price of ethanol along with sensitivity analysis</p> <ul style="list-style-type: none"> <li>• <b>Life cycle analysis:</b> NA</li> <li>• <b>Risk analysis:</b> Yes, Probability of non-negative NPV</li> </ul>	<ul style="list-style-type: none"> <li>• Minimum selling price of ethanol varies between 633 US\$/m<sup>3</sup> and 933 US\$/m<sup>3</sup> for a less probable non-negative NPV and a more probable non-negative NPV.</li> </ul>
Jana & De, 2017	<ul style="list-style-type: none"> <li>• <b>Product/Products:</b> Power, ethanol, cooling, heating</li> <li>• <b>Ethanol production technology:</b> Polygeneration</li> <li>• <b>Economic assessment:</b> No</li> <li>• <b>Life cycle analysis:</b> <b>Scope-</b> Cradle to gate <b>System boundary-</b> Rice straw procurement, polygeneration <b>Functional unit-</b> 1 kWh of electricity, 1 kg of ethanol, 1 tonne-h of refrigeration, 1 GJ of steam <b>Comparison-</b> polygeneration with standalone power generation unit <b>Platform-</b> SimaPro 7.2</li> <li>• <b>Risk analysis:</b> NA</li> </ul>	<ul style="list-style-type: none"> <li>• Thermo-chemical ethanol factory construction has significant impact on the environment.</li> <li>• CO<sub>2</sub> emission vary with the variation of the biomass transportation.</li> <li>• No significant change in the environmental impact parameters could be observed due to ethanol production instead of power generation.</li> </ul>
Handler et al., 2016	<ul style="list-style-type: none"> <li>• <b>Product/Products:</b> Ethanol</li> </ul>	<ul style="list-style-type: none"> <li>• For every MJ of ethanol the GHG emission was</li> </ul>

	<ul style="list-style-type: none"> <li>• <b>Ethanol production technology:</b> fermentation of steel mill waste and biomass gasification and syngas fermentation.</li> <li>• <b>Economic assessment:</b> NA</li> <li>• <b>Life cycle analysis:</b>  <b>Scope-</b> Cradle to grave  <b>System boundary-</b> Biomass procurement, biomass gasification, syngas fermentation and ethanol combustion  <b>Functional unit-</b> 1 MJ of ethanol  <b>Comparison-</b> Among various biomass to ethanol along with industrial waste gas fermentation  <b>Platform-</b> SimaPro 7.3</li> <li>• <b>Risk analysis:</b> NA</li> </ul>	<p>calculated to be 31.4 g <math>CO_2</math> eq. for industrial off gas, 8 g <math>CO_2</math> eq. for corn stover, 11.7 g <math>CO_2</math> eq. for switchgrass and 1.5 g <math>CO_2</math> eq. for forest residue.</p> <ul style="list-style-type: none"> <li>• Compared to petroleum gasoline standard forest residue derived ethanol provided a 98% reduction in GHG emission.</li> </ul>
Diederichs et al., 2016	<ul style="list-style-type: none"> <li>• <b>Product/Products:</b> Jet fuel</li> <li>• <b>Ethanol production technology:</b> Different ethanol production routes namely gasification and Fischer-Tropsh synthesis, Bio-chemical conversion to ethanol, gasification and syngas</li> </ul>	<ul style="list-style-type: none"> <li>• Minimum selling price of jetfuel was calculated to be 249.5 cents in the gasification-fermentation route which is third lowest among the five routes.</li> </ul>

	<p>fermentation, Hydro-processing of vegetable oils and sucrose fermentation using sugarcane juice followed by upgradation to jet fuel.</p> <ul style="list-style-type: none"> <li>• <b>Economic assessment:</b> Yes, calculation of minimum jetfuel selling price and economic sensitivity</li> <li>• <b>Life cycle analysis:</b> NA</li> <li>• <b>Risk analysis:</b> NA</li> </ul>	<ul style="list-style-type: none"> <li>• The minimum selling price of jetfuel is most sensitive towards the feedstock cost.</li> </ul>
Jana & De, 2015	<ul style="list-style-type: none"> <li>• <b>Product/Products:</b> Power, ethanol, refrigeration and <math>CO_2</math> removal</li> <li>• <b>Ethanol production technology:</b> Catalytic conversion of <math>CO</math> and <math>H_2</math>.</li> <li>• <b>Economic assessment:</b> Yes, calculation of different economic performance parameters.</li> <li>• <b>Life cycle analysis:</b> NA</li> <li>• <b>Risk analysis:</b> NA</li> </ul>	<ul style="list-style-type: none"> <li>• Total annualized fixed cost and operating cost were found to be 32 million and 17 million INR respectively.</li> <li>• Payback period for this polygeneration was 5.25 years with a return on investment of 14.9%.</li> </ul>
Yang & Chen, 2013	<ul style="list-style-type: none"> <li>• <b>Product/Products:</b> Bio-ethanol</li> <li>• <b>Ethanol production technology:</b> Corn fermentation</li> <li>• <b>Economic assessment:</b> No</li> </ul>	<ul style="list-style-type: none"> <li>• GHG emission of this corn-ethanol production is higher than the normal gasoline.</li> </ul>

	<ul style="list-style-type: none"> <li>• <b>Life cycle analysis:</b>  <b>Scope-</b> Cradle to gate  <b>System boundary-</b> corn cultivation and collection, ethanol production, ethanol purification and waste water treatment.  <b>Functional unit-</b> 1 kg of corn ethanol  <b>Comparison-</b> Standalone system  <b>Platform-</b> SimaPro 7.2</li> <li>• <b>Risk analysis:</b> NA</li> </ul>	<ul style="list-style-type: none"> <li>• The amount of GHG emission is 11.12 kg <math>CO_2</math> equivalent.</li> </ul>
Borrion et al., 2012	<ul style="list-style-type: none"> <li>• <b>Product/Products:</b> Bio-ethanol</li> <li>• <b>Ethanol production technology:</b> Enzymatic hydrolysis and fermentation</li> <li>• <b>Economic assessment:</b> Yes</li> <li>• <b>Life cycle analysis:</b>  <b>Scope-</b> Cradle to grave  <b>System boundary-</b> wheat cultivation and straw collection, ethanol production, ethanol distribution and blending, fuel use in vehicles</li> </ul>	<ul style="list-style-type: none"> <li>• E85 blend reduced 73% of GHG emission compared to the conventional petrol.</li> <li>• A significant increase in terrestrial ecotoxicity can be seen in case of E15 and E85 blends.</li> <li>• Pre-treatment of biomass in this method causes maximum damage to the environment.</li> </ul>

	<b>Functional unit-</b> 1 km travel in a small passenger car  <b>Comparison-</b> comparison among petrol, E15 and E85 blends  <b>Platform-</b> SimaPro 7.2  <ul style="list-style-type: none"> <li>• <b>Risk analysis:</b> NA</li> </ul>	
	<ul style="list-style-type: none"> <li>• <b>Product/Products:</b> Bio-ethanol</li> <li>• <b>Ethanol production technology:</b> waste wood gasification and syngas fermentation of wheat straw</li> <li>• <b>Economic assessment:</b> Calculation of minimum ethanol selling price with sensitivity analysis</li> <li>• <b>Life cycle analysis:</b> NA</li> <li>• <b>Risk analysis:</b> NA</li> </ul>	<ul style="list-style-type: none"> <li>• Minimum ethanol selling price (MESP) calculated was 2.05 \$/gallon of ethanol.</li> <li>• Plant capacity is the highest contributing factor in the calculation of MESP followed by the internal rate of return.</li> </ul>

### 2.5.1 Research gaps in economic, life cycle and risk assessment of bio-ethanol production technologies:

Comprehensive literature review in this topic suggested that various researcher delved into economic, life cycle and risk analysis of various bio-ethanol production technologies. Yet there exists significant research gap in overall sustainability analysis involving economic, investment risk and environmental analysis of the bio-ethanol production process. There is scarcity of research involving the overall sustainability analysis of co-gasification and syngas fermentation as well.

## 2.6 Research objectives

After identifying the research gaps in the comprehensive literature review the following objectives have been identified for this study

- Equilibrium modelling and thermodynamic performance assessment of biomass co-gasification in Aspen plus using three of the most abundantly available lignocellulosic Indian agro-wastes, namely rice straw, sugarcane bagasse and wheat straw fed in the combination of two.
- Assessment of thermodynamic performance and optimization of the co-gasification process parameters to maximize the energy and exergy efficiency of the process using Response Surface Methodology.
- Elimination of the least performing biomass combination for further studies.
- Kinetic modelling and optimization of process parameters of biomass co-gasification in Aspen plus for the two combinations of biomass feedstocks.
- Analysis of the combined effect of various input parameters on the energy and exergy efficiency of the kinetic model.
- Optimization of the process parameters to maximize the energy and exergy efficiency of the process and selection of best performing biomass blend for syngas production.
- Equilibrium modelling and parametric optimization of biomass co-gasification and syngas fermentation process using the best performing biomass mixture in the co-gasification kinetic model in Aspen plus.
- Sensitivity analysis of various gasification and fermentation parameters like  $LHV_{\text{synags}}$ ,  $H_2/CO$  ratio, CGE, Ethanol production rate and overall energy efficiency with temperature and equivalence ratio.
- Optimization of input variables to maximize the ethanol production rate and energy efficiency along with the reduction of total  $CO_2$  emission from the process model.
- Integration of power generation and heat and resource recovery in the co-gasification-syngas fermentation model.

- Comprehensive techno economic analysis of the modified model to determine the minimum selling cost of ethanol, net present value and payback period.
- Investment risk analysis using Monte-Carlo simulation to determine the probability a non-negative NPV
- Life cycle analysis of the developed co-gasification fermentation model to determine the environmental impact of the process.

## **2.7 Scope of the research work**

This research aims to contribute in the field of bio-fuel research in the Indian context. As per the Indian biofuel policy ethanol has appeared as a potential candidate to be mixed with gasoline. To produce ethanol in a sustainable manner the hybrid pathway of biomass co-gasification and syngas fermentation has been explored to replace the conventional ethanol production process of sugar fermentation. The overall sustainability analysis of the overall process is also important to determine the possible commercialization aspect of the entire process.





## Chapter 3. Materials and Methods

### 3.1 Introduction

This thesis is focused on the exploration of Indian agro-waste for the production of bio-ethanol. As already discussed India has an abundance agricultural waste. The feedstocks used and the methodology followed for the simulation process have been discussed in this chapter.

### 3.2 Materials

Wheat straw, sugarcane bagasse and rice straw have been selected as the feedstock in this study. The reason for selecting these three agro-waste is because of their abundant availability in most of the parts of India.

The elemental composition of the three biomass has been presented in Table 3.1

**Table 3.1:** Elemental analysis of the feedstock (Livingston, 1991; Miles et al., 1995)

Analysis		Rice Straw	Wheat Straw	Sugarcane Bagasse
<b>Proximate Analysis</b> (% As received basis)	Moisture	7.93	15.10	10.39
	Fixed Carbon	14.60	14.98	10.71
	Volatile Matter	60.28	62.32	76.72
	Ash	17.19	7.60	2.19
<b>Ultimate Analysis</b> (% dry basis)	Carbon (C)	38.24	43.92	48.64
	Hydrogen (H)	4.79	5.52	5.87
	Nitrogen (N)	0.87	0.73	0.16
	Oxygen (O)	36.44	40.88	42.89
	Sulphur (S)	0	0	0
	Ash	18.67	8.95	2.44
<b>Heating Value</b> (MJ/kg)	Lower Heating Value (LHV)	13.95 MJ/kg	16.45 MJ/kg	17.71 MJ/kg

### 3.3 Methodology of modelling in Aspen plus

Two type of process models have been developed using Aspen plus namely equilibrium and kinetic model.

#### 3.3.1 Aspen plus simulation of equilibrium models

Equilibrium models of gasification have been developed using aspen plus for a long time now. Aspen plus is a software that simulates various chemical processes with inbuilt unit operation blocks or user defined blocks with the help of its large quantity of physical and chemical data library of various components. Gasification is not present in Aspen plus as a single unit operation block so it is necessary to connect various unit operation, transfer and manipulator blocks to form a consolidated simulation. The whole process is completed in a number of steps. The flow diagram is provided in Figure 3.1

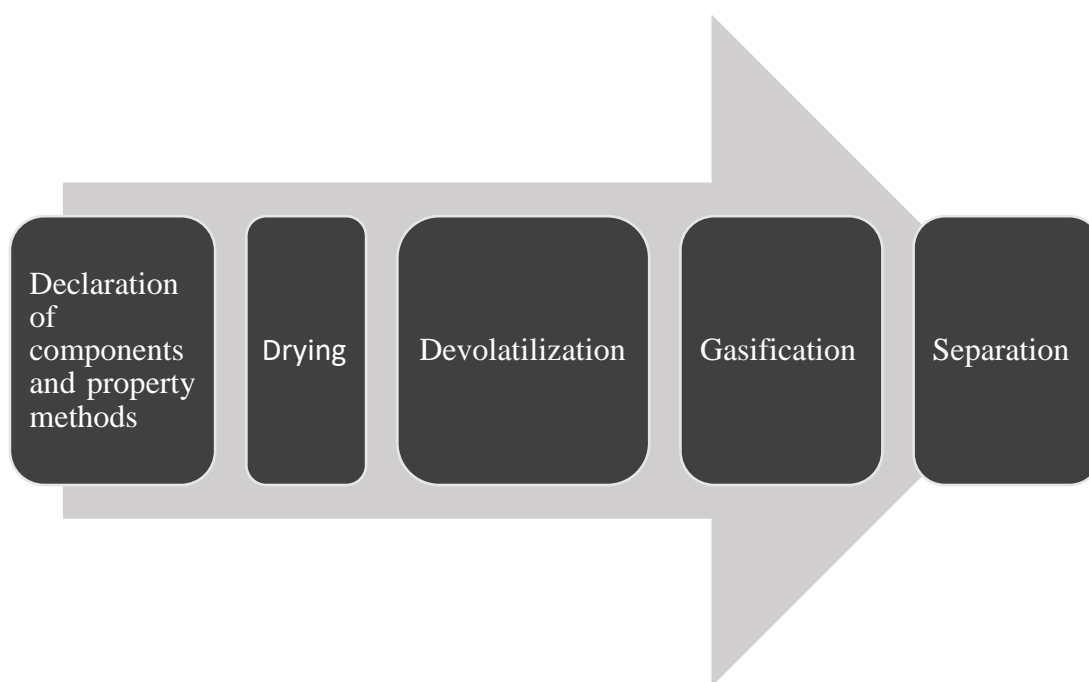


**Figure 3.1:** Methodical representation of Aspen plus equilibrium modelling

#### Declaration of components and property methods

Firstly in Aspen plus, it is necessary to declare the components participating in the gasification process. It is known that the biomass is not defined by a particular molecular formula so biomass is declared as a non-conventional component in aspen plus. As a non-conventional component it is necessary for biomass to provide its ultimate and proximate analysis along with

an enthalpy and density model. Enthalpy and density models chosen in most of the literatures are HCOALGEN and DCOALIGT (Pati et al., 2020). Other conventional components are also specified from the aspen plus database. A suitable property method stating the equation of state for the gaseous and liquid elements is then selected to calculate the thermodynamic parameters of various elements. In gasification modelling IDEAL method (Tungalag et al., 2020), Peng-Robinson cubic equation of state (PENG-ROB) (Adnan et al., 2017; Gagliano et al., 2017a; Okolie et al., 2020), Peng-Robinson cubic equation of state with Boston-Mathias alpha function (PR-BM) (Doherty et al., 2013; Safarian, Richter, et al., 2019; Wan, 2016; Zhai et al., 2016), Redlich-Kwong cubic equation of state, Redlich-Kwong cubic equation of state with Boston Mathias alpha function (RK-BM), Redlich-Kwong-Soave cubic equation of state and Redlich-Kwong-Soave cubic equation of state with Boston Mathias alpha function (RKS-BM) (Begum et al., 2014; Tavares et al., 2020) are the most utilised property methods. Using these property methods the properties of gaseous elements are needed to be determined by running the property analysis.

### 3.3.1.1 Drying

The simulation is conducted first by passing the biomass through a stoichiometric block (RStoic) for drying. Here with the help of dry air a pseudo stoichiometric reaction is assumed and moisture is released from biomass at a temperature range of 100-150°C. The equation for drying is as follows.



### 3.3.1.2 Devolatilization

The dry biomass is then transferred to a decomposer block (RYield) to convert the non-conventional biomass into conventional elements according to its ultimate analysis at a temperature range of 350-500°C. A calculator block is employed to specify the yields of the products. This process is basically a simulative assumption of the pyrolysis process where most of the researchers have approached it with breaking the biomass according to its ultimate analysis (Barrera et al., 2014; Doherty et al., 2008; Han et al., 2017). But in some cases researchers have also tried to specify the yields of pyrolysis products from actual experimental results. Another interesting way to model this devolatilization process is to break the biomass into its elemental composition of lignin, cellulose and hemicellulose and then according to the pyrolysis data of these elemental constituents, model the devolatilization.

### **3.3.1.3 Gasification**

Furthermore, RStoic or RGibbs blocks are used to carry out the oxidation and reduction equations of gasification. In the RStoic block reaction equilibrium is performed with the help of equilibrium constants of various oxidation and reduction gasification reactions. Whereas the RGibbs block performs the elemental equilibrium by minimizing the Gibbs free energy of the reactant and product mixture. Now, the simulation of gasification reactions can be performed in two methods. First one is to separate the solid char from the pyrolysis mixture and performing the heterogeneous reactions separately. The second one is to consider all the products at the same time and then send them to an RGibbs block for simultaneous reaction simulation.

### **3.3.1.4 Separation**

After the gasification is complete the gas-solid mixture is sent to a separator block for the removal of ash and any other solid impurities present after gasification.

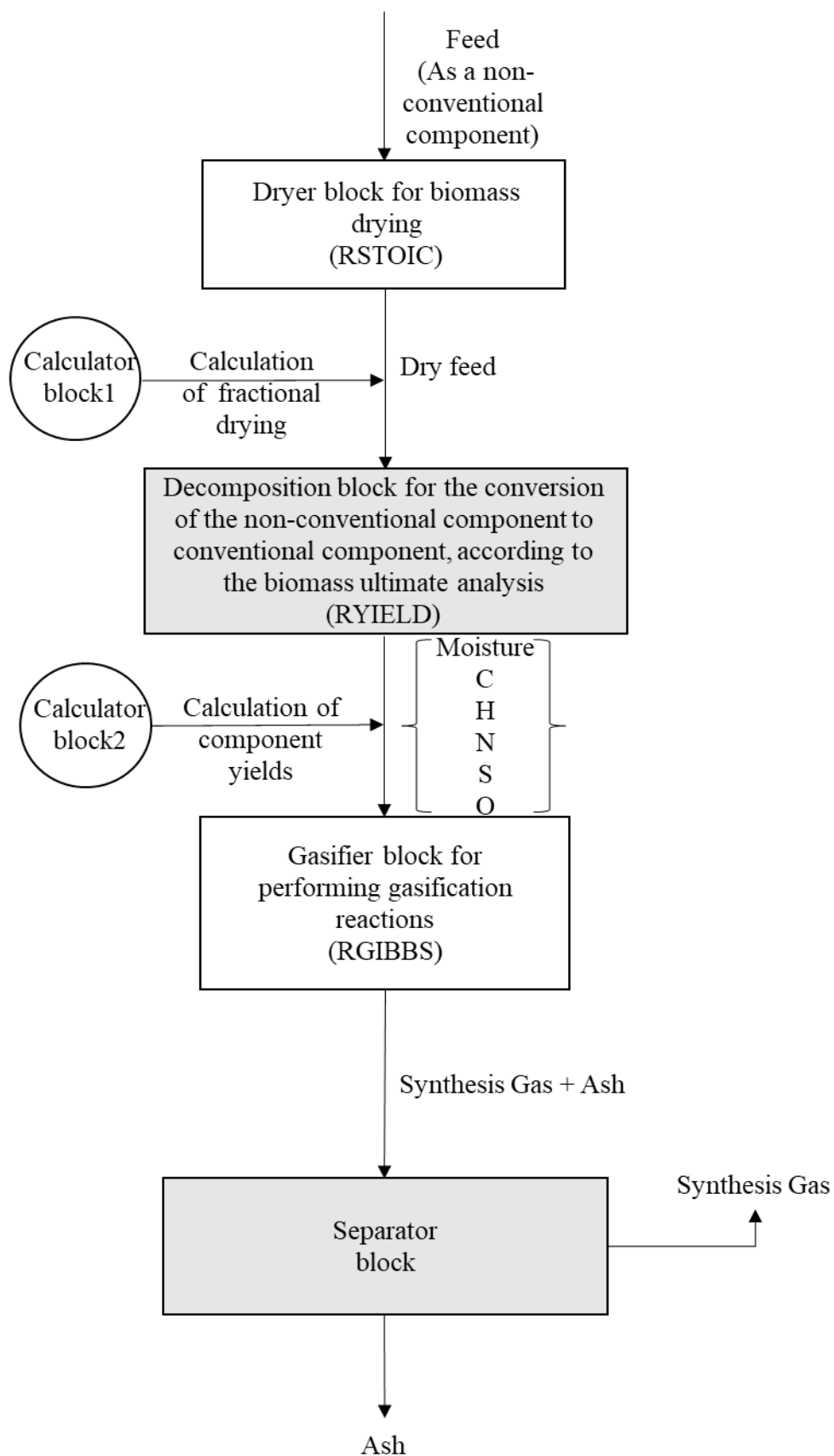


**Figure 3.2:** Process flow diagram of Aspen plus equilibrium modelling

### **3.3.1.5 Aspen plus simulation of kinetic models**

In Aspen plus, reactors like RCSTR and RPLUG use reaction kinetics for the simulation. The kinetic model of gasification varies from the equilibrium model only in the gasification part. In kinetic modelling also, it is necessary to declare the property method. It facilitates the calculation of various thermodynamic quantities according to the chosen equation of state. Biomass drying is also modelled as discussed in 3.3.1.1. The devolatilization step is generally modelled using the process discussed in 3.3.1.2. However, some researchers have also employed pyrolysis kinetics in determining the pyrolysis products (Ardila et al., 2014; Pauls et al., 2016). Modelling of the heterogeneous and homogeneous char combustion and gasification reactions is the main feature where various models differ. It is a general practice to separately model the heterogeneous and homogeneous reactions (Yu & Smith, 2018). Heterogeneous reactions being a process of gas-solid interaction poses more complicated reaction kinetic expression compared to the homogeneous reactions where gas is only reacting state. Some studies have also modelled gasification kinetics by using user defined block where all the kinetic expressions have been entered as FORTRAN subroutines (Nikoo & Mahinpey, 2008). Tar formation and cracking reactions can also be handled in Aspen plus kinetic models. In Aspen plus tar components are specified as aromatic hydrocarbons, phenols etc.. Figure 3.3 shows the modelling procedure of gasification involving reaction kinetics in Aspen plus.

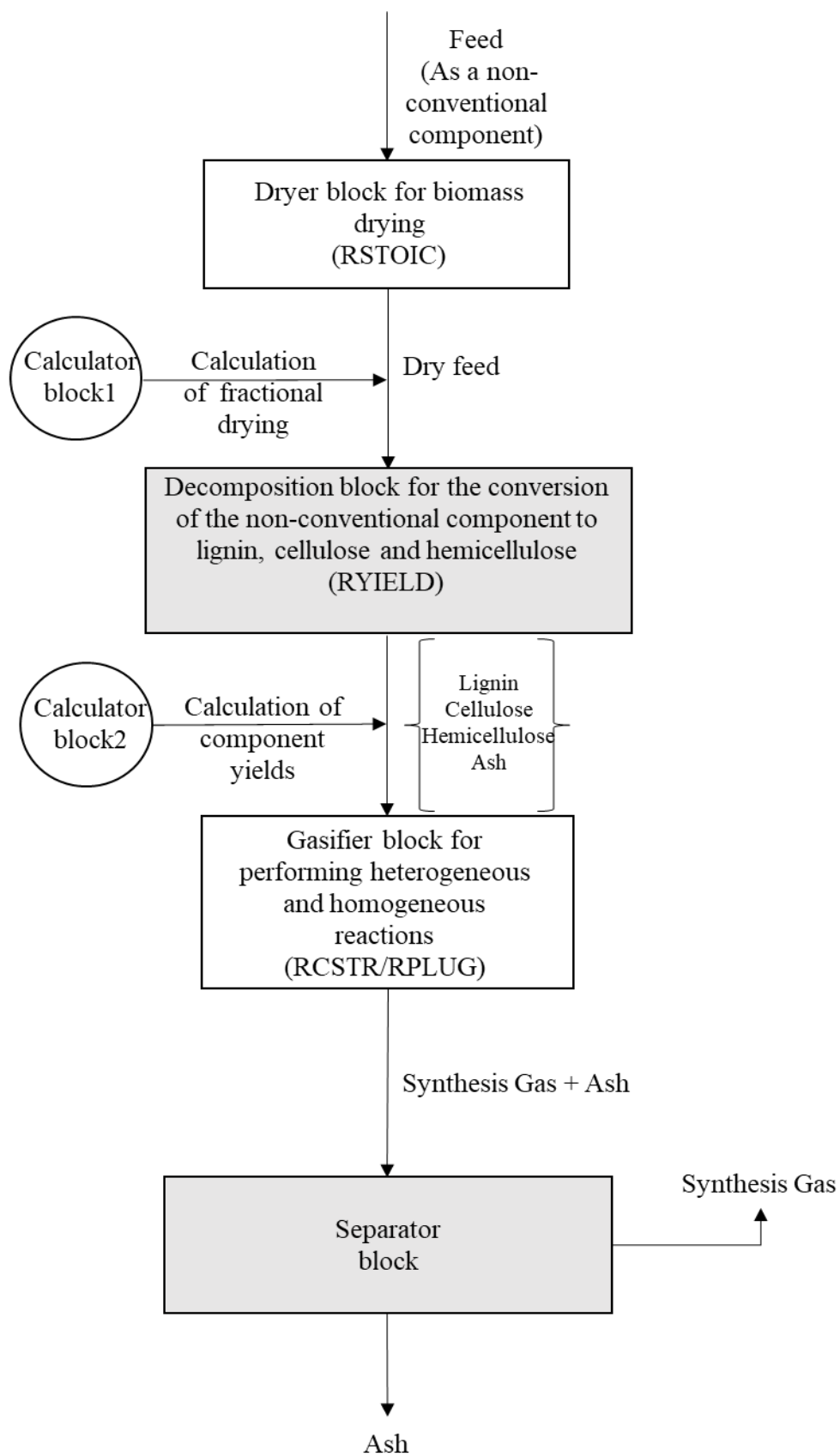


**Figure 3.3:** Process flow diagram of Aspen plus kinetic modelling

### **3.4 Aspen plus modelling of syngas fermentation**

The process of syngas fermentation modelling in Aspen plus is in its early stage. Generally the complexities involved in the gas- liquid mass transfer is ignored and the process is modelled assuming stoichiometric equilibrium. The RSTOIC block is used for this purpose and the reactions 3-6 are used in the model for predicting the ethanol production. A suitable fraction conversion for CO and H<sub>2</sub> is provided from the literature. The fermentation medium is considered to be water in Aspen plus as nutrients are not available in the Aspen plus library.

### **3.5 Chapter summary**

Selection of material and methodology is one of the most crucial thing in any simulation study. The particulars of the simulation methodology has been discussed in the following chapters where the individual modelling are conducted.



---

## **Chapter 4. Equilibrium modelling and thermodynamic analysis of Indian lignocellulosic biomass co-gasification using Aspen plus**

---

### **4.1 Objective of the chapter**

Main objectives of the present study are-

- i. Modelling of a fixed-bed downdraft gasification process based on Gibbs free energy minimization for the co-gasification of mixed lignocellulosic biomass using Aspen plus.
- ii. Thermodynamic evaluation based on energetic and exergetic performance to assess the process performance.
- iii. Optimization of the input parameters for the maximization of energy and exergy efficiency
- iv. Selection of suitable feedstock for co-gasification.

### **4.2 Modelling aspect**

Aspen plus software has been widely explored as a potential tool for the modelling of complex chemical processes. The modelling process of biomass co-gasification has its complexity due to the chemical reactions and product formation at different stages. Co-gasification follows four basic steps: drying of the biomass, devolatilization or pyrolysis, combustion of the volatile particles, and finally gasification of the char particles. For simulation modelling, three biomass from Indian origin, viz., rice straw, wheat straw and sugarcane bagasse are used as feedstock. They are fed to the gasification model as a combination of two biomass at a time. The modelling assumptions are:

- i. The process is isothermal and all blocks are considered to be zero dimensional and fully insulated.
- ii. Residence time of all elements inside a particular block is long enough to attain chemical equilibrium.
- iii. This is a kinetic-free and tar-free model.

In Aspen plus, biomass is not specified as a conventional component with chemical formulae but as a non-conventional component specifying elemental analysis. For this study, the elemental analysis of biomass along with their lower heating values are provided in Table 3.1.

Enthalpy and density model selected for the modelling are HCOALGEN, DCOALIGT respectively. Peng- Robinson equation of state with Boston-Mathias modifications (PR-BM) has been used as the property method (Jana & De, 2014) for calculating physical properties of conventional components and MIXCINC is the stream class used here. The approach of Gibbs free energy minimization has been utilized to develop a steady state model for this study

Figure 4.1 shows the Aspen plus flowsheet of the co-gasification model using air-steam mixture as the gasifying agent.

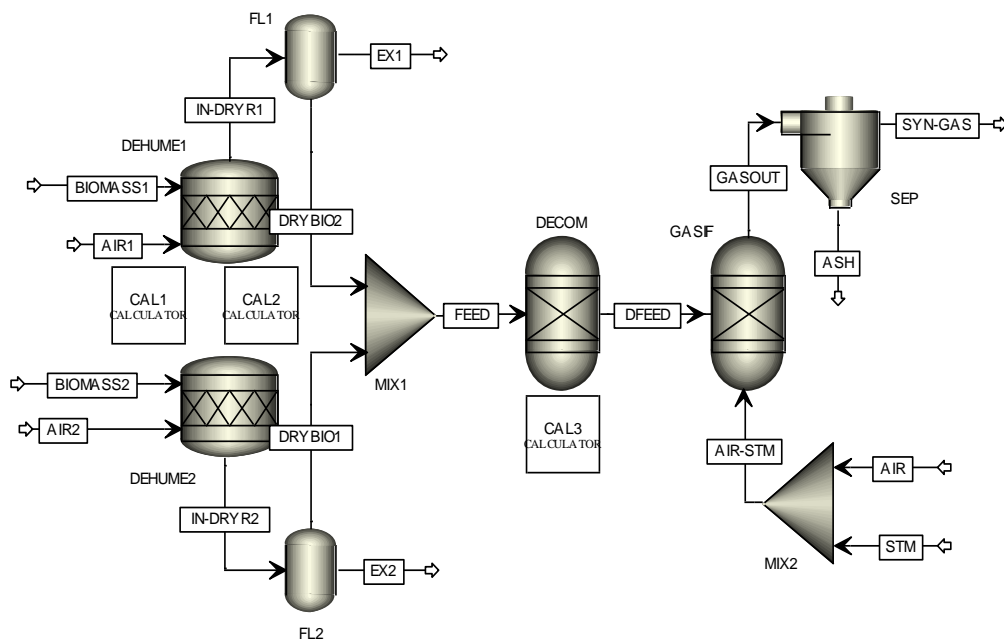


**Figure 4.1:** Co-gasification model developed in Aspen plus

Table 4.1 describes the utility of each block used in this co-gasification modelling.

**Table 4.1:** Description of the blocks used in co-gasification model

Block name in the Model	Block ID in Aspen plus®	Utility
<b>DEHUME1 and DEHUME2</b>	RStoic	Removes moisture from the LBs with the help of AIR1 and AIR2 stream following given stoichiometry and conversion factor
<b>FL1 and FL2</b>	Flash2	Separates moisture and dried biomass
<b>MIX1</b>	Mixer	Blends both the dried LBs

<b>DECOMP</b>	RYield	Converts biomass into conventional elements with the help of a calculator block.
<b>MIX2</b>	Mixer	Blends both the gasifying streams HOT-AIR and STM and forwards further
<b>GASIF</b>	RGibbs	Carries out gasification according to the Gibbs free energy minimization technique
<b>SEP</b>	SSplit	Separates ash from the rest of the gas mixture

The model is clearly divided into four sub-models: drying, devolatilization, gasification and separation. Despite the simultaneous feeding of biomass, the drying process shows the dehumidification, taking place in two separate stoichiometric reactors namely DEHUME1 and DEHUME2, with the help of hot-air blown over the palletized biomass. From the dryer block, the dehumidified biomass moves for devolatilization in the DECOMP block. This block is RYield block where the non-conventional biomass turns into conventional elements according to the ultimate analysis of the feedstock (i.e. C, H<sub>2</sub>, N<sub>2</sub>, O<sub>2</sub> and Ash). The conversion is done with the help of an embedded FORTRAN subroutine connected to a calculator block that calculates the product yields in DCOMP block. After the devolatilization, the constituent elements react with air-steam mixture shown in the model as AIR-STM stream for gasification in the block GASIF which is an RGibbs block and produces a mixture of CO, H<sub>2</sub>, CO<sub>2</sub>, H<sub>2</sub>O, CH<sub>4</sub>, NH<sub>3</sub> and Ash. The co-gasification reactions taking place inside the RGibbs reactor are R3- R14. Finally, the ash is separated from the gas mixture by passing the whole mixture through a SEP block.

### 4.3 Thermodynamic Performance Assessment

In the course of thermodynamic performance assessment the energy balance equation for a steady-state steady-flow process can be written as:

$$\sum \dot{m}_i h_i = \sum \dot{m}_e h_e \quad (4.1)$$

where,  $\dot{m}_i$ ,  $\dot{m}_e$ ,  $h_i$  and  $h_e$  represent the mass flow rates and specific enthalpies at entry and exit respectively.

Exergy balance can be carried out as provided in Eq. 4.2 (Sreejith et al., 2014).

$$Ex_{rec} = I_{proc} + Ex_{prod} \quad (4.2)$$

Here,  $Ex_{rec}$  is exergy flow in the reactant stream, while  $Ex_{prod}$  and  $I_{proc}$  refer to exergy flow of product stream and total irreversibility present in the process, respectively.

Equation 4.3 shows The LHV of mixed lignocellulosic biomass ( $LHV_{mlb}$ ):

$$\dot{m}_{total} \times LHV_{mlb} = \dot{m}_{biomass1} \times LHV_{biomass1} + \dot{m}_{biomass2} \times LHV_{biomass2} \quad (4.3)$$

where ,  $\dot{m}_{biomass1}$  and  $\dot{m}_{biomass2}$  are the mass flow rates of total and individual biomass and  $LHV_{biomass1}$  and  $LHV_{biomass2}$  are the lower heating values of respective biomass.

The lower heating value of the produced syngas ( $LHV_{syngas}$ ) is represented as given in Eq. 4.4 (Yu & Smith, 2018)-

$$LHV_{syngas} = 12.636 \times V_{frac_{H_2}} + 10.798 \times V_{frac_{CO}} + 35.818 \times V_{frac_{CH_4}} \quad (4.4)$$

where,  $V_{frac_{H_2}}$ ,  $V_{frac_{CO}}$  and  $V_{frac_{CH_4}}$  represent the respective volume fractions of  $H_2$ ,  $CO$  and  $CH_4$  in the produced syngas.

The required energy efficiency can now be formulated as-

$$\eta_{energy} = \frac{\dot{m}_{syngas} \times LHV_{syngas}}{\dot{m}_{total} \times LHV_{mlb} + \dot{m}_{air} \times C_{p,air} \times \Delta T + \dot{m}_{water} \times C_{p,water} \times \Delta T + \dot{m}_{water} \times L_{water}} \quad (4.5)$$

where  $\dot{m}_{syngas}$ ,  $\dot{m}_{air}$  and  $\dot{m}_{water}$  are the total mass flow rates of syngas, air and water.  $C_{p,air}$  and  $C_{p,water}$  are specific heat capacities of air and water respectively,  $\Delta T$  is the temperature difference and  $L_{water}$  is the latent heat of vaporisation of water.

Total exergy ( $Ex_{tot}$ ) of any flowing stream consists of two major parts, viz. physical exergy ( $Ex_{phy}$ ) and chemical exergy ( $Ex_{chem}$ ).

$$Ex_{tot} = Ex_{phy} + Ex_{chem} \quad (4.6)$$

Physical exergy is defined as

$$Ex_{phy} = h - h_0 - T_0(s - s_0) \quad (4.7)$$

where  $h$  and  $s$  are the enthalpy and entropy at any specified temperature ( $T$ ) and pressure ( $P$ ) and  $h_0$  and  $s_0$  are enthalpy and entropy at atmospheric condition ( $T_0 = 298.15^\circ C$ ,  $P_0 = 1 \text{ atm}$ ).

Chemical exergy is estimated by Eq. 4.8 which is as follows (Monir et al., 2020):

$$Ex_{chem} = \sum_i X_i Ex_{0,i} + RT_0 \sum_i X_i \ln X_i \quad (4.8)$$

where  $X_i$  is the mole fraction of  $i^{\text{th}}$  component,  $Ex_{0,i}$  is the standard chemical exergy of the  $i^{\text{th}}$  component and  $R$  is the universal gas constant.

As the biomass is fed to the gasifier at atmospheric condition, its physical exergy is considered to be negligible. So, exergy of biomass is practically the chemical exergy of it as stated below (Rupesh et al., 2016b):

$$Ex_{biomass} = \beta \times LHV \quad (4.9)$$

where  $Ex_{biomass}$  is the total exergy of any biomass and  $\beta$  is a multiplying factor which is calculated by utilizing Eq. 4.10 (Rupesh et al., 2016b).

$$\beta = \frac{1.0414 + 0.0177 \left[ \frac{H}{C} \right] - 0.3328 \left[ \frac{O}{C} \right] \{ 1 + 0.537 \left[ \frac{H}{C} \right] \}}{1 - 0.4021 \left[ \frac{O}{C} \right]} \quad (4.10)$$

where hydrogen ( $H$ ), carbon ( $C$ ), nitrogen ( $N$ ) and oxygen ( $O$ ) are obtained from the ultimate analysis of biomass.

Thus exergy efficiency can be determined by Eq. 4.11 as:

$$\eta_{Exergy} = \frac{Ex_{syngas}}{Ex_{biomass1} + Ex_{biomass2} + Ex_{air} + Ex_{steam}} \quad (4.11)$$

Where  $\eta_{Exergy}$  is the exergetic efficiency of the simulation model,  $Ex_{syngas}$ ,  $Ex_{air}$  and  $Ex_{steam}$  are the total exergy of syngas, air, and steam respectively.

## 4.4 Results and Discussions

### 4.4.1 Model Validation

To validate the equilibrium model developed in Aspen plus, the experimental study on co-gasification of wood and Indian coal in a fixed bed downdraft gasifier by Sharma et al., 2015 has been selected. In both literature and our study, air-steam mixture acts as the gasifying agent. The feedstock characteristics are provided in Table 4.2.

**Table 4.2:** Elemental analysis of the feedstock used in the experiments of Sharma et al., 2015

Analysis		Wood	Indian coal
<b>Proximate analysis</b> (% dry basis)	Moisture	10	8
	Fixed Carbon	8.7	41
	Volatile matter	81	30
	Ash	0.3	21
<b>Ultimate Analysis</b> (% dry basis)	Carbon (C)	44.4	53.2
	Hydrogen (H)	6.3	3.2
	Nitrogen (N)	0.6	3.2
	Oxygen (O)	48.8	39.9
	Sulphur (S)	0	0.42

The feedstock for the simulation model has been tuned to the ultimate and proximate analysis of wood (W) and Indian coal (C) and validated against the results obtained from experiments conducted at 85% W + 15% C and 75%W + 25% C. Similar gasification parameters like feed rate, temperature, air-steam flow rate are maintained. Figure 4.2 describes the comparison

between simulated and experimental volume percentage of  $H_2$ ,  $CO$ ,  $CO_2$  and  $CH_4$  production in the form of a bar chart.

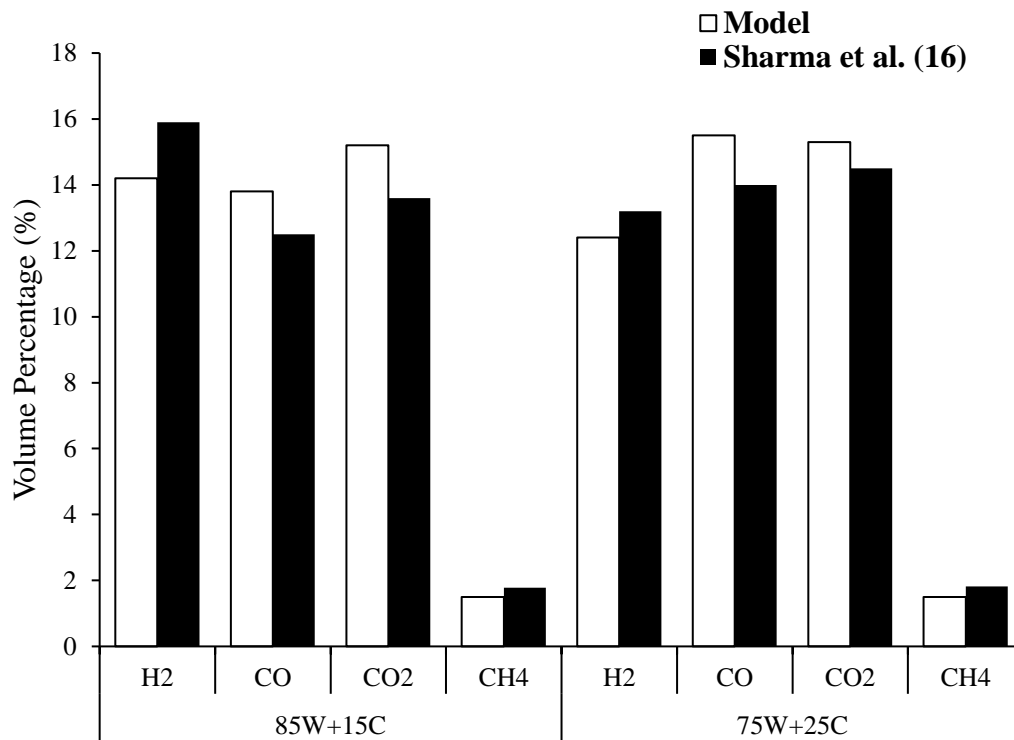


**Figure 4.2:** Comparison of volume percentage between model and experimental results of Sharma et al. 2015

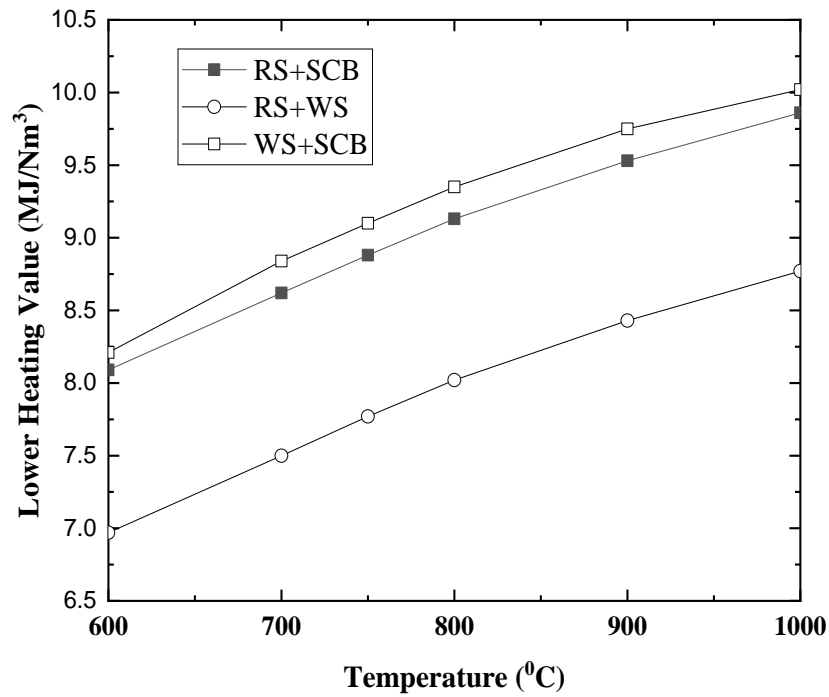
The figure clearly indicates that the experimental values are higher than model values in case of  $H_2$  and  $CH_4$  yield, but lower in case of  $CH_4$  and  $CO_2$ . Calculating the percentage error in the model for each of the constituent gas yield, it can be inferred that the percentage error is not more than 10% for each case.

#### 4.4.2 Thermodynamic performance results

The simulation model runs at the base condition of 100 kg/hr feed rate, gasifier temperature of 750°C, equivalence ratio of 0.35 and steam to biomass ratio of 0.5. In this condition, using rice straw and sugarcane bagasse at 1:1 mass ratio as feedstock, the model yields 24.75% v/v of  $H_2$ , 19.71% v/v of  $CO$  and 1.3% v/v of  $CH_4$ . Now, using rice straw and wheat straw at 1:1 mass ratio as feedstock, it yields 24.4% v/v of  $H_2$ , 18.8% v/v of  $CO$  and 1.9% v/v of  $CH_4$ . Finally, using wheat straw and sugarcane bagasse as feedstock, it yields 30.6% v/v of  $H_2$ , 25.3% v/v of  $CO$  and 0.9% v/v of  $CH_4$ . Evidently, syngas yield is higher for the combined feedstock of wheat straw and sugarcane bagasse, because of their higher carbon and hydrogen content in the

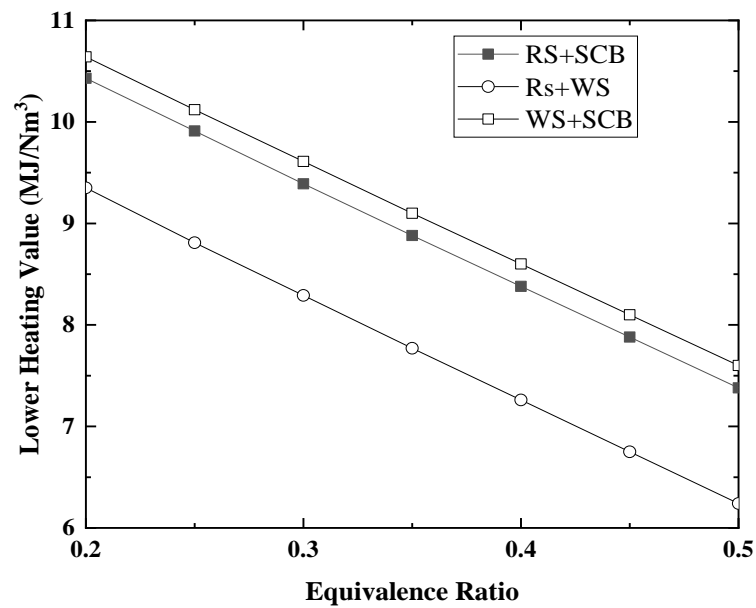
ultimate analysis.

The lower heating value (LHV) is an important measure of the energy potential of the produced syngas. To find out the variation of LHV with temperature the gasification temperature is varied from 600°C to 1000°C keeping the other operating variables constant. Figure 4.3 depicts the variation of LHV with temperature. It can be seen that the LHV increases with gasifier temperature rise, due to the increase in the production of syngas at elevated temperatures. Zhai et al., 2016 observed similar results as observed in the present study.



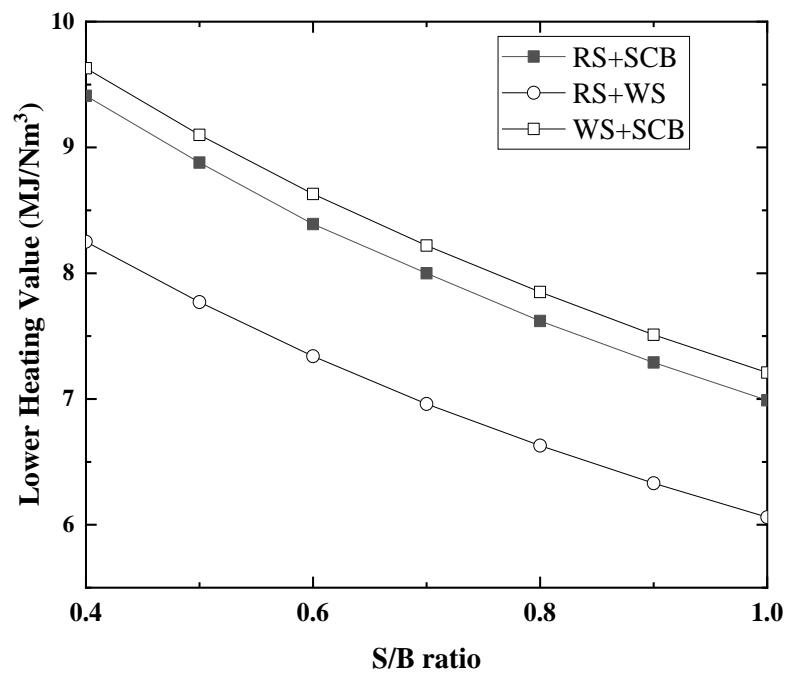
**Figure 4.3:** Variation of LHV of syngas with gasification temperature

Figure 4.4 shows the variation of LHV with equivalence ratio. Figure shows that increasing equivalence ratio adversely affects the gasification yield as well as the LHV.



**Figure 4.4:** Variation of LHV of syngas with equivalence ratio

Figure 4.5 shows the variation of LHV with steam to biomass ratio. Here also, an adverse effect is observed due to the decrease in  $CO$  production. However,  $H_2$  production increases with the presence of more steam in the system.



**Figure 4.5:** Variation of LHV of syngas with steam to biomass ratio



The variation of energy and exergy efficiency with temperature is presented in Figure 4.6(a) and Figure 4.6(b). Along with the variation of temperature from 600°C to 1000°C, both efficiencies increase and energy efficiency is higher than exergy efficiency. However, the rate of increase of the exergy efficiency is considerably lower after 700°C. Energetic efficiency rises from 50.7% to 64.8% in case of rice straw and sugarcane bagasse mixture, which is the highest among the rest biomass mixtures. In case of exergy efficiency, the highest rise is observed in wheat straw and sugarcane bagasse mixture which is 34% to 36.4%. The constant rise happens as the molar yield of syngas gets elevated at higher temperature, thus increasing the LHV of the produced syngas. But with the rise in temperature, the physical exergy of the gasifying agent (air-steam) rises significantly. Henceforth, the exergy efficiency curve is more or less horizontal after 700°C. Mojaver et al., 2019 used different biomass for the performance analysis of the gasification system and concluded that increase in temperature improves both the energy and exergy efficiencies, which is at per the findings of the present study. Wang & Chen, 2013 also reached similar conclusions while investigating co-gasification of biomass and coal. This literature also concluded that, at a particular temperature energy efficiency is higher than the exergy efficiency, which supports the finding of the present study.

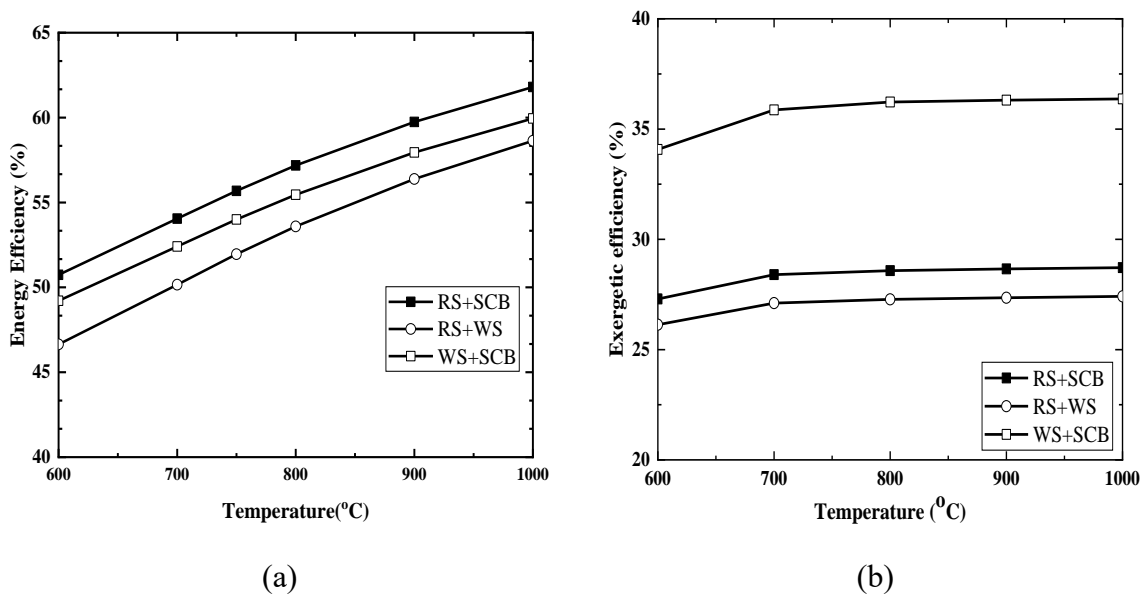


**Figure 4.6:** Variation of (a) energy efficiency and (b) exergy efficiency with Temperature (°C) at an equivalence ratio 0.35 and steam/biomass ratio 0.5

Figure 4.7 (a) and Figure 4.7(b) show the variation of energy and exergy efficiencies with the change in equivalence ratio from 0.2 to 0.5. A monotonically decreasing trend is seen for both efficiencies in all the biomass mixtures. But, energy efficiency is highest in case of rice straw

and sugarcane bagasse mixture, which is 65.6% at 0.2 equivalence ratio. However, wheat straw and sugarcane bagasse mixture shows most improved exergy efficiency of 49.7% at 0.2 equivalence ratio. This is because increased air flow shifts the gasification reactions towards combustion. Hence, LHV of the syngas decreases while decreasing both the efficiencies. The study of Adnan & Hossain, 2018 favours the finding of the present study. Patel et al., 2017 investigated the exergy efficiency of biomass co-gasification at various equivalence ratio and found similar trends depicted in the present study.

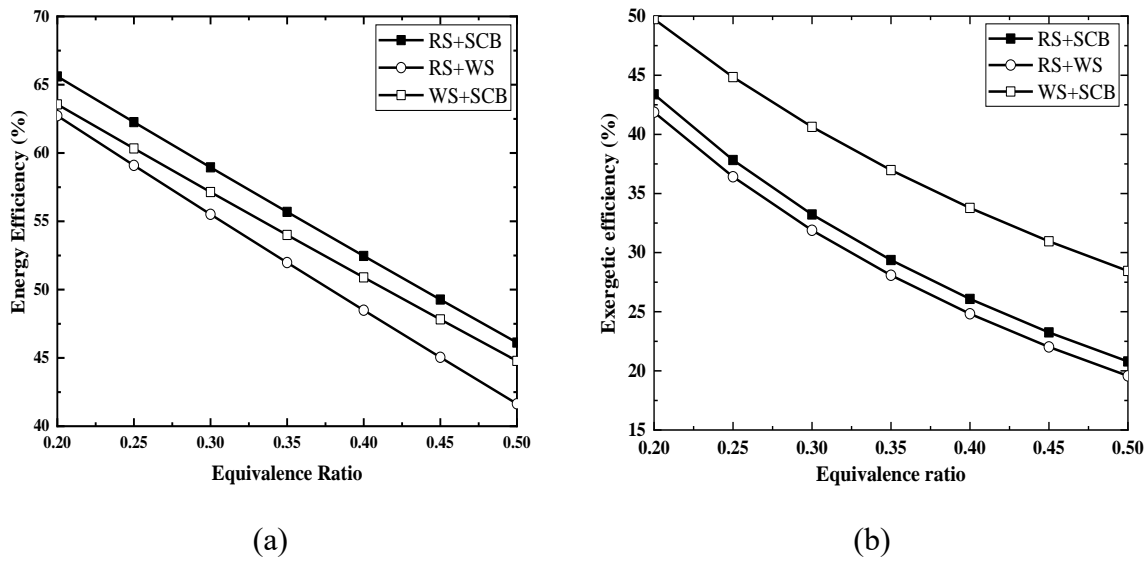


**Figure 4.7:** Variation of (a) energy efficiency and (b) exergy efficiency with equivalence ratio at a gasifier temperature 750°C and steam/biomass ratio 0.5

Figure 4.8(a) and Figure 4.8(b) show effects of steam to biomass ratio on energy and exergy efficiencies. Here also, a decreasing trend is observed with the increase in steam to biomass ratio from 0.4 to 1. Rice straw and sugarcane bagasse mixture shows highest energy efficiency of 59.9% at 0.4 steam to biomass ratio and it decreases further to 40.7 % as the ratio increases. Wheat straw and sugarcane bagasse mixture shows highest exergy efficiency of 38.2% at 0.4 steam to biomass ratio, while it decreases further to 31.8 % as the ratio increases. Increase in the steam flow elevates the  $CO$  produced in water-gas reaction towards a more stable water-gas shift reaction, resulting in an enhanced  $CO_2$  and  $H_2$  production. This phenomenon in turn decreases the LHV of the syngas which adversely affects the energy and exergy efficiencies. The findings of Mojaver et al., 2019 and Yan et al., 2016 lead to similar conclusion as both the literature concluded that increase in steam to biomass ratio adversely affect the energy and exergy efficiency of the biomass co-gasification.

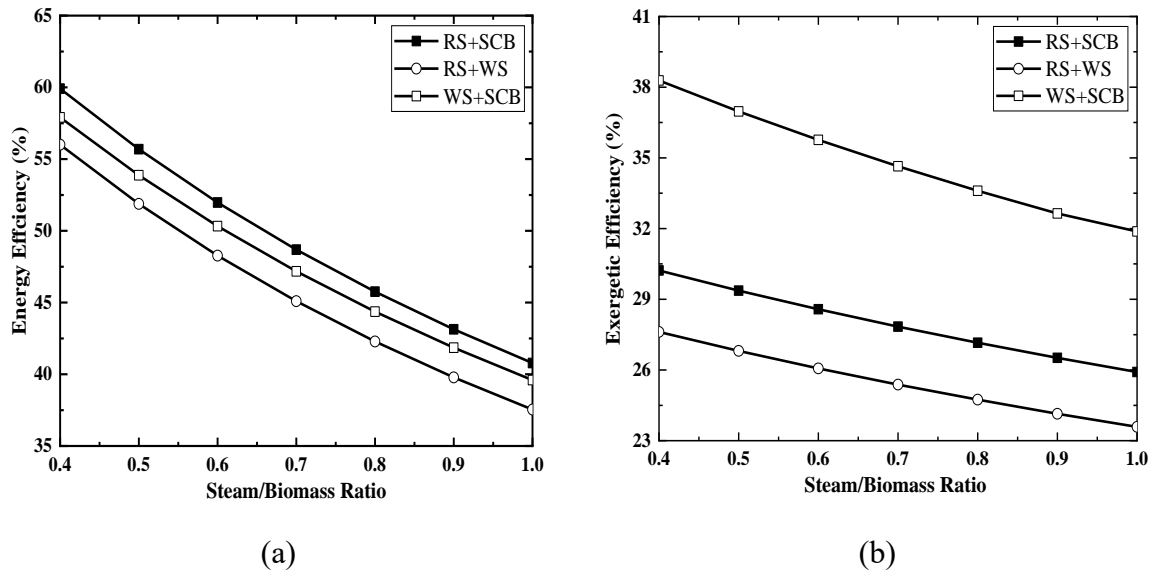


**Figure 4.8:** Variation of (a) energy efficiency and (b) exergy efficiency with steam/biomass ratio at gasifier temperature 750°C and equivalence ratio 0.35

#### 4.4.3 Statistical analysis using Response Surface Methodology

The experimental design to optimize the simulation of biomass co-gasification has been carried out using Response Surface Methodology (RSM). Response surface methodology is an effective tool to carry out statistical optimization of any process that depends upon numerous independent variables (Lv et al., 2014). As seen in the previous section, the combination of rice straw and wheat straw is seen to be the least efficient combination. Therefore, the optimization is conducted for the biomass combinations of rice straw- sugarcane bagasse (RS-SCB) and wheat straw- sugarcane bagasse (WS-SCB). The gasification temperature, equivalence ratio and steam to biomass ratio are selected as input variables whereas the energy efficiency and exergy efficiency are the response variable. The experimental scheme is designed based on Box- Benhnken model in Design Expert V11 software. A total of 17 data points are prepared with 3 independent variables and 3 levels. The levels are provided in Table 4.3

**Table 4.3:** List of independent variables

Variables (units)		+1 level	-1 level
Gasification temperature (°C)		0.8	0.2
		1000	600
Equivalence ratio (wt/wt)		0.5	0.2
Steam/Biomass		1	0.4

#### 4.4.3.1 Statistical analysis for rice straw and sugarcane bagasse mixture

The analysis of variance (ANOVA) is conducted for both energy and exergy efficiency of rice straw and sugarcane bagasse mixture in co-gasification. The ANOVA tables are provided in Table 4.4 and Table 4.5 respectively

**Table 4.4:** ANOVA table of energy efficiency (RS-SCB)

Source	Sum of Squares	df	Mean Square	F-value	p-value
<b>Model</b>	1737.89	7	248.18	58.49	< significant 0.0001
<b>A-Temperature</b>	426.32	1	426.32	100.47	< 0.0001
<b>B-Equivalence ratio</b>	139.86	1	139.86	32.96	< 0.0001
<b>C-Steam/Biomass</b>	1098.63	1	1098.63	258.92	< 0.0001
<b>AC</b>	25.76	1	25.76	6.07	0.0359
<b>BC</b>	25.00	1	25.00	5.89	0.0381
<b>A<sup>2</sup></b>	8.42	1	8.42	1.99	0.1924
<b>B<sup>2</sup></b>	14.45	1	14.45	3.41	0.0981
<b>Residual</b>	38.19	9	4.24		
<b>Lack of Fit</b>	38.19	3	7.64		
<b>Pure Error</b>	0.0000	4	0.0000		
<b>Cor Total</b>	1775.47	16			
<b>Std. Dev.</b>				2.06	
<b>Mean</b>				50.39	
<b>R<sup>2</sup></b>				0.9785	
<b>Adjusted R<sup>2</sup></b>				0.9618	
<b>Predicted R<sup>2</sup></b>				0.8585	
<b>Adeq Precision</b>				27.0468	

**Table 4.5:** ANOVA table of exergy efficiency (RS-SCB)

Source	Sum of Squares	df	Mean Square	F-value	p-value
<b>Model</b>	919.38	9	102.15	228.70	< significant 0.0001
<b>A-Equivalence ratio</b>	777.17	1	777.17	1739.89	< 0.0001
<b>B-Temperature</b>	3.48	1	3.48	7.80	0.0268
<b>C-Steam/Biomass</b>	96.81	1	96.81	216.74	< 0.0001
<b>AB</b>	0.8100	1	0.8100	1.81	0.2201
<b>AC</b>	15.80	1	15.80	35.37	0.0006
<b>BC</b>	0.8836	1	0.8836	1.98	0.2024
<b>A<sup>2</sup></b>	23.68	1	23.68	53.00	0.0002
<b>B<sup>2</sup></b>	1.14	1	1.14	2.56	0.1536
<b>C<sup>2</sup></b>	0.0072	1	0.0072	0.0160	0.9028
<b>Residual</b>	3.13	7	0.4467		
<b>Lack of Fit</b>	3.13	3	1.04		
<b>Pure Error</b>	0.0000	4	0.0000		
<b>Cor Total</b>	922.51	16			
<b>Std. Dev.</b>				0.6683	
<b>Mean</b>				29.69	
<b>R<sup>2</sup></b>				0.9966	
<b>Adjusted R<sup>2</sup></b>				0.9923	
<b>Predicted R<sup>2</sup></b>				0.9458	
<b>Adeq Precision</b>				52.0297	

According to the analysis of variance (ANOVA) results of energy and exergy efficiency models provided in Table 4.4 and 4.5 the F-values of both the models are 58.49 and 228.70 respectively which indicate that all input parameters are having significant influence on the response variable and there is less than 0.001% chance that an F-value this large could have occurred due to noise.

The corresponding p-value for the models are less than 0.0001 respectively. As both the p-values are less than 0.05, it indicates that the models are significant. R<sup>2</sup> value of 0.9785 for the energy efficiency model and 0.9966 for the exergy efficiency model signify that models can explain up to 97.85% and 99.66% changes in input variables respectively. Adjusted and predicted R<sup>2</sup> values for the energy efficiency model are found to be 0.9618 and 0.8585 respectively. For the exergy efficiency model these values are found to be 0.9923 and 0.9458

respectively. In both the models the difference between the adjusted and predicted  $R^2$  values are less than 0.2 which indicate that both the values are in reasonable agreement with each other for both the models. Adequate precision is the measure of signal to noise ratio in the model. Respective adequate precession values for both the models are greater than 4 which suggest that impact noise over signals in both the models is negligible. Figures 4.9 and 4.10 show the random yet close distribution of the actual values on both sides of the prediction diagonal for both the responses respectively.

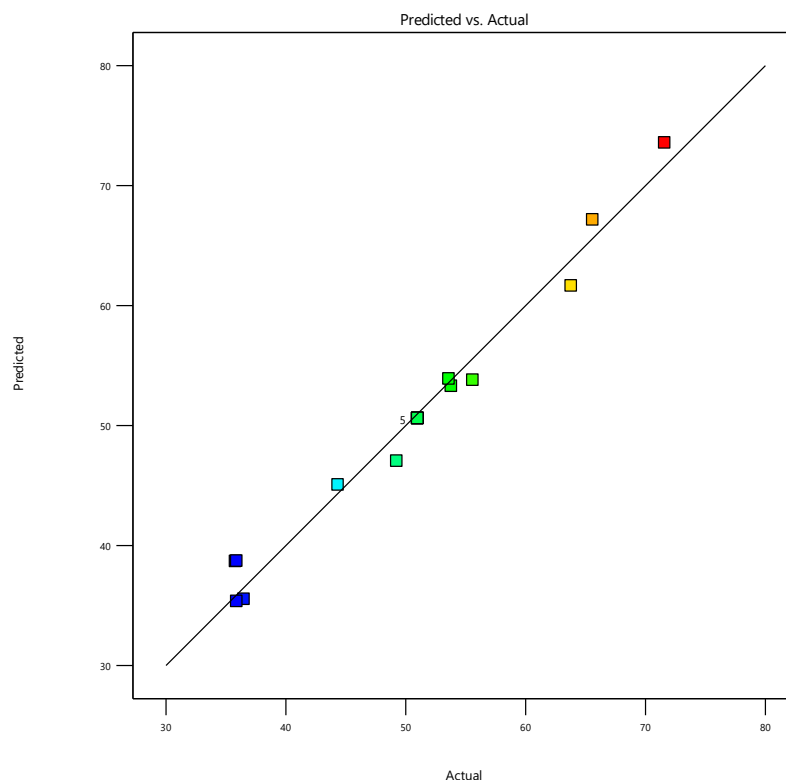


**Figure 4.9:** Deviation of the actual responses from predicted response values of energy efficiency regression model (RS-SCB)

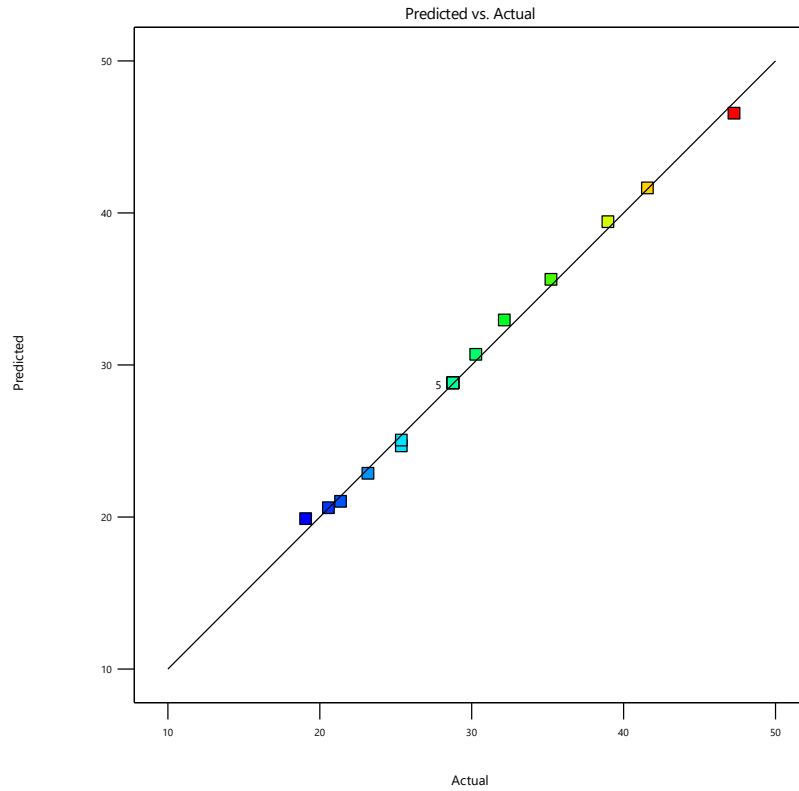


**Figure 4.10:** Deviation of the actual responses from predicted response values of exergy efficiency regression model (RS-SCB)

The ANOVA tables provided in Table 4.4 and 4.5 give a regression equation for energy efficiency in terms of the input variables. The coded factors for the equation are as follows  
 $A = (\text{Temperature}-600)/200$ ,  $B = (\text{Equivalence ratio}-0.2)/0.15$  and  $C = (\text{Steam to biomass ratio} - 0.4)/0.3$ . The binomial equation in coded factors is given as

$$\text{Energy efficiency} = 50.60 - 7.30*A + 4.18*B - 11.72*C + 2.54*AC - 2.50*BC + 1.41*A^2 - 1.85*B^2 \quad (4.12)$$

$$\text{Exergy efficiency} = 28.8 - 9.86*A + 0.66*B - 3.48*C - 0.45*AB + 1.99*AC - 0.47*BC + 2.37*A^2 - 0.52*B^2 + 0.04*C^2 \quad (4.13)$$

The regression equation helps us to study the effect of any two parameters over the response.

After obtaining the regression equation the optimization is conducted to maximize the energy and exergy efficiency for the co-gasification.

#### 4.4.3.2 Statistical analysis for wheat straw and sugarcane bagasse mixture

The analysis of variance (ANOVA) is conducted for both energy and exergy efficiency of wheat straw and sugarcane bagasse mixture in co-gasification. The ANOVA tables are provided in Table 4.6 and Table 4.7 respectively

**Table 4.6:** ANOVA table of energy efficiency (WS-SCB)

Source	Sum of Squares	df	Mean Square	F-value	p-value
<b>Model</b>	1287.89	9	143.10	2047.55	< significant 0.0001
<b>A-Temperature</b>	215.03	1	215.03	3076.83	< 0.0001
<b>B-Equivalence ratio</b>	278.64	1	278.64	3986.97	< 0.0001
<b>C-Steam/Biomass</b>	769.06	1	769.06	11004.23	< 0.0001
<b>AB</b>	2.39	1	2.39	34.23	0.0006
<b>AC</b>	4.39	1	4.39	62.86	< 0.0001
<b>BC</b>	5.01	1	5.01	71.70	< 0.0001
<b>A<sup>2</sup></b>	2.13	1	2.13	30.43	0.0009
<b>B<sup>2</sup></b>	0.0568	1	0.0568	0.8124	0.3974
<b>C<sup>2</sup></b>	11.71	1	11.71	167.49	< 0.0001
<b>Residual</b>	0.4892	7	0.0699		
<b>Lack of Fit</b>	0.4892	3	0.1631		
<b>Pure Error</b>	0.0000	4	0.0000		
<b>Cor Total</b>	1288.38	16			
<b>Std. Dev.</b>				0.2644	
<b>Mean</b>				54.60	
<b>C.V. %</b>				0.4841	
<b>R<sup>2</sup></b>				0.9996	
<b>Adjusted R<sup>2</sup></b>				0.9991	
<b>Predicted R<sup>2</sup></b>				0.9939	
<b>Adeq Precision</b>				165.0124	



**Table 4.7:** ANOVA table of exergy efficiency (WS-SCB)

Source	Sum of Squares	df	Mean Square	F-value	p-value
<b>Model</b>	833.68	9	92.63	244.21	< significant 0.0001
<b>A-Temperature</b>	7.92	1	7.92	20.88	0.0026
<b>B-Equivalence ratio</b>	676.40	1	676.40	1783.22	< 0.0001
<b>C-Steam/Biomass</b>	116.50	1	116.50	307.13	< 0.0001
<b>AB</b>	1.07	1	1.07	2.83	0.1363
<b>AC</b>	0.3591	1	0.3591	0.9467	0.3630
<b>BC</b>	13.87	1	13.87	36.56	0.0005
<b>A<sup>2</sup></b>	3.08	1	3.08	8.11	0.0248
<b>B<sup>2</sup></b>	13.46	1	13.46	35.48	0.0006
<b>C<sup>2</sup></b>	1.38	1	1.38	3.64	0.0980
<b>Residual</b>	2.66	7	0.3793		
<b>Lack of Fit</b>	2.66	3	0.8851		
<b>Pure Error</b>	0.0000	4	0.0000		
<b>Cor Total</b>	836.34	16			
<b>Std. Dev.</b>				0.6159	
<b>Mean</b>				33.20	
<b>C.V. %</b>				1.85	
<b>R<sup>2</sup></b>				0.9968	
<b>Adjusted R<sup>2</sup></b>				0.9927	
<b>Predicted R<sup>2</sup></b>				0.9492	
<b>Adeq Precision</b>				55.0898	

According to the analysis of variance (ANOVA) results of energy and exergy efficiency models provided in Table 4.6 and 4.7 the F-values of both the models are 2047.55 and 244.21 respectively which indicate that all input parameters are having significant influence on the response variable and there is less than 0.001% chance that an F-value this large could have occurred due to noise.

The corresponding p-value for the models are less than 0.0001 respectively. As both the p-values are less than 0.05, it indicates that the models are significant. R<sup>2</sup> value of 0.9996 for the energy efficiency model and 0.9968 for the exergy efficiency model signify that models can explain up to 99.96% and 99.68% changes in input variables respectively. Adjusted and predicted R<sup>2</sup> values for the energy efficiency model are found to be 0.9991 and 0.9931

respectively. For the exergy efficiency model these values are found to be 0.9927 and 0.9492 respectively. In both the models the difference between the adjusted and predicted  $R^2$  values are less than 0.2 which indicate that both the values are in reasonable agreement with each other for both the models. Adequate precision is the measure of signal to noise ratio in the model. Respective adequate precession values for both the models are greater than 4 which suggest that impact noise over signals in both the models is negligible. Figures 4.11 and 4.12 show the random yet close distribution of the actual values on both sides of the prediction diagonal for both the responses respectively.

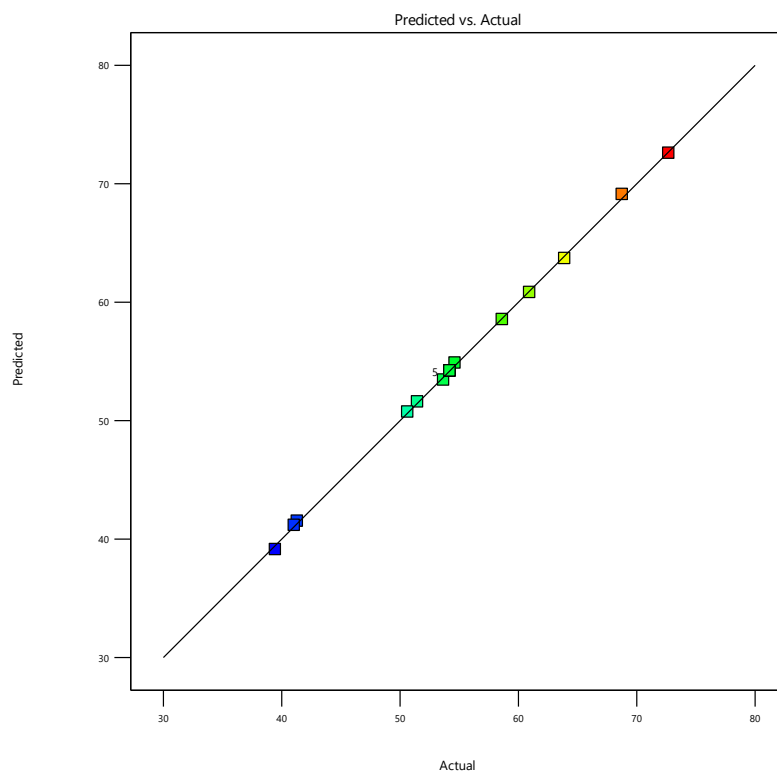


**Figure 4.11:** Deviation of the actual responses from predicted response values of energy efficiency regression model (WS-SCB)

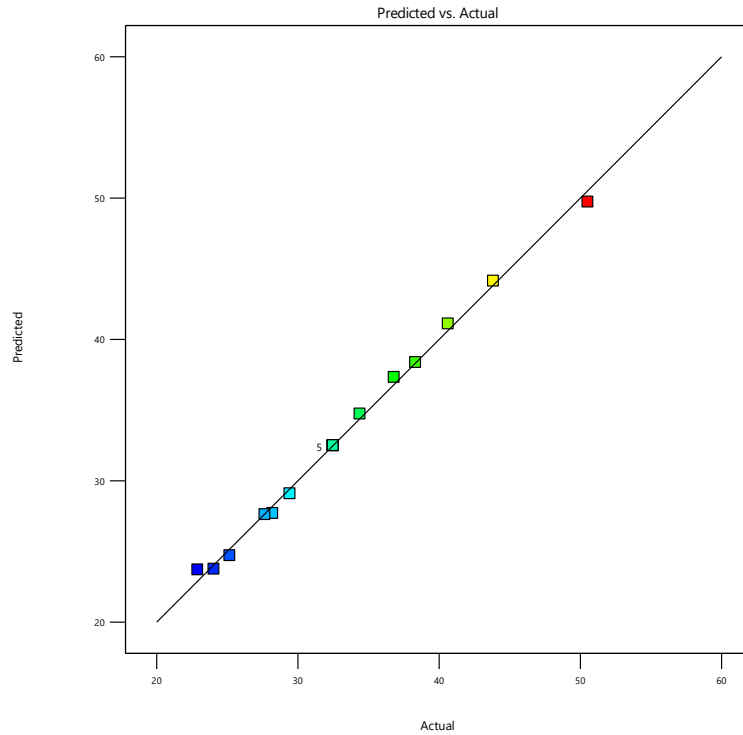


**Figure 4.12:** Deviation of the actual responses from predicted response values of exergy efficiency regression model (WS-SCB)

The ANOVA tables provided in Table 4.6 and 4.7 give a regression equation for energy efficiency in terms of the input variables. The coded factors for the equation are as follows  
 $A = (\text{Temperature} - 600)/200$ ,  $B = (\text{Equivalence ratio} - 0.2)/0.15$  and  $C = (\text{Steam to biomass ratio} - 0.4)/0.3$  The binomial equation in coded factors is given as

$$\text{Energy efficiency} = 54.21 + 5.18*A - 5.90*B - 9.8*C + 0.77*AB + 1.05*AC + 1.12*BC - 0.71*A^2 - 0.12*B^2 + 1.67*C^2 \quad (4.13)$$

$$\text{Exergy efficiency} = 32.49 + 0.995*A - 9.20*B - 3.82*C - 0.52*AB - 0.30*AC + 1.86*BC - 0.85*A^2 + 1.79*B^2 + 0.57*C^2 \quad (4.15)$$

The regression equation helps us to study the effect of any two parameters over the response.

#### 4.4.4 Optimization of process parameters

After obtaining the regression equation the optimization is conducted to maximize the energy and exergy efficiency for the co-gasification. The optimization suggest that for the rice straw and sugarcane bagasse mixture a temperature of 993.87°C, equivalence ratio of 0.2 and steam to biomass ratio of 0.4 provided the maximum energy efficiency of 76.8% and maximum exergy efficiency of 46.38% respectively.

For the wheat straw and sugarcane bagasse mixture a temperature of 967.83°C, equivalence ratio of 0.2 and steam to biomass ratio of 0.4 provided the maximum energy efficiency of 74.25% and maximum exergy efficiency of 50.56% respectively.

#### 4.5 Chapter summary

From the above study, the following observations can be summarized:

- I. Developed model can be satisfactorily used for performance assessment of biomass co-gasification experiment considering the satisfactory validation results.
- II. At 993.87°C temperature 0.2 equivalence ratio and 0.4 steam to biomass ratio, rice straw and sugarcane bagasse mixture provides highest energy efficiency of 76.8% whereas wheat straw and sugarcane bagasse mixture shows the highest exergy efficiency of 50.56% at 967.83°C temperature 0.2 equivalence ratio and 0.4 steam to biomass ratio.
- III. Increase in temperature increases the LHV of syngas, and the performance efficiency of the gasification while equivalence ratio and steam to biomass ratio are kept constant. Similar trends has been observed by Zhai et al., 2016.
- IV. Equivalence ratio and steam to biomass ratio adversely effects the LHV of syngas and performance efficiencies.
- V. Steam as a gasifying agent improves  $H_2$  production but reduces CO in the syngas mixture.

Higher temperature and lower equivalence ratio and steam to biomass ratio has been found to be more viable for an energy rich and efficient co-gasification process. Optimization results suggest that energy efficiency is high for the rice straw and sugarcane bagasse mixture whereas for the wheat straw and sugarcane bagasse mixture exergy efficiency is high. Therefore a kinetic model of biomass co-gasification is developed in the next chapter with the expectation of finding the most efficient biomass mixture in co-gasification. Also steam is not used as a gasifying agent for the further studies as it reduces the CO production.

---

## **Chapter 5. Kinetic modelling and thermodynamic performance optimization of Indian lignocellulosic biomass co-gasification**

---

### **5.1 Objective of the chapter**

The present study focuses on the development of a steady state kinetic model of downdraft co-gasification of the two biomass combinations namely rice straw- sugarcane bagasse (RS-SCB) and wheat straw- sugarcane bagasse (WS-SCB) using Aspen plus. The Response surface methodology has also been utilised to optimize the energy and exergy efficiency of the whole system using biomass ratio, gasification temperature and equivalence ratio as input variables.

The primary objective of this chapter is to observe the combined effect of the input variables on the response variables and to find out the best performing biomass combination for the ethanol production via syngas fermentation.

### **5.2 Methodology**

The Ultimate, proximate and elemental analysis of the feedstocks along with their LHV's have been provided in Table 3.1.

Here in this work, the elemental analysis of biomass has been given emphasis upon. A constant amount of 5% moisture has been included to each biomass and the drying process is skipped. Thermodynamic equilibrium method using Gibb's free energy minimization considers infinite residence time for the reactants inside the reactor which in turn provides the highest yield for the products. But in reality the gas residence time inside the reactor is comparatively very small. This factor along with temperature dependency of gasification reactions are taken care of in the kinetic model which brings the kinetic model more close to reality. Drying, pyrolysis, oxidation and reduction are the chemical processes taking place inside the gasifier. Although these processes take place simultaneously inside the gasifier, for simplicity of the study, zone demarcation has been made according to Yu & Smith, 2018. The highest temperature is attained at the oxidation zone due to exothermic nature of the reaction. The endothermic gasification reactions occur as soon as the temperature is favourable. Following assumptions are made in this gasification model

- i. Mass flow rate does not change with time i.e. steady state conditions.

- ii. Char contains only carbon and ash.
- iii. Pyro-gas contains  $CO$ ,  $CO_2$ ,  $H_2$  and  $CH_4$ .
- iv. Pyro-oil contains only phenol.
- v. All the reactors are isothermal.

No synergistic effect is present during co-gasification of the biomass under study. All gasification characteristics of the two biomass feedstocks follow linear and additive correlation among themselves. This is due to the fact that unlike the combinations of coal-biomass and food waste-biomass mixtures, the H:C and H:O values of two dry biomass feedstocks, namely RS and SB under study, are of the same order (Edreis et al., 2014; Howaniec et al., 2011; Quan & Gao, 2016; Wei et al., 2017; Zhang et al., 2015).

Aspen plus provides inbuilt power-law kinetics for a continuously stirred tank reactor following Arrhenius equation. The rate constant is expressed as

$$k = A \left( \frac{T}{T_0} \right) \exp \left[ -\frac{E_a}{R} \left( \frac{1}{T} - \frac{1}{T_0} \right) \right] \quad (5.1)$$

Where A is the frequency factor, T is reactor temperature,  $T_0$  is ambient temperature,  $E_a$  is activation energy and R is the universal gas constant.

All the reactions with their rate constant expressions are given in Table 5.1.

**Table 5.1:** Rate constants for different gasification reactions (Eikeland et al., 2015; Gremyachkin, 2006; Umeki et al., 2012)

Reaction name	Equation	Rate Constant
<b>Full combustion reaction</b>	$C + O_2 \xrightarrow{K_1} CO_2$	$K_1 = 4.31 \times 10^{11} \times \sqrt{T} \times C_{O_2} e^{-\left(\frac{184000}{RT}\right)}$
<b>Boudouard reaction</b>	$C + CO_2 \xrightleftharpoons[K'_2]{K_2} 2CO$	$K_2 = 1.272 \times m_s T \times C_{CO_2} e^{-\left(\frac{188270.5}{RT}\right)}$ $K'_2 = 1.044 \times 10^{-4} \times m_s T^2 \times C_{CO}^2 e^{-\left(\frac{19646}{RT} - 20.92\right)}$
<b>Steam gasification reaction</b>	$C + H_2O \xrightleftharpoons[K'_3]{K_3} CO + H_2$	$K_3 = 1.272 \times m_s T \times C_{H_2O} e^{-\left(\frac{188270.5}{RT}\right)}$ $K'_3 = 1.044 \times 10^{-4} \times m_s T^2 \times C_{H_2} \times C_{CO} e^{-\left(\frac{52536}{RT} - 20.92\right)}$
<b>Water-gas shift reaction</b>	$CO + H_2O \xrightleftharpoons[K'_4]{K_4} CO_2 + H_2$	$K_4 = 7.68 \times 10^{10} \times T \times C_{CO}^{0.5} \times C_{H_2O} e^{-\left(\frac{304635}{RT}\right)}$

		$K'_4 = 6.4 \times 10^9 \times T \times C_{H_2}^{0.5}$ $\times C_{CO} e^{-\left(\frac{326407.6}{RT}\right)}$
<b>Methane reforming reaction</b>	$CH_4 + H_2O \xrightleftharpoons[K'_5]{K_5} CO + 3H_2$	$K_5 = 3.1005 \times C_{CH_4} \times C_{H_2O} e^{-\left(\frac{124710}{RT}\right)}$ $K'_5 = 3.556 \times 10^{-3} \times T \times C_{CO}$ $\times C_{H_2}^2 e^{-\left(\frac{124710}{RT}\right)}$
	$C_6H_6O \xrightarrow{K_6} 0.5C_{10}H_8 + CO + H_2$	$K_6 = 10^7 \times C_{C_6H_6O} e^{-\left(\frac{100000}{RT}\right)}$
<b>Tar cracking reaction</b>	$C_{10}H_8 \xrightarrow{K_7} 10C(s) + 4H_2$	$K_7 = 7 \times 10^{14} \times C_{H_2}^{-0.7}$ $\times C_{C_{10}H_8}^2 e^{-\left(\frac{360000}{RT}\right)}$
	$C_{10}H_8 + 4.75H_2 \xrightarrow{K_8} 1.25C_6H_6 + 2.5CH_4$	$K_8 = 10^{14} \times C_{H_2}^{0.4} \times C_{C_{10}H_8} e^{-\left(\frac{324000}{RT}\right)}$

### 5.3 Model development

Based on these following assumptions, an Aspen plus model is developed nested with FORTRAN subroutine for the co-gasification process. The first step is to enlist the components that participate in the process. Aspen plus has a huge library of physical components and thermodynamic data sets related to them. Since the properties of biomass and ash, are not available in Aspen plus data banks they are specified as non-conventional components in the simulation model. Enthalpy and density model chosen for these two components are HCOALGEN and DCOALGAI respectively. Lignin cellulose and hemicellulose are included as user defined components according to Wooley & Putsche, 1996. Non-random two liquid equation of state with Redlich-kwong function has been chosen as the property method to calculate the property of the components. First the mixed biomass is fed to a RYIELD block BRKDWN at different mass ratios where it is disintegrated to the hydrocarbon polymers, namely, lignin, cellulose, hemicellulose and ash. This is a pseudo step to convert the biomass to conventional component. The pyrolysis data of lignin, cellulose and hemicellulose, as available in the literature have been used (Qu et al., 2011). Accordingly, the constituent polymers are converted to pyro-gas ( $CO$ ,  $H_2$ ,  $CO_2$ ,  $CH_4$ ), pyro-oil and char at 500°C in another RYIELD block, PYRO. Compositions of different constituents in both of these unit operations are provided by calculator block using FORTRAN subroutine. From the pyrolysis block the char is separated by separator block SEP1. Main gasification reactions are modelled according

to the oxidation and gasification reaction kinetics enlisted in Table 5.1. Separated char moves to the first RCSTR block COMBUST where the primary combustion reaction occurs and carbon is converted to  $CO_2$  in the presence of externally supplied air. Temperature of the reactor is kept at  $1000^\circ C$ . This is the main energy producing reaction in the gasification process. Air is supplied at different equivalence ratio. Equivalence ratio is defined in equation 5.2.

$$Eq\ ratio = \frac{actual\ air}{stoichiometric\ air} \quad (5.2)$$

After the char combustion, SEP2 block separates the ash from unburnt carbon and produced  $CO_2$ . The unburnt carbon and  $CO_2$  further gets mixed with the other pyrolysis products ( $CO$ ,  $H_2$ ,  $CO_2$  and Phenol) in the second RCSTR block GASIF. Here the gasification reactions occur according to the rate kinetics specified in Table 5.1. The Aspen plus flow sheet is provided in Figure 5.1.

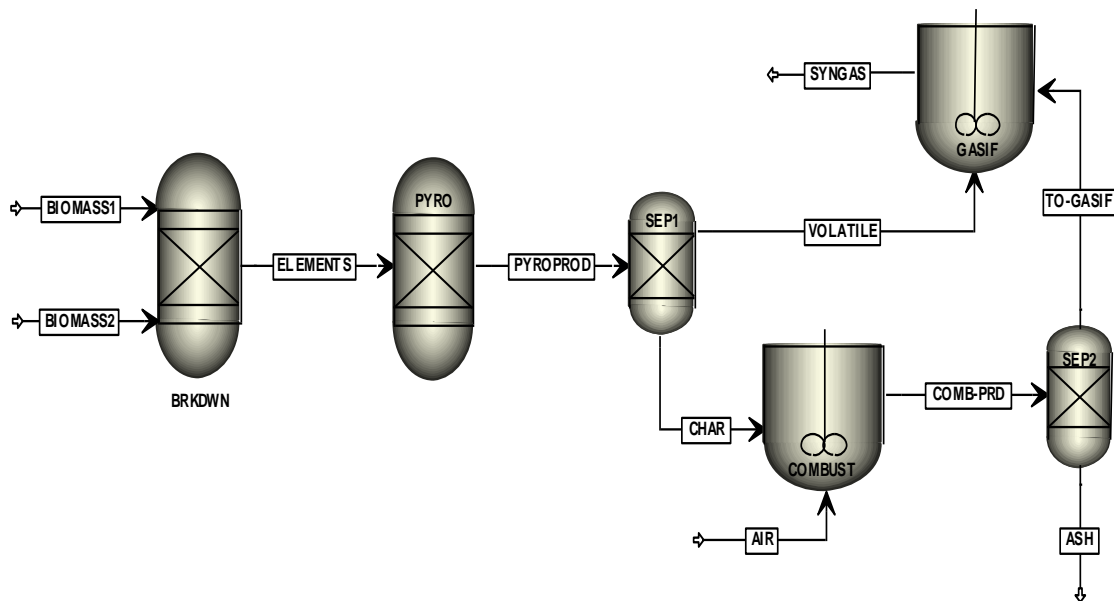


**Figure 5.1:** Aspen plus flow sheet for kinetic model of co-gasification

The overall process model using Aspen plus was run at different combinations of RS-SCB and WS- SCB mass flow rate ratio, equivalence ratio and gasification temperature.

#### 5.4 Thermodynamic performance analysis

Thermodynamic performance of this system has been analysed by the first law and second law of thermodynamics, thereby calculating the energy and exergy efficiency of the product gases. Mass, energy and exergy balance equations have been employed and from there the efficiency parameters are calculated. The efficiency equations are similar to those described in chapter 4.



But as there is no steam present as gasifying agent in this analysis the energy and exergy efficiency equations are rewritten as

$$\eta_{energy} = \frac{\dot{m}_{syngas} \times LHV_{syngas}}{\dot{m}_{total} \times LHV_{mlb} + \dot{m}_{air} \times C_{p,air} \times \Delta T} \quad (5.3)$$

$$\eta_{Exergy} = \frac{Ex_{syngas}}{Ex_{biomass1} + Ex_{biomass2} + Ex_{air}} \quad (5.4)$$

## 5.5 Experimental design

As discussed in chapter 4, the experimental scheme is designed based on Box- Benhnken model in Design Expert V11 software. A total of 17 data points are prepared with 3 independent variables and 3 levels. The levels are listed in Table 5.2. Mass fraction of rice straw or wheat straw in biomass mixture is varied from 0.8 i.e. 80% rice straw or wheat straw and 20 % sugarcane bagasse to 0.2 i.e. 20% rice straw or wheat straw and 80% sugarcane bagasse. Temperature is varied from 600°C to 900°C and the equivalence ratio is varied from 0.2 to 0.5.

**Table 5.2:** List of independent variables

Variables (units)	+1 level	-1 level
Mass fraction of rice straw or wheat straw in biomass mixture (rice straw:total biomass)(% wt/wt)	0.8	0.2
Gasification temperature (°C)	900	600
Equivalence ratio (wt/wt)	0.5	0.2

## 5.6 Results and discussions

### 5.6.1 Model Validation

The co-gasification simulation model is validated by comparing the syngas yield of the model with the experiment done by Monir et al., 2020 using forest residue and wood charcoal as feedstock. Monir et al., 2020 performed experimental investigations feeding various ratios of the biomass mixture in a downdraft gasifier. The simulation model of the present study is manipulated according to the ultimate, proximate and elemental analysis of forest residue and wood charcoal provided in literature (Monir et al., 2020). The feedstock properties are provided in Table 5.3.

**Table 5.3:** Elemental analysis of the feedstock used in the experiments of (Monir et al., 2020)

Analysis		Forest Residue	Wood charcoal
<b>Proximate analysis</b> (% dry basis)	Moisture	5	6
	Fixed Carbon	30	35
	Volatile matter	57	31
	Ash	8	28
<b>Ultimate Analysis</b> (% dry basis)	Carbon (C)	42.75	54.17
	Hydrogen (H)	4.66	1.48
	Nitrogen (N)	4.81	0.64
	Oxygen (O)	47.77	43.66
	Sulphur (S)	0.01	0.05

Gasification parameters such as temperature for gasification, equivalence ratio along with other experimental data are also in the simulation. Yields of  $CO$ ,  $H_2$ ,  $CO_2$  and  $CH_4$  are obtained from the simulation for mass fraction of forest residue to wood charcoal ratios of 100:0, 90:10 and 80:20.

Good agreement can be observed between the simulated and experimental data available in the literature. The experimental and simulation results are shown in Table 5.4 .

**Table 5.4:** yield variation between experimental and simulation results

Volume%	Monir et. al (Monir et al., 2020)			Present simulation			Mean Error
	100:0	90:10	80:20	100:0	90:10	80:20	
<b>CO</b>	20.11	21.53	21.74	18.68	18.96	19.13	0.107
<b>H<sub>2</sub></b>	9.92	11.39	11.86	8.79	9.67	10.24	0.122
<b>CO<sub>2</sub></b>	8.45	8.35	8.24	10.16	10.45	10.58	0.248
<b>CH<sub>4</sub></b>	1.15	1.10	1.15	1.59	1.72	1.68	0.474

The sum of square method has been used to determine the mean error of each product yield in the proposed simulation (Nikoo & Mahinpey, 2008).

$$Squared\ sum = \sum_{i=1}^N \left( \frac{y_{im} - y_{ic}}{y_{ic}} \right)^2 \quad (5.5)$$

where  $y_{im}$  is the predicted yield in the simulation model and  $y_{ic}$  is the gas yield reported in experiment.

$$mean\ squared\ sum = \frac{Squared\ sum}{N} \quad (5.6)$$

N is the total number of readings taken.

$$mean\ error = \sqrt{mean\ squared\ sum} \quad (5.7)$$

The mean error recorded for  $CO$ ,  $H_2$ ,  $CO_2$  and  $CH_4$  yields are found to be 0.107, 0.122, 0.248 and 0.474 respectively. The bar chart shown in Figure 5.2 shows the comparison between the experimental data and model prediction at different biomass ratios.

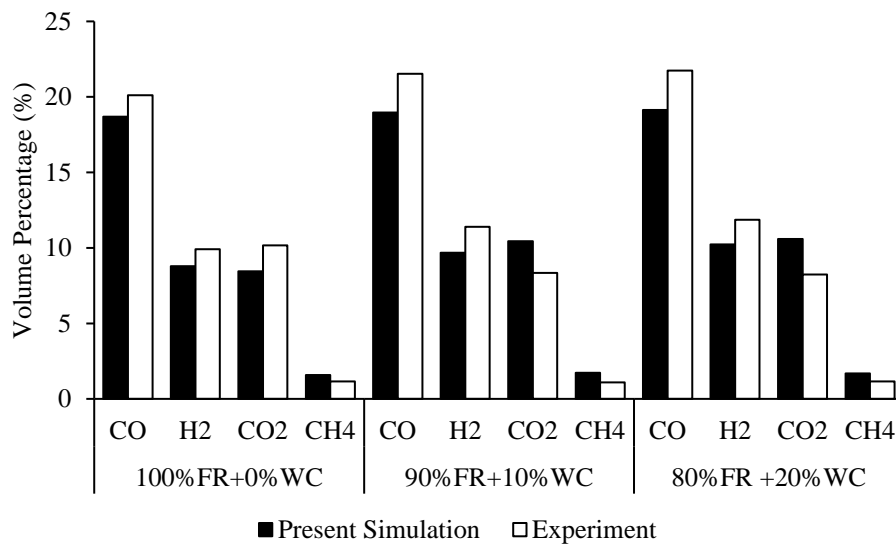


**Figure 5.2:** Bar chart showing the comparison of experimental to simulated values

The model predictions for  $CO$ ,  $H_2$  and  $CO_2$  are in good agreement with experimental findings of Monir et al., 2020. However, the mean error in case of  $CH_4$  yield is high. This may be due to the occurrence of other tar cracking reactions which have not been considered under the present model. Tar compounds have been assumed to be both benzene ( $C_6H_6$ ) and naphthalene ( $C_{10}H_8$ ) (Font Palma, 2013) in this model and the yield of tar in this model is 5.7% (v/v).

### 5.6.2 Optimization of the performance of mixed biomass gasification process

For the data provided in Table 5.5 obtained from the simulation model for the combination of rice straw and sugarcane bagasse, multiple regression analysis are performed in the Design Expert software.

**Table 5.5:** Results of the experimental conditions.

	<b>Factor 1</b>	<b>Factor 2</b>	<b>Factor 3</b>	<b>Response 1</b>	<b>Response 2</b>
<b>Run</b>	A: Mass fraction of rice straw in biomass mixture	B:Temperature ( $^{\circ}\text{C}$ )	C:Equivalence ratio	Energy efficiency ( $\eta$ )	Exergy efficiency ( $\psi$ )
<b>1</b>	0.5	750	0.35	34.04	27.8
<b>2</b>	0.8	750	0.2	40.34	39.5
<b>3</b>	0.8	900	0.35	41.18	34.19
<b>4</b>	0.5	600	0.5	28.48	25.77
<b>5</b>	0.2	600	0.35	36.01	21.83
<b>6</b>	0.2	750	0.2	43.94	32.28
<b>7</b>	0.5	750	0.35	34.04	27.8
<b>8</b>	0.5	900	0.2	43.33	36.92
<b>9</b>	0.5	900	0.5	30.53	26.48
<b>10</b>	0.2	750	0.5	30.77	23.9
<b>11</b>	0.5	750	0.35	34.04	27.8
<b>12</b>	0.2	900	0.35	38.01	34.58
<b>13</b>	0.8	750	0.5	40.17	40.25
<b>14</b>	0.5	750	0.35	34.04	27.8
<b>15</b>	0.5	750	0.35	34.04	27.8
<b>16</b>	0.8	600	0.35	39.88	38.2
<b>17</b>	0.5	600	0.2	41.74	23.9

The results obtained from that analysis is listed in Table 5.6. According to the analysis of variance (ANOVA) results of energy and exergy efficiency models provided in Table 5.6, the F-values of both the models are 12.77 and 40.04 respectively which indicate that all input parameters are having significant influence on the response variable and there is less than 0.001% chance that this influence could have occurred due to noise.

**Table 5.6:** ANOVA table of the response variables (RS-SCB)

Variables	R1: Energy efficiency ( $\eta$ )				R2: Exergy efficiency ( $\psi$ )			
	Co-efficient	Sum of Squares	df	p-value	Co-efficient	Sum of Squares	df	p-value
<b>Model</b>		335.16	9	0.0014		536.68	9	< 0.0001
<b>A</b>	+1.61	20.61	1	0.0326	+4.94	195.53	1	< 0.0001
<b>B</b>	+0.8675	6.02	1	0.1941	+2.81	63.11	1	0.0003
<b>C</b>	-4.93	194.04	1	< 0.0001	-2.03	32.80	1	0.0022
<b>AB</b>	-0.1750	0.1225	1	0.8435	-4.19	70.22	1	0.0002
<b>AC</b>	+3.25	42.25	1	0.0067	+2.28	20.84	1	0.0073
<b>BC</b>	+0.1150	0.0529	1	0.8967	-3.08	37.88	1	0.0015
<b>A<sup>2</sup></b>	+3.76	59.45	1	0.0028	+5.06	107.70	1	< 0.0001
<b>B<sup>2</sup></b>	+0.9725	3.98	1	0.2810	-0.6575	1.82	1	0.3054
<b>C<sup>2</sup></b>	+1.01	4.27	1	0.2655	+1.13	5.33	1	0.1004
Residual		20.43	7			10.42	7	
<b>Lack of Fit</b>		20.43	3			10.42	3	
<b>Pure Error</b>		0.0000	4			0.0000	4	
<b>Total</b>		355.59	16			547.10	16	
<b>R<sup>2</sup></b>		0.9425				0.9809		
<b>Adjusted R<sup>2</sup></b>		0.8687				0.9565		
<b>Predicted R<sup>2</sup></b>		0.0807				0.6952		
<b>Adequate Precision</b>		12.4779				20.2219		
<b>Std. Dev.</b>		1.71				1.22		

The corresponding p-value for the models are 0.0014 and less than 0.0001 respectively. As both the p-values are less than 0.05, it indicates that the models are significant. R<sup>2</sup> value of 0.9425 for the energy efficiency model and 0.9809 for the exergy efficiency model signify that models can explain up to 94.25% and 98.09% changes in experimental parameters respectively. Adjusted R<sup>2</sup> values are found to be 0.8687 for the energy efficiency model and 0.9565 for the exergy efficiency model furthermore vouch for the model reliability. Adequate precision is the measure of signal to noise ratio in the model. Respective adequate precession values for both

the models are greater than 4 which suggest that impact noise over signals in both the models is negligible. The predicted  $R^2$  value of 0.0807 for energy efficiency model and 0.6952 for exergy efficiency model are not close enough to their adjusted  $R^2$  values of 0.8687 and 0.9565 respectively. It implies that some necessary modification is needed for both the models. Revised models have been prepared neglecting most of the insignificant model terms and the revised ANOVA results are listed in Table 5.7.

**Table 5.7:** Modified ANOVA table of the response models (RS-SCB)

Variables	R1: Energy efficiency ( $\eta$ )				R2: Exergy efficiency ( $\psi$ )			
	Co-efficient	Sum of Squares	df	p-value	Co-efficient	Sum of Squares	df	p-value
Model		326.27	5	< 0.0001		529.84	7	< 0.0001
<b>A</b>	+1.61	20.61	1	0.0179	+4.94	195.53	1	< 0.0001
<b>B</b>	+0.8675	6.02	1	0.1610	+2.81	63.11	1	0.0003
<b>C</b>	-4.93	194.05	1	< 0.0001	-2.03	32.81	1	0.0025
<b>AC</b>	+3.25	42.25	1	0.0022	-4.19	70.22	1	0.0002
<b>A<sup>2</sup></b>	+3.87	63.35	1	0.0005	+2.28	20.84	1	0.0093
					-3.08	37.88	1	0.0016
					+5.08	109.45	1	< 0.0001
Residual		29.32	11			17.26	9	
<b>Lack of Fit</b>		29.32	7			17.26	5	
<b>Pure Error</b>		0.0000	4			0.0000	4	
<b>Total</b>	355.59		16		547.10		16	
<b>R<sup>2</sup></b>		0.9175				0.9684		
<b>Adjusted R<sup>2</sup></b>		0.8801				0.9439		
<b>Predicted R<sup>2</sup></b>		0.6970				0.7796		
<b>Adequate Precision</b>		16.8567				19.2267		
<b>Std. Dev.</b>		1.63				1.39		

The table clearly shows that the predicted  $R^2$  values have improved significantly to 0.6970 and 0.7796 respectively which are closer to the adjusted  $R^2$  values nullifying any kind of problem in the model. Figure 5.3 shows the random yet close distribution of the actual values on both sides of the prediction diagonal for both the responses.

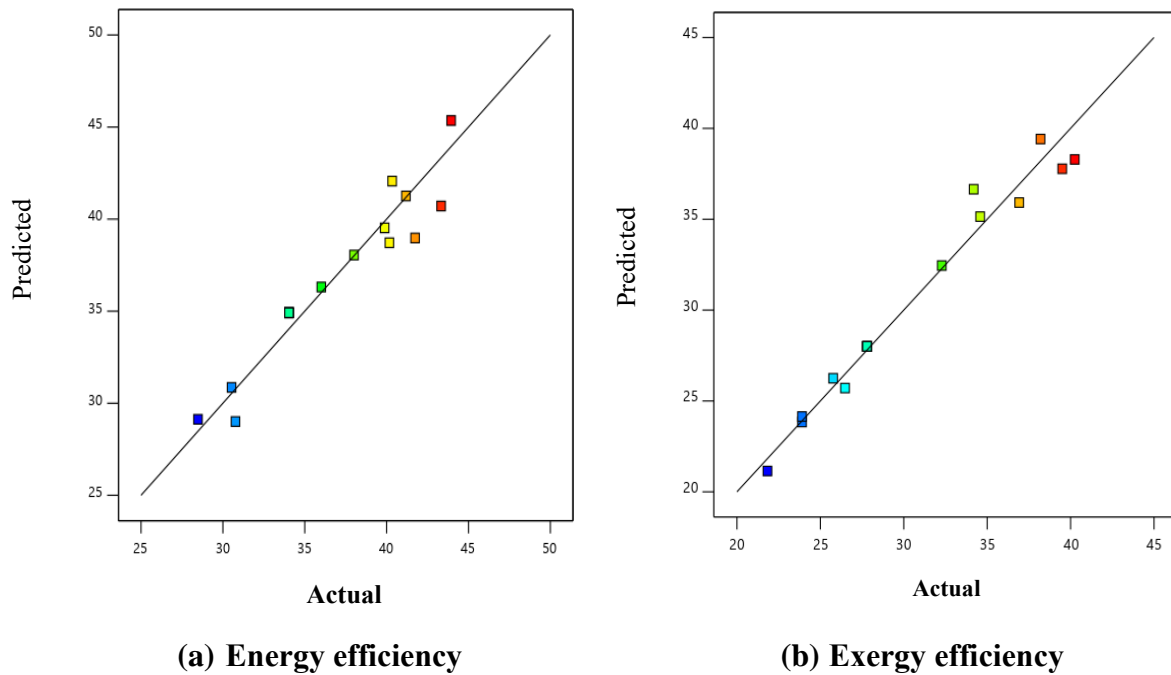


**Figure 5.3:** Deviation of the actual responses from predicted response values of regression model (RS-SCB)

Table 5.8 shows the modified ANOVA table for wheat straw and sugarcane bagasse mixture for the response variables energy and exergy efficiencies.

**Table 5.8:** Modified ANOVA table of the response models (WS-SCB)

Variables	R1: Energy efficiency ( $\eta$ )				R2: Exergy efficiency ( $\psi$ )			
	Co-efficient	Sum of Squares	df	p-value	Co-efficient	Sum of Squares	df	p-value
<b>Model</b>		328.27	6	< 0.0001		648.73	8	< 0.0001
<b>A</b>	+2.01	21.61	1	0.0240	+5.16	203.24	1	< 0.0001
<b>B</b>	+0.7675	6.02	1	0.1816	+2.81	63.11	1	0.0003
<b>C</b>	-4.53	197.15	1	< 0.0001	-1.96	34.66	1	0.0025
<b>AB</b>	-0.1750	0.122	1	0.6418	-4.19	70.46	1	0.0002
<b>AC</b>	+3.25	44.21		0.0035	+2.28	20.84		
<b>BC</b>					-3.08	37.88		
<b>A<sup>2</sup></b>	+4.16	64.32	1	0.0005	+6.66	187.56	1	0.0093
<b>C<sup>2</sup></b>					+2.73	31.53	1	< 0.0001
<b>Residual</b>		29.20	11			26.02	9	
<b>Lack of Fit</b>		29.20	7			13.85	5	
<b>Pure Error</b>		0.0000	4			0.0000	4	
<b>Total</b>	355.59		16			647.75	16	
<b>R<sup>2</sup></b>		0.9179				0.9614		
<b>Adjusted R<sup>2</sup></b>		0.8686				0.9229		
<b>Predicted R<sup>2</sup></b>		0.6975				0.7779		
<b>Adequate Precision</b>		16.8567				15.1467		
<b>Std. Dev.</b>		1.71				1.80		



The F-values of both the models are 18.63 and 24.93 respectively which indicate that all input parameters are having significant influence on the response variable and there is less than 0.001% chance that this influence could have occurred due to noise. The corresponding p-values for both the models are less than 0.0001. As both the p-values are less than 0.05, it indicates that the models are significant.  $R^2$  value of 0.9179 for the energy efficiency model and 0.9614 for the exergy efficiency model signify that models can explain up to 91.79% and 96.14% changes in input variables respectively. Adjusted and predicted  $R^2$  values for the energy efficiency model are found to be 0.8686 and 0.6975 respectively. For the exergy efficiency model these values are found to be 0.9229 and 0.7779 respectively. In both the models the difference between the adjusted and predicted  $R^2$  values are less than 0.2 which indicate that both the values are in reasonable agreement with each other for both the models. Adequate precision is the measure of signal to noise ratio in the model. Respective adequate precession values for both the models are greater than 4 which suggest that impact noise over signals in both the models is negligible.

Figure 5.3 shows the random yet close distribution of the actual values on both sides of the prediction diagonal for both the responses.

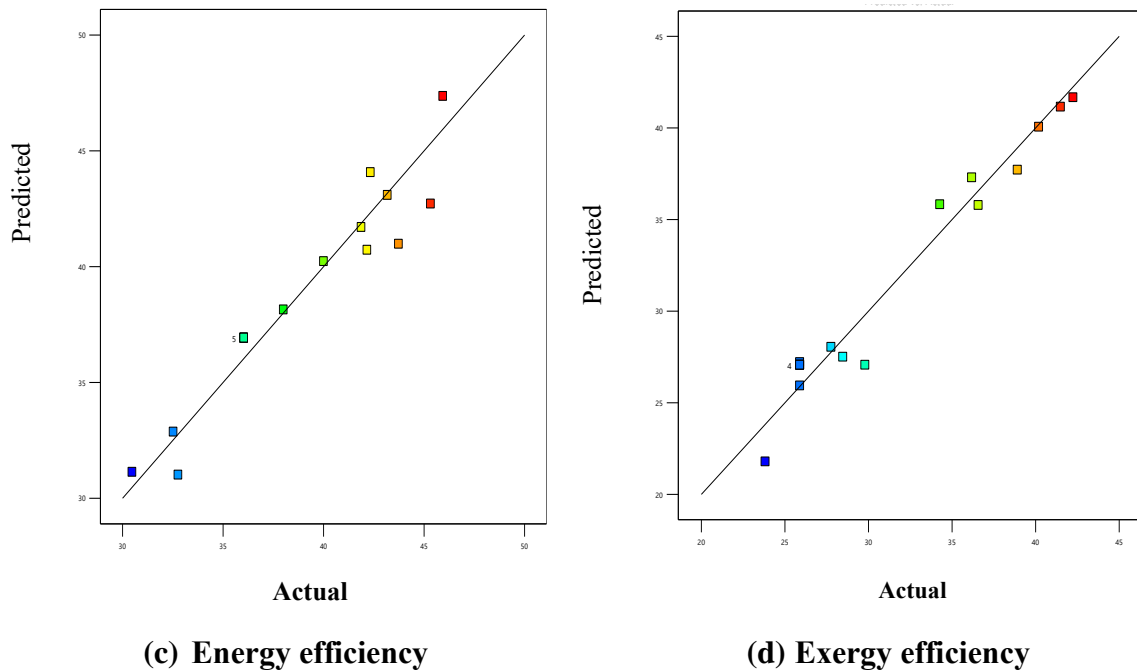


**Figure 5.4:** Deviation of the actual responses from predicted response values of regression model (WS-SCB)

The ANOVA tables provided in Table 5.7 and Table 5.8 gives a regression equation for energy efficiency in terms of the input variables. The coded factors for the equation are as follows

$A = (\text{Mass fraction of rice straw or wheat straw in biomass mixture} - 0.2)/0.3$ ,  $B = (\text{Temperature} - 600)/150$ ,  $C = (\text{Equivalence ratio} - 0.2)/0.15$ . The binomial equations in coded factors for RS-SCB are given as

$$\eta = 34.92 + 1.61*A + 0.8675*B - 4.93*C - 3.25*AC + 3.87*A^2 \quad (5.8)$$

The regression equation in coded factors for exergy efficiency is as follows-

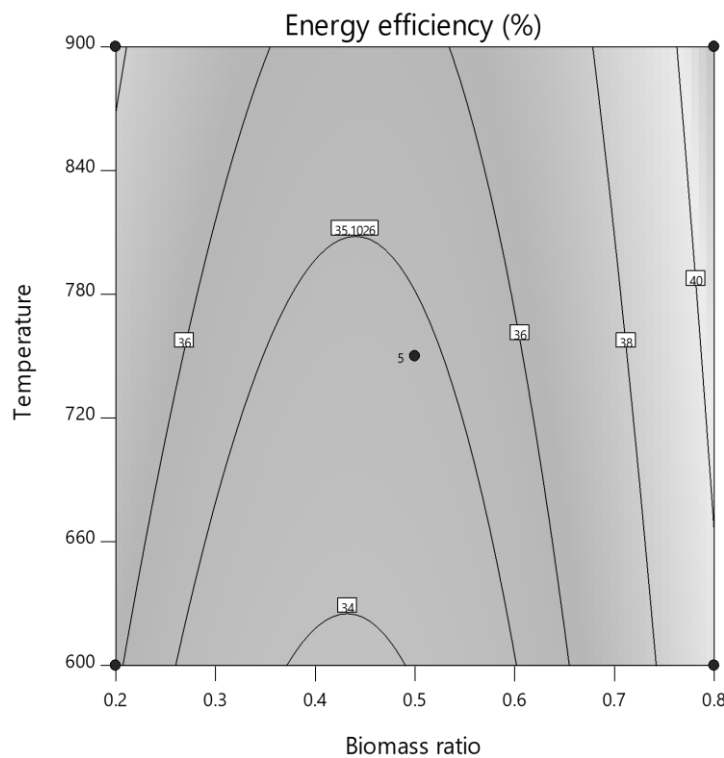
$$\psi = 28.01 + 4.94*A + 2.81*B - 2.03*C - 4.19*AB + 2.28*AC - 3.08*BC + 5.08*A^2 \quad (5.9)$$

The binomial equations in coded factors for WS-SCB are given as

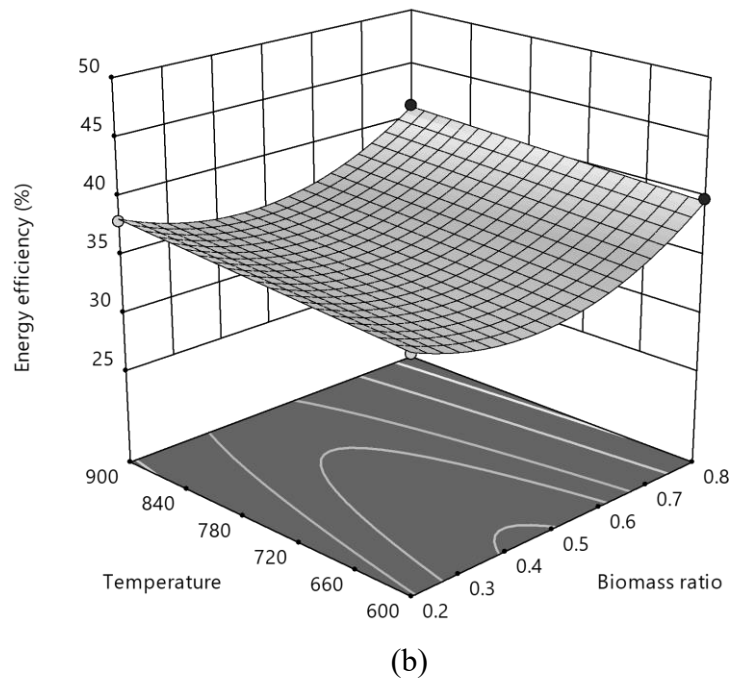
$$\eta = 36.92 + 2.01*A + 0.7675*B - 4.53*C - 0.175*AB + 3.25*AC + 4.16*A^2 \quad (5.10)$$

$$\psi = 27.06 + 5.16*A + 2.81*B - 1.96*C - 4.19*AB + 2.28*AC - 3.08*BC + 6.66*A^2 + 2.73*C^2 \quad (5.11)$$

The regression equation helps us to study the effect of any two parameters over the response.

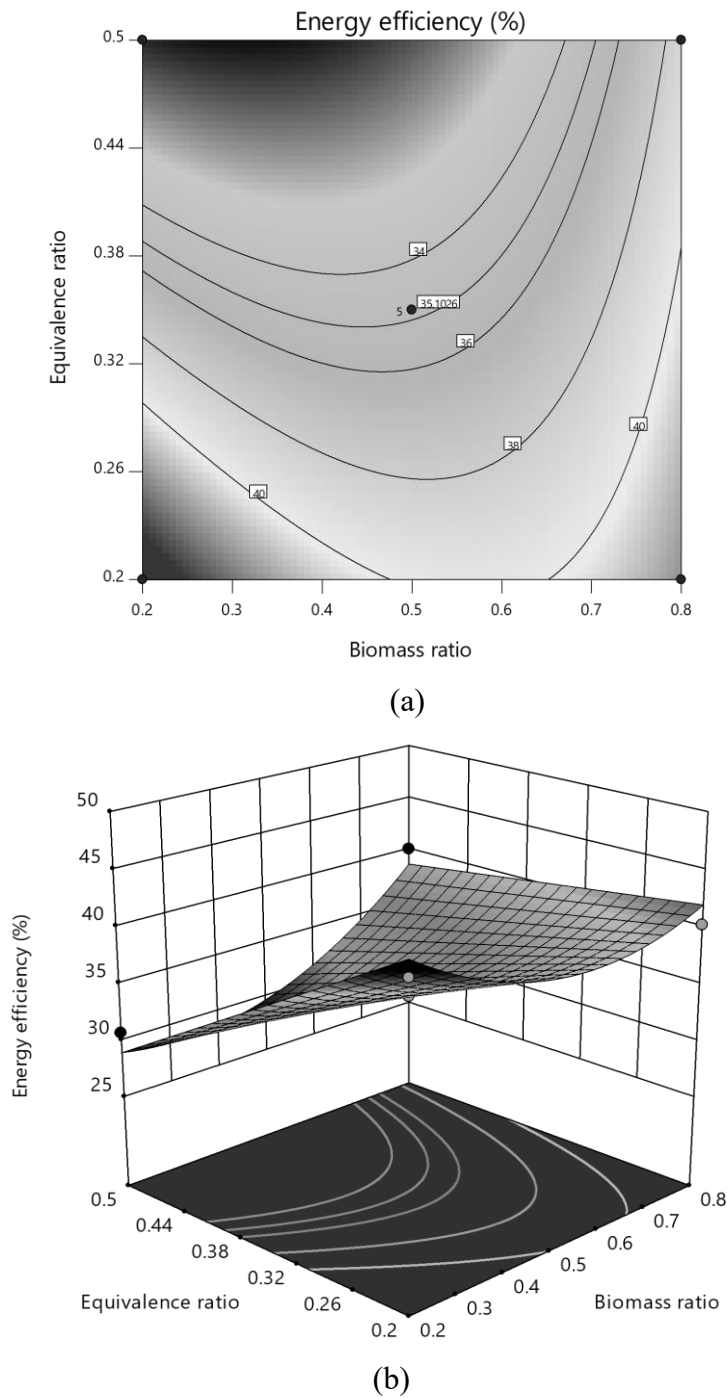


(a)



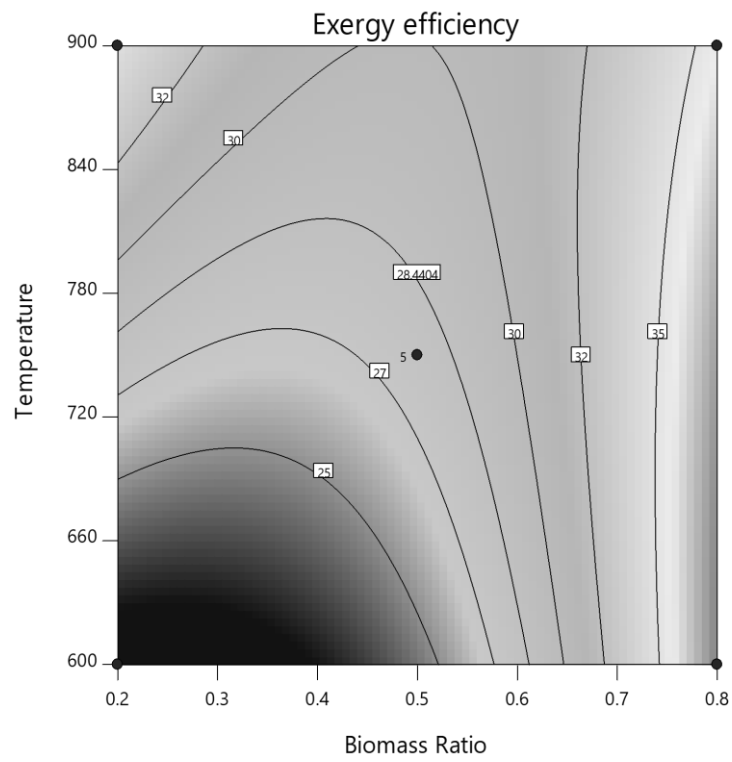
**Figure 5.5:** Effect of biomass ratio and gasification temperature on energy efficiency ( $\eta$ )

Figure 5.5 shows the effect of biomass ratio and gasification temperature on energy efficiency in the form of contour and surface plot respectively. The equivalence ratio is kept constant at 0.35. A substantial rise in energy efficiency can be observed with the addition of sugarcane bagasse in the biomass mixture even at lower temperatures. This can be because of the higher carbon content in the bagasse. Shen et al., 2012 and Mehrpooya et al., 2018 reported an enhancement of energy efficiency with the addition of feedstock with higher carbon content. Mansur et al., 2019 reported enhanced efficiency with the increase in temperature. The result in the present study is also at par to the reported literature.

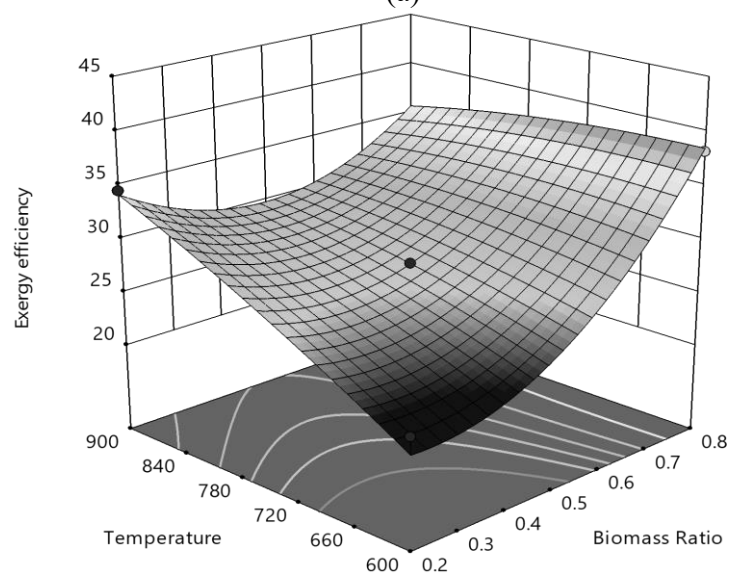


**Figure 5.6:** Effect of biomass ratio and equivalence ratio on energy efficiency ( $\eta$ )

Figure 5.6 shows the contour and surface plot depicting the effect of biomass ratio and equivalence ratio on energy efficiency at 750°C temperature. Energy efficiency is high at lower equivalence ratios and it decreases gradually with increase in air supply to the gasifier. This effect is mainly due to the susceptibility of total combustion reaction with increased air flow at any particular temperature. Ghassemi & Shahsavan-Markadeh, 2014 reported similar trends in case of biomass gasification.



(a)

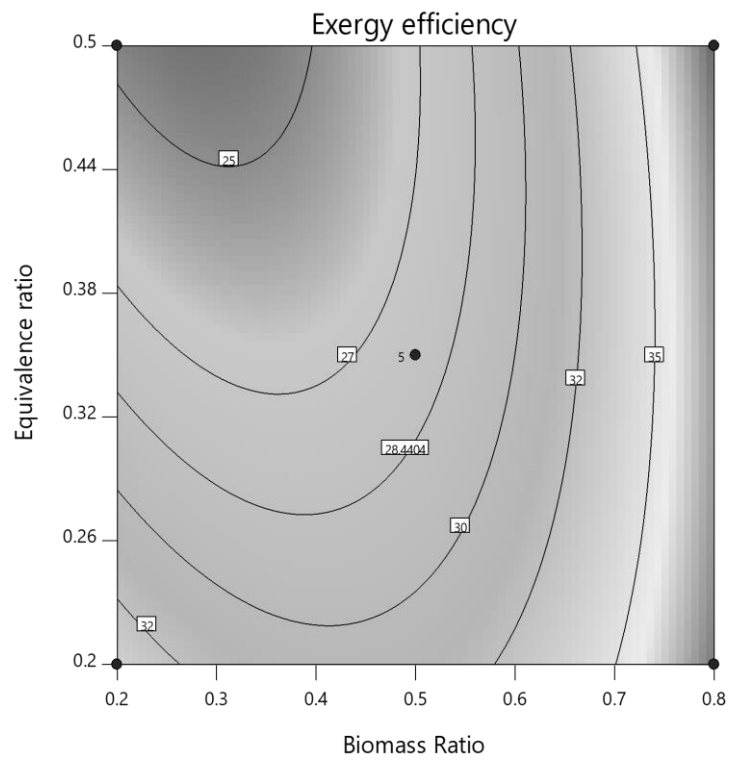


(b)

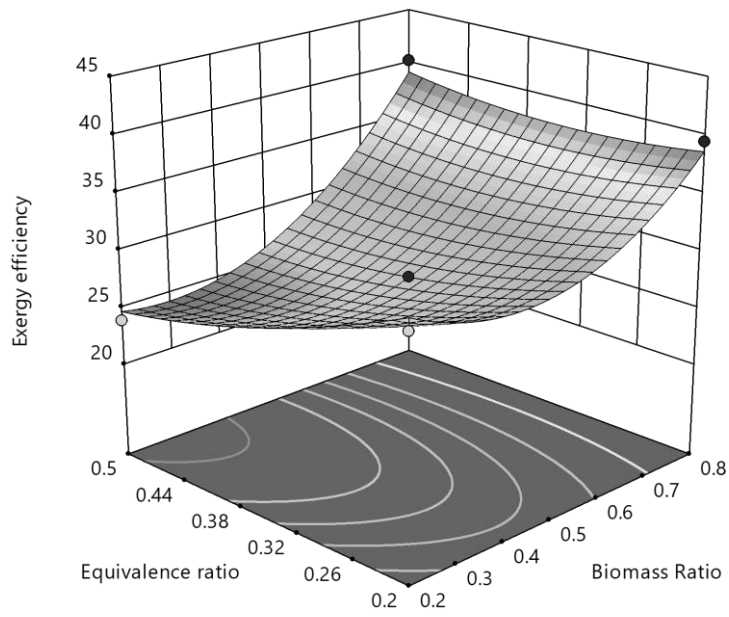
**Figure 5.7:** Effect of biomass ratio and gasification temperature on exergy efficiency ( $\psi$ )

Figure 5.7 shows the contour and surface plot respectively for exergy efficiency varying the biomass ratio and gasification temperature while the equivalence ratio is fixed at 0.35. The plots suggest that exergy efficiency is high at lower temperatures when rice straw content is high in the feedstock mixture but at higher temperatures addition of more sugarcane bagasse enhances the exergy efficiency. As the LHV of sugarcane bagasse is substantially higher than that of rice straw, the total chemical exergy of the feedstock is low when biomass ratio is high. So, at lower temperatures when syngas yield is comparatively low exergy efficiency is high when more rice straw is present in the feedstock mixture. In their study Karamarkovic & Karamarkovic, 2010 also observed high exergetic efficiency at high temperature for carbon rich biomass.

Figure 5.8 represents the effect of biomass ratio and equivalence ratio on exergy efficiency at 750°C temperature in the form of contour and surface plot. The plots show a decline in energy efficiency with rising equivalence ratio. This adverse effect can be because of the total combustion taking place in the presence of more air. Hosseini et al., 2012 also reported an adverse and most impactful effect of increasing equivalence ratio on exergy efficiency. Tapasvi et al., 2015 observed that the most influencing parameter in the biomass gasification process is the equivalence ratio.

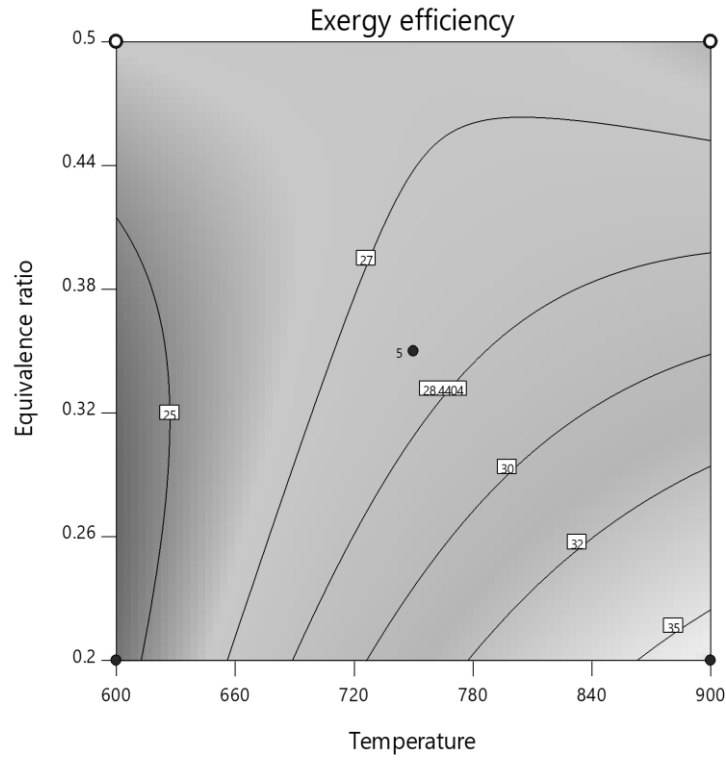


(a)

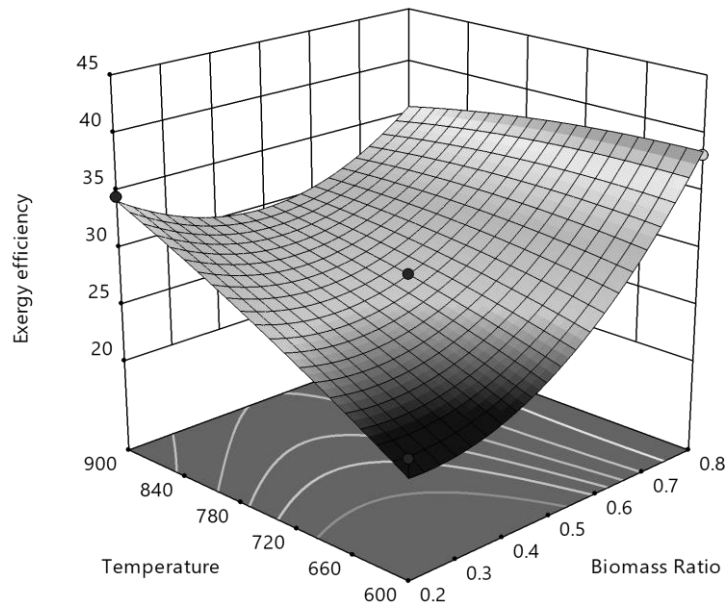


(b)

**Figure 5.8:** Effect of biomass ratio and equivalence ratio on exergy efficiency ( $\psi$ )



(a)



(b)

**Figure 5.9:** Effect of gasification temperature and equivalence ratio on exergy efficiency ( $\psi$ )

Figure 5.9 shows the effect of temperature and equivalence ratio on exergy efficiency at constant biomass ratio of 0.5. Exergy efficiency is high at reduced equivalence ratio and high temperature. At higher temperature and low equivalence ratio, the char breaks down to form  $CO$  at higher amount which in turn increases the syngas exergy increasing the overall exergy



efficiency. Srinivas et al., 2009 also observed positive and adverse influences of temperature and equivalence ratio respectively during their research study on gasification of Indian biomass. The wheat straw and sugarcane bagasse mixture show similar trend in the interaction plots. Therefore the interaction plot has not been shown for the wheat straw and sugarcane bagasse mixture.

Optimization of the process parameters have been conducted to find the maximum energy and exergy efficiency points for both the biomass mixtures for the rice straw and sugarcane bagasse mixture a biomass ratio of 0.343, temperature of 891.64°C, equivalence ratio of 0.217 provided the maximum energy efficiency of 45.35% and maximum exergy efficiency of 40.18% respectively.

For the wheat straw and sugarcane bagasse mixture a biomass ratio of 0.684, temperature of 894.2°C, equivalence ratio of 0.217 provided the maximum energy efficiency of 46.75% and maximum exergy efficiency of 42.51% respectively.

## 5.7 Chapter summary

In the present research, an Aspen plus model has been developed for the co-gasification of two biomass combinations RS-SCB and WS-SCB based on reaction kinetics a regression analysis has been conducted on their thermodynamic performances. Interesting findings have also been obtained through the optimization of efficiencies of energy and exergy. The following conclusions can be drawn from this study:

- i. Biomass co-gasification can be modelled more realistically and reliably using Aspen plus if kinetics of gasification is employed.
- ii. The mean errors recorded for the yield of CO, H<sub>2</sub>, CO<sub>2</sub> and CH<sub>4</sub> while doing the validation are 0.107, 0.122, 0.248 and 0.474 respectively.
- iii. Tar yield of the model is 5.67% (v/v).
- iv. Values of energy and exergy efficiency can be calculated from the regression equation shown in equations 5.8 - 5.11 within the said boundary condition that follows-  
 $0.2 \leq \text{biomass ratio} \leq 0.8$ ,  $600^{\circ}\text{C} \leq \text{gasification temperature} \leq 900^{\circ}\text{C}$ ,  $0.2 \leq \text{equivalence ratio} \leq 0.5$ .
- v. Highest energy efficiency and exergy efficiency for the RS-SCB mixture were achieved to be 45.35% and 40.18% respectively.
- vi. Highest energy efficiency and exergy efficiency for the WS-SCB mixture were achieved to be 46.75% and 42.51% respectively.

Form this study it can be concluded that the mixture of WS-SCB performs better in co-gasification. This has been rigorously tested in both equilibrium and kinetic models of co-gasification. In the next chapter, this combination will be utilized for the production of bio-ethanol via the hybrid route of co-gasification and syngas fermentation.

---

## **Chapter 6. Bio-ethanol production via syngas platform: model development and multi-objective optimization**

---

### **6.1 Objective of the chapter**

This study aims to develop a simulation model of the novel co-gasification fermentation process for the production of bioethanol with the help of Aspen plus software, using wheat straw and sugarcane bagasse as feedstock as suggested by the previous study. The process model aims to be used in modelling the co-gasification fermentation pathway for any Indian lignocellulosic biomass. After proper validation of the co-gasification module, Regression equations for a number of various performance parameters like ethanol production rate, LHV of syngas, CGE, overall energy efficiency and  $CO_2$  emission has been developed in terms of biomass mass ratio (wheat straw: sugarcane bagasse), gasification temperature, and equivalence ratio using Response Surface Methodology (RSM) as these performance parameters majorly indicate whether the process is sustainable or not. Finally a multi-objective optimization has been conducted to maximize the ethanol production rate and overall energy efficiency of the process and minimize the amount of  $CO_2$  exerted at the end of the process, thus trying to achieve a cleaner ethanol production.

### **6.2 Feedstock selection and mathematical background**

#### **6.2.1 Feedstock selection**

Wheat straw and sugarcane bagasse have been selected as the feedstock for this modelling study. The ultimate and proximate analysis of both biomasses as well as their lower heating values is listed in Table 3.1.

#### **6.2.2 Mathematical methodology**

The gasification process is modelled in Aspen plus following non-stoichiometric equilibrium. In the non-stoichiometric equilibrium process, the product gas composition is determined using the Gibbs free energy minimization method.

### 6.3 Model development

The co-gasification fermentation model, developed in Aspen plus using wheat straw and sugarcane bagasse as feedstock, is shown in Figure 6.1. As chemical formulas of both the biomasses are not available conventionally, they have been declared as non-conventional component, specified by the ultimate and proximate analysis, as per the input criterion of Aspen plus. Enthalpy and density model of the biomass is provided by the packages HCOALGEN and DCOALIGT respectively in Aspen plus (Acar & Böke, 2019). The ultimate and proximate analysis of wheat straw and sugarcane bagasse is provided in Table 3.1. Basic model assumptions are as follows:

1. All the unit operations are in steady state.
2. All the reactors are isothermal.
3. All the reactions are considered to attain equilibrium.
4. Product gases of gasification obey the ideal gas law.
5. Tar formation is neglected in case of the gasifier.
6. Water is the medium for syngas fermentation.

As the simulation model deals with both liquid and gaseous states, the non-random two liquid (NRTL) model is utilised as the equation of state to calculate the thermodynamic parameters. The major processes in this modelling involve three stages namely gasification, fermentation, and separation. The first step of this gasification is drying which is simulated by using two stoichiometric blocks (RStoic), DEMOIST1 and DEMOIST2, for the purpose of dehumidification: the moisture separates from the biomass streams namely BIOMASS1 (wheat straw) and BIOMASS2 (Sugarcane bagasse) in flash separator blocks DRYR1 and DRYR2. The mass flow rate of both the biomasses is kept at 30 tonnes/h. Both the non-conventional streams of dry biomass then decompose in the yield block, DECOMP to conventional components as provided in its ultimate analysis.

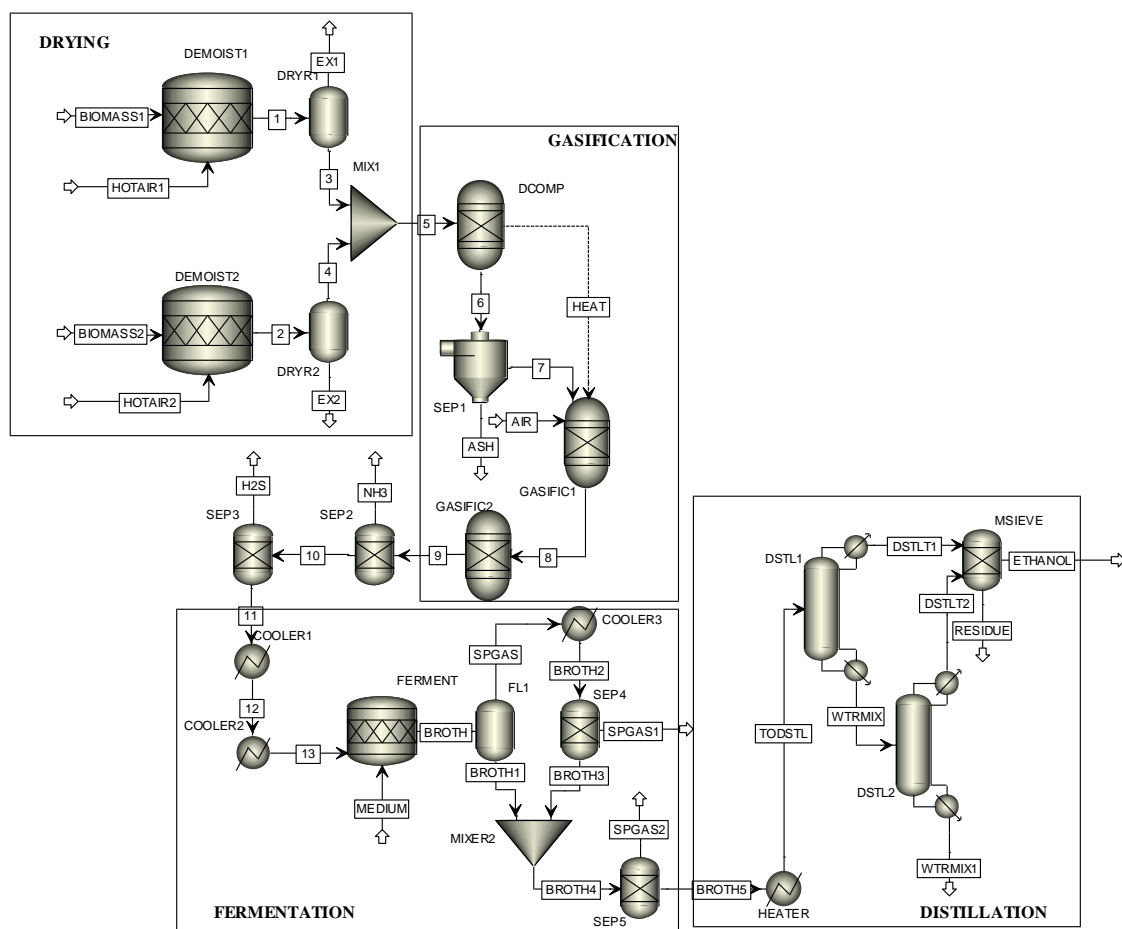


**Figure 6.1:** Co-gasification and fermentation simulation flow-sheet in Aspen plus

A calculator block CAL1 is combined with the DECOMP block for this purpose. The ash present in the biomass is separated using a cyclone separator SSplit block SEP1. The gasification process is modelled using two Gibbs free energy minimization block (RGibbs), GASIFIC1 and GASIFIC2. In the block GASIFIC1, the combustion reactions are modelled following reactions R3-R7 listed in Table 1.2. Heat required for the gasification reaction is supplied from the DECOMP block. The gasifier temperature is set at 750°C for the base case. Air is being used as the gasifying agent in GASIFIC1 block for the combustions reactions to complete. Air is provided according to the equivalence ratio given in equation 5.2. An equivalence ratio of 0.28 is assumed for the base simulation which is in accordance with the previous literatures (Ramzan et al., 2011). The reduction reactions take place at the GASIFIC2 block following the restricted chemical equilibrium approach. The reactions modelled at this stage are reactions R8-R12 in Table 1.2. Both the RGibbs blocks (GASIFIC1 and GASIFIC2) are kept at atmospheric pressure in this simulation study. With the completion of this gasification process, a mixture of  $CO$ ,  $H_2$ ,  $CO_2$ ,  $CH_4$ ,  $NH_3$ ,  $H_2S$ , and  $N_2$  is received. In the next

step, the traces of  $NH_3$  and  $H_2S$  are removed from the gas mixture by passing the gas mixture through a  $NH_3$  and  $H_2S$  removal unit, respectively. Removal of  $NH_3$  involves absorption which is conducted in the SEP2 block (Frilund et al., 2021). As  $NH_3$  protonates in water, the SEP2 block is assumed to conduct water wash of the syngas. Subsequent removal of  $H_2S$  is conducted in an activated Carbon bed, which is modelled by SEP3 block in the present model (Liakakou et al., 2021). After the hot gas clean up, the cleaned gas mixture is passed through two syngas coolers namely COOLER1 and COOLER2 to bring the temperature down to 37°C which is ideal for further fermentation process (Pardo-Planas et al., 2017a). Next, the syngas mixture is provided into the stoichiometric block FERMENT to carry out the fermentation process in the presence of proper fermentation medium. In this simulation, water is used as the fermentation medium as the various nutrients used in syngas fermentation are not available in Aspen plus (Okolie et al., 2020). In the FERMENT block, the fermentation of  $CO$  and  $H_2$  takes place in the presence of acetogenic bacteria *Clostridium Ljungdahlii* following the acetyl-CoA pathway. The fermentation reactions considered are reactions R19-R22. The alcohol-acetate mixture produced in the FERMENT block needs to be separated from the rest of the gas, mostly  $CO_2$ , and for this purpose a flash separator FL1 is employed. The liquid portion leaves as BROTH1 material stream and the vapour portion leaves as SPGAS gaseous stream. The SPGAS stream then cools down to 25°C in COOLER3 block, for further vapour separation in SEP4 block, and it finally separates from the total gas as BROTH3 liquid stream and SPGAS1 vapour stream. The BROTH3 stream mixes with the BROTH1 stream coming from the flash separator in MIXER2 block and moves to SEP5 block for a final separation of vapour from the liquid mixture. The final liquid mixture is then preheated up to a temperature of 90°C in HEATER block as preheating of the broth is necessary for proper distillation. The distillation process is carried out in two consecutive RadFrac distillation columns DSTL1 and DSTL2. In DSTL1, the number of stages is set at 30 and reflux ratio is 5.4. The exact reflux ratio for this distillation process is found out by setting a design specification using the mass purity as the target variable, and varying the input of reflux ratio from 1 to 10. A mass purity of 94 % is set through the first distillation. And, the second distillation is conducted in DSTL2 where a reflux ratio of 6.448 is obtained using design specification in the RadFrac block. The final ethanol and water mixture is then transferred to a molecular sieve SEP4, which has been modelled using a separator block, and a purity of 99 % is achieved.

## 6.4 Response Surface Methodology

RSM is a globally used optimization method in statistics, based on non-linear multivariable model (Lv et al., 2014). This methodology provides a robust procedure to optimize process variables causing fluctuation in any experimental design. A mathematical model best fitting to the experimental data is also obtained by this method. In our study, Box- Benhnken design is used to carry out the RSM. Biomass ratio (wheat straw: sugarcane bagasse), gasification temperature, and ER are used as the input variables; whereas, ethanol production rate, LHV, CGE, overall energy efficiency ( $\eta$ ) and total CO<sub>2</sub> emission are the output variables. The range of biomass ratio, temperature, and equivalence ratio is set at 0.2- 0.8, 500°C-1000°C and 0.15- 0.5, respectively. So, a total of 17 experiment sets along with 3 variables and 3 levels are obtained. The output values obtained using Aspen plus are utilised to form an output matrix to perform the analysis of variance (ANOVA). This ANOVA is useful for obtaining the regression model for each output response. Significance of each input parameter as well as their interaction can also be evaluated through this ANOVA model. The accuracy of the model is calculated by the values of regression coefficient ( $R^2$ ), adjusted  $R^2$ , and predicted  $R^2$  respectively.

## 6.5 Performance parameters

The performance parameters utilised in this model are the ethanol production rate, lower heating value of the syngas, cold gas efficiency of gasification, and overall energy efficiency ( $\eta$ ) of the gasification-fermentation process.

Ethanol production rate is the output rate of ethanol (t/h) coming through the overhead product stream of the distillation tower.

Lower heating value of the syngas is determined by the summation of the product of volume fraction of all constituents, and their corresponding lower heating values (Pati et al., 2021). This has been provided in equation 4.4.

CGE is the ratio of the total lower heating value of syngas to the total lower heating value of supplied biomass per hour.

$$CGE = \frac{\text{Syngas volumetric flow rate (Nm}^3/\text{hr}) \times LHV_{\text{syngas}}(\text{MJ/Nm}^3)}{\text{Biomass flow rate (Kg/h)} \times LHV_{\text{biomass}}(\text{MJ/Kg})} \quad (6.1)$$

The overall energy efficiency ( $\eta$ ) of the co-gasification fermentation process has been calculated as the ratio of the total energy content of produced ethanol to the energy content of biomass and is expressed as:

$$\eta = \frac{\text{mass flow rate of ethanol (Kg/h)} \times \text{LHV}_{\text{ethanol}}(\text{MJ/Kg})}{\text{Biomass flow rate (Kg/h)} \times \text{LHV}_{\text{biomass}}(\text{MJ/Kg})} \quad (6.2)$$

## 6.6 Results and Discussions

### 6.6.1 Model validation

The gasification module of the above simulation model is validated by comparing the simulation results with the experimental results of Gabbrielli et al., 2022 and Mallick et al., 2020 at similar operating conditions. Gabbrielli et al., 2022 conducted air gasification in a fixed bed downdraft gasifier using sewage sludge and woodchips as feedstock. Subsequently, Mallick et al., 2020 conducted their experiments using rice husk and saw dust as feedstock in a circulating fluidised bed gasifier. The proximate and ultimate analysis of various biomasses used in the respective experimental studies and the operating conditions are listed in Table 6.1. The models with literature data have been simulated using the same Aspen blocks described in section 6.3. The model outputs have been compared with the literature findings. Deviation of the model from experimental results was estimated in terms of root mean square error which is calculated as presented in equation 6.3.

$$rmse = \sqrt{\frac{\sum (y_{exp} - y_{model})^2}{N}} \quad (6.3)$$



**Table 6.1:** Elemental analysis of the feedstock to be used for validation purpose

	<b>Gabbrielli et al.</b>		<b>Mallick et al. [22]</b>	
	Woodchips	Sewage sludge	Rice husk	Saw dust
<b>Proximate analysis</b>				
<b>Moisture</b>	13.2	21.2	8.7	9.4
<b>Fixed carbon</b>	15.4	2.6	12.0	15.6
<b>Volatile matter</b>	83.4	28.0	60.2	73.8
<b>Ash</b>	0.8	69.4	19.7	1.1
<b>Ultimate analysis</b>				
<b>Ash</b>	0.8	69.4	19.7	1.1
<b>C</b>	49.9	14.9	38.5	52.3
<b>H</b>	6.1	1.9	4.8	5.2
<b>N</b>	0.2	1.1	1.0	0.3
<b>Cl</b>	nd	0.2	nd	nd
<b>S</b>	nd	0.2	nd	nd
<b>O</b>	43.0	12.9	36.1	41.7

The variations of experimental and simulated mole percentage can be found in Figure 6.2. While comparing the model with sewage sludge and wood chips co-gasification in Figure 6.2(a), an rmse value of 2.6 is obtained. Whereas, in case of rice husk and sawdust co-gasification the rmse value is found to be 1.34, which are in accordance with the literature (Kombe et al., 2022; Rupesh et al., 2016a) In case of both the models the predicted values are in good agreement with the experimental data considering equilibrium modelling of biomass co-gasification (Gagliano et al., 2017a). However, in Figure 6.2(b), the yield of methane is very low in the model compared to the experimental value which attributes to the fact that in equilibrium gasification, the conversion in the water gas shift reaction is much higher at higher temperatures (Kombe et al., 2022). This problem can be addressed by the usage of kinetic modelling.

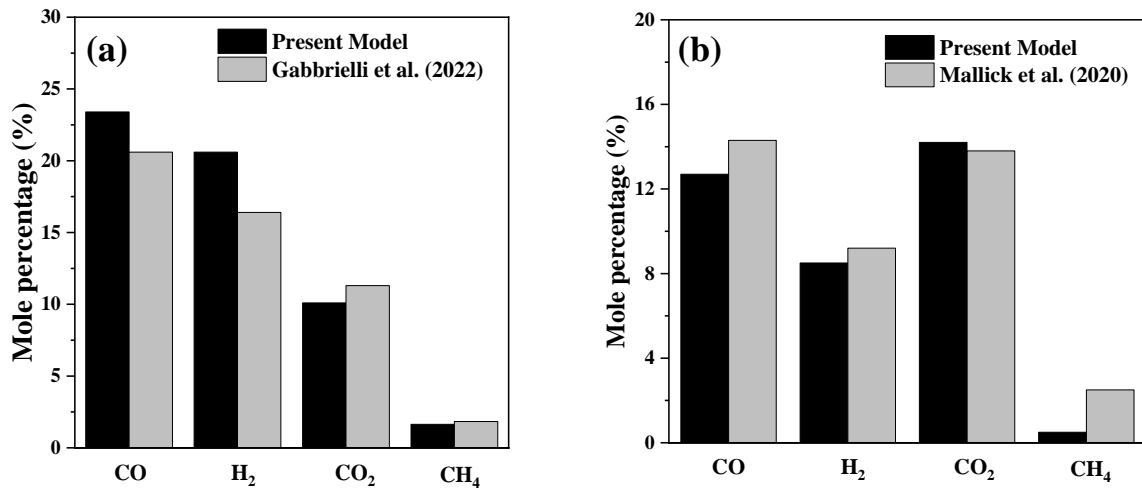
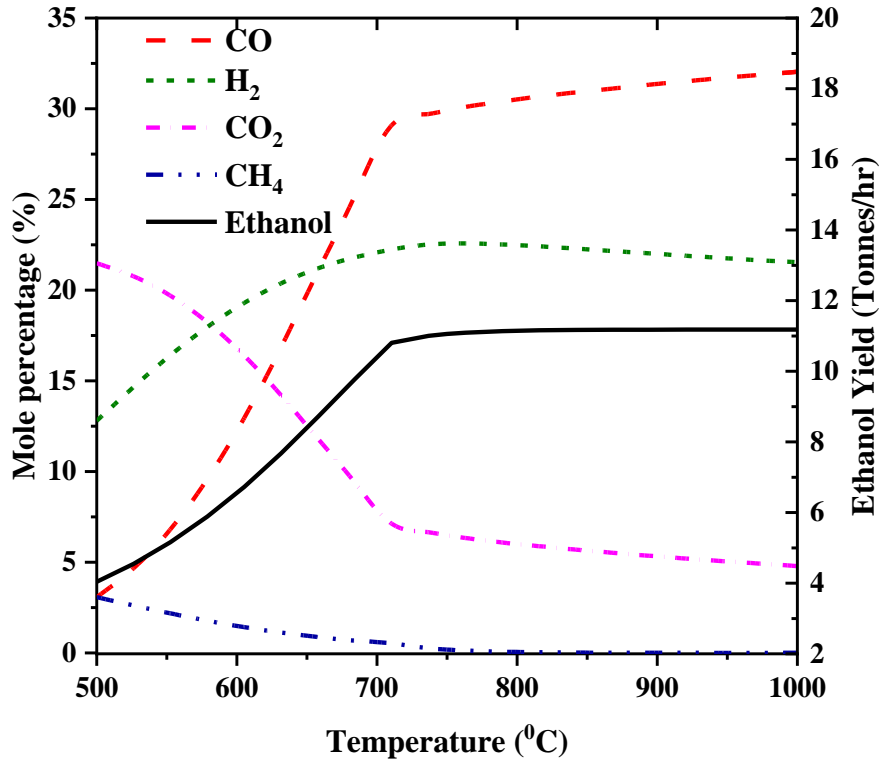


**Figure 6.2:** Variation of model yields with experimental results

### 6.6.2 Sensitivity analysis

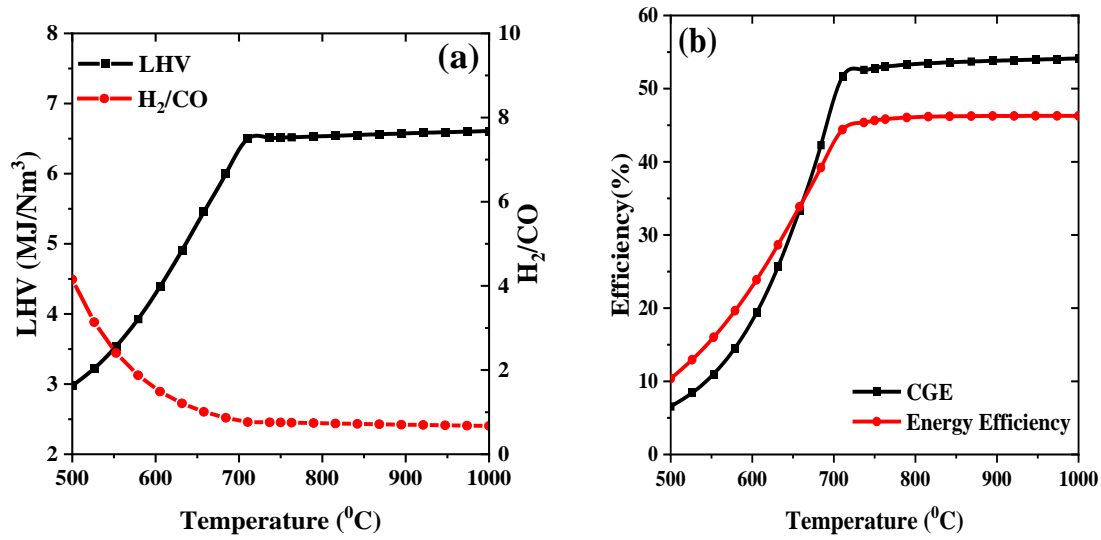
Sensitivity of this model has been tested against the variation of temperature and equivalence ratio. Temperature of co-gasification has been varied from 500°C to 1000°C keeping the biomass ratio and equivalence ratio constant at 1 and 0.28, respectively. For equivalence ratio sensitivity, the equivalence ratio has been varied from 0.1 to 0.5 where biomass ratio and temperature are fixed at 1 and 750°C, respectively.

Figure 6.3 shows the variation in the mole percentage syngas components and ethanol with temperature. Very high slope of the *CO* versus temperature plot can be seen from Figure 6.3 which indicates that *CO* production increases significantly with the increase of temperature till 700°C. Beyond that, up to 1000°C the percentage-increase in *CO* production is not that much significant. In case of *H<sub>2</sub>*, the production increases from 500°C to 760°C, and above that, there is a slight decrease in production with the increase in temperature. The production of *CO<sub>2</sub>* and *CH<sub>4</sub>* decreases with the increase in temperature. Kombe et al., 2022 reported similar trends in their simulation study. The increase in the concentration of *H<sub>2</sub>* can be attributed to the occurrence of water-gas shift reaction (Abdelrahim et al., 2020). The slight decrease in the *H<sub>2</sub>* production beyond 700°C can be due to the decrease in equilibrium constant of water gas shift reaction (Franco et al., 2003). As the ethanol production rate is directly proportional to the yield of *CO* and *H<sub>2</sub>*, with the increase of *CO* and *H<sub>2</sub>* production the ethanol production also increases with gasification temperature.



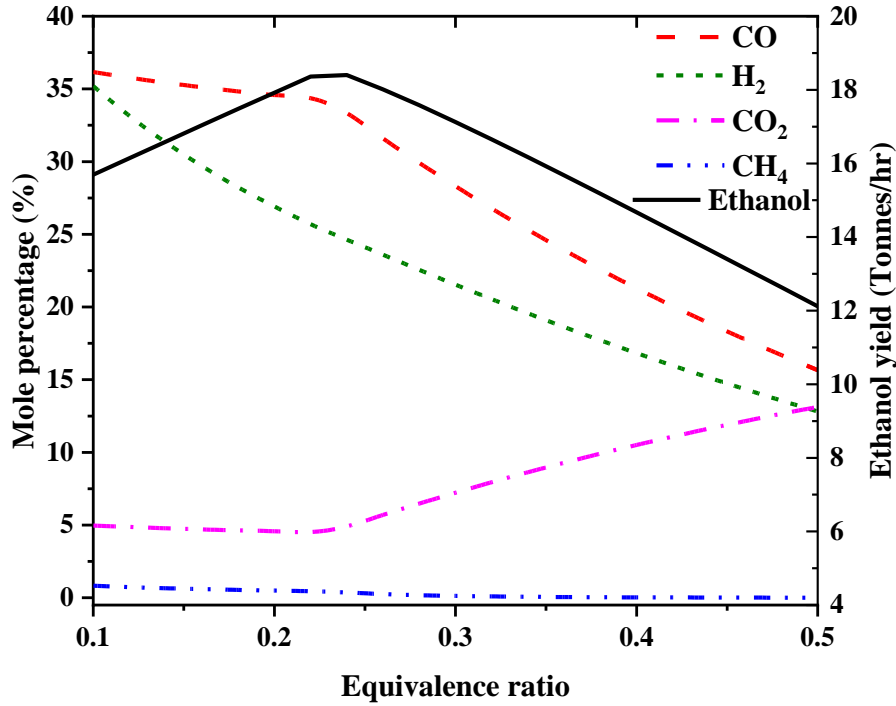
**Figure 6.3:** Variation of syngas and ethanol yield with temperature

Figure 6.4 (a) and (b) depict the variation of  $LHV_{\text{syngas}}$ ,  $H_2/CO$  ratio, CGE and overall energy efficiency. Increase in temperature affects the  $LHV_{\text{syngas}}$  positively as  $LHV_{\text{syngas}}$  improves in Figure 6.4(a) with increasing temperature. High temperature promotes the yield of  $CO$  and  $H_2$  as already mentioned in Figure 6.3 which in turn increases the lower heating value of the syngas. The plot of  $H_2/CO$  against temperature is a constantly decreasing curve which becomes constant beyond  $700^\circ\text{C}$ . Due to the relatively slow increase in forward rate constant with respect to the backward water-gas reaction, the  $CO$  production becomes stagnant and the production of  $H_2$  decreases slightly. Han et al., 2017 reported similar results in their simulation work. From Figure 6.4(b), it can be observed that the CGE of syngas continuously increases with the increase in temperature, which can be attributed to the increase in both the yield and LHV of syngas with the increase in temperature. This finding is in accordance with the published work of Abdelrahim et al., 2020 as they reported similar variation of CGE with temperature. Overall energy efficiency also steeply increases up to  $700^\circ\text{C}$  temperature, and passes through a plateau above  $700^\circ\text{C}$  temperature till  $1000^\circ\text{C}$  is reached. Such variations can be due to the consistent ethanol yield at elevated gasification temperatures beyond  $700^\circ\text{C}$ .



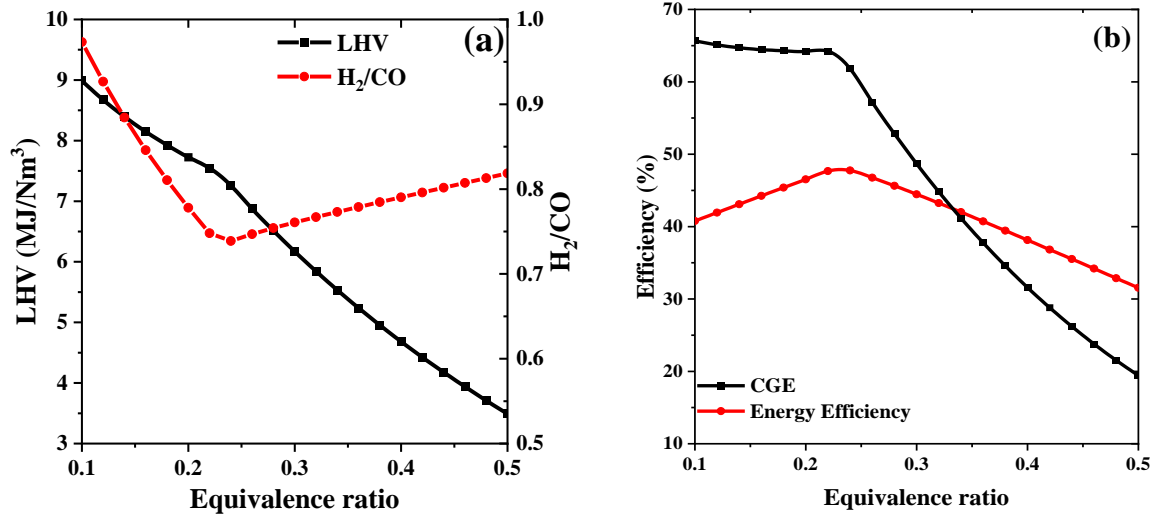
**Figure 6.4:** Variation of (a) LHV of syngas and  $H_2/CO$  ratio and (b) CGE and overall energy efficiency with temperature

Figure 6.5 demonstrates the variation of syngas mole percentage and ethanol production rate against varying equivalence ratio while keeping the temperature constant at 750°C. The  $CO$  and  $H_2$  production reduces with increasing equivalence ratio. As a consequence, the yield of  $CO_2$  increases with increasing equivalence ratio. The yield of  $CH_4$  also reduces with the increase in equivalence ratio. The decrease of  $CO$  and  $H_2$  production is due to the increase in air flow in the gasifier which increases the oxidation and steam formation reaction through combustion (Pauls et al., 2016). This can be attributed to the reticence of the methane formation reaction at higher temperatures (Mendiburu et al., 2014). Ngamchompoo & Triratanasirichai, 2017 in their experimental work and Aydin et al., 2017 in their modelling study found similar results. The ethanol production against equivalence ratio exhibits a positive slope up to an equivalence ratio of 0.28, while proceeding further, the slope becomes negative as the amount of  $CO$  and  $H_2$  in the syngas decreases. Safarian et al., 2020 reported similar variation of specific ethanol mass flow rate against equivalence ratio.



**Figure 6.5:** Variation of syngas and ethanol yield with equivalence ratio

Figure 6.6 (a) and (b) demonstrate the influence of the variation of equivalence ratio on the performance parameters namely  $LHV_{\text{syngas}}$ ,  $H_2/CO$  ratio, CGE and overall energy efficiency ( $\eta$ ). It can be observed that the value of  $LHV_{\text{syngas}}$  decreases continuously with increasing ER whereas the value of  $H_2/CO$  ratio primarily decreases and then increases. The  $LHV_{\text{syngas}}$  is directly associated with the yield of  $CO$ ,  $H_2$  and  $CH_4$  which decreases with increasing equivalence ratio hence reducing the  $LHV_{\text{syngas}}$  (Devi et al., 2003). With increased supply of air the rate of carbon combustion reaction becomes more prominent than steam formation reaction hence the depletion of  $CO$  is higher than  $H_2$  which results in the increase of  $H_2/CO$  ratio at higher equivalence ratio. The CGE follows similar trend as that of the  $LHV_{\text{syngas}}$  as the feedstock input is constant and the  $LHV_{\text{syngas}}$  decreases with the increase in ER. The overall energy efficiency ( $\eta$ ) increases till an ER value of 0.28 and beyond that it decreases. This can be explained by the trend of ethanol yield with the ER shown in Figure 6.5. Figure 6.5 suggests that the ethanol production increases up to a certain value ( $\approx 0.28$ ) of ER, beyond which it decreases. As the energy contribution of ethanol is also included in the definition of  $\eta$ , the observed influence of ER on  $\eta$  can be thus explained. Han et al. also proposed a range of equivalence ratio of 0.2-0.3 for the optimal value of performance parameters which is in accordance with the present study (Han et al., 2017).



**Figure 6.6:** Variation of (a) LHV of syngas and H<sub>2</sub>/CO ratio and (b) CGE and overall energy efficiency with equivalence ratio

### 6.6.3 Statistical analysis results

#### 6.6.3.1 ANOVA results

The ANOVA results of the regression analysis for each of the response variables have been listed in the table provided in the supplementary section. It indicates that the p-values for each of the statistical model is significant. The  $R^2$  values for ethanol productivity, LHV<sub>syngas</sub>, CGE, overall energy efficiency ( $\eta$ ), and CO<sub>2</sub> emission are 0.9599, 0.9686, 0.9593, 0.9598 and 0.9982, respectively. The difference between the adjusted and predicted  $R^2$  values for each of the regression model is less than 0.2 which indicates that the signal to noise ratio in each of the statistical model is minimal (Inayat et al., 2021). Also, the amount of adequate precision is high enough (more than 4) for the models which discard the chance of error due to erroneous calculation or measurements (Sim et al., 2007). The ANOVA table has been provided in Table 6.2.

**Table 6.2:** ANOVA results for response variables of the hybrid model

	<b>Ethanol productivity</b>		<b>LHV<sub>syngas</sub></b>		<b>CGE</b>		<b>Overall energy Efficiency</b>		<b>CO<sub>2</sub> emission</b>	
<b>constants</b>	F- value	p- value	F- value	p- value	F- value	p- value	F- value	p- value	F- value	p- value
<b>Model</b>	30.81	< 0.000 1	39.60	< 0.000 1	30.34	< 0.000 1	30.70	< 0.000 1	442.10	< 0.000 1
<b>BR</b>	0.764 9	0.404 5	0.008 5	0.928 6	0.049 7	0.828 6	0.380 9	0.552 4	5.73	0.047 8
<b>Temp</b>	101.3 9	< 0.000 1	37.30	0.000 2	51.64	< 0.000 1	102.0 8	< 0.000 1	51.90	0.000 2
<b>ER</b>	42.08	0.000 1	208.6 6	< 0.000 1	115.4 4	< 0.000 1	41.86	0.000 1	3857.3 4	< 0.000 1
<b>BR× Temp</b>	0.064 7	0.804 9	0.027 7	0.871 6	0.006 7	0.936 6	0.077 4	0.787 1	0.0662	0.804 4
<b>BR ×ER</b>	0.000 2	0.988 8	0.005 3	0.943 4	0.003 8	0.952 1	0.004 4	0.948 7	0.3801	0.557 1
<b>Temp × ER</b>	30.89	0.000 4	17.77	0.002 3	29.00	0.000 4	30.73	0.000 4	38.57	0.000 4
<b>BR × BR</b>	-	-	-	-	-	-			0.6554	0.444 8
<b>Temp × Temp</b>	40.48	0.000 1	13.42	0.005 2	16.23	0.003 0	39.76	0.000 1	22.63	0.002 1
<b>ER × ER</b>	-	-	-	-	-	-			0.5715	0.474 3
<b>Model fit statistics</b>										
<b>R<sup>2</sup></b>	0.9599		0.9686		0.9593		0.9598		0.9982	
<b>Adj-R<sup>2</sup></b>	0.9288		0.9441		0.9277		0.9285		0.9960	
<b>Pred-R<sup>2</sup></b>	0.7583		0.7969		0.7310		0.7574		0.9719	
<b>Adq. Prec.</b>	18.4806		21.1849		18.9247		18.4957		68.6440	

The regression equations for each of the response variables are presented in equations 6.4-6.8. These equations are useful in predicting the values of response variables for any set of values within the given range.

$$\begin{aligned} \text{Ethanol productivity} = & -68100.76167 + 743.64 \times \text{Biomass ratio} + 176.195 \times \\ & + 52836.8 \times \text{Eq ratio} - 2.22 \times \text{Biomass ratio} \times \text{Temp} - 144.2857 \times \text{Biomass ratio} \times \\ & \text{Eq ratio} - 83.1 \times \text{Temp} \times \text{Eq ratio} - 0.081 \times \text{Temp}^2 \quad (6.4) \end{aligned}$$

$$\begin{aligned} \text{LHV} = & -14.11 + 0.652 \times \text{Biomass ratio} + 0.046 \times \text{Temp} + 8.74 \times \text{Eq ratio} - \\ & 0.0006 \times \text{Biomass ratio} \times \text{Temp} - 0.314 \times \text{Biomass ratio} \times \text{Eq ratio} - 0.027 \times \\ & \text{Temp} \times \text{Eq ratio} - 0.0004 \times \text{Temp}^2 \quad (6.5) \end{aligned}$$

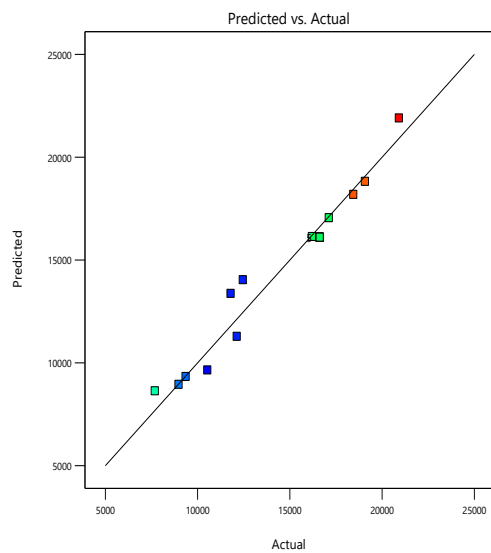
$$\begin{aligned} \text{CGE} = & -289.8 + 6.0846 \times \text{Biomass ratio} + 0.71 \times \text{Temp} + 244.37 \times \text{Eq ratio} - \\ & 0.004 \times \text{Biomass ratio} \times \text{Temp} - 3.58 \times \text{Biomass ratio} \times \text{Eq ratio} - 0.468 \times \text{Temp} \times \\ & \text{Eq ratio} - 0.0002 \times \text{Temp}^2 \quad (6.6) \end{aligned}$$

$$\begin{aligned} \text{Overall energy efficiency } (\eta) = & -167.93 + 3.45 \times \text{Biomass ratio} + 0.433 \times \text{Temp} + \\ & 130.98 \times \text{Eq ratio} - 0.006 \times \text{Biomass ratio} \times \text{Temp} - 1.63 \times \text{Biomass ratio} \times \\ & \text{Eq ratio} - 0.205 \times \text{Temp} \times \text{Eq ratio} - 0.0002 \times \text{Temp}^2 \quad (6.7) \end{aligned}$$

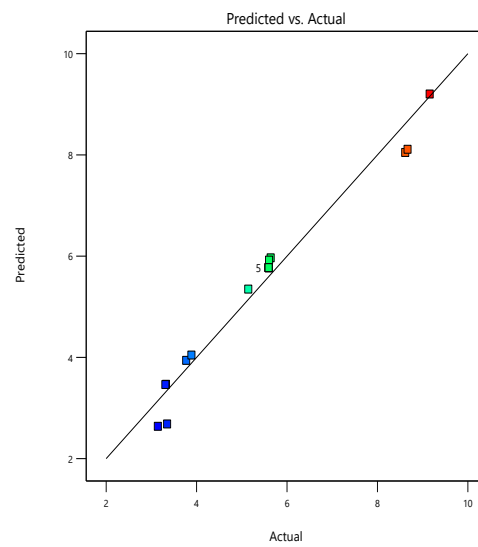
$$\begin{aligned} \text{CO}_2 \text{ emission} = & -37342.96 + 3898.51 \times \text{Biomass ratio} + 101.795 \times \text{Temp} + 1.558 \times \\ & 10^5 \times \text{Eq ratio} - 1.61 \times \text{Biomass ratio} \times \text{Temp} - 4415.173 \times \text{Biomass ratio} \times \\ & \text{Eq ratio} - 66.71 \times \text{Temp} \times \text{Eq ratio} - 3296.24 \times \text{Biomass ratio}^2 - 0.0436 \times \\ & \text{Temp}^2 - 9045.6 \times \text{Eq ratio}^2 \quad (6.8) \end{aligned}$$

Figure 6.7 (a)-(e) depict the amount of deviation of the actual response values from the response surface regression model values. The straight lines indicate the predicted values of the statistical model whereas the dots indicate the actual values obtained by Aspen simulation data. All the figures indicate that there is not much deviation between any predicted value by the model, and the actual values obtained from the simulation, which in turn justifies that the quadratic regression models can be used for predicting the response variables.

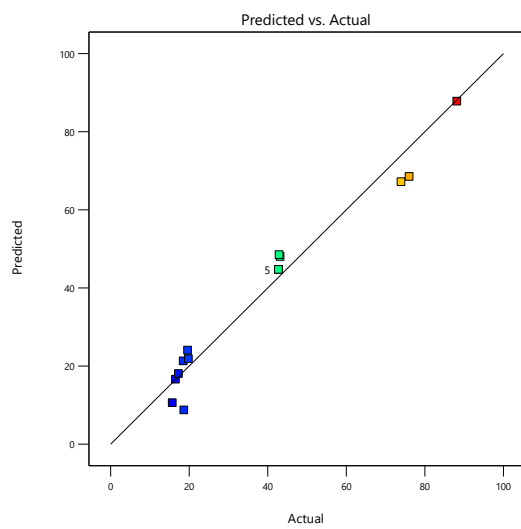




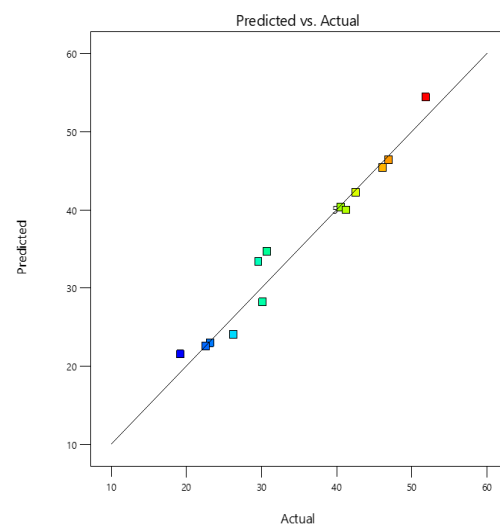
(a) Ethanol production rate



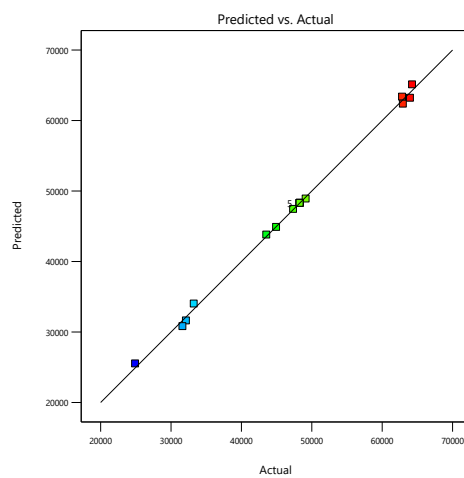
(b) Lower heating value



(c) Cold gas efficiency



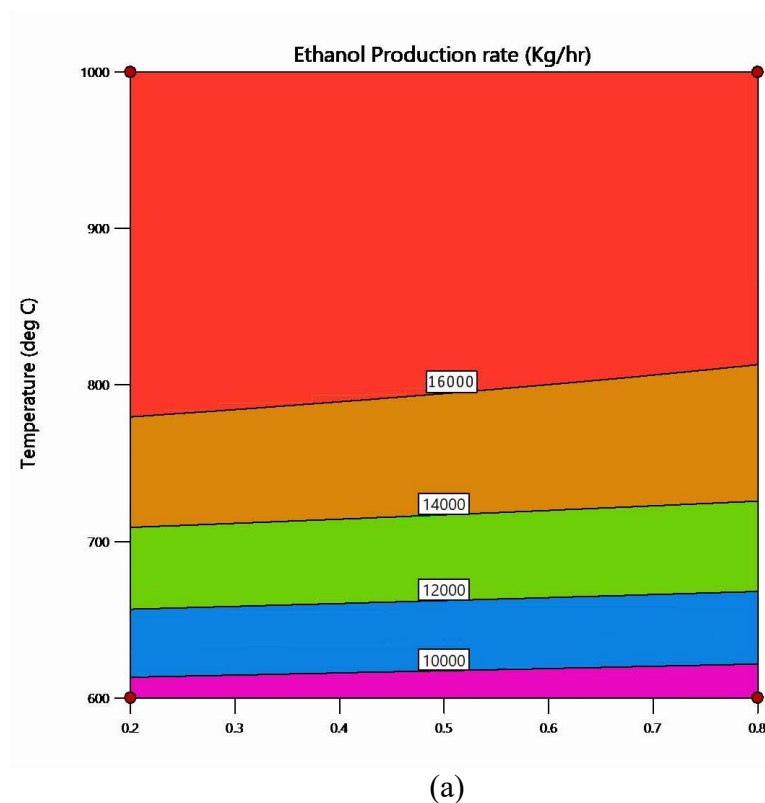
(d) Overall energy efficiency

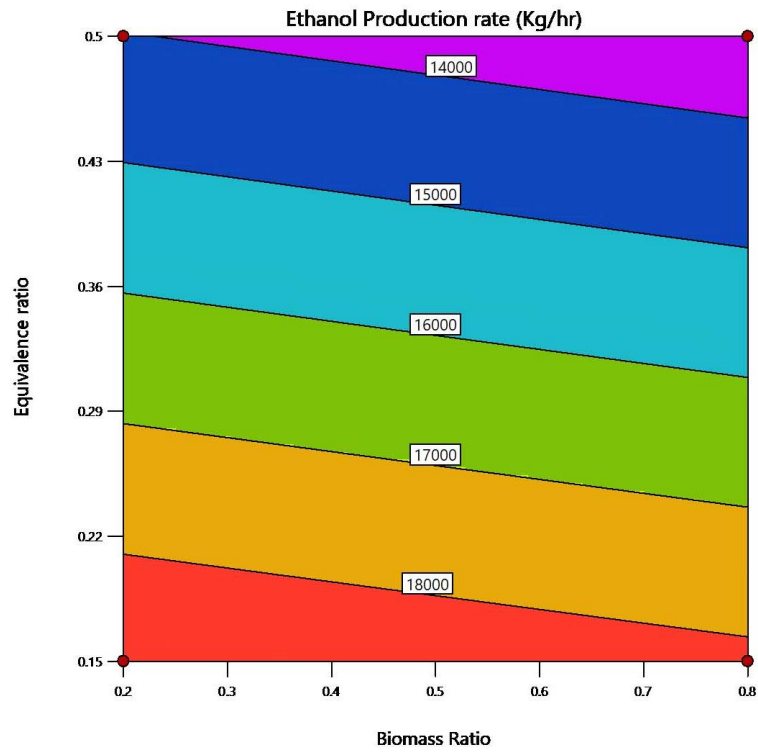


(e) CO<sub>2</sub> emission

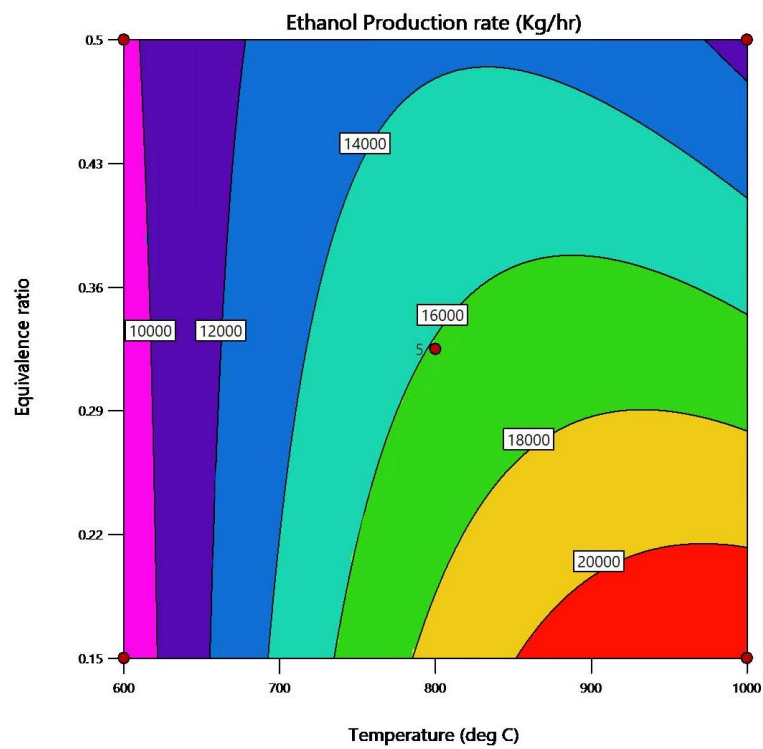
**Figure 6.7:** Deviation of the actual responses from predicted response values of regression model

Interaction effect of the operating variables over the response variables is necessary to optimize these operating variables. Figure 6.8 shows the effects of biomass ratio, temperature, and equivalence ratio on ethanol production rate. Figure 6.8 (a) depicts the contour plot of ethanol production upon a combined effect of biomass ratio and temperature. It can be inferred from the figure that the ethanol production increases at higher temperature. Also, from Figure 6.8 (b), it can be observed that lower equivalence ratio and higher biomass ratio increase the ethanol production of the system. Figure 6.8 (c) depicts the combined effects of temperature and equivalence on ethanol production. From the contour of ethanol production, it is evident that high temperature and low equivalence ratio increase the hourly yield of ethanol, whereas at higher values of equivalence ratio, the ethanol production is low irrespective of temperature. So the production rate of ethanol increases at high biomass ratio, high temperature and low equivalence ratio.





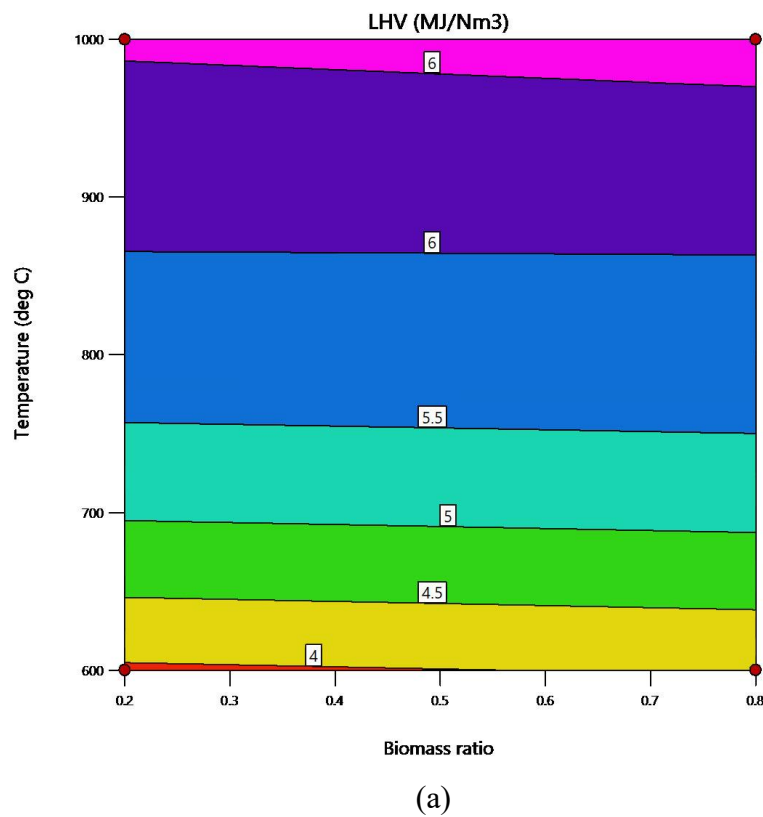
(b)

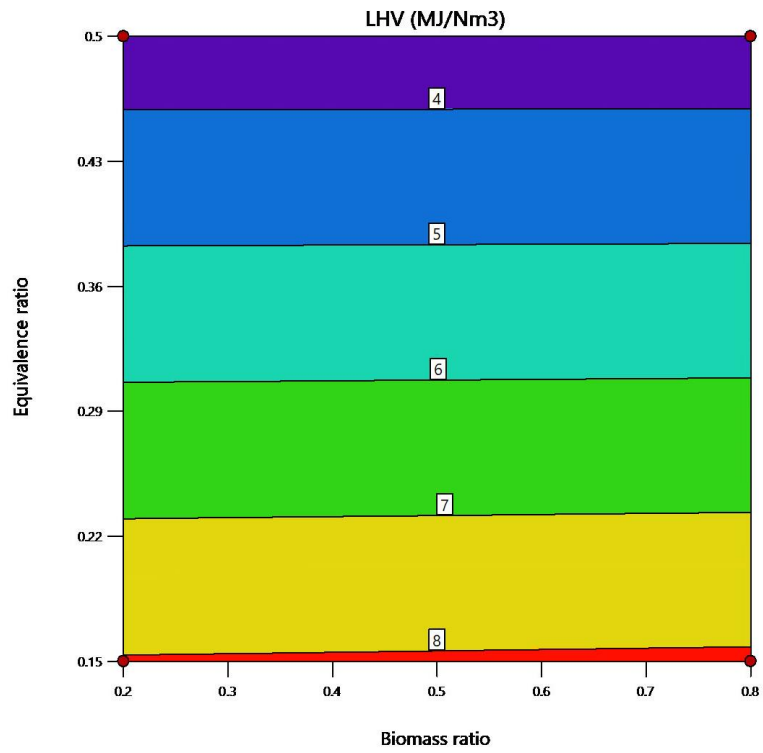


(c)

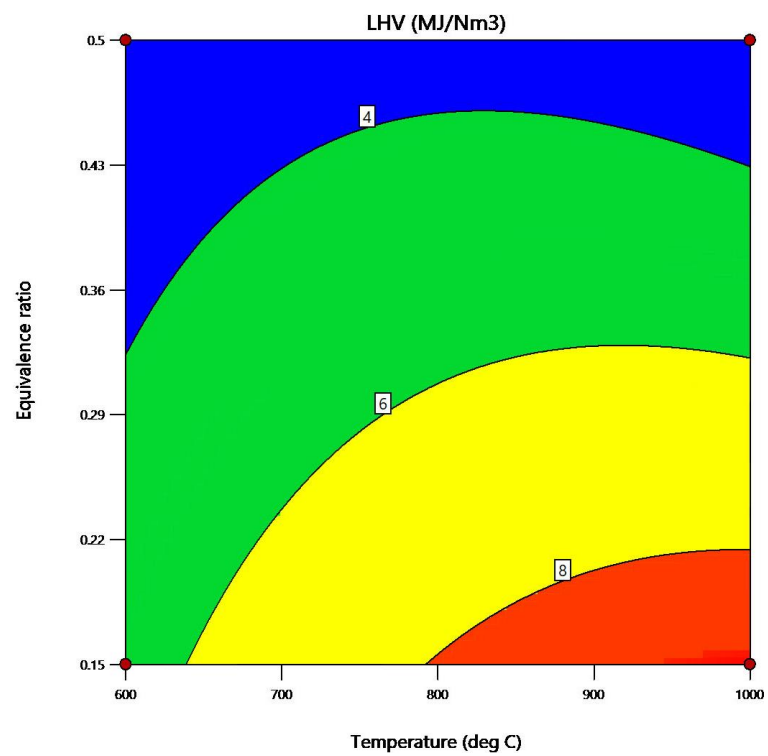
**Figure 6.8:** Interaction effects of input variables on Ethanol production rate

Figure 6.9 shows the combined effect of operating variables on the syngas LHV. Figure 6.9 (a) and (b) demonstrate that the LHV of the syngas increases with increasing temperature and decreasing equivalence ratio where a high value of biomass ratio is preferred. This can be due to the higher yield of  $CO$  and  $H_2$  at high temperature and low equivalence ratio. Figure 6.9 (c) indicates the combined effects of temperature and equivalence ratio on LHV of syngas. It can be observed that high temperature and low equivalence ratio increase the LHV of the syngas. Similar observations were made in the simulation study of previous literature (Kombe et al., 2022).





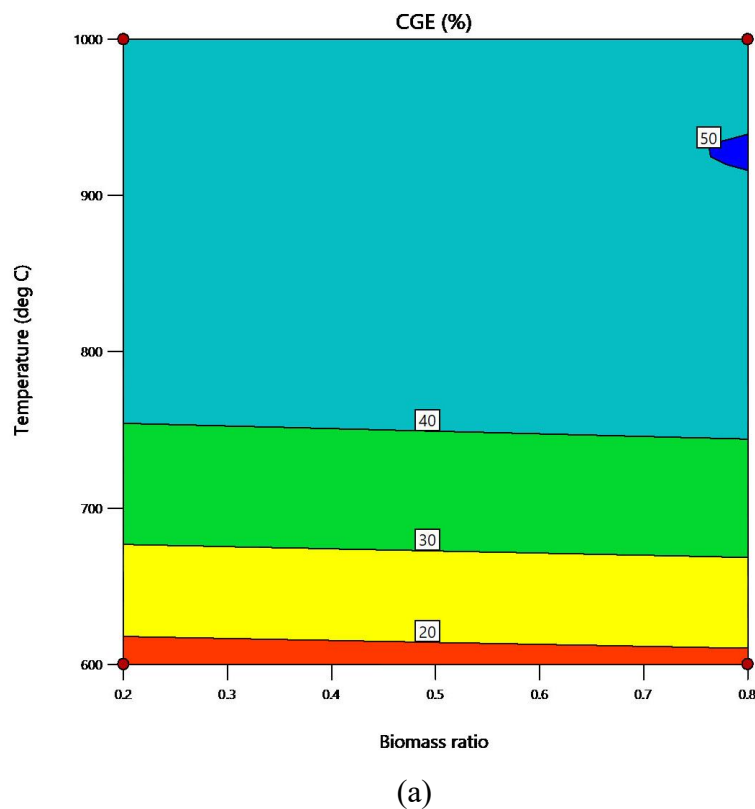
(b)

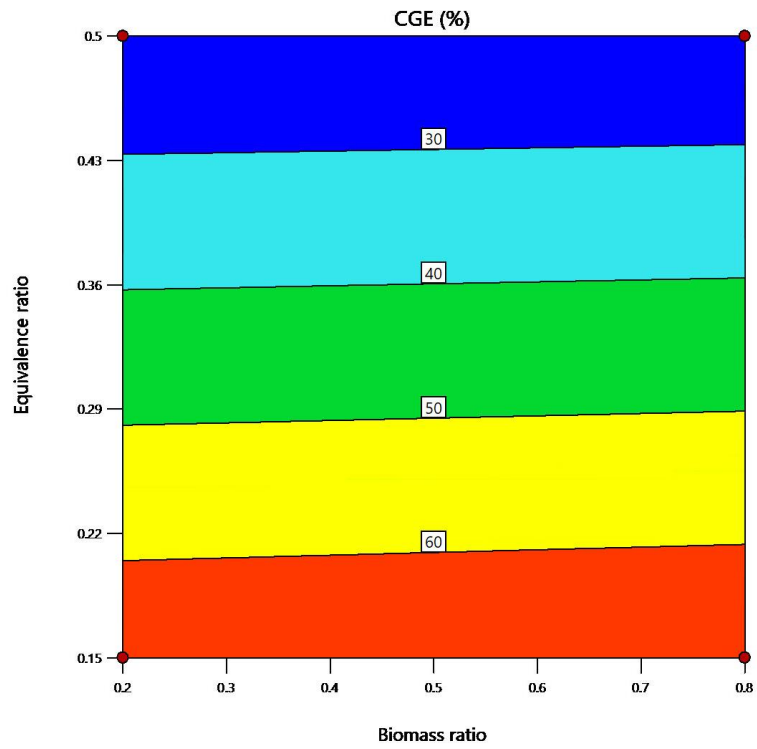


(c)

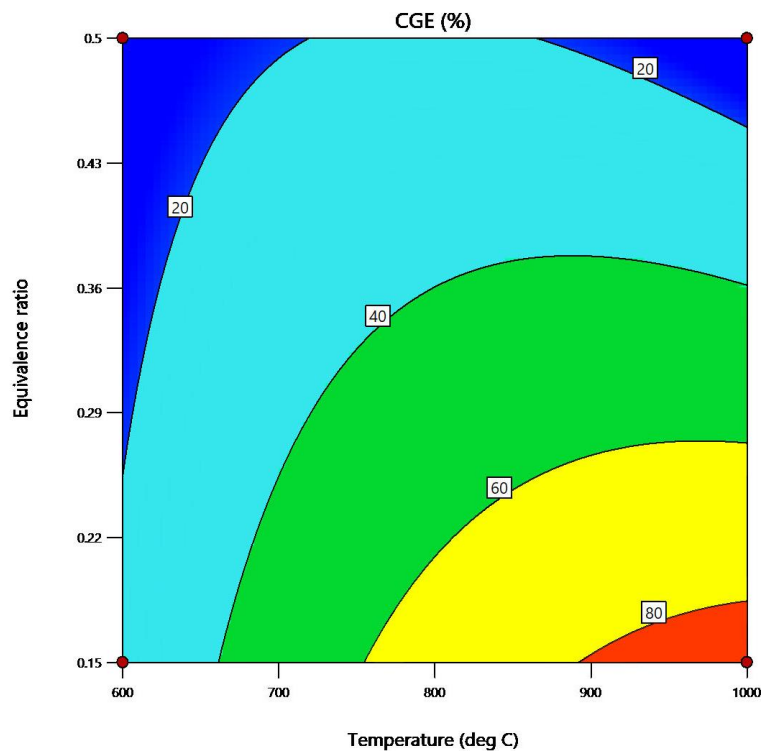
**Figure 6.9:** Interaction effect of input variables on syngas LHV (MJ/Nm<sup>3</sup>)

Figure 6.10 depicts the combined effects on cold gas efficiency by the operating variables. In Figures 6.10 (a) and (b), effects of biomass ratio and temperature, and biomass ratio and equivalence ratio on CGE have been illustrated. It can be clearly understood from the figures that high temperature and high biomass ratio cause an escalation in the CGE of the co-gasification system, whereas, CGE is adversely affected when both the values of temperature and biomass ratio are increased. From Figure 6.10 (c), we can clearly observe that the combination of high temperature and low equivalence ratio strongly improve the CGE of the produced syngas.





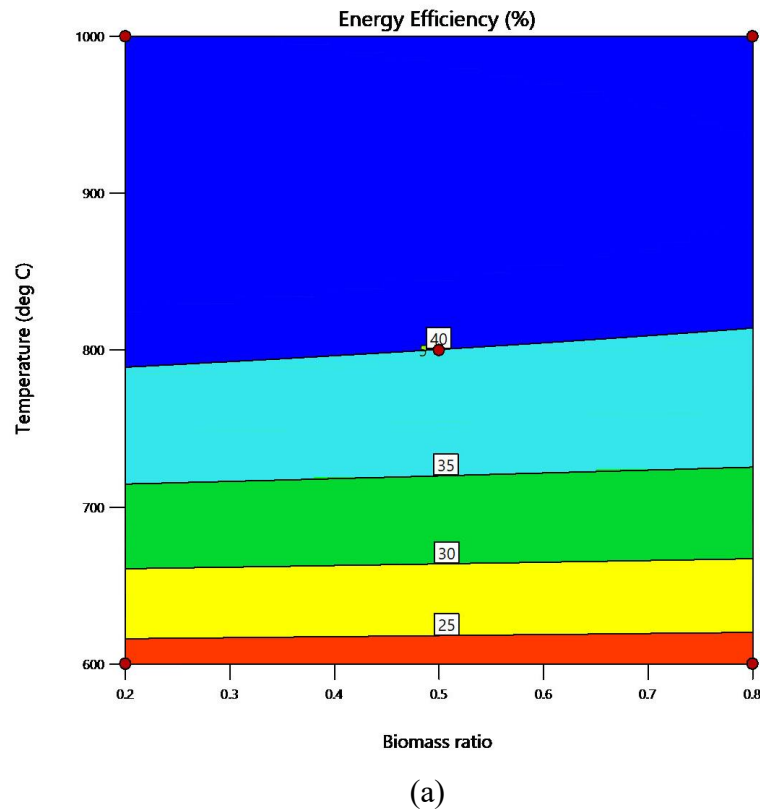
(b)



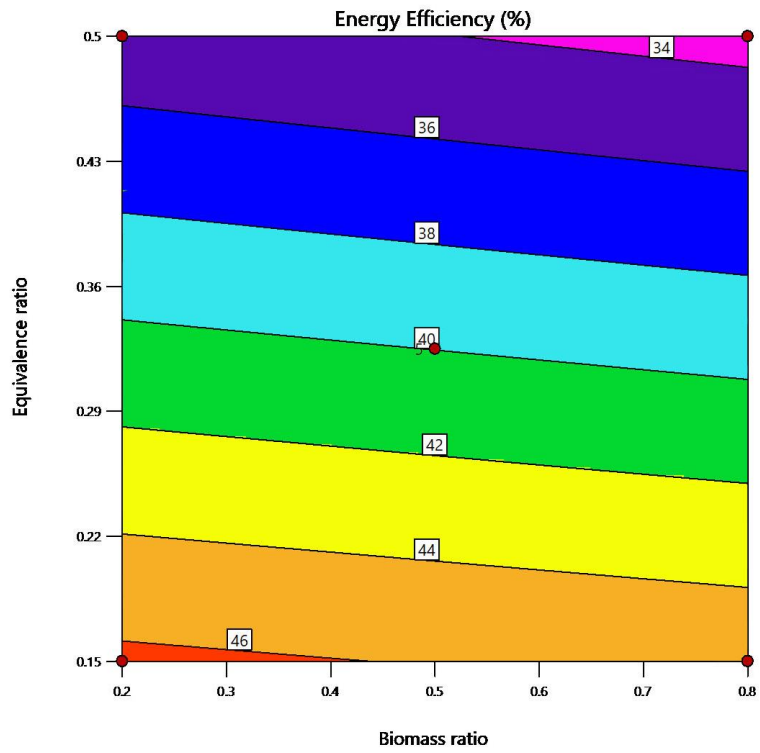
(c)

**Figure 6.10:** Interaction effect of input variables on cold gas efficiency (CGE)

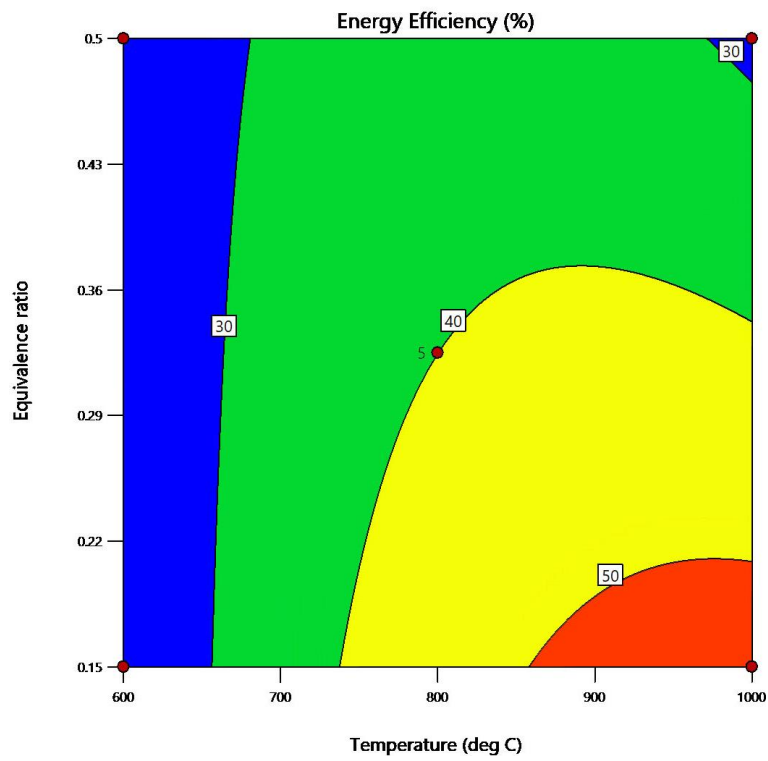
Figure 6.11 indicates the effect of operating parameters on overall energy efficiency of the co-gasification fermentation system. Figure 6.11 (a) shows an upward tendency of energy efficiency with increasing temperature, whereas for Figure 6.11 (b), the trend is exactly the opposite. Here, the energy efficiency decreases with increasing equivalence ratio. Figure 6.11 (c) depicts the combined effects of temperature and equivalence ratio on energy efficiency. The figure suggests that the high efficiency zone exists at high temperature and low equivalence ratio.







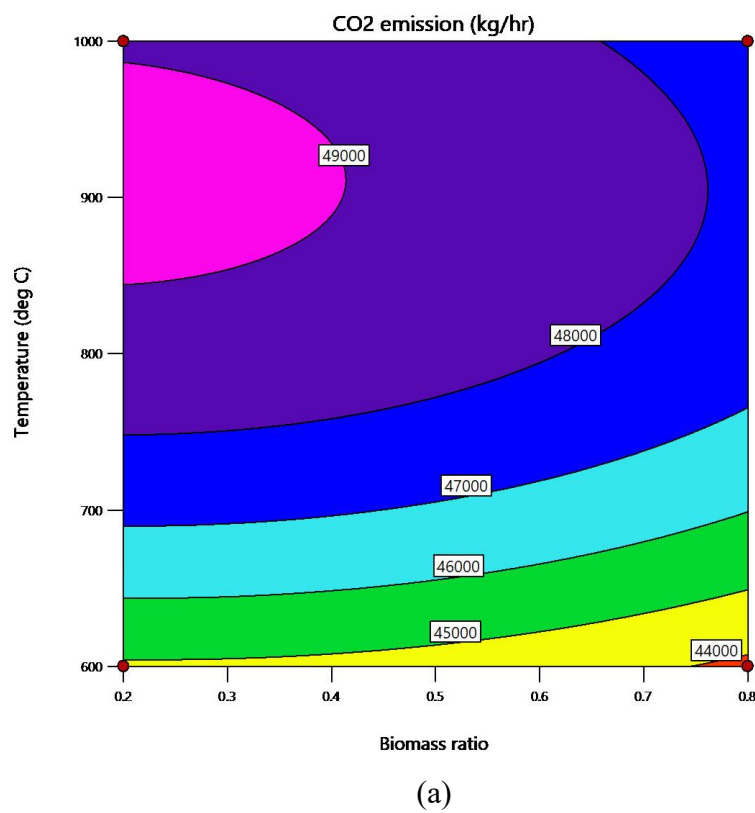
(b)



(c)

**Figure 6.11:** Interaction effect of input variables on energy efficiency

Figure 6.12 indicates the effects of operating parameters on the  $CO_2$  emission. Figure (a) and (b) depict the effects of biomass ratio and temperature, and biomass ratio and equivalence ratio on  $CO_2$  emission, respectively. Here, from Figure 6.12 (a) it can be observed that  $CO_2$  emission is high at low biomass ratio and high temperature. Also, from Figure 6.12 (b), it is evident that  $CO_2$  emission increases with increasing equivalence ratio. Figure 6.12 (c) depicts the combined effects of temperature and equivalence ratio on overall  $CO_2$  emission of the system. It can be observed that the high  $CO_2$  emitting zone occurs at high equivalence ratio, whereas, the combination of low temperature and low equivalence ratio causes less emission of  $CO_2$  to the atmosphere.



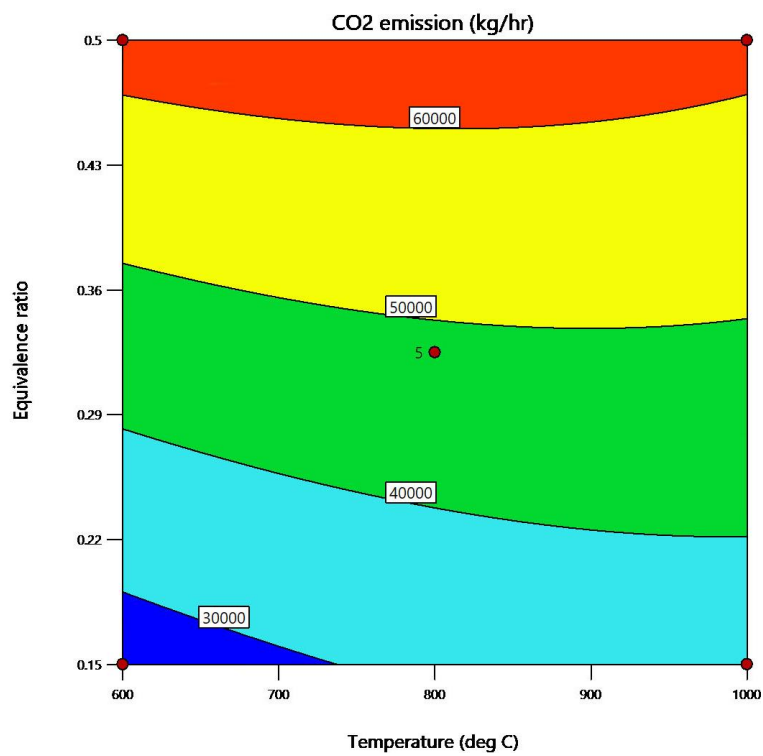
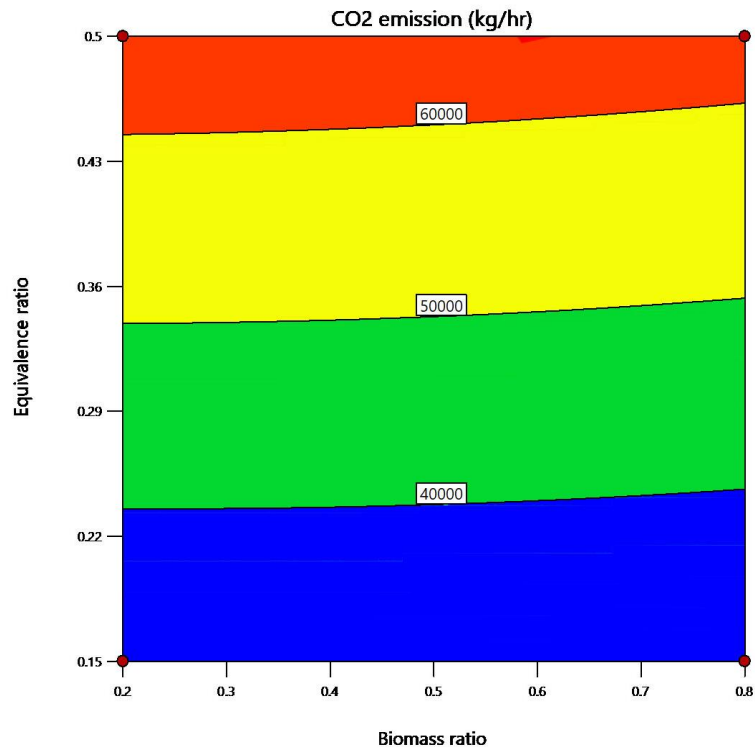


**Figure 6.12:** Interaction effect of input variables on  $CO_2$  emission

#### 6.6.4 Multi-objective optimization

The contour plots obtained by the response surface methodology indicate that all the response variables respond positively to the temperature and biomass ratio, and adversely to the equivalence ratio. A multi-objective optimization has been carried out in the Design Expert software itself which tries to maximize the ethanol productivity and overall energy efficiency of ethanol production while minimizing the  $CO_2$  emission of the system. As observed earlier, high biomass ratio, high temperature and low equivalence ratio promote the ethanol production rate and overall energy efficiency ( $\eta$ ) whereas  $CO_2$  emission is low at low temperatures. A trade-off is therefore necessary to find out an optimum point so that the ethanol production is sustainable as well as clean. The optimization results suggest that the biomass ratio of 0.8, temperature of 919.5°C and equivalence ratio of 0.15 give the highest ethanol productivity of 20.917 tonnes/ hr, overall efficiency of 52.184 %, and a minimum  $CO_2$  emission of 32669.862 kg/ hr.

#### 6.7 Chapter summary

The co-gasification fermentation model, developed under the present study, can predict the quantity of ethanol produced corresponding to the input biomass feedstock for co-gasification unit. The model has been validated through successful comparison of simulated predictions with the reported experimental results on yield and composition of syngas obtained from co-gasification. The values of  $LHV_{\text{syngas}}$ , CGE, ethanol production rate, overall energy efficiency, and  $CO_2$  emission can be calculated using the regression equations 7.4-7.8, within stipulated input variable range of  $0.2 \leq \text{biomass ratio} \leq 0.8$ ,  $500^\circ\text{C} \leq \text{gasification temperature} \leq 1000^\circ\text{C}$ , and  $0.1 \leq \text{equivalence ratio} \leq 0.5$ . The sensitivity analysis has also been performed for syngas yields, LHV of syngas, CGE, ethanol production rate, and overall system efficiency against temperature and ER used for co-gasification. Temperature increment in a co-gasification system enhances the rate of endothermic reactions, thus increasing the yield of  $CO$ ,  $H_2$ , and ethanol. Whereas, increasing ER adversely affects the syngas production. Through optimization using RSM, the maximum values of ethanol production of 20.92 ton/hr and overall energy efficiency of 52.184, and minimum value of  $CO_2$  emission of 32669.86 kg/hr have been obtained at wheat straw: sugar cane bagasse ratio of 4:1; co-gasification temperature, and ER of 919.5°C and 0.15, respectively.

---

## **Chapter 7. Integration of power generation and heat and resource recovery in the co-gasification- syngas fermentation model**

---

### **7.1 Objective of the chapter**

The objectives of the current study are,

- i. To integrate a power production unit from unconverted syngas along with heat recovery in the form of process steam
- ii. To recycle the fermentation medium and the distillation entrainer to reduce the overall water and resource consumption along with proper heat integration to use all the available energies generated in the process.

### **7.2 Model development**

The previous model developed by the authors was limited in fully utilizing the energy potential and resources. There was significant amount of unfermented syngas without any medium recycle. Biomass co-gasification and syngas fermentation process model has been modified in the present study using Aspen plus and shown in Figure 7.1. The assumptions for the model are as follows:

- a. Equilibrium is attained for both the processes (Co-gasification and fermentation).
- b. Tar content of output syngas is negligible
- c. Ash is considered to be inert.

Two biomass streams enter the gasifier at ambient condition and as non-conventional feeds in Aspen plus. The feed rate is 60 ton/h with an equal supply of wheat straw and SCB of 30 ton/h. The gasifier has been modelled using a RYield and an RGibbs reactor, respectively. The RYield reactor breaks the non-conventional biomass into conventional components as per their ultimate analysis. A FORTRAN subroutine is written in such a manner that it can convert both the non-conventional LCBs to conventional components if their ultimate analysis is provided. The previous model developed by the authors found 919.5°C temperature and 0.15 equivalence ratio for optimum ethanol production. However, it lacked in utilizing the overall heat generated in the system and a significant amount of fermentation medium was wasted unutilized. A temperature of 919.5°C is maintained in the RGibbs reactor and the major gasification reactions take place in the RGibbs reactor. After the removal of ash in a cyclone separator, syngas is sent

toward a heat exchanger for heat recovery. The recovered heat has been stored as high-temperature steam, and some amount of it is used to preheat the supply air up to 150°C for better gasification efficiency (Zachl et al., 2022). With the help of the heat exchangers, HEATX and HEATX2, the temperature of the syngas has been brought down to 37°C which is preferred for fermentation. After that, gas fermentation is conducted using an RStoic block assuming CO and H<sub>2</sub> conversion to ethanol of 70 % and 50 %, respectively (Okolie et al., 2021). The prevalent gasification and fermentation reactions are given in the supplementary information section. The fermented broth, then, leaves the fermenter and the excess CO and H<sub>2</sub> mixture is provided to a combustor - gas turbine setup for energy generation. The fermented broth goes through rigorous distillation in a RadFrac column. Ethanol and water form an azeotropic mixture at 78.1°C and 89% molar concentration of ethanol at atmospheric pressure (Gil et al., 2012).

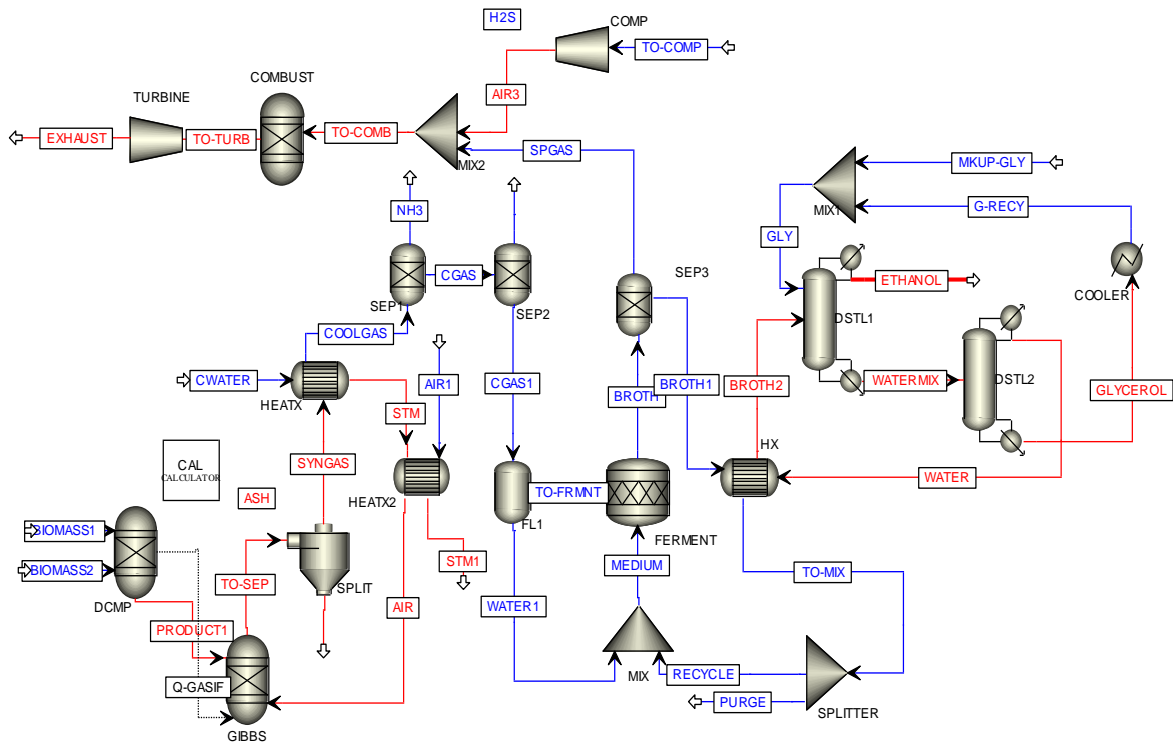


**Figure 7.1:** Aspen plus flowsheet of the modified co-gasification and fermentation process including power generation and heat and resource recovery.

So, it is not possible to achieve more than 89% of ethanol purity if conventional distillation is performed at the atmospheric pressure. In this simulation, extractive distillation has been performed using glycerol as an entrainer which increases the relative volatility of the components, and enables the distillation process to achieve more than 99.5% pure ethanol. In

the first column, ethanol has been separated from the glycerol water mixture, and in the second column, glycerol has been recovered and recycled back to the initial distillation column where ethanol is being separated. The extractive distillation process to obtain bio-ethanol is another important inclusion in the current model. The water recovered at the top of the second distillation column is recycled to the fermentation reactor after purging a portion to reduce excessive accumulation of cells in the fermenter (Pardo-Planas et al., 2017b). Before entering the fermentation reactor, the recycle medium stream exchanges heat with the incoming broth from the fermenter to achieve a temperature of 65°C to enhance the distillation performance. This medium recycle helps in reducing the water consumption of the entire process. The power generation unit is modelled using a compressor to compress syngas mixture, an RGibbs block which acts as the gas combustor, and finally, is followed by a gas turbine where gas is expanded to generate power. Compressed air is supplied to the combustor as combusting agent. So, there are two recycle streams in the flowsheet, one is the glycerol recycle for distillation purpose, and another is the medium recycle for fermentation purpose. The three outputs of this process model are bio-ethanol, power, and process steam whereas the previous model output was only bio-ethanol.

## **7.3 Results and discussions**

### **7.3.1 Mass and energy balance**

The mass and energy balance for the process model is shown in Figure 7.2. Here, 60 ton/h of mixed biomass is supplied to the gasifier producing 17300 kg/h of ethanol with 48433.6 kg/h of air supply. A total 59946 kg/h of syngas is produced at a 0.15 equivalence ratio and 919.5°C temperature. While cooling the syngas, 35 ton/h of process steam is generated. A medium recycle has reduced the medium flow rate to 5278.5 kg/hr. The output glycerol (183.16kg/h) from the distillation column is fully recycled, and is fed to the column in combination with the make-up glycerol stream (91.7 kg/h). The excess syngas from the fermentation process produces 32 MW of shaft work when fitted to a power producing combustor-turbine setup. The work of Pardo-Planas et al., 2017 presented a total ethanol production of 17270 L/h with 50 ton/h of switchgrass supply. Michailos et al., 2019 estimated an ethanol production of 28300 L/h with 100 ton/h of SCB. Comparing the ethanol production with other ethanol production processes, Barbanera et al., 2018 presented an estimate of 283 L/ton of biomass following the enzymatic hydrolysis and fermentation pathway.

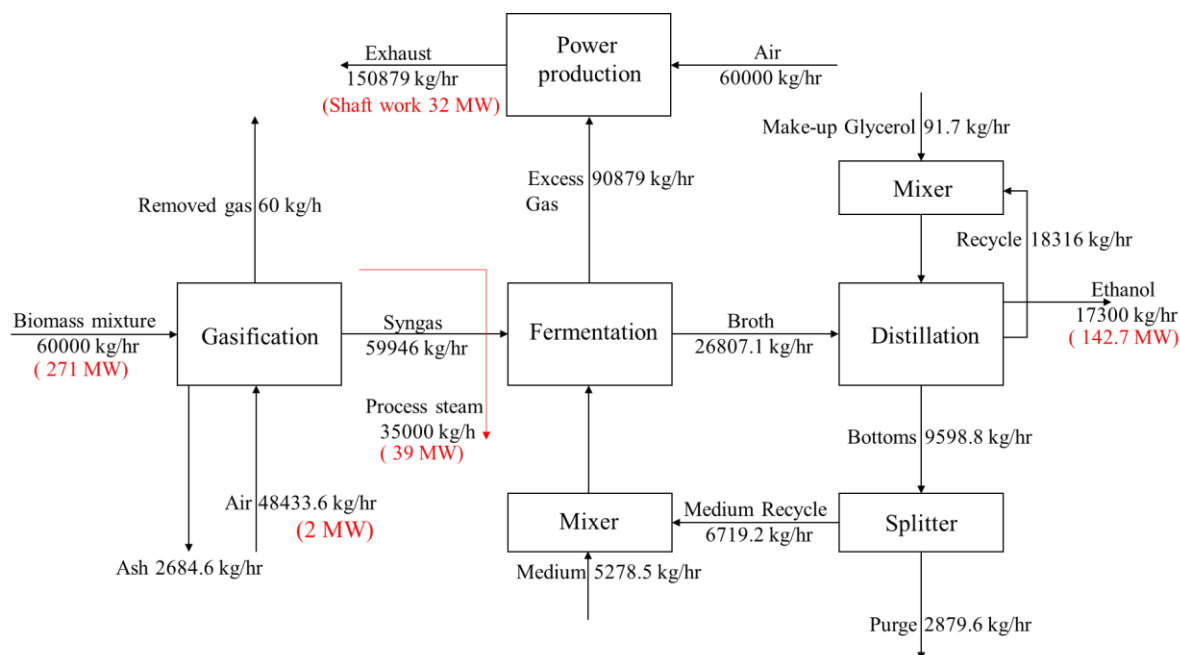


**Figure 7.2:** Mass and energy balance block diagram

## 7.4 Chapter summary

The co-gasification fermentation process model developed by the authors in their previous work has been modified with fermentation medium recycle and glycerol recycle as well as heat recovery in the form of process steam and power generation from the unconverted syngas from the fermentation reactor. The modelling has been conducted at a wheat straw and sugar cane bagasse mass ratio of 1:1, equivalence ratio of 0.15, co-gasification temperature 919.5°C, and fermentation temperature of 37°C. With a feed rate of 60 ton/h, a production of 17,300 kg/h of ethanol is achieved which is a yield of 0.29 kg/ kg of feedstock. Along with the bio-ethanol, 35 MW of process heat and 32 MW of power is also generated from the system. The produced power is consumed in the distillation process making the process more sustainable. The fermentation medium and glycerol recycle have significantly reduced the medium and glycerol requirement of the process which in turn improves the resource utilization of the process.



---

## **Chapter 8. Techno-economic analysis, investment risk analysis and life cycle analysis of the co-gasification fermentation model**

---

### **8.1 Objective of the chapter**

The modified co-gasification fermentation model in the previous chapter needs to go through rigorous sustainability analysis in order to be commercially viable.

The main objectives of this chapter are

- i. To perform a comprehensive techno-economic, investment risk and life cycle assessment on the co-gasification and fermentation process with waste heat recovery and resource recycle to assess its economic feasibility and environmental sustainability.
- ii. To conduct comparative analysis of the performance of the currently developed scheme with conventional bio-ethanol production processes.

### **8.2 Methodology**

#### **8.2.1 Methodology of Techno-economic analysis**

The techno-economic analysis of the ethanol production process is carried out to understand the economic feasibility of the project, and to determine the minimum selling price of bio-ethanol. The detailed cash flow analysis along with the estimation of net present value (NPV), internal rate of return (IRR), and payback period (PBP) have also been conducted here. A risk analysis on the basis of variable economic parameters has been carried out to find out the probability of achieving a non-negative NPV. The Monte Carlo simulation has been used to conduct the risk analysis. Total working life of the bio-ethanol plant has been assumed to be 20 years with 8000 hours of yearly production. Straight line depreciation with 10 % of interest rate and 30 % of tax rate has also been assumed in the modelling.

The procurement cost of each equipment has been estimated using CAPCOST software developed by Turton et al., 2009. The reference year for the calculation of capital cost was selected to be 2022, and all the equipment costs have been calculated using the Chemical Engineering Plant Cost Indices (CEPCI) of the year 2022.

$$Equipment\ cost_{2022} = \frac{CEPCI_{2022}}{CEPCI_{base\ year}} \times Equipment\ cost_{base\ year} \quad (8.1)$$

The base year is considered to be 2010 in the software.

The total equipment purchase cost is then multiplied by the Lang factor for the total direct cost and total indirect cost, respectively. The total capital investment is calculated from the total direct and indirect costs. The equipment cost break up is provided in the supplementary information section. It is assumed that 40% of the fixed capital investment is invested in the first year, 50% in the second year, and the remaining 10% in the third year. It is also assumed that during the first year of operation, the plant works on a production capacity of 70% and the capacity increases by 10% every year. The capital investment depreciation is for 15 years using straight line depreciation. The total operating life of the plant is, however, 20 years, and the plant works with 95% of its capacity for the 16<sup>th</sup> and the 17<sup>th</sup> year, and for the last three years, the plant produces at 90% of its capacity. The tax rate is assumed to be 30 % and the interest rate is assumed to be 10% per annum. The annual operating hours of the plant is assumed to be 8000 hours.

The annual operation and maintenance costs are calculated by adding up the variable and the fixed costs for the plant operation. The variable costs include utilities, raw material, operating labour, supervision, operating supply, maintenance and repair, laboratory charges, patents, and royalties. The fixed costs, on the other hand, include depreciation, financing, local taxes, and insurances. The plant overhead charges and general administrative costs are also included in the operation and maintenance charges. Other than the utility and raw material cost, all the other expenses are shown as a function of the equipment purchase cost in the supplementary information section. After calculating the annual operating cost, the production cost of 1 litre of ethanol is calculated by dividing the total annual cost by the annual production rate.

$$Production\ cost = \frac{Total\ Annual\ cost}{Annual\ production\ rate} \quad (8.2)$$

$$Total\ annual\ cost = Annualised\ capital\ cost + Annual\ operating\ cost \quad (8.3)$$

Total annual cost is expressed as the sum of the annualised capital cost (ACC) and the annual operating cost where the annualised capital cost is calculated as

$$Annualised\ capital\ cost = \frac{i \times (1+i)^t}{(1+i)^t - 1} \times Total\ capital\ investment \quad (8.4)$$

Where *i* is the interest rate and *t* is the total time period of plant life. The economic performance of the project is calculated in terms of the NPV, ACC, IRR, and PBP. The estimation of NPV, IRR, and PBP have been done using the following equations:

$$NPV = -TCI + \sum_{t=1}^{20} \frac{Cash\ flow}{(1+i)^t} \quad (8.5)$$

$$\sum_{i=1}^{20} \frac{Cash\ flow}{1+IRR} = 0 \quad (8.6)$$

$$PBP = \frac{Total\ Investment\ Cost}{Annual\ Income} \quad (8.7)$$

Using the equation, the production cost of ethanol can be calculated, and after that, the minimum selling price of ethanol can be calculated by making the NPV break even (NPV=0).

### 8.2.2 Methodology of investment risk analysis

Risk analysis is one of the fundamental aspects of any economic investment. It is important to assess the risk associated with any kind of investment so that the investors become aware of what they are investing in and what the chances of loss are in any particular project. The Monte Carlo simulation is a globally accepted method for determining this uncertainty in any economic investment (Colantoni et al., 2021). In this simulation approach, the analysis is modelled by considering the probability distribution in the annual operating hours, daily ethanol production, minimum ethanol selling price, operating cost, and total capital investment. The base value and probability distribution of these parameters are determined after conducting the economic analysis. 10,000 Monte Carlo iterations are then performed using Crystal Ball add-in in MS Excel, and the economic risk of the system in terms of NPV is determined. The sensitivity analysis of the NPV with the variation of the operating variables has also been incorporated in the study.

### 8.2.3 Life cycle impact assessment methodology

Life cycle impact of the modelled co-gasification-fermentation process has been conducted following the ISO 14040/14044 guideline frameworks (Klopffer & Grahl, 2014). The main constituent elements of this framework are goal and scope definition of the project, inventory analysis, impact assessment, and interpretation of the generated impacts. The input and the output data of ethanol production are collected from the Aspen plus simulation as well as the Eco-invent database 3.1, developed by the Swiss Centre for Life Cycle Inventories. The impact of the ethanol production process is quantified according to the ReCiPe Midpoint (H) and endpoint (H) 1.13 method using the SimaPro software package (version 9.1). All the inventory processes have been quantified to a number of indicators, and the indicators determine the relative severity of the ethanol production process in a particular category. A total of 18 impact categories are involved in the midpoint approach. The midpoint categories have further been

conglomerated to form three endpoint categories namely human health, eco-system, and resources.

### 8.2.3.1 Definition of goal and scope

The environmental feasibility of ethanol production via this thermochemical - biochemical pathway is defined as the goal of this LCA exercise. The combined impact of both co-gasification and fermentation processes is considered here. Wheat straw and sugarcane bagasse are the two agricultural wastes used as feedstock for this process. The cultivation process of these biomass is considered, but further, only the allocated impact of the waste is considered for this study. An economic allocation has been done in the case of the agricultural products as the main product and wastes vary in market price. The boundary of this study has been kept confined to cradle to gate as the ethanol production process is the point of concern here. A comparison with the similar technologies available in the market will provide important insights about the environmental sustainability of the co-gasification fermentation process. Therefore, A methodical comparison of environmental impacts of ethanol production from the co-gasification fermentation route (CGF), the conventional route of 2G bio-ethanol production involving pre-treatment of LB, enzymatic hydrolysis of pre-treated LB and fermentation (EHF) route, and the 1G ethanol production via sugar fermentation (SF) route has been incorporated within the scope of this study.

### 8.2.3.2 Functional unit definition

Defining the functional unit is one of the most rudimentary yet quintessential task in an LCA exercise. Here in this simulation, the ethanol production unit produces power and process heat as by-products. These three products are not comparable by the means of mass or economics, but all of them are energies of different grade. Exergy is the maximum available work that a system can provide to its surroundings (Hosseini et al., 2012). Every output in this system possesses some amount of exergy which can easily be calculated. The calculation of the exergy of all these products homogenizes the system and makes the outputs comparable. Exergy flow rates of ethanol, power, and process heat are calculated as

$$\dot{Ex}_{Ethanol} = \dot{m}_{ethanol} \times Ex_{ethanol} \quad (8.8)$$

$$\dot{Ex}_{power} = \dot{W} \quad (8.9)$$

$$\dot{Ex}_{process\ heat} = \left(1 - \frac{T_{outlet}}{T_{ambient}}\right) \times \dot{Q}_{Process\ heat} \quad (8.10)$$

Where  $\dot{Ex}_{Ethanol}$ ,  $\dot{Ex}_{power}$ ,  $\dot{Ex}_{process\ heat}$  are the exergy flow rates of ethanol, power, and process heat, respectively, and  $\dot{m}_{ethanol}$  is the mass flow rate of ethanol. The exergy from any form of energy is chosen as the allocation method of the system (Jana & De, 2017). The environmental impact of an individual output is allocated according to the percentage of total exergy in it. After the allocation, the functional unit for ethanol production is considered to be 1 kg of ethanol.

### 8.2.3.3 System boundaries

The cradle to gate approach has been selected as the impact assessment strategy here. Wheat straw and sugarcane bagasse are available from the cultivation of wheat and sugarcane, respectively. Wheat straw can be collected from the wheat collection facility and sugarcane bagasse can be collected from the sugar mill after the extraction of the juice from the sugarcane. The procurement process of wheat straw and sugarcane bagasse has been incorporated in the analysis as bio-based energy or fuel generation including the biomass cultivation as well (Shafie et al., 2014). The gasification facility is assumed to be 20 km away from the straw and bagasse collection points. The sugar mill is assumed to be adjacent to the sugarcane fields. The system boundary is shown in Figure 8.1. Ethanol is regarded as the primary output of the system. The system boundary does not include the utilization of the output products as it is a cradle to gate assessment for the comparison of the three ethanol production options viz. CGF, EHF, and SF routes.

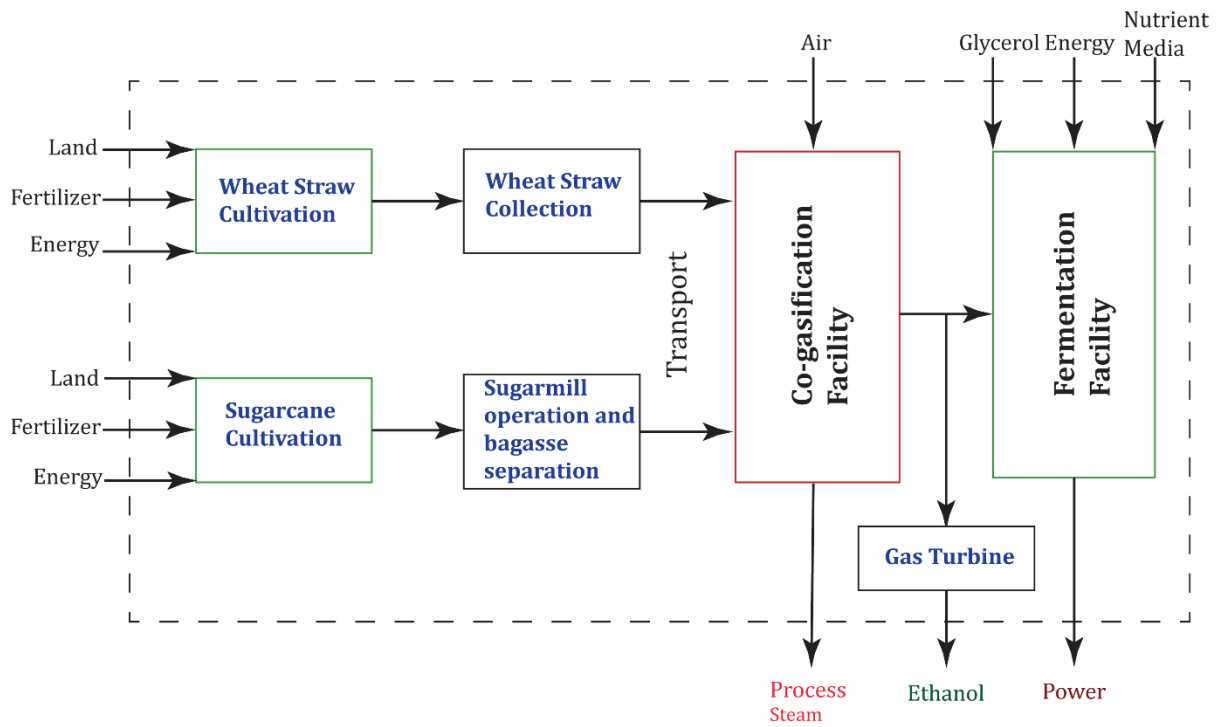


**Figure 8.1:** System boundary of the system for life cycle assessment

#### 8.2.3.4 Inventory analysis

The inventory for this particular assessment is prepared on the basis of 1 ton of mixed biomass supply. The data of wheat cultivation and straw collection are obtained from previous literature (Borrion et al., 2012a). The data on sugarcane production and separation of the bagasse from sugar and molasses are taken from Santoyo-Castelazo et al., 2023. The ethanol production plant is assumed to be situated at a distance of 20 km from the straw and bagasse collection facility, and they are assumed to be carried in a 16-32 tons truck of EURO4 standard whose data has been taken from the Ecoinvent database (Dübendorf, 2014). The simulation data from Aspen plus have been used to define the input and output of the co-gasification and fermentation process. The co-gasification process is conducted in self sustained manner, and hence, it is assumed that no external energy supply is required for this process (Fernández-Lobato et al., 2022). All the inventory data used in the LCA have been provided in Table 8.1.

**Table 8.1:** LCA inventory for 1 ton of mixed biomass use

<b>Inputs</b>	<b>Item in database</b>	<b>amount</b>
<b>Wheat straw(Borrion et al., 2012b)</b>	Unit process modelled in SimaPro from literature data	500 kg
<b>Sugarcane bagasse (Santoyo-Castelazo et al., 2023b)</b>	Unit process modelled in SimaPro from literature data	500 kg
<b>Air</b>	Air from nature	1550.15 kg
<b>Transport (straw and bagasse collection point to production facility)</b>	Transport freight, lorry 16-32 metric ton, euro4 {RoW} market for transport, APOS, U	20 ton-km (assumed)
<b>Syngas production unit</b>	Synthetic gas factory {RoW} construction, APOS, U	1440 t/day capacity
<b>Nutrient media for fermentation (Handler et al., 2016)</b>	Unit process modelled in SimaPro from literature data	Accounted for the stoichiometric requirement of the fermentation process
<b>Process water for fermentation</b>	Tap water {IN} tap water production, conventional treatment, APOS, U	88 kg
<b>Glycerol</b>	Glycerine {RoW} market for glycerine, APOS, U	1.53 kg
<b>Electricity</b>	Electricity, medium voltage {IN-Eastern grid}  market for electricity, medium voltage   APOS, S	5.4 MJ
<b>Transport (Ethanol transportation form production to distribution facility)</b>	Transport freight, lorry 16-32 metric ton, euro4 {RoW} market for transport, APOS, U	20 ton-km

Syngas has been assumed to be produced in a synthesis gas factory. This factory installation data have been taken from the eco-invent database. Syngas, derived from the co-gasification process, cools down in heat exchangers generating steam. The fermentation of the produced syngas occurs inside a continuous stirred tank reactor. The fermentation process receives nutrient media and syngas as input, and produces ethanol as output. The data for nutrient media preparation have been taken from Handler et al., 2016. For the extractive distillation process, glycerol has been used as an entraining media. Two distillation columns have been installed for

the purification of the ethanol. The emission data of the simulation process have been collected from the Aspen plus model. The outlet gas stream from the fermenter containing unreacted syngas and product  $CO_2$  is then further sent to a combustor turbine combination which in turn produces power. The generated power is then utilized to make up for the power requirement in the distillation unit. Hence, Ethanol, process steam, and power are the three major outputs from this particular bio-refinery setup.

### 8.3 Results and discussions

#### 8.3.1 Capital investment and MFSP estimation:

The simulated co-gasification fermentation plant has been divided into five different units to demonstrate the equipment purchase cost. The five units are co-gasification unit, gas cleaning unit, fermentation unit, distillation unit, and power production unit. Using the CAPCOST software, the total equipment purchase cost of 36.2 M\$ has been calculated. The purchase cost share of each unit has been shown in Figure 8.2 which reflects that the gasification unit has the maximum share of 43.3 % followed by the power production unit (33.4 %) and the fermentation unit (19 %). The results are in good agreement with the study conducted by Michailos et al., 2019. It needs to be mentioned that the heat recovery unit from the hot syngas has been incorporated in the gasification unit, and the medium recycle has been included in the fermentation unit.

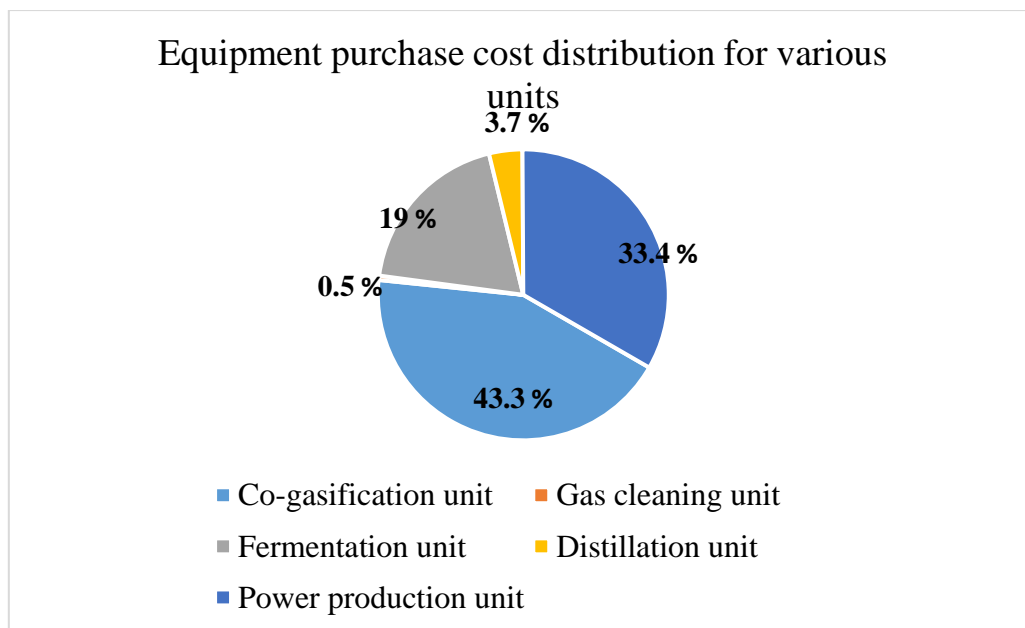


**Figure 8.2:** Equipment purchase cost distribution of various units in the simulated co-gasification fermentation plant



The estimation of total capital investment has been conducted in Table 8.2, where all the cost involved in different stages of plant set up and other logistics are presented.

**Table 8.2:** Assessment of total capital investment

<b>Total equipment purchase cost (TEPC)</b>		<b>\$ 3,61,92,700.00</b>
<b>Equipment Installation</b>	39 % of TEPC	
<b>Instrumentation and control</b>	26 % of TEPC	
<b>Piping</b>	31 % of TEPC	
<b>Electrical systems</b>	10 % of TEPC	
<b>Buildings</b>	29 % of TEPC	
<b>Yard improvement</b>	12 % of TEPC	
<b>Total Direct Cost (TDC)</b>	2.47*TEPC	
		<b>\$ 8,94,00,000.00</b>
<b>Engineering and supervision</b>	32 % of TEPC	
<b>Construction expenses</b>	34 % of TEPC	
<b>Legal expenses</b>	4 % of TEPC	
<b>Contractor's fee</b>	19 % of TEPC	
<b>Total Indirect Cost (TIC)</b>	89% of TEPC	
		<b>\$ 3,22,11,500.00</b>
<b>Contingency</b>	0.02*(TDC+TIC)	<b>\$ 2,43,22,300.00</b>
<b>Working Capital</b>	0.15*(TDC+TIC+ Contingency)	<b>\$ 2,18,90,000.00</b>
<b>Land</b>	0.06*Equipment purchase cost	<b>\$ 21,71,600.00</b>
<b>Total Capital Investment</b>		<b>\$ 17,00,00,000.00</b>

The operation and maintenance costs of the proposed plant have been calculated in terms of the equipment purchase cost. In Table 8.3, the results from the economic analysis are presented in the form of various economic indicators, like annualised capital cost, net present value (NPV), internal rate of return (IRR), payback period, and ethanol production cost. These economic indicators have been calculated in MS Excel 2013. The NPV of the project has been calculated to be 18.7 M\$ considering an internal rate of return of 13.33 % and payback period of 6.7 years. The ethanol production cost for a production rate of 21926 L/h has been calculated to be 0.61 \$/L, however, for a zero NPV scenario or NPV break-even, 0.65 \$/L of minimum ethanol selling price (MESP) was determined.

**Table 8.3:** Results of economic analysis and economic indicators

<b>Total annual operation and maintenance cost</b>	<b>\$ 8,65,00,000.00</b>
<b>Ethanol production rate</b>	21926 L/h
<b>Ethanol yield</b>	365 L/tonne of biomass
<b>Production cost of Ethanol</b>	0.61 \$/L
<b>Minimum ethanol selling price (MESP)</b>	0.65 \$/L
<b>Selling price of ethanol in India</b>	0.70 \$/L
<b>Total Product sales</b>	\$ 9,59,32,500.00
<b>Net present value</b>	\$ 3,84,25,395.20
<b>Internal rate of Return</b>	13.33%
<b>Payback period</b>	6.7 years

### 8.3.2 Comparison of economic indicators

The techno-economic analysis results have been compared to other bio-ethanol production processes following EHF and SF route. Various economic indicators of these routes have been provided in table 8.4

The model provides the indicators of the CGF route whereas the indicators for the EHF and SF route have been collected from the literature.

**Table 8.4:** Comparison of the economic indicators of the CGF, EHF and SF route

Conversion Routes	Feedstock	Capacity	Economic Indicators	References
<b>CGF route</b>	Wheat straw and SCB	60 t/h	NPV- 38 M\$ IRR- 13.33 % PBP- 6.7 years MESP- 0.65 \$/L Probability of having non-negative NPV- 81.8 %	This study
<b>EHF route</b>	Wheat straw	13 t/h	NPV- 5.05 M\$ IRR- NA PBP- 10 years MESP- 1.43 \$/L Probability of having non-negative NPV- 62 %	(Hasanly et al., 2018)
<b>SF route</b>	Sugarcane juice	612 t/h	NPV- 43 M\$ IRR- 13.5 % PBP- NA MESP- 0.44 \$/L Probability of having non-negative NPV- 75.7 %	(J. F. L. Silva et al., 2017)

The comparison suggests that the SF route of 1G bioethanol production provides the least MESP of 0.44 \$/L but the CGF route provides highest probability of having a non-negative NPV. The economic performance of the CGF route is much better compared to the EHF route.

### 8.3.3 Uncertainty analysis on NPV

The Monte Carlo simulation has been performed to analyse the uncertainty of NPV with the varying input parameters of the techno-economic model. The sensitivity analysis of NPV with the variation of the input parameters was also performed using the Monte Carlo simulation. The input variables considered in the study are working hours, hourly ethanol production, total capital investment, total operating cost (including the biomass cost), and depreciation. The

NPV of this project is the forecasted variable. The probability distribution of various input variables has been selected from literature and provided in table 8.5.

**Table 8.5:** Probability distribution and specifications of the input variables

<b>Variable</b>	<b>Distribution</b>	<b>Specifications</b>
<b>Annual hours</b>	Triangular	Min- 4000 h Most likely-7000 h Maximum-8000 h
<b>Hourly ethanol production</b>	Normal	Mean- 21926 L/h Standard deviation (SD)- 1461.7 L/h
<b>MESP</b>	Normal	Mean- 0.65 \$/L Standard deviation (SD)- 0.04 \$/L
<b>Operating cost</b>	Normal	Mean-8,65,00,000 \$ Standard deviation (SD)- 8650000 \$
<b>Total capital investment</b>	Normal	Mean- 17,00,00,000 \$ Standard deviation (SD)- 1,70,00,000 \$

A triangular probability distribution is selected for the total working hours, and all other input variables are assumed to follow normal probability distribution. 10,000 Monte Carlo iterations were performed and the frequency distribution of various NPV values were plotted for a mean ethanol price of 0.65 \$/litre. Figure 8.3 shows the frequency distribution histogram plot for a range of NPV values.

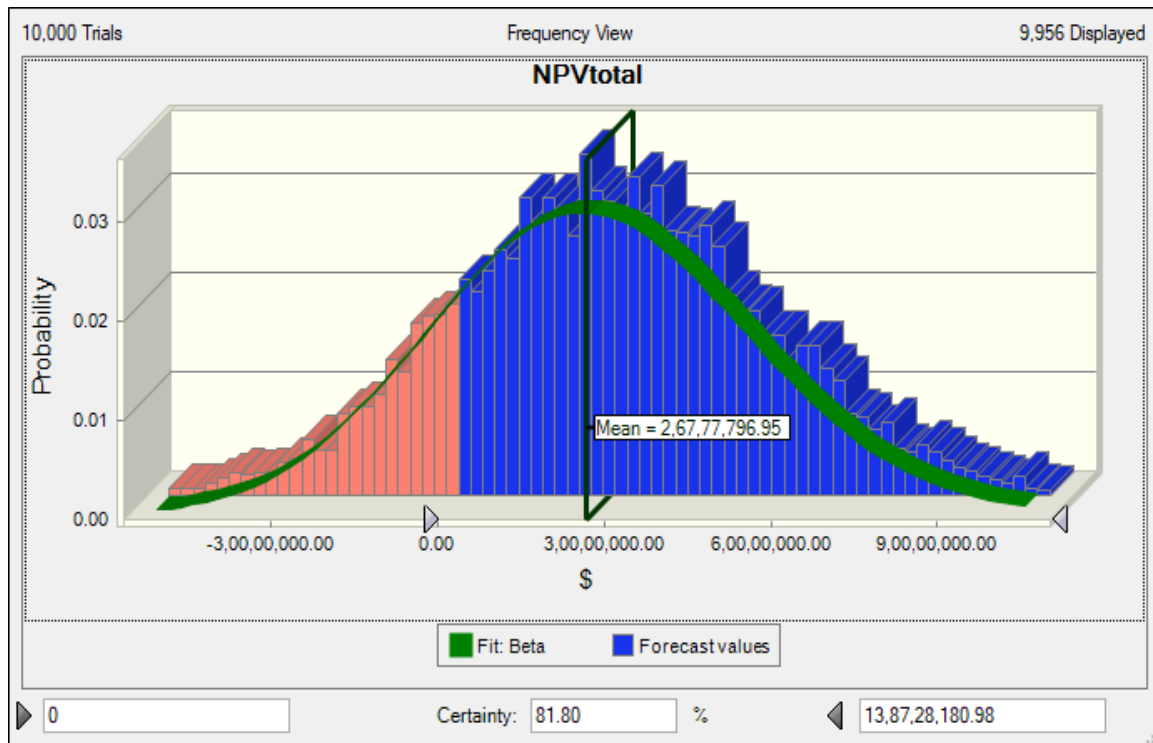


**Figure 8.3:** Probability distribution histogram for total NPV variation

The mean value of NPV has been found to be 26.7 M\$ and 81.80 % is the probability of getting a non-negative NPV value. The red portion of the curve depicts the negative NPV values and the blue portion of the curve depicts the non-negative NPV values. Non-negative NPV values suggest that setting up the plant will be profitable and the investors can expect a good return against their investment, and in this modelling, there is 81.80 % chance that the business is going to be profitable. de Medeiros et al., 2017 presented an ethanol selling price of 0.78 \$ per litre for more than 80 % positive NPV value in Monte Carlo simulation. The individual effect or sensitivity of NPV with the changes in operating variables like operating cost (includes raw material cost), daily ethanol production, minimum fuel selling price, annual operating hours, and total capital investment has been depicted in figure 6. From the figure, it can be observed that the total operating cost imposes most significant effect on the NPV and 38.2 % is the obtained value. The negative value indicates that an increase in the operating cost will decrease the NPV of the overall process. The operating cost is followed by the daily production, MESP, and annual operating hours. All these positively affect the NPV of the process, and the NPV has a respective sensitivity of 23.8 %, 19.4 % and 18.6 % of the aforementioned variables. However, the total capital investment does not have any significant impact on the total NPV as can be seen in Figure 8.4 which can be explained as it is a one-time investment and does not have any recurring effect on the overall process. According to the findings of Colantoni et al.,

2021 the investment cost is the least sensitive parameter on NPV, and with increasing capacity of the plant, the investment cost becomes less and less important.

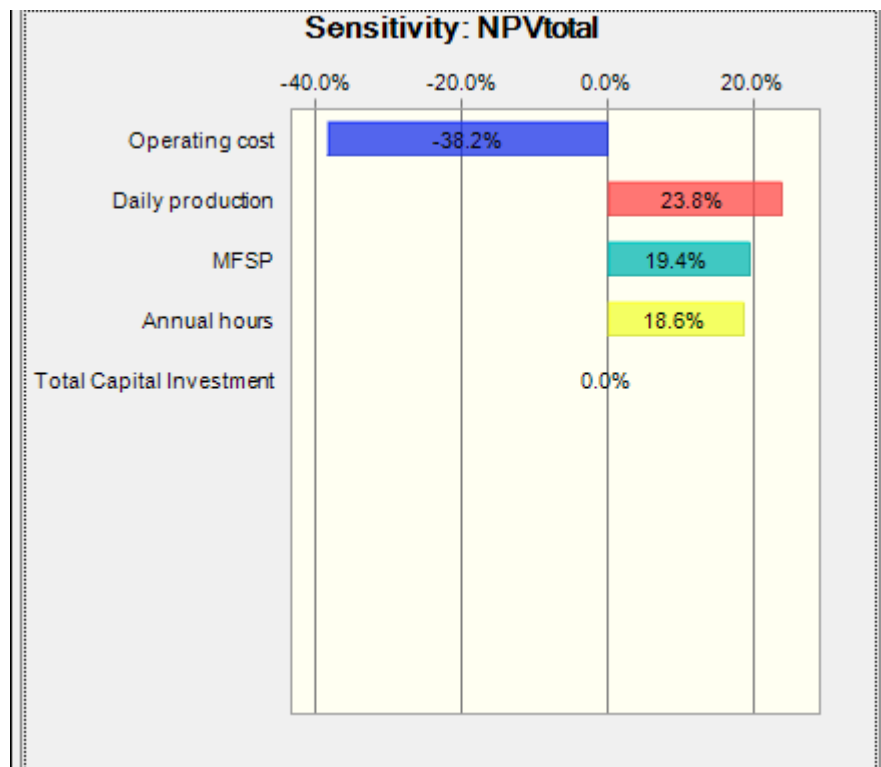


**Figure 8.4:** Sensitivity of NPV on the operating variables

### 8.3.4 Life cycle assessment results

The life cycle impacts of the co-gasification fermentation hybrid process have been conducted with a cradle to gate approach. The impacts of each individual process have been assessed and the current technology has been compared to the EHF and SF route. Here, the assessment has been conducted using the ReCiPe 2016 hierarchist methodology of version 1.04 both at the midpoint and endpoint level. This methodology considers a time horizon of 100 years for the calculation of the environmental impacts. Both midpoint and endpoint results of this process have been considered for the analysis.

#### 8.3.4.1 Impacts of the co-gasification fermentation process:

In this section, the percentage impact of the individual processes participating in the co-gasification fermentation process and the overall process are discussed. Figure 8.5 shows the impacts of the unit processes that eventually culminate to the final ethanol production in 14 different impact categories.

The global warming potential is defined as the amount of  $CO_2$  emitted in a particular process and is expressed as kg  $CO_2$  equivalent per kg of bio-ethanol. The highest contributor to the global warming is the generation of electricity that is required for the distillation purpose. As the production of electricity in India is still largely dependent on the burning of fossil fuel, it is justifiable that the greenhouse gas emission during the electricity generation will also be high. After that, the excess  $CO$  emitted post combustion in the gas turbine contributes to the global warming potential. The construction of the synthesis gas factory and the ethanol production also significantly contribute to the global warming.

The grid energy to be supplied for distillation in excess of the electricity generated from unconverted syngas is also the highest contributor in the impact categories like Ozone depletion, Ozone formation effect on both human health and terrestrial ecosystem, fine particulate matter formation, terrestrial acidification, freshwater eutrophication, and fossil resource scarcity.

The ethanol fermentation plant setup that consists of both the fermentation and distillation unit installation, majorly contribute to the impact categories like ionizing radiation, terrestrial ecotoxicity, terrestrial ecotoxicity, freshwater ecotoxicity, marine ecotoxicity, human carcinogenic toxicity, human non-carcinogenic toxicity, mineral resource scarcity, and water consumption. The reason of such high impact of these processes on the environment can be due to the heavy machinery and reactor setup for the process of fermentation and distillation for a plant that produces ethanol up to 500 ton/ day.

Another important contributor to the environmental damage is the synthesis gas factory construction. This factory set up consists of both the gasification and power generation unit. This is another heavy machinery setup which involve usage of metals, chemicals, and precession equipment for its construction.

Usage of glycerol mainly contributes to the marine eutrophication as the conventional glycerol production process emits various chemicals which are responsible for disturbing the marine nutrient balance. The sugarcane and wheat cultivation also contribute to the environmental impact because of the fertilisers, energy, and heavy machineries used during the process. Steam generated as process heat has been treated here as an avoided product which significantly reduces the global warming potential, terrestrial acidification, and fossil resource scarcity. The highest negative impact can be gained through the avoidance of the usage of fossil fuel in steam generation.

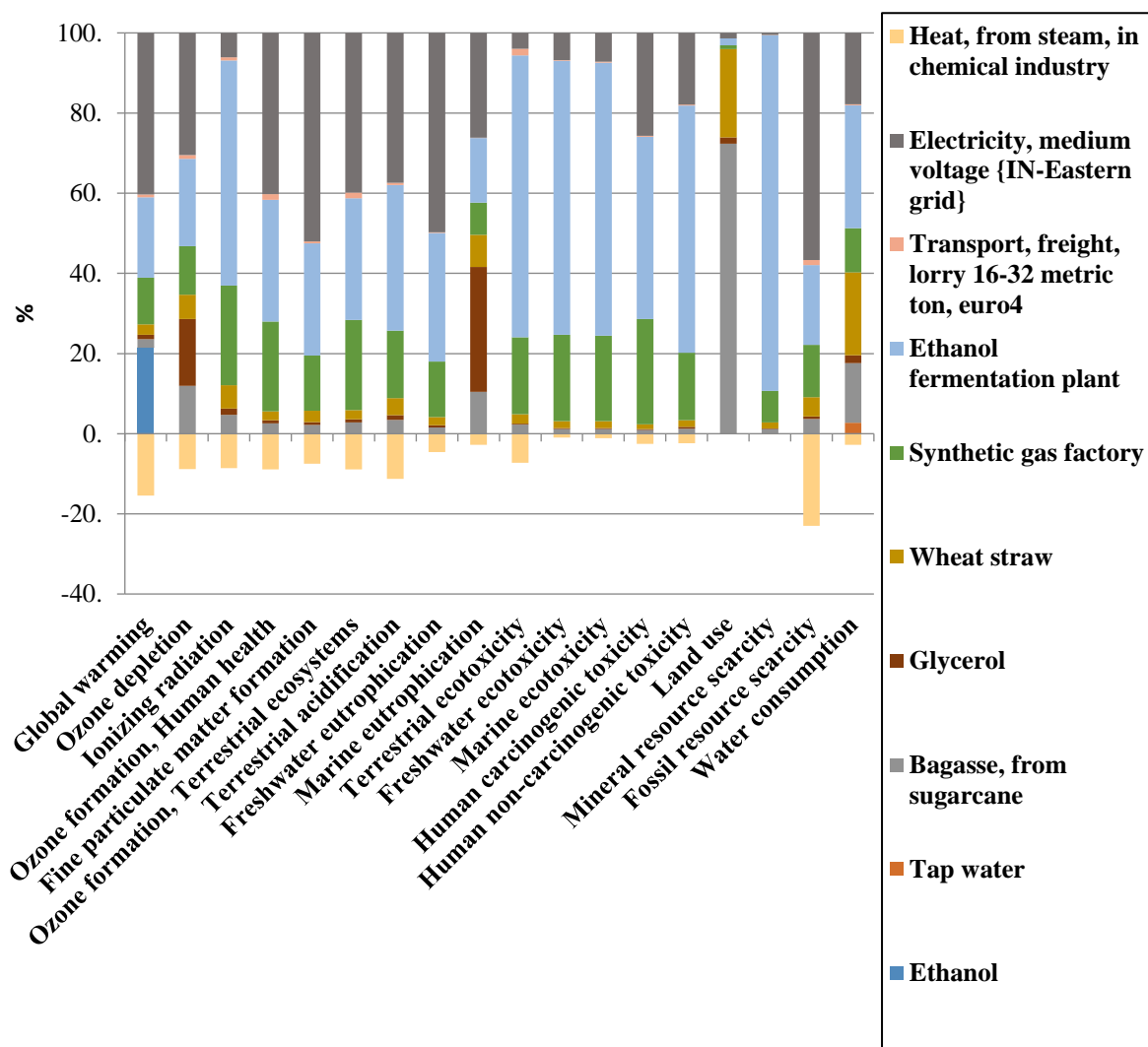


**Figure 8.5:** Percentage of environmental impact in ReCiPe 2016 Midpoint (H) 1.13 method for different unit processes

### 8.3.4.2 Comparison of life cycle impacts with other ethanol production technologies

A comparative analysis of the percentage impacts of the CGF, EHF, and SF route has been shown in Figure 8.6. It can be inferred that the EHF pathway causes more damage in 11 impact categories. The impact was highest in 5 impact categories for the CGF pathway. However, the SF pathway had the highest impact in ozone depletion and land use. In the categories like Ozone depletion, Ozone formation, fine particulate matter formation, terrestrial acidification, marine eutrophication, and water consumption, the impact of the present process under discussion is less than the conventional ethanol production process. The high environmental impact of the EHF path is mainly due to the energy dense pre-treatment involved to remove the lignin from the biomass. Also, the requirement of chemicals like sulfuric acid ( $\text{H}_2\text{SO}_4$ ),



sodium hydroxide (NaOH), ammonium phosphate ((NH<sub>4</sub>)<sub>3</sub>PO<sub>4</sub>), and magnesium sulphate (MgSO<sub>4</sub>) is also an important factor in this regard.

Following a cradle-to-gate approach, the total amount of CO<sub>2</sub> emitted during the production process was found to be 1.4 kg per kg of bio-ethanol. Handler et al., 2016, reported a total GWP of 1.5 kg of CO<sub>2</sub> per litre of bio-ethanol while working with the gasification fermentation route in a similar approach using corn stover as the feedstock. Stratospheric Ozone depletion, which is termed as kg CFC-11 equivalent, is 5.34E-7 kg per kg of ethanol for the CGF process. The terrestrial acidification value is 0.0053 kg of SO<sub>2</sub> equivalent which indicates the deposition of chemicals in the surface of the earth. Freshwater and marine eutrophication are two important categories that express the amount of chemical and nutrient deposition in the freshwater and sea, respectively. The values for the process are 0.0006 kg P equivalent and 7.44E-5 kg S equivalent, respectively. The values of eco-toxicity manifested in various sectors like terrestrial, freshwater, marine as well as in human beings are high in the hybrid process which is a result of the complicated machineries involved. The equivalent values of environmental burden in quantified manner imposed by each ethanol production pathway in each category as standardized by the ReCiPe 2016 midpoint (H) category has been provided in Table 8.6.

**Table 8.6:** Environmental impacts according to ReCiPe 2016 Midpoint (H) methodology for various ethanol production pathway

Impact category	Unit	2G ethanol (Hybrid production) (CGF)	2G Ethanol Enzymatic hydrolysis and fermentation (EHF)	1G Ethanol (SF)
<b>Global warming</b>	kg CO <sub>2</sub> eq	1.40	2.63	0.92
<b>Ozone depletion</b>	kg CFC11 eq	5.34E-07	6.15E-06	9E-06
<b>Ionizing radiation</b>	kBq Co-60 eq	0.02	0.19	0.024
<b>Ozone formation, Human health</b>	kg NOx eq	0.003	0.005409	0.004
<b>Fine particulate matter formation</b>	kg PM2.5 eq	0.003074	0.003605	0.003232
<b>Ozone formation, Terrestrial ecosystems</b>	kg NOx eq	0.003526	0.005543	0.004745
<b>Terrestrial acidification</b>	kg SO2 eq	0.005289	0.016606	0.009821
<b>Freshwater eutrophication</b>	kg P eq	0.000627	0.000638	0.000269
<b>Marine eutrophication</b>	kg N eq	7.44E-05	0.001688	0.001561
<b>Terrestrial ecotoxicity</b>	kg 1,4-DCB	11.32298	14.83026	4.415011
<b>Freshwater ecotoxicity</b>	kg 1,4-DCB	0.191253	0.135737	0.058766
<b>Marine ecotoxicity</b>	kg 1,4-DCB	0.245851	0.151555	0.052487
<b>Human carcinogenic toxicity</b>	kg 1,4-DCB	0.105777	0.042321	0.026109
<b>Human non- carcinogenic toxicity</b>	kg 1,4-DCB	3.283299	3.129515	1.721533
<b>Land use</b>	m2a crop eq	12.53638	20.90329	45.80513
<b>Mineral resource scarcity</b>	kg Cu eq	0.041218	0.024616	0.005753
<b>Fossil resource scarcity</b>	kg oil eq	0.243332	0.764545	0.172877
<b>Water consumption</b>	m3	0.010861	0.150819	0.124062

The endpoint analysis finally culminates the various midpoint impacts into three broad categories namely human health, ecosystem, and resources. From figure 8.7, it can be clearly seen that the endpoint impact on human health and resources is highest for the EHF pathway whereas on the ecosystem, the SF does the maximum damage. Although the CGF route has significant effects on human health, it does not pose the highest impact in any endpoint category.

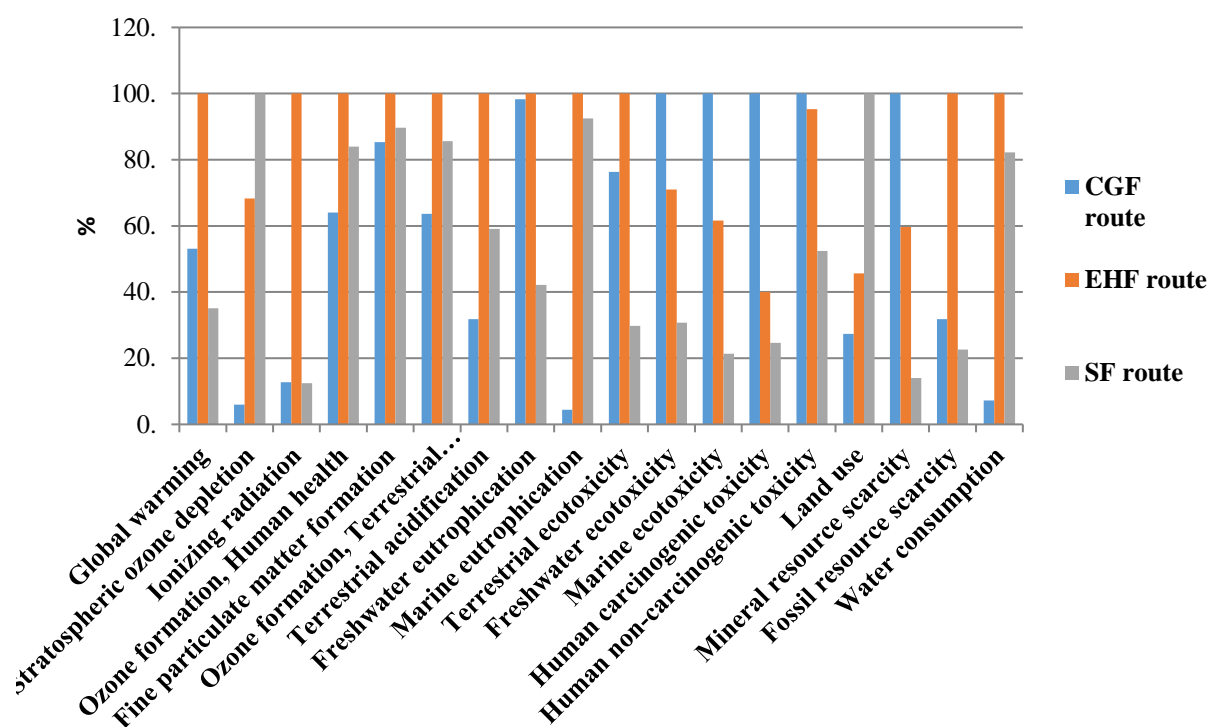


**Figure 8.6:** Midpoint comparison of impacts of three different ethanol production methodologies

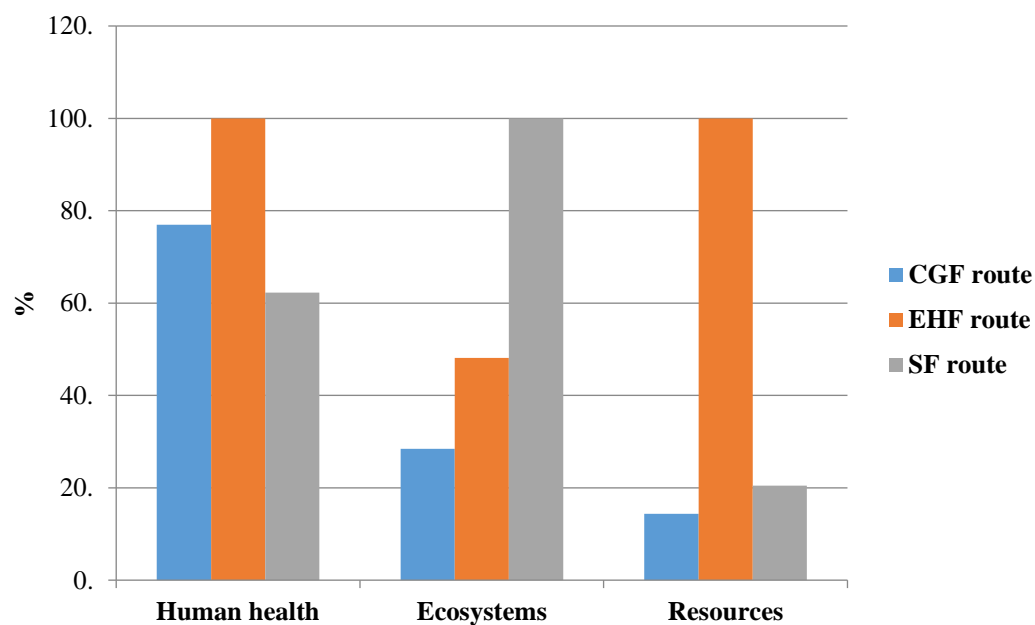


**Figure 8.7:** Endpoint comparison of ethanol production methodologies

## 8.4 Chapter summary

The techno-economic analysis of the process provided a minimum ethanol selling price of 0.65\$/kg which is lesser than the market price of ethanol in India. The other economic indicators like NPV, IRR and payback period are 18.7 M\$, 13.33 %, and 6.7 years, respectively. An insight into the dynamism of the economic model has been provided with the help of risk assessment using the Monte Carlo simulation. The operating cost of the plant has been found to be the most impactful parameter in terms of economic sensitivity. An 81.8 % probability of a non-negative NPV was achieved considering probabilistic distribution for each economic parameter. The individual life cycle assessment of the CGF route suggest a global warming potential of 1.40 kg CO<sub>2</sub> eq. Ozone depletion of 5.34e-07 kg CFC11 eq. terrestrial acidification of 0.005289 kg SO<sub>2</sub> eq. per kg of ethanol. The life cycle comparison of the CGF, EHF, and SF routes indicates that the EHF route is the most environmentally damaging amongst the three. The midpoint impacts suggest that the CGF route is the least impactful in 9 impact categories. The endpoint comparison of the three routes indicate that the CGF route is the least impactful towards ecosystem and resources.

This study does not consider the variation of fermentation parameters and dynamism of the process which can result in over-prediction of the results to some extent. However, this work can be considered as an important step towards the valorisation of LCBs available in India. The co-gasification - fermentation pathway has been observed as an economically robust and environmentally sustainable process that can be industrially applicable.

---

## Chapter 9. Conclusions and future scope

---

### 9.1 Conclusions

The present research has focused on the theoretical attempt towards commercially standardizing the 2G-Bioethanol production process following the syngas platform. The routes of biomass co-gasification and syngas fermentation have been extensively reviewed on the basis of previously published research. The twin problem of resource wastage and environmental pollution has been addressed by incorporating Indian lignocellulosic biomass as feedstock for the process. These biomass are generally regarded as waste and would have been burnt away instead. Utilizing them in this process should provide a more sustainable as well as profitable alternative. The exact work that has been conducted during the course of this study under the objectives stated in chapter 2 has brought in certain findings which have been discussed in the thesis.

From the results of the studies on the first aim of the present research, i.e., “development of equilibrium model and thermodynamic performance assessment of biomass co-gasification”, it has been concluded that

- Increase in temperature increases the LHV of syngas, and the performance efficiency of the gasification while equivalence ratio and steam to biomass ratio are kept constant.
- Equivalence ratio and steam to biomass ratio adversely effects the LHV of syngas and performance efficiencies.
- The mixture of wheat straw and sugarcane bagasse performed better in terms of exergy efficiency whereas the energy efficiency was better for the rice straw and sugarcane bagasse mixture co-gasification.
- Highest energy efficiency of 76.8% has been calculated for rice straw- sugarcane bagasse mixture whereas highest exergy efficiency Of 50.56% has been calculated for wheat straw and sugarcane

As it was necessary to provide a suitable gasifying agent for co-gasification, air was used as a gasifying agent despite of the adverse effect it was causing. But steam was not included for further studies.

From the results of the studies on the second aim of the present research, i.e “Kinetic modelling and optimization of process parameters of biomass co-gasification” it has been concluded that

- Kinetic modelling improved the prediction accuracy of syngas while increasing the complexity of the model.
- Methane and tar were more correctly predicted than in case of the equilibrium model.
- Highest energy and exergy efficiency were obtained for wheat straw and sugarcane bagasse mixture and the values were 46.75% and 42.51% respectively.

Kinetic model performed better in the prediction of  $CH_4$  while the prediction of  $CO$  and  $H_2$  was similar to a great extent to that of the equilibrium model. As this work is primarily focused on the production of syngas which is essentially the mixture of  $CO$  and  $H_2$ , further simulations were conducted considering the equilibrium model of co-gasification.

From the results of the studies on the third and fourth aims of the present research, i.e., “Equilibrium modelling and parametric optimization of biomass co-gasification and syngas fermentation process” and “Implication of power generation and heat and resource recovery in the co-gasification- syngas fermentation model”, it can be concluded that

- The model is capable of predicting the ethanol production rate, energy efficiency and overall  $CO_2$  emission of the process within a stipulated range of specified input variables by using the regression equations developed using response surface methodology.
- Multi-objective optimization clearly indicated that high gasification temperature, high biomass ratio (wheat straw: sugarcane bagasse) and low equivalence ratio will give optimum ethanol production with less  $CO_2$  emission. A maximum of 20.92 ton/hr ethanol production could be achieved in the model.
- Integration of power production unit, steam generation unit and resource recycle in the form of fermentation medium and glycerol significantly improves the resource utilization as the syngas is fully utilized and waste heat from the system could be harnessed.
- Along with 17.3 ton/hr of bio-ethanol, 35 MW of process heat and 32 MW of power is also generated from the system.

Finally, from the results of the studies on the fifth aim of the present research, i.e.,” Techno-economic analysis, investment risk analysis and investment risk analysis of the model “it can be concluded that

- The minimum selling price of ethanol (0.65\$/kg) is well less than the current market price.

- The process becomes profitable within 7 years of its function.
- Fluctuation in the economic parameters affected the NPV of the process less significantly.
- Other ethanol production routes performed less in terms of the non-negative NPV of the process.
- Electricity and plant development are the most damaging factors in this process towards the environment.
- Bio-ethanol from the CGF route was more suitable environmentally rather than the SF and EHF route.

It is expected that the process modelling, optimization and overall sustainability analysis for the combined co-gasification-fermentation unit will be useful for the prediction of the performance of similar units handling other biomass feedstock. The integrated co-gasification-fermentation process for the generation of ethanol from lignin-rich agricultural wastes will ultimately strengthen the pathway of transition from fossil-fuel based economy towards the green bio-economy.

## **9.2 Scope for future work**

This research can be seen as a comprehensive overview and analysis of the Indian agro-waste co-gasification and syngas fermentation. Both kinetic and equilibrium co-gasification model and equilibrium fermentation model have been developed in this work. However, the kinetic modelling of syngas fermentation is an interesting area of study. Also, the variation of different fermentation parameters can be incorporated in the kinetic modelling. This can be seen as a possible scope for future work.

Other than that the optimization studies can be conducted using other optimization techniques to make the results more robust.

Finally, with the development of machine learning based algorithms, predictive models of bio-ethanol production can also be developed using available data sets of ethanol production.





## References

- Abdelrahim, A., Brachi, P., Ruoppolo, G., Fraia, S. Di, & Vanoli, L. (2020). Experimental and Numerical Investigation of Biosolid Gasification: Equilibrium-Based Modeling with Emphasis on the Effects of Different Pretreatment Methods. *Ind. Eng. Chem. Res.* <https://doi.org/10.1021/acs.iecr.9b03902>
- Acar, M. C., & Böke, Y. E. (2019). Simulation of biomass gasification in a BFBG using chemical equilibrium model and restricted chemical equilibrium method. *Biomass and Bioenergy*, 125(December 2018), 131–138. <https://doi.org/10.1016/j.biombioe.2019.04.012>
- Adeyemi, I., & Janajreh, I. (2015). Modeling of the entrained flow gasification: Kinetics-based ASPEN Plus model. *Renew. Energy*, 82, 77–84. <https://doi.org/10.1016/j.renene.2014.10.073>
- Adnan, M. A., & Hossain, M. M. (2018). Co-gasification of Indonesian coal and microalgae – A thermodynamic study and performance evaluation. *Chem. Eng. Process. - Process Intensif.*, 128(February), 1–9. <https://doi.org/10.1016/j.cep.2018.04.002>
- Adnan, M. A., Susanto, H., Binous, H., Muraza, O., & Hossain, M. M. (2017). Feed compositions and gasification potential of several biomasses including a microalgae: A thermodynamic modeling approach. *Int. J. Hydrogen Energy*, 42(27), 17009–17019. <https://doi.org/10.1016/j.ijhydene.2017.05.187>
- Ali, D. A., Gadalla, M. A., Abdelaziz, O. Y., Hulteberg, C. P., & Ashour, F. H. (2017). Co-gasification of coal and biomass wastes in an entrained flow gasifier: Modelling, simulation and integration opportunities. *J. Nat. Gas Sci. Eng.*, 37, 126–137. <https://doi.org/10.1016/j.jngse.2016.11.044>
- Ardila, Y. C., Figueroa, J. E. J., Lunelli, B. H., Filho, R. M., & Maciel, M. R. W. (2014). Simulation of ethanol production via fermentation of the synthesis gas using aspen plus. *Chem. Eng. Trans.*, 37(2), 637–642. <https://doi.org/10.3303/CET1437107>
- Aydin, E. S., Yucel, O., & Sadikoglu, H. (2017). Development of a semi-empirical equilibrium model for downdraft gasification systems. *Energy*, 130, 86–98. <https://doi.org/10.1016/j.energy.2017.04.132>
- Baccar, I., Hnich, K. Ben, Khila, Z., Pons, M. N., Romdhane, M., & Hajjaji, N. (2022). Environmental Life Cycle Assessment of Second-Generation Bioethanol from Tunisian Waste Dates. *Bioenergy Res.*, 15(4), 1982–1995. <https://doi.org/10.1007/s12155-022->

- Barbanera, M., Lascaro, E., Foschini, D., Cotana, F., & Buratti, C. (2018). Optimization of bioethanol production from steam exploded hornbeam wood (*Ostrya carpinifolia*) by enzymatic hydrolysis. *Renew. Energy*, *124*, 136–143. <https://doi.org/10.1016/j.renene.2017.07.022>
- Barman, N. S., Ghosh, S., & De, S. (2012). Gasification of biomass in a fixed bed downdraft gasifier - A realistic model including tar. *Bioresour. Technol.*, *107*, 505–511. <https://doi.org/10.1016/j.biortech.2011.12.124>
- Barontini, F., Frigo, S., Gabbrielli, R., & Sica, P. (2021). Co-gasification of woody biomass with organic and waste matrices in a down-draft gasifier : An experimental and modeling approach. *Energy Convers. Manag.*, *245*, 114566. <https://doi.org/10.1016/j.enconman.2021.114566>
- Barrera, R., Salazar, C., & Pérez, J. F. (2014). Thermochemical equilibrium model of synthetic natural gas production from coal gasification using Aspen Plus. *Int. J. Chem. Eng.*, *2014*. <https://doi.org/10.1155/2014/192057>
- Baruah, D., & Baruah, D. C. (2014). Modeling of biomass gasification: A review. *Renew. Sustain. Energy Rev.*, *39*, 806–815. <https://doi.org/10.1016/j.rser.2014.07.129>
- Basu, P. (2010). *Biomass Gasification and Pyrolysis: Practical Design and Theory*. Academic Press.
- Begum, S., Rasul, M. G., & Akbar, D. (2014). A numerical investigation of municipal solid waste gasification using aspen plus. *Procedia Eng.*, *90*, 710–717. <https://doi.org/10.1016/j.proeng.2014.11.800>
- Beheshti, S. M., Ghassemi, H., & Shahsavan-Markadeh, R. (2015). Process simulation of biomass gasification in a bubbling fluidized bed reactor. *Energy Convers. Manag.*, *94*, 345–352. <https://doi.org/10.1016/j.enconman.2015.01.060>
- Bengelsdorf, F. R., Straub, M., & Dürre, P. (2013). Bacterial synthesis gas (syngas) fermentation. *Environ. Technol. (United Kingdom)*, *34*(13–14), 1639–1651. <https://doi.org/10.1080/09593330.2013.827747>
- Bhuvaneshwari, S., Hettiarachchi, H., & Meegoda, J. N. (2019). Crop residue burning in India: policy challenges and potential solutions. *Int. J. Environ. Res. Public Health*, *16*(5), 832.
- Borrion, A. L., McManus, M. C., & Hammond, G. P. (2012a). Environmental life cycle assessment of bioethanol production from wheat straw. *Biomass and Bioenergy*, *47*, 9–19. <https://doi.org/10.1016/j.biombioe.2012.10.017>
- Borrion, A. L., McManus, M. C., & Hammond, G. P. (2012b). Environmental life cycle

- assessment of bioethanol production from wheat straw. *Biomass and Bioenergy*, 47, 9–19. <https://doi.org/10.1016/j.biombioe.2012.10.017>
- Cao, Y., Bai, Y., & Du, J. (2021). Air-steam gasification of biomass based on a multi-composition multi-step kinetic model: A clean strategy for hydrogen-enriched syngas production. *Sci. Total Environ.*, 753. <https://doi.org/10.1016/j.scitotenv.2020.141690>
- Cao, Y., Bai, Y., & Du, J. (2022). Co-gasification of rice husk and woody biomass blends in a CFB system : A modeling approach. *Renew. Energy*, 188, 849–858.
- Catalanotti, E., Porter, R. T. J., & Mahgerefteh, H. (2022). An Aspen Plus Kinetic Model for the Gasification of Biomass in a Downdraft Gasifier. *Chem. Eng. Trans.*, 92(February), 679–684. <https://doi.org/10.3303/CET2292114>
- Chen, C., Jin, Y. Q., Yan, J. H., & Chi, Y. (2013). Simulation of municipal solid waste gasification in two different types of fixed bed reactors. *Fuel*, 103, 58–63. <https://doi.org/10.1016/j.fuel.2011.06.075>
- Chen, J., Gomez, J. A., Höffner, K., Barton, P. I., & Henson, M. A. (2015). Metabolic modeling of synthesis gas fermentation in bubble column reactors. *Biotechnol. Biofuels*, 8(1), 1–12.
- Chowdhury, R., Ghosh, S., Debnath, B., & Manna, D. (2018). Indian agro-wastes for 2G biorefineries: Strategic decision on conversion processes. *Green Energy Technol.*, 9789811071874, 353–373. [https://doi.org/10.1007/978-981-10-7188-1\\_16](https://doi.org/10.1007/978-981-10-7188-1_16)
- Chowdhury, R., & Sarkar, A. (2012). Reaction Kinetics and Product Distribution of Slow Pyrolysis of Indian Textile Wastes. *Int. J. Chem. React. Eng.*, 10. <https://doi.org/10.1515/1542-6580.2662>
- Colantoni, A., Villarini, M., Monarca, D., Carlini, M., Mosconi, E. M., Bocci, E., & Rajabi Hamedani, S. (2021). Economic analysis and risk assessment of biomass gasification CHP systems of different sizes through Monte Carlo simulation. *Energy Reports*, 7, 1954–1961. <https://doi.org/10.1016/j.egyr.2021.03.028>
- de Medeiros, E. M., Posada, J. A., Noorman, H., Osseweijer, P., & Filho, R. M. (2017). Hydrous bioethanol production from sugarcane bagasse via energy self-sufficient gasification-fermentation hybrid route: Simulation and financial analysis. *J. Clean. Prod.*, 168, 1625–1635. <https://doi.org/10.1016/j.jclepro.2017.01.165>
- de Souza-Santos, M. L. (2010). Solid fuels combustion and gasification: Modeling, simulation, and equipment operations. In *CRC Press* (2nd ed.). CRC Press. <https://doi.org/10.1201/9781420047509>
- Devi, L., Ptasinski, K. J., & Janssen, F. J. J. G. (2003). A review of the primary measures for tar elimination in biomass gasification processes. *Biomass and Bioenergy*, 24(2), 125–

140. [https://doi.org/10.1016/S0961-9534\(02\)00102-2](https://doi.org/10.1016/S0961-9534(02)00102-2)
- Diederichs, G. W., Ali Mandegari, M., Farzad, S., & Görgens, J. F. (2016). Techno-economic comparison of biojet fuel production from lignocellulose, vegetable oil and sugar cane juice. *Bioresour. Technol.*, 216, 331–339. <https://doi.org/10.1016/j.biortech.2016.05.090>
- Doherty, W., Reynolds, A., & Kennedy, D. (2008). Simulation of a circulating fluidised bed biomass gasifier using ASPEN Plus - A performance analysis. *ECOS 2008 - Proc. 21st Int. Conf. Effic. Cost, Optim. Simul. Environ. Impact Energy Syst.*, 1241–1248.
- Doherty, W., Reynolds, A., & Kennedy, D. (2013). Aspen plus simulation of biomass gasification in a steam blown dual fluidised bed. *Mater. Process Energy*, 212–220.
- Dübendorf, C. (2014). *Ecoinvent database 3.1*. [www.ecoinvent.org](http://www.ecoinvent.org)
- Dutta, A., Talmadge, M., Hensley, J., Worley, M., Dudgeon, D., Barton, D., Groenendijk, P., Ferrari, D., Stears, B., Searcy, E. ., Wright, C. ., & Hess, J. . (2011). Process design and economics for conversion of lignocellulosic biomass to ethanol. *NREL Tech. Rep. NREL/TP-5100-51400*, 303(May 2011), 275–3000. <http://www.nrel.gov/docs/fy11osti/51400.pdf>5Cnpapers2://publication/uuid/49A5007E-9A58-4E2B-AB4E-4A4428F6EA66
- Edreis, E. M. A., Luo, G., Li, A., Xu, C., & Yao, H. (2014). Synergistic effects and kinetics thermal behaviour of petroleum coke / biomass blends during H<sub>2</sub>O co-gasification. *Energy Convers. Manag.*, 79, 355–366. <https://doi.org/10.1016/j.enconman.2013.12.043>
- Eikeland, M. S., Thapa, R. K., & Halvorsen, B. M. (2015). Aspen Plus Simulation of Biomass Gasification with Known Reaction Kinetic. *Proc. 56th Conf. Simul. Model. (SIMS 56)*, October, 7-9, 2015, Linköping Univ. Sweden, 119, 149–156. <https://doi.org/10.3384/ecp15119149>
- Fernández-Lobato, L., Aguado, R., Jurado, F., & Vera, D. (2022). Biomass gasification as a key technology to reduce the environmental impact of virgin olive oil production: A Life Cycle Assessment approach. *Biomass and Bioenergy*, 165(August). <https://doi.org/10.1016/j.biombioe.2022.106585>
- Font Palma, C. (2013). Modelling of tar formation and evolution for biomass gasification: A review. *Appl. Energy*, 111, 129–141. <https://doi.org/10.1016/j.apenergy.2013.04.082>
- Franco, C., Pinto, F., Gulyurtlu, I., & Cabrita, I. (2003). The study of reactions influencing the biomass steam gasification process. *Fuel*, 82(7), 835–842. [https://doi.org/10.1016/S0016-2361\(02\)00313-7](https://doi.org/10.1016/S0016-2361(02)00313-7)
- Frilund, C., Tuomi, S., Kurkela, E., & Simell, P. (2021). Small- to medium-scale deep syngas purification: Biomass-to-liquids multi-contaminant removal demonstration. *Biomass and*

- Bioenergy*, 148(March), 106031. <https://doi.org/10.1016/j.biombioe.2021.106031>
- Gabbrielli, R., Barontini, F., Frigo, S., & Bressan, L. (2022). Numerical analysis of biomethane production from biomass-sewage sludge oxy-steam gasification and methanation process. *Appl. Energy*, 307(July 2021). <https://doi.org/10.1016/j.apenergy.2021.118292>
- Gagliano, A., Nocera, F., Bruno, M., & Cardillo, G. (2017a). Development of an Equilibrium-based Model of Gasification of Biomass by Aspen Plus. *Energy Procedia*, 111, 1010–1019. <https://doi.org/10.1016/j.egypro.2017.03.264>
- Gagliano, A., Nocera, F., Bruno, M., & Cardillo, G. (2017b). Development of an Equilibrium-based Model of Gasification of Biomass by Aspen Plus. *Energy Procedia*, 111, 1010–1019. <https://doi.org/10.1016/j.egypro.2017.03.264>
- Gautam, R., & Seider, W. D. (1979). Computation of phase and chemical equilibrium: Part I. Local and constrained minima in Gibbs free energy. *AIChE J.*, 25(6), 991–999. <https://doi.org/10.1002/aic.690250610>
- Ghassemi, H., & Shahsavan-Markadeh, R. (2014). Effects of various operational parameters on biomass gasification process; A modified equilibrium model. *Energy Convers. Manag.*, 79, 18–24. <https://doi.org/10.1016/j.enconman.2013.12.007>
- Gil, I. D., Gómez, J. M., & Rodríguez, G. (2012). Control of an extractive distillation process to dehydrate ethanol using glycerol as entrainer. *Comput. Chem. Eng.*, 39, 129–142. <https://doi.org/10.1016/j.compchemeng.2012.01.006>
- Gordon, S., & McBride, B. J. (1971). Computer program for calculation of complex chemical equilibrium compositions rocket performance incident and reflected shocks, and Chapman-Jouguet detonations. *Comput. Progr. Calc. Complex Chem. Equilib. Compos. Rocket Perform. Incid. Reflected Shock. ChapmanJouguet Detonations*, 250.
- Gremyachkin, V. M. (2006). Kinetics of heterogeneous reactions of carbon and oxygen during combustion of porous carbon particles in oxygen. *Combust. Explos. Shock Waves*, 42(3), 254–263. <https://doi.org/10.1007/s10573-006-0048-0>
- Gunatilake, H., Roland-holst, D., & Sugiyarto, G. (2014). Energy security for India : Biofuels ,energy efficiency and food productivity. *Energy Policy*, 65, 761–767. <https://doi.org/10.1016/j.enpol.2013.10.050>
- Gunes, B. (2021). A critical review on biofilm-based reactor systems for enhanced syngas fermentation processes. *Renew. Sustain. Energy Rev.*, 143, 110950.
- Han, J., Liang, Y., Hu, J., Qin, L., Street, J., Lu, Y., & Yu, F. (2017). Modeling downdraft biomass gasification process by restricting chemical reaction equilibrium with Aspen Plus. *Energy Convers. Manag.*, 153(October), 641–648.

<https://doi.org/10.1016/j.enconman.2017.10.030>

- Handler, R. M., Shonnard, D. R., Griffing, E. M., Lai, A., & Palou-Rivera, I. (2016). Life Cycle Assessments of Ethanol Production via Gas Fermentation: Anticipated Greenhouse Gas Emissions for Cellulosic and Waste Gas Feedstocks. *Ind. Eng. Chem. Res.*, 55(12), 3253–3261. <https://doi.org/10.1021/acs.iecr.5b03215>
- Hasanly, A., Khajeh Talkhonchah, M., & Karimi Alavijeh, M. (2018). Techno-economic assessment of bioethanol production from wheat straw: a case study of Iran. *Clean Technol. Environ. Policy*, 20(2), 357–377. <https://doi.org/10.1007/s10098-017-1476-0>
- Henstra, A. M., Sipma, J., Rinzema, A., & Stams, A. J. (2007). Microbiology of synthesis gas fermentation for biofuel production. *Curr. Opin. Biotechnol.*, 18(3), 200–206. <https://doi.org/10.1016/j.copbio.2007.03.008>
- Hiloidhari, M., Das, D., & Baruah, D. C. (2014). Bioenergy potential from crop residue biomass in India. *Renew. Sustain. Energy Rev.*, 32, 504–512. <https://doi.org/10.1016/j.rser.2014.01.025>
- Horowitz, C. A. (2016). Paris agreement. *Int. Leg. Mater.*, 55(4), 740–755.
- Hosseini, M., Dincer, I., & Rosen, M. A. (2012). Steam and air fed biomass gasification: Comparisons based on energy and exergy. *Int. J. Hydrogen Energy*, 37(21), 16446–16452. <https://doi.org/10.1016/j.ijhydene.2012.02.115>
- Howaniec, N., Smolinski, A., Stanczyk, K., & Pichlak, M. (2011). Steam co-gasification of coal and biomass derived chars with synergy effect as an innovative way of hydrogen-rich gas production. *Int. J. Hydrogen Energy*, 36. <https://doi.org/10.1016/j.ijhydene.2011.08.017>
- Inayat, M., Sulaiman, S. A., Inayat, A., Shaik, N. B., Gilal, A. R., & Shahbaz, M. (2021). Modeling and parametric optimization of air catalytic co-gasification of wood-oil palm fronds blend for clean syngas (H<sub>2</sub>+CO) production. *Int. J. Hydrogen Energy*, 46(59), 30559–30580. <https://doi.org/10.1016/j.ijhydene.2020.10.268>
- Jana, K., & De, S. (2014). Biomass integrated gasification combined cogeneration with or without CO<sub>2</sub> capture - A comparative thermodynamic study. *Renew. Energy*, 72, 243–252. <https://doi.org/10.1016/j.renene.2014.07.027>
- Jana, K., & De, S. (2015). Polygeneration using agricultural waste: Thermodynamic and economic feasibility study. *Renew. Energy*, 74, 648–660. <https://doi.org/10.1016/j.renene.2014.08.078>
- Jana, K., & De, S. (2017). Environmental impact of biomass based polygeneration – A case study through life cycle assessment. *Bioresour. Technol.*, 227, 256–265.

- <https://doi.org/10.1016/j.biortech.2016.12.067>
- Jarungthammachote, S., & Dutta, A. (2007). Thermodynamic equilibrium model and second law analysis of a downdraft waste gasifier. *Energy*, 32(9), 1660–1669. <https://doi.org/10.1016/j.energy.2007.01.010>
- Kapoor, R., Ghosh, P., Kumar, M., Sengupta, S., Gupta, A., Kumar, S. S., Vijay, V., Kumar, V., Kumar Vijay, V., & Pant, D. (2020). Valorization of agricultural waste for biogas based circular economy in India: A research outlook. *Bioresour. Technol.*, 304(December 2019). <https://doi.org/10.1016/j.biortech.2020.123036>
- Karamarkovic, R., & Karamarkovic, V. (2010). Energy and exergy analysis of biomass gasification at different temperatures. *Energy*, 35(2), 537–549. <https://doi.org/10.1016/j.energy.2009.10.022>
- Kaushal, P., & Tyagi, R. (2017). Advanced simulation of biomass gasification in a fluidized bed reactor using ASPEN PLUS. *Renew. Energy*, 101, 629–636. <https://doi.org/10.1016/j.renene.2016.09.011>
- Klopffer, W., & Grahl, B. (2014). *Life Cycle Assessment (LCA) A guide to best practice*. Wiley-VCH.
- Kombe, E. Y., Lang'at, N., Njogu, P., Malessa, R., Weber, C. T., Njoka, F., & Krause, U. (2022). Numerical investigation of sugarcane bagasse gasification using Aspen Plus and response surface methodology. *Energy Convers. Manag.*, 254(December 2021), 115198. <https://doi.org/10.1016/j.enconman.2021.115198>
- Ku, X., Wang, J., Jin, H., & Lin, J. (2019). Effects of operating conditions and reactor structure on biomass entrained-flow gasification. *Renew. Energy*, 139, 781–795. <https://doi.org/10.1016/j.renene.2019.02.113>
- La Villetta, M., Costa, M., & Massarotti, N. (2017). Modelling approaches to biomass gasification: A review with emphasis on the stoichiometric method. *Renew. Sustain. Energy Rev.*, 74(February), 71–88. <https://doi.org/10.1016/j.rser.2017.02.027>
- Lan, W., Chen, G., Zhu, X., Wang, X., Liu, C., & Xu, B. (2018). Biomass gasification-gas turbine combustion for power generation system model based on ASPEN PLUS. *Sci. Total Environ.*, 628–629, 1278–1286. <https://doi.org/10.1016/j.scitotenv.2018.02.159>
- Lenton, T. M., Xu, C., Abrams, J. F., Ghadiali, A., Loriani, S., Sakschewski, B., Zimm, C., Ebi, K. L., Dunn, R. R., Svenning, J. C., & Scheffer, M. (2023). Quantifying the human cost of global warming. *Nat. Sustain.*, 6(10), 1237–1247. <https://doi.org/10.1038/s41893-023-01132-6>
- Li, M., Zhao, W., Xu, Y., Zhao, Y., Yang, K., Tao, W., & Xiao, J. (2019). Comprehensive Life

- Cycle Evaluation of Jet Fuel from Biomass Gasification and Fischer-Tropsch Synthesis Based on Environmental and Economic Performances. *Ind. Eng. Chem. Res.*, 58(41), 19179–19188. <https://doi.org/10.1021/acs.iecr.9b03468>
- Liakakou, E. T., Infantes, A., Neumann, A., & Vreugdenhil, B. J. (2021). Connecting gasification with syngas fermentation: Comparison of the performance of lignin and beech wood. *Fuel*, 290, 120054. <https://doi.org/10.1016/j.fuel.2020.120054>
- Liu, Q., Proust, C., Gomez, F., Luart, D., & Len, C. (2020). The prediction multi-phase, multi reactant equilibria by minimizing the Gibbs energy of the system: Review of available techniques and proposal of a new method based on a Monte Carlo technique. *Chem. Eng. Sci.*, 216. <https://doi.org/10.1016/j.ces.2019.115433>
- Lv, X., Xiao, J., Du, Y., Shen, L., & Zhou, Y. (2014). Experimental study on biomass steam gasification for hydrogen-rich gas in double-bed reactor. *Int. J. Hydrogen Energy*, 39(36), 20968–20978. <https://doi.org/10.1016/j.ijhydene.2014.10.083>
- Ma, S., Dong, C., Hu, X., Xue, J., Zhao, Y., & Wang, X. (2022). Techno-economic evaluation of a combined biomass gasification-solid oxide fuel cell system for ethanol production via syngas fermentation. *Fuel*, 324(PA), 124395. <https://doi.org/10.1016/j.fuel.2022.124395>
- Mallick, D., Mahanta, P., & Moholkar, V. S. (2020). Co-gasification of biomass blends: Performance evaluation in circulating fluidized bed gasifier. *Energy*, 192. <https://doi.org/10.1016/j.energy.2019.116682>
- Mansur, F. Z., Faizal, C. K. M., Samad, A. F. A., Atnaw, S. M., & Sulaiman, S. A. (2019). Performance modelling and validation on co-gasification of coal and sawdust pellet in research-scale downdraft reactor. *IOP Conf. Ser. Mater. Sci. Eng.*, 702(1). <https://doi.org/10.1088/1757-899X/702/1/012023>
- Marcantonio, V., Ferrario, A. M., Carlo, A. Di, Zotto, L. Del, Monarca, D., & Bocci, E. (2020). Biomass steam gasification: A comparison of syngas composition between a 1-d matlab kinetic model and a 0-d aspen plus quasi-equilibrium model. *Computation*, 8(4), 1–15. <https://doi.org/10.3390/computation8040086>
- Mehrpoooya, M., Khalili, M., Mehdi, M., & Sharifzadeh, M. (2018). Model development and energy and exergy analysis of the biomass gasification process ( Based on the various biomass sources ). *Renew. Sustain. Energy Rev.*, 91(2), 869–887. <https://doi.org/10.1016/j.rser.2018.04.076>
- Mendiburu, A. Z., Carvalho, J. A., & Coronado, C. J. R. (2014). Thermochemical equilibrium modeling of biomass downdraft gasifier: Stoichiometric models. *Energy*, 66, 189–201. <https://doi.org/10.1016/j.energy.2013.11.022>



- Mendiburu, A. Z., Carvalho, J. A., Zanzi, R., Coronado, C. R., & Silveira, J. L. (2014). Thermochemical equilibrium modeling of a biomass downdraft gasifier: Constrained and unconstrained non-stoichiometric models. *Energy*, 71, 624–637. <https://doi.org/10.1016/j.energy.2014.05.010>
- Michailos, S., Parker, D., & Webb, C. (2019). Design, Sustainability Analysis and Multiobjective Optimisation of Ethanol Production via Syngas Fermentation. *Waste and Biomass Valorization*, 10(4), 865–876. <https://doi.org/10.1007/s12649-017-0151-3>
- Mohammadi, M., Mohamed, A. R., Najafpour, G. D., Younesi, H., & Uzir, M. H. (2014). Kinetic studies on fermentative production of biofuel from synthesis gas using clostridium ljungdahlii. *Sci. World J.*, 2014(1). <https://doi.org/10.1155/2014/910590>
- Mojaver, P., Jafarmadar, S., Khalilarya, S., & Chitsaz, A. (2019). Study of synthesis gas composition, exergy assessment, and multi-criteria decision-making analysis of fluidized bed gasifier. *Int. J. Hydrogen Energy*, 44(51), 27726–27740. <https://doi.org/10.1016/j.ijhydene.2019.08.240>
- Monir, M. U., Abd Aziz, A., Kristanti, R. A., & Yousuf, A. (2020). Syngas Production from Cogasification of Forest Residue and Charcoal in a Pilot Scale Downdraft Reactor. *Waste and Biomass Valorization*, 11(2), 635–651. <https://doi.org/10.1007/s12649-018-0513-5>
- Morley, C. (2005). *gaseq.co.uk*.
- Ngamchompoo, W., & Triratanasirichai, K. (2017). Experimental investigation of high temperature air and steam biomass gasification in a fixed-bed downdraft gasifier. *Energy Sources, Part A Recover. Util. Environ. Eff.*, 39(8), 733–740. <https://doi.org/10.1080/15567036.2013.783657>
- Nikoo, M. B., & Mahinpey, N. (2008). Simulation of biomass gasification in fluidized bed reactor using ASPEN PLUS. *Biomass and Bioenergy*, 32(12), 1245–1254. <https://doi.org/10.1016/j.biombioe.2008.02.020>
- Okolie, J. A., Nanda, S., Dalai, A. K., & Kozinski, J. A. (2020). Hydrothermal gasification of soybean straw and flax straw for hydrogen-rich syngas production: Experimental and thermodynamic modeling. *Energy Convers. Manag.*, 208(February), 112545. <https://doi.org/10.1016/j.enconman.2020.112545>
- Okolie, J. A., Tabat, M. E., Gunes, B., Epelle, E. I., Mukherjee, A., Nanda, S., & Dalai, A. K. (2021). A techno-economic assessment of biomethane and bioethanol production from crude glycerol through integrated hydrothermal gasification, syngas fermentation and biomethanation. *Energy Convers. Manag.*, X, 12, 100131. <https://doi.org/10.1016/j.ecmx.2021.100131>

- Pardo-Planas, O., Atiyeh, H. K., Phillips, J. R., Aichele, C. P., & Mohammad, S. (2017a). Process simulation of ethanol production from biomass gasification and syngas fermentation. *Bioresour. Technol.*, 245(July), 925–932. <https://doi.org/10.1016/j.biortech.2017.08.193>
- Pardo-Planas, O., Atiyeh, H. K., Phillips, J. R., Aichele, C. P., & Mohammad, S. (2017b). Process simulation of ethanol production from biomass gasification and syngas fermentation. *Bioresour. Technol.*, 245(August), 925–932. <https://doi.org/10.1016/j.biortech.2017.08.193>
- Patel, V. R., Patel, D., Varia, N., & Patel, R. N. (2017). *Co-gasification of lignite and waste wood in a pilot-scale ( 10 kW<sub>e</sub> ) downdraft gasifier*. 119, 834–844.
- Pati, S., De, S., & Chowdhury, R. (2020). “Process modelling and thermodynamic performance optimization of mixed Indian lignocellulosic waste co-gasification. In *International Journal of Energy Research*. <https://doi.org/10.1002/er.6052>
- Pati, S., De, S., & Chowdhury, R. (2021). Process modelling and thermodynamic performance optimization of mixed Indian lignocellulosic waste co-gasification. *Int. J. Energy Res.*, 45(12), 17175–17188. <https://doi.org/10.1002/er.6052>
- Patra, T. K., & Sheth, P. N. (2015). *Biomass gasification models for downdraft gasifier : A state-of-the-art review*. 50, 583–593.
- Pauls, J. H., Mahinpey, N., & Mostafavi, E. (2016). Simulation of air-steam gasification of woody biomass in a bubbling fluidized bed using Aspen Plus: A comprehensive model including pyrolysis, hydrodynamics and tar production. *Biomass and Bioenergy*, 95, 157–166. <https://doi.org/10.1016/j.biombioe.2016.10.002>
- Perry, R. ., & Green, D. . (2007). *Perry's Chemical Engineers' Handbook* (8th ed.). McGraw-Hill.
- Phillips, J. R., Huhnke, R. L., & Atiyeh, H. K. (2017). Syngas fermentation: a microbial conversion process of gaseous substrates to various products. *Fermentation*, 3(2), 28.
- Puig-Arnabat, M., Bruno, J. C., & Coronas, A. (2010). Review and analysis of biomass gasification models. *Renew. Sustain. Energy Rev.*, 14(9), 2841–2851. <https://doi.org/10.1016/j.rser.2010.07.030>
- Qu, T., Guo, W., Shen, L., Xiao, J., & Zhao, K. (2011). Experimental Study of Biomass Pyrolysis Based on Three Major Components : Hemicellulose , Cellulose , and Lignin. *Ind. Eng. Chem. Res.*, 10424–10433. <https://doi.org/10.1021/ie1025453>
- Quan, C., & Gao, N. (2016). Copyrolysis of Biomass and Coal : A Review of Effects of Copyrolysis Parameters , Product Properties , and Synergistic Mechanisms. *Biomed Res.*

*Int.*, 2016.

- Rabea, K., Michailos, S., Akram, M., Hughes, K. J., Ingham, D., & Pourkashanian, M. (2022). An improved kinetic modelling of woody biomass gasification in a downdraft reactor based on the pyrolysis gas evolution. *Energy Convers. Manag.*, 258(March). <https://doi.org/10.1016/j.enconman.2022.115495>
- Ragsdale, S. W. (2008). Enzymology of the Wood–Ljungdahl pathway of acetogenesis. *Ann. N. Y. Acad. Sci.*, 1125(1), 129–136.
- Ragsdale, S. W., & Pierce, E. (2008). Acetogenesis and the Wood–Ljungdahl pathway of CO<sub>2</sub> fixation. *Biochim. Biophys. Acta (BBA)-Proteins Proteomics*, 1784(12), 1873–1898.
- Ramzan, N., Ashraf, A., Naveed, S., & Malik, A. (2011). Simulation of hybrid biomass gasification using Aspen plus: A comparative performance analysis for food, municipal solid and poultry waste. *Biomass and Bioenergy*, 35(9), 3962–3969. <https://doi.org/10.1016/j.biombioe.2011.06.005>
- Regis, F., Monteverde, A. H. A., & Fino, D. (2023). A techno-economic assessment of bioethanol production from switchgrass through biomass gasification and syngas fermentation. *Energy*, 274(September 2022), 127318. <https://doi.org/10.1016/j.energy.2023.127318>
- Roadmap for ethanol blending in india 2020-25. (n.d.). <https://www.iea.org/policies/17007-roadmap-for-ethanol-blending-in-india-2020-25>
- Rosha, P., & Ibrahim, H. (2022). Technical feasibility of biomass and paper-mill sludge co-gasification for renewable fuel production using Aspen Plus. *Energy*, 258(July), 124883. <https://doi.org/10.1016/j.energy.2022.124883>
- Ruggiero, G., Lanzillo, F., Raganati, F., Russo, M. E., Salatino, P., & Marzocchella, A. (2022). Bioreactor modelling for syngas fermentation: Kinetic characterization. *Food Bioprod. Process.*, 134, 1–18. <https://doi.org/10.1016/j.fbp.2022.04.002>
- Rupesh, S., Muraleedharan, C., & Arun, P. (2016a). ASPEN plus modelling of air–steam gasification of biomass with sorbent enabled CO<sub>2</sub> capture. *Resour. Technol.*, 2(2), 94–103. <https://doi.org/10.1016/j.reffit.2016.07.002>
- Rupesh, S., Muraleedharan, C., & Arun, P. (2016b). Energy and exergy analysis of syngas production from different biomasses through air-steam gasification. *Front. Energy*, 1–13. <https://doi.org/10.1007/s11708-016-0439-1>
- Safarian, S., Ebrahimi Saryazdi, S. M., Unnthorsson, R., & Richter, C. (2020). Artificial neural network integrated with thermodynamic equilibrium modeling of downdraft biomass gasification-power production plant. *Energy*, 213, 118800.

<https://doi.org/10.1016/j.energy.2020.118800>

- Safarian, S., Richter, C., & Unnthorsson, R. (2019). Waste Biomass Gasification Simulation Using Aspen Plus: Performance Evaluation of Wood Chips, Sawdust and Mixed Paper Wastes. *J. Power Energy Eng.*, 07(06), 12–30. <https://doi.org/10.4236/jpee.2019.76002>
- Safarian, S., Unnthorsson, R., & Richter, C. (2020). Simulation and Performance Analysis of Integrated Gasification-Syngas Fermentation Plant for Lignocellulosic Ethanol Production. *Fermentation*, 6(3). <https://doi.org/10.3390/FERMENTATION6030068>
- Safarian, S., Unnþórsson, R., & Richter, C. (2019). A review of biomass gasification modelling. *Renew. Sustain. Energy Rev.*, 110(November 2018), 378–391. <https://doi.org/10.1016/j.rser.2019.05.003>
- Santoyo-Castelazo, E., Santoyo, E., Zurita-García, L., Camacho Luengas, D. A., & Solano-Olivares, K. (2023a). Life cycle assessment of bioethanol production from sugarcane bagasse using a gasification conversion Process: Bibliometric analysis, systematic literature review and a case study. *Appl. Therm. Eng.*, 219(PA), 119414. <https://doi.org/10.1016/j.applthermaleng.2022.119414>
- Santoyo-Castelazo, E., Santoyo, E., Zurita-García, L., Camacho Luengas, D. A., & Solano-Olivares, K. (2023b). Life cycle assessment of bioethanol production from sugarcane bagasse using a gasification conversion Process: Bibliometric analysis, systematic literature review and a case study. *Appl. Therm. Eng.*, 219(PA), 119414. <https://doi.org/10.1016/j.applthermaleng.2022.119414>
- Sapkota, T. B., Vetter, S. H., Jat, M. L., Sirohi, S., Shirsath, P. B., Singh, R., Jat, H. S., Smith, P., Hillier, J., & Stirling, C. M. (2019). Cost-effective opportunities for climate change mitigation in Indian agriculture. *Sci. Total Environ.*, 655, 1342–1354. <https://doi.org/10.1016/j.scitotenv.2018.11.225>
- Shafie, S. M., Masjuki, H. H., & Mahlia, T. M. I. (2014). Life cycle assessment of rice straw-based power generation in Malaysia. *Energy*, 70, 401–410. <https://doi.org/10.1016/j.energy.2014.04.014>
- Sharma, M., Attanoor, S., & Dasappa, S. (2015). Investigation into co-gasifying Indian coal and biomass in a down draft gasifier — Experiments and analysis. *Fuel Process. Technol.*, 138, 435–444.
- Sharma, P., Gupta, B., Pandey, M., Singh Bisen, K., & Baredar, P. (2020). Downdraft biomass gasification: A review on concepts, designs analysis, modelling and recent advances. *Mater. Today Proc.*, 46(xxxx), 5333–5341. <https://doi.org/10.1016/j.matpr.2020.08.789>
- Shen, C., Chen, W., Hsu, H., Sheu, J., & Hsieh, T. (2012). Co-gasification performance of coal

- and petroleum coke blends in a pilot-scale pressurized entrained-flow gasifier. *Int. J. Energy Res.*, 36(4), 499–508. <https://doi.org/10.1002/er>
- Shen, N., Dai, K., Xia, X.-Y., Zeng, R. J., & Zhang, F. (2018). Conversion of syngas (CO and H<sub>2</sub>) to biochemicals by mixed culture fermentation in mesophilic and thermophilic hollow-fiber membrane biofilm reactors. *J. Clean. Prod.*, 202, 536–542.
- Silva, I. P., Lima, R. M. A., Silva, G. F., Ruzene, D. S., & Silva, D. P. (2019). Thermodynamic equilibrium model based on stoichiometric method for biomass gasification: A review of model modifications. *Renew. Sustain. Energy Rev.*, 114(July), 109305. <https://doi.org/10.1016/j.rser.2019.109305>
- Silva, J. F. L., Selicani, M. A., Junqueira, T. L., Klein, B. C., Vaz, S., & Bonomi, A. (2017). Integrated furfural and first generation bioethanol production: Process simulation and technoeconomic analysis. *Brazilian J. Chem. Eng.*, 34(3), 623–634. <https://doi.org/10.1590/0104-6632.20170343s20150643>
- Sim, J. H., Kamaruddin, A. H., Long, W. S., & Najafpour, G. (2007). Clostridium aceticum-A potential organism in catalyzing carbon monoxide to acetic acid: Application of response surface methodology. *Enzyme Microb. Technol.*, 40(5), 1234–1243. <https://doi.org/10.1016/j.enzmictec.2006.09.017>
- Smith, J. D., Alembath, A., Al-Rubaye, H., Yu, J., Gao, X., & Golpour, H. (2019). Validation and Application of a Kinetic Model for Downdraft Biomass Gasification Simulation. *Chem. Eng. Technol.*, 42(12), 2505–2519. <https://doi.org/10.1002/ceat.201900304>
- Sreejith, C. C., Muraleedharan, C., & Arun, P. (2014). Performance prediction of steam gasification of wood using an ASPEN PLUS thermodynamic equilibrium model. *Int. J. Sustain. Energy*, 33(2), 416–434. <https://doi.org/10.1080/14786451.2012.755977>
- Srinivas, T., Gupta, A. V. S. S. K. S., & Reddy, B. V. (2009). Thermodynamic Equilibrium Model and Exergy Analysis of a Biomass Gasifier. *J. Energy Resour. Technol.*, 131(September), 1–7. <https://doi.org/10.1115/1.3185354>
- Stanley Sandler. (2006a). *chemical biochemical and engineering thermodynamics* (4th ed.). Jhon Wiley and Sons.
- Stanley Sandler. (2006b). *chemical biochemical and engineering thermodynamics* (4th ed.). Jhon Wiley and Sons.
- Sun, X., Atiyeh, H. K., Kumar, A., & Zhang, H. (2018). Enhanced ethanol production by Clostridium ragsdalei from syngas by incorporating biochar in the fermentation medium. *Bioresour. Technol.*, 247(July 2017), 291–301. <https://doi.org/10.1016/j.biortech.2017.09.060>

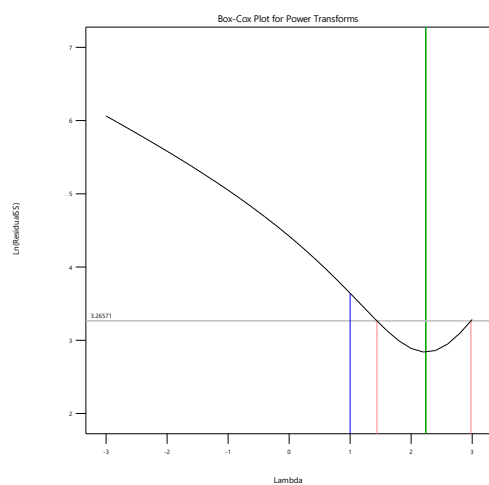
- Tapasvi, D., Kempegowda, R. S., Tran, K., Skreiberg, Ø., & Grønli, M. (2015). A simulation study on the torrefied biomass gasification. *Energy Convers. Manag.*, 90, 446–457. <https://doi.org/10.1016/j.enconman.2014.11.027>
- Tavares, R., Monteiro, E., Tabet, F., & Rouboa, A. (2020). Numerical investigation of optimum operating conditions for syngas and hydrogen production from biomass gasification using Aspen Plus. *Renew. Energy*, 146, 1309–1314. <https://doi.org/10.1016/j.renene.2019.07.051>
- Tinaut, F. V., Melgar, A., Pérez, J. F., & Horrillo, A. (2008). Effect of biomass particle size and air superficial velocity on the gasification process in a downdraft fixed bed gasifier. An experimental and modelling study. *Fuel Process. Technol.*, 89(11), 1076–1089. <https://doi.org/10.1016/j.fuproc.2008.04.010>
- Tungalag, A., Lee, B. J., Yadav, M., & Akande, O. (2020). Yield prediction of MSW gasification including minor species through ASPEN plus simulation. *Energy*, 198, 117296. <https://doi.org/10.1016/j.energy.2020.117296>
- Turton, R., Bailie, R. C., Whiting, W. B., & Shaeiwitz, J. A. (2009). *Analysis, Design and Synthesis of Chemical Processes* (3rd ed.). Prentice Hall.
- Umeki, K., Namioka, T., & Yoshikawa, K. (2012). Analysis of an updraft biomass gasifier with high temperature steam using a numerical model. *Appl. Energy*, 90(1), 38–45. <https://doi.org/10.1016/j.apenergy.2010.12.058>
- Wan, W. (2016). An innovative system by integrating the gasification unit with the supercritical water unit to produce clean syngas: Effects of operating parameters. *Int. J. Hydrogen Energy*, 41(33), 14573–14582. <https://doi.org/10.1016/j.ijhydene.2016.04.237>
- Wang, H.-J., Dai, K., Xia, X.-Y., Wang, Y.-Q., Zeng, R. J., & Zhang, F. (2018). Tunable production of ethanol and acetate from synthesis gas by mesophilic mixed culture fermentation in a hollow fiber membrane biofilm reactor. *J. Clean. Prod.*, 187, 165–170.
- Wang, L., & Chen, Z. (2013). Gas generation by co-gasification of biomass and coal in an autothermal fluidized bed gasifier. *Appl. Therm. Eng.*, 59, 278–282. <https://doi.org/10.1016/j.applthermaleng.2013.05.042>
- Wang, Y.-Q., Yu, S.-J., Zhang, F., Xia, X.-Y., & Zeng, R. J. (2017). Enhancement of acetate productivity in a thermophilic (55 C) hollow-fiber membrane biofilm reactor with mixed culture syngas (H<sub>2</sub>/CO<sub>2</sub>) fermentation. *Appl. Microbiol. Biotechnol.*, 101, 2619–2627.
- Wei, J., Guo, Q., Gong, Y., Ding, L., & Yu, G. (2017). Synergistic effect on co-gasification reactivity of biomass-petroleum coke blended char. *Bioresour. Technol.*, 234, 33–39. <https://doi.org/10.1016/j.biortech.2017.03.010>

- Wooley, R. J., & Putsche, V. (1996). Development of an ASPEN PLUS Physical Property Database for Biofuels Components. *Natl. Renew. Energy Lab.*, 1–32.
- Yan, L., Yue, G., & He, B. (2016). Thermodynamic analyses of a biomass – coal co-gasification power generation system. *Bioresour. Technol.*, 205, 133–141. <https://doi.org/10.1016/j.biortech.2016.01.049>
- Yang, Q., & Chen, G. Q. (2013). Greenhouse gas emissions of corn-ethanol production in China. *Ecol. Modell.*, 252(1), 176–184. <https://doi.org/10.1016/j.ecolmodel.2012.07.011>
- Yu, J., & Smith, J. D. (2018). Validation and application of a kinetic model for biomass gasification simulation and optimization in updraft gasifiers. *Chem. Eng. Process. - Process Intensif.*, 125(January), 214–226. <https://doi.org/10.1016/j.cep.2018.02.003>
- Zachl, A., Buchmayr, M., Gruber, J., Anca-Couce, A., Scharler, R., & Hochenauer, C. (2022). Air preheating and exhaust gas recirculation as keys to achieving an enhanced fuel water content range in stratified downdraft gasification. *Fuel*, 323(November 2021), 124429. <https://doi.org/10.1016/j.fuel.2022.124429>
- Zainal, Z. A., Ali, R., Lean, C. H., & Seetharamu, K. N. (2001). Prediction of performance of a downdraft gasifier using equilibrium modeling for different biomass materials. *Energy Convers. Manag.*, 42(12), 1499–1515. [https://doi.org/10.1016/S0196-8904\(00\)00078-9](https://doi.org/10.1016/S0196-8904(00)00078-9)
- Zaman, S. A., & Ghosh, S. (2021). A generic input–output approach in developing and optimizing an Aspen plus steam-gasification model for biomass. *Bioresour. Technol.*, 337(x), 125412. <https://doi.org/10.1016/j.biortech.2021.125412>
- Zhai, M., Guo, L., Wang, Y., Zhang, Y., Dong, P., & Jin, H. (2016). Process simulation of staging pyrolysis and steam gasification for pine sawdust. *Int. J. Hydrogen Energy*, 41(47), 21926–21935. <https://doi.org/10.1016/j.ijhydene.2016.10.037>
- Zhang, B., Zhong, Z., Min, M., Ding, K., Xie, Q., & Ruan, R. (2015). Catalytic fast co-pyrolysis of biomass and food waste to produce aromatics: Analytical Py – GC / MS study. *Bioresour. Technol.*, 189, 30–35. <https://doi.org/10.1016/j.biortech.2015.03.092>
- Zhang, F., Ding, J., Zhang, Y., Chen, M., Ding, Z.-W., van Loosdrecht, M. C. M., & Zeng, R. J. (2013). Fatty acids production from hydrogen and carbon dioxide by mixed culture in the membrane biofilm reactor. *Water Res.*, 47(16), 6122–6129.
- Zhang, W., Gu, Y., Fang, H., Chen, J., Chen, H., Zhu, Y., & Mu, L. (2023). Thermodynamic modeling and performance analysis on co-gasification of *Chlorella vulgaris* and petrochemical industrial sludge via Aspen plus combining with response surface methodology. *Int. J. Hydrogen Energy*, November 2022. <https://doi.org/10.1016/j.ijhydene.2023.11.169>

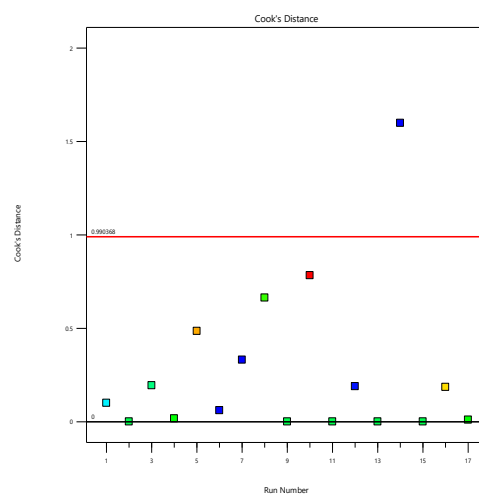
Zheng, H., & Morey, R. V. (2014). An unsteady-state two-phase kinetic model for corn stover fluidized bed steam gasification process. *Fuel Process. Technol.*, 124, 11–20.



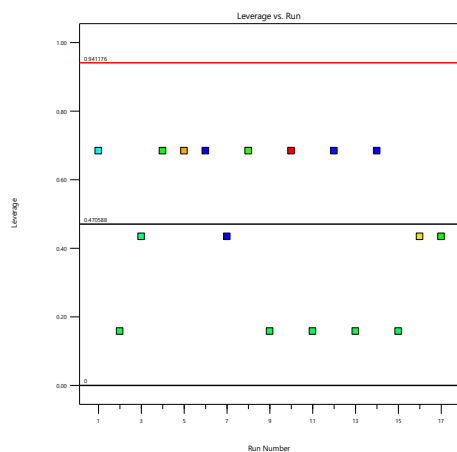
# Appendix



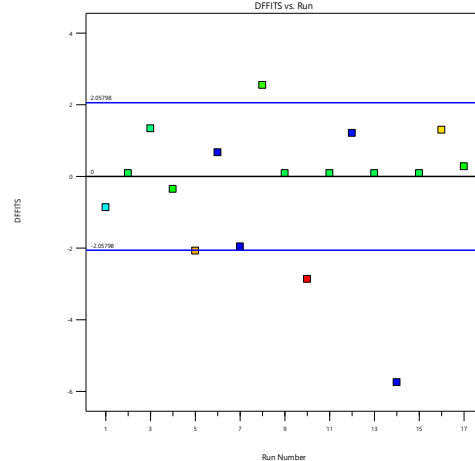
(a)



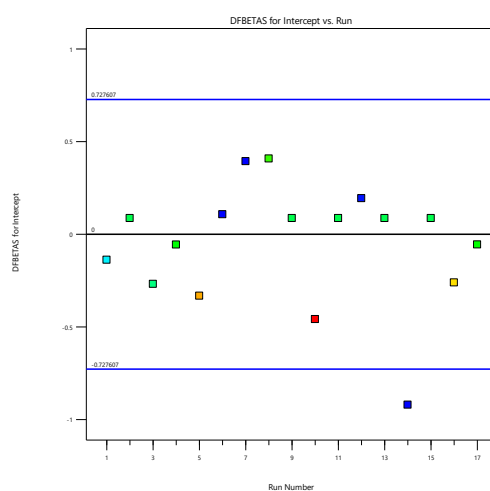
(b)



(c)

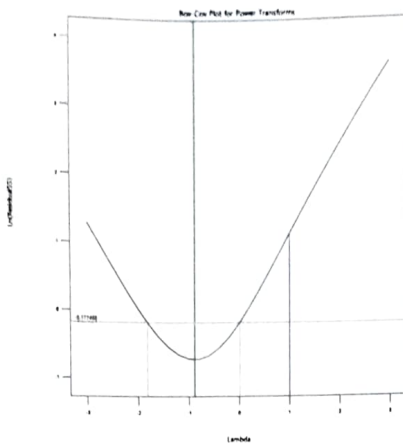


(d)

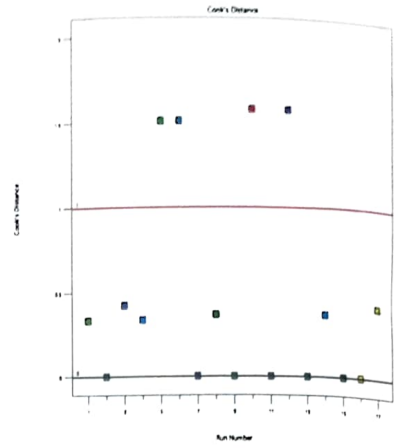


(e)

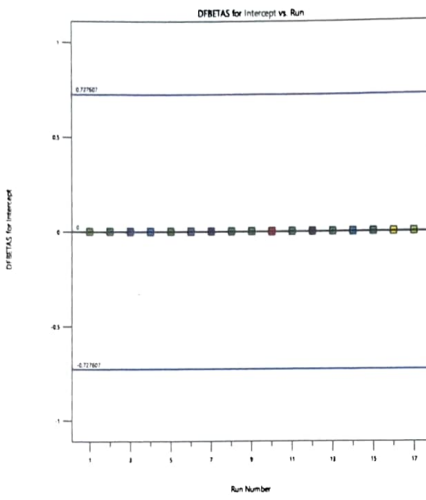
**Figure 1-A:** Diagnostic plots for energy efficiency optimization for RS-SCB mixture in equilibrium modelling



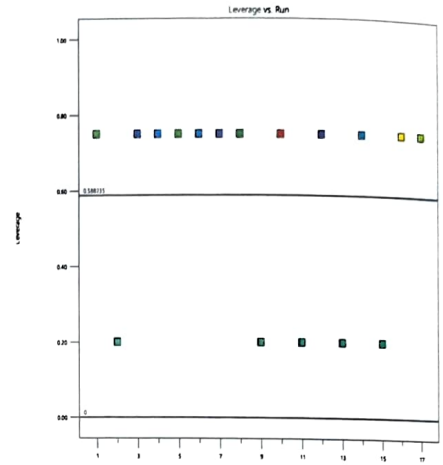
(a)



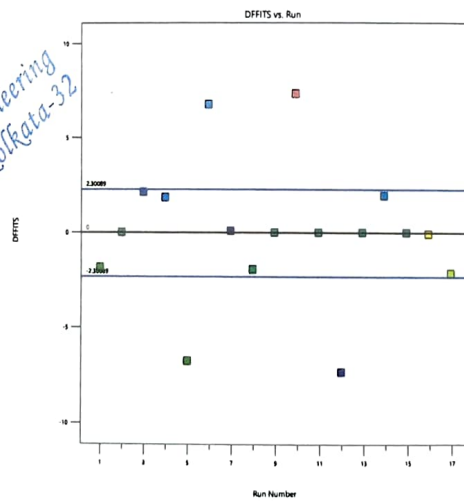
(b)



(c)



(d)



(e)

Figure 2-A: Diagnostic plots for exergy efficiency optimization for RS-SCB mixture